

Can Parallel Multi-Compartment *In Vitro* Drug Binding Measurements Improve the Prediction of In Vivo PK Measurements?

Declaration

I declare that this thesis is an original report of my research, has been written by myself and has not been submitted for any previous degree. The experimental work is entirely my own and references has been acknowledged and provided for supporting literature.

Author:

Wayne Ludlow Wright

Acknowledgements

This thesis has only been possible thanks to help from a wide range of people. Firstly, I would like to thank my supervisors, Dr Scott Summerfield, Prof. Simon Mackay, Dr Andrew Paul and Prof. Yvonne Perrie.

I would also like to thank Jackie Bloomer for helping to launch this GSK - University of Strathclyde programme.

Others to thank, my colleagues in Bioanalysis, Immunogenicity and Biomarkers (BIB).

Dedication

This work is dedicated to sons Bjorn, Jayden, Dontae and Tahjae Wright and my late mother Mrs Rose Gordon-Wright.

Abstract

Measurement of unbound drug concentration (C_u), plasma protein binding (PPB), volume of distribution (VD) are important pharmacokinetic parameters for understanding drug distribution *in-vivo*. However, experimentation is generally performed *in-vitro* under non-competitive conditions across single tissues; this does not adequately reflect the *in-vivo* situation where drug binds competitively between blood components (e.g., plasma) and tissues (proteins and lipids). Several assays are therefore required across multiple tissues and species which can be time consuming. The aim of this thesis was to evaluate a new device (Competitive Rapid Equilibrium Dialysis – “CRED”) which allows for plasma protein and tissue binding to be conducted in parallel from several tissues (as occurs *in-vivo*). The unbound drug compartments of the CRED are interconnected thereby mimicking how unbound drug is the fraction available for *in vivo* drug distribution. This thesis investigates the use of the CRED device toward the goal of improving *in-vitro* predictions of *in-vivo* drug distribution by comparison of plasma protein binding and volume of distribution data obtained using column chromatography and observed literature respectively. The 6 compartment CRED system was adopted in order to study a set of tool compounds that span a wide range of physicochemical properties, and therefore binding affinities. Chapter 2 explores a simple model combining human serum albumin (HSA) and phosphatidylcholine (PC) acting as competitive binding surrogates of plasma and tissues protein, respectively. A correlation coefficient R^2 of 0.7 was obtained for plasma protein binding (PPB) when compared to HSA binding measured using column chromatography. Applying a more complex mixture of phospholipids (phosphatidylethanolamine, phosphatidylserine and phosphatidylinositol) to better reflect the lipid content of tissues *in-vivo*, the volume of distribution correlation coefficient R^2 was improved from 0.5 (PC only) to 0.80 (comparison to literature data). Some researchers have reported a general increase in PPB with increasing size of preclinical species and finally to humans. Investigation of PPB across species in parallel enabled this to be further investigated and was found to be dependent on both compound and protein load which aids the predictability *in-vivo* (Chapter3). The major bottleneck using CRED is the time to equilibrium which is a particular drawback when studying multiple compounds. The throughput was improved using a cassette of compounds along with a highly optimised LC-MS approach for rapid analysis from 4.0hrs to under 1hr per 96 well block (RapidSep, Chapter4). Overall, the competitive binding environment provides the platform to improve *in vivo* drug distribution and facilitate the advancement of better chemical leads.

Contents

Acknowledgements.....	i
Abstract.....	ii
Chapter 1: Drug Attrition in Discovery and Development and the Birth of DMPK as a Key Discipline.....	1
1.1. Introduction.....	2
1.2. Role of Pharmacokinetics in Drug Development.....	5
1.2.1. Absorption.....	5
1.2.2. Distribution.....	7
1.2.3. Metabolism.....	8
1.2.4. Drug Elimination.....	9
1.3. Free Drug Concentration: The Driving force for PK and PD.....	12
1.3.1. The Free Drug Hypothesis.....	13
1.3.2. Impact of Free Drug Hypothesis on CNS Drug Development.....	13
1.3.3. Impact of Free Drug Hypothesis in Relation to Drug Clearance.....	15
1.3.4. Free Drug Hypothesis Impacting Volume of Distribution.....	17
1.4. An Overview of <i>In-Vitro</i> Systems used to Determine the Binding Characteristics of Drug molecules to Plasma Protein.....	19
1.4.1. Microdialysis.....	19
1.4.2. Ultrafiltration.....	21
1.4.3. Immobilised Artificial Membranes.....	22
1.4.4. Equilibrium Dialysis.....	23
1.4.5. Competitive Rapid Equilibrium Dialysis (CRED).....	24
1.4.6. Aims and Objectives.....	24
Chapter 2: Validating a Simple Model of the Competitive Rapid Equilibrium Dialysis.....	26
2.1. Creating an <i>in-vitro</i> Drug Distribution System using Surrogate Matrices.....	27
2.1.1. Introduction.....	27
2.1.2. Tissue Composition with Respect to Drug Binding.....	27
2.1.3. Plasma Composition with Respect to Drug Binding.....	28
2.2. Factors Affecting Plasma Protein Binding Using Equilibrium Dialysis.....	28
2.2.1. Membrane Permeability.....	29
2.2.2. Time to Equilibrium.....	30
2.2.3. Stability of Compounds during Binding Studies.....	30
2.3 Methods and Experimental Procedures.....	30

2.3.1 Compound Selection, Reagents, and Instrumentation.....	30
2.3.2. Reagents	30
2.3.3. Physicochemical Properties and Structures of Tool Compounds.....	31
2.3.4. Instrumentation.....	48
2.3.5. Matrix Effects.....	48
2.4. Experiments and Results to Aid Preliminary Assessments:.....	49
2.4.1. Membrane Permeability	49
2.4.2. Time to Equilibrium	50
2.4.3. Stability of Compounds during Binding Studies.....	51
2.4.4. Feasibility Study.....	51
2.5. Simple Model: Drug Distribution within the CRED using Surrogate Phosphatidylcholine as the lipid component of Cell membrane:	54
2.5.1. Preparation of Buffer.....	54
2.5.2. Preparation of Tissue Surrogate	54
2.5.3. Preparation of Plasma Surrogate	54
2.5.4. Preparation of Analyte concentration (2µm) in Plasma Surrogate.....	54
2.5.5. Preparation of Base Plate.....	54
2.5.6. Preparation of Samples within CRED Device Prior to Incubation	54
2.5.6. Preparation of Calibrations standards.....	55
2.5.6. Chromatographic and Mass Spectroscopy Conditions.....	56
2.5.7. Data Acquisition and Processing.....	56
2.6. Calculations:.....	57
2.6.1. Percentage Bound.....	57
2.6.2. Fraction unbound.....	57
2.6.3. Tissue Dilution	57
2.6.4. Determination of Tissue Dilution Factor.....	59
2.6.5. <i>In-vivo</i> Volume of Distribution (V _{dss}).....	59
2.7. Discussion of Preliminary studies	59
2.7.1 Results Simple Model: Drug Distribution within the CRED using Phosphatidylcholine as the major lipid component of Cell membrane.....	60
2.7.2. Trend Analysis of the Volume of the Distribution obtained using the CRED across Molecular Descriptors for acids, bases, neutrals and Zwitterions.....	74
2.7.3. Validation Study Conducted in Parallel using analytical techniques CRED and Column Chromatography	81

2.7.4. Discussion: Simple Design Model of the CRED	81
2.8. Investigation in Improving the Drug Distribution between Human Serum Albumin and the major phospholipids to better mimic the in-vivo situation:	85
2.8.1. Physiological Concentration of Major Phospholipids.....	86
2.8.2. Compound Selection and Reagents	86
2.8.3. Preparation of Samples within CRED Device Prior to Incubation	86
2.8.4. Preparation of Calibrations standards.....	87
2.8.5. Volume of Distribution (VDss) <i>In-vivo</i>	87
2.8.6. Results	88
2.8.7. Trend Analysis of VDss with Physico-chemical descriptors	92
2.8.8. Variation of VDss Across Different CRED Designs Compared to the Observed Literature VDss as Standard.....	93
2.8.9. Replot of Volume of Distribution across neutrals, acids and bases for Observed Literature and CRED Excluding Outliers.....	94
2.9. Data summary	94
2.10. Discussion	94
Chapter 3: Feasibility of the Competitive Rapid Equilibrium Dialysis in the Reduction, Refinement and Replacement of Animals in Scientific testing (3Rs) Error! Bookmark not defined.	
3.1. An Investigation into Plasma protein Binding of Different Species in Parallel using the CRED.	98
3.1.1. Method.....	99
3.1.2. Preparation of Calibrations standards.....	100
3.1.3. Chromatographic and Mass Spectroscopy Conditions.....	100
3.1.4. Data Acquisition and Processing.....	100
3.2. Experimental Data obtained from Plasma protein Binding of Different Species in Parallel using the CRED	101
3.2.1. Experiment 1: Concentration of GSK248560 Post CRED using Protein Precipitation.....	101
3.2.2. Experiment 2: Concentration of GSK248560 Post CRED using Protein Precipitation.....	102
3.2.3. Experiment 3: Concentration of GSK248560 Post CRED using Protein Precipitation.....	103
3.2.4. Results	104
3.2.5. Discussion.....	105

3.3. Further Investigation into Plasma protein Binding Across Different Species in Parallel using subset of tool Compounds	106
3.3.1. Results	107
3.3.2. Discussion.....	109
Chapter 4: An Investigation into Increasing the Throughput of PPB using RapidSeparation Technology	Error! Bookmark not defined.
4.1. Introduction	111
4.2. Material and Methods.....	112
4.2.1. Preparation of Buffer	113
4.2.2. Preparation of Tissue Surrogate	113
4.2.3. Preparation of Analyte concentration (2µm) in Phosphate Buffer	113
4.2.4. Preparation of Base Plate	113
4.2.5. Preparation of Samples	114
4.2.6. LC-MS/MS Quantitative Analysis.....	114
4.3. Results	115
4.3.1. Examples of Chromatographic Profiles obtained using Conventional HPLC and RapidSep Technology	115
4.3.2. Comparison of Human Plasma Protein Binding Obtained using RapidSep and Conventional Liquid Chromatographic System	115
4.3.3. Comparison of Mouse Plasma Protein Binding of RapidSep with Conventional LC system	117
4.3.4. Comparison of Rat Plasma Protein Binding of RapidSep with Conventional LC system	119
4.3.5. Comparison of Dog Plasma Protein Binding of RapidSep with Conventional LC system	121
4.3.6. Discussion.....	124
Chapter 5: Competitive Rapid Equilibrium Dialysis Its Application in Liposome Technology: Proof of Concept	Error! Bookmark not defined.
5.1. Introduction	127
5.2. Comparison of the Distribution of Doxorubicin Loaded Liposome Formulations Using the Competitive Rapid Equilibrium Dialysis.	127
5.2.1. Method.....	128
5.2.2. Preparation of Calibrations standards.....	130
5.2.3. Chromatographic and Mass Spectroscopy Conditions.....	130
5.2.4. Data Acquisition and Processing.....	131

5.3. Result.....	131
5.4. Discussion	135
5.5. Conclusion.....	136
Chapter 6: Improving in vitro prediction of <i>in-vivo</i> drug distribution using the Competitive Rapid Equilibrium Dialysis.....	Error! Bookmark not defined.
6.1. Discussion	139
6.2. Conclusion.....	140
6.3. Further Work.....	141
<i>Appendix 1</i> Stability of Compounds in Human Serum Albumin and Phosphate Buffered Saline	143
<i>Appendix 2</i> Mass Spectrometer Acquisition Parameters	152
<i>Appendix 3</i> Pilot Study <i>In-Vitro</i> Pharmacokinetic Parameters	154
<i>Appendix 4</i> Main Study <i>In-Vitro</i> Pharmacokinetic Parameters	173
<i>Appendix 5</i> Back Calculated Calibration Standard Data and Associated Parameters for Acidic Series.....	214
<i>Appendix 6</i>	217
<i>In-Vitro</i> Pharmacokinetic Parameters of Acidic series using CRED Device for Mouse, Rat, Dog and Human Plasma in Parallel with RapidSep and Standard LC for Chromatographic Separation	217
<i>In-Vitro</i> Pharmacokinetic Parameters of Basic series using CRED Device for Mouse, Rat, Dog and Human Plasma in Parallel with RapidSep and Standard LC for Chromatographic Separation	227
<i>In-Vitro</i> Pharmacokinetic Parameters of Neutral series using CRED Device for Mouse, Rat, Dog and Human Plasma in Parallel with RapidSep and Standard LC for Chromatographic Separation	235
<i>References</i>	242

Chapter 1: Drug Attrition in Discovery and Development and the Birth of DMPK as a Key Discipline

1.1. Introduction

The modern Drug Development process is often depicted by a division into 4 contiguous phases shown below in Figure 1.

1. Preclinical (target identification, lead identification, lead optimisation and efficacy/safety testing)
2. Clinical (e.g., human trials)
3. Regulatory Approval and Launch
4. Post Market monitoring

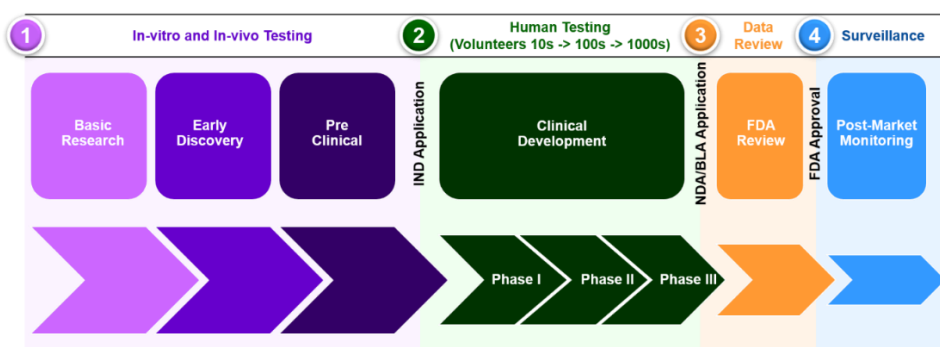


Fig 1 Taken from Agile Bioanalysis Services CRO showing stages of the drug development process

Prior to this (ca. 2-3 decades ago), Drug Discovery scientists focused mostly on improving potency against the identified drug target, generally using *in-vitro* experiments, (Wang and Urban 2004). Pharmacology's best practice of the time was to standardise drug administration to generic formulations often *via* the intraperitoneal, subcutaneous or intramuscular bolus routes while tending to compare results across compounds on the basis of drug dose. Administered doses tended to be high (>10 mg/Kg) because observation of pharmacology was the key driver. The result of this process was an efficient Drug Discovery engine selecting many candidates of high potency, however, attrition in the subsequent Drug Development phase was high and became a significant concern within the pharmaceutical industry (Fig 2). Introspection of these high rates of drug attrition concluded that key molecular properties and flaws were not being screened out prior to initiation of toxicology studies and early clinical studies (Fig 3).

Notably, solubility in gastrointestinal fluid and permeability through the gut wall were rarely tested, despite oral administration being the most convenient administration route in the clinical setting. Furthermore, comparison of different compounds based on dose is a relatively blunt instrument because no understanding of concentration in blood or tissue is gained nor indeed losses by limited oral absorption. These attrition concerns laid the foundations for a new scientific discipline Drug Metabolism and Pharmacokinetics (DMPK) that has become an essential partner for building in drug-like properties during Lead Identification/Optimisation (such as good oral absorption) (Prentis, Lis et al. 1988). More recent work (Basavaraj and Betageri 2014) helped highlight that poor DMPK properties and lack of efficacy were the major reason for drug attrition arising from selection of poor physicochemical properties.

Scientists constantly endeavour to address drug attrition as the implications are enormous, from including (1) millions of dollars of wasted expenditure and time as a result of drugs failing to reach market; (2) dissatisfied shareholders; (3) lack of filling of drug pipelines to offset expiring patents of established marketed drugs; and lastly (4) tighter regulatory criteria. In the

1990s drug attrition was roughly 40% (Pammolli, Magazzini et al. 2011), which was largely due to inadequate drug profiling and suboptimal PK parameters causing drug failure at the development phase of the molecule.

The ensuing decade saw the emergence of Discovery DMPK functions that sat alongside Pharmacology and Medicinal Chemistry teams to build in desirable drug-like properties prior to the initiation of toxicology studies (Summerfield and Jeffrey 2009). Screening and mechanistic work became commonplace for metabolism, solubility, cellular permeability and latterly drug interaction potential and propensity for the formation of reactive metabolites (Ballard, Brassil et al. 2012). This resulted in a marked improvement in progressing drugs through early toxicology studies to clinical trials. However, attrition in late phase clinical trials was still substantial, which was attributed to a poor appreciation of drug concentration-effect relationships and how preclinical pharmacology and/or disease models translated to human pharmacology or human disease (Morgan, Van Der Graaf et al. , Kola 2008). In the last 5 years Translation Medicine has introduced biomarkers to understand target engagement in human as early as possible, thereby reducing clinical attrition due to efficacy ((Cook, Brown et al. 2014),(Kraus 2018)).

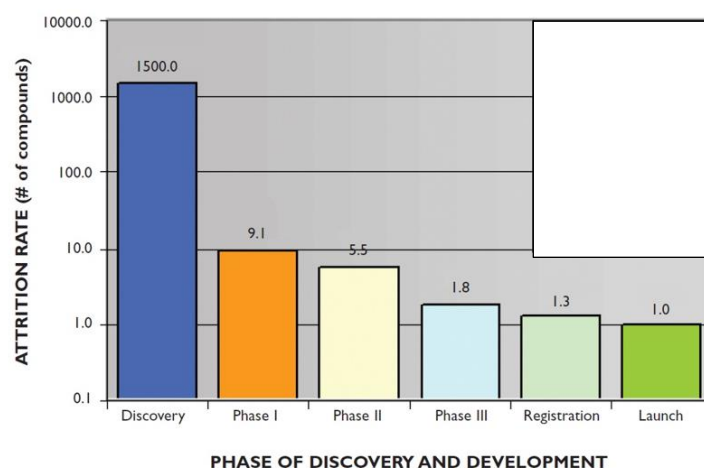


Fig 2 Taken from (Wang and Urban 2004) showing attrition rates of drug candidates, as denoted by the number of compounds that would be required to generate a new drug at the different phases of discovery and development.

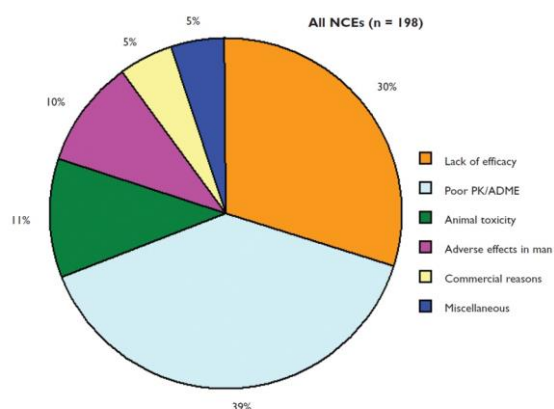


Fig 3 Taken from (Wang and Urban 2004) showing analysis of the reasons for failure of 198 drug candidates in clinical development

With the rising cost to discover and develop a drug (Fig 4) a new strategy was adopted early on in drug discovery utilising DMPK, a scientific discipline which evaluates molecular

properties such as bioavailability, half-life, clearance, metabolic profile and volume of distribution.

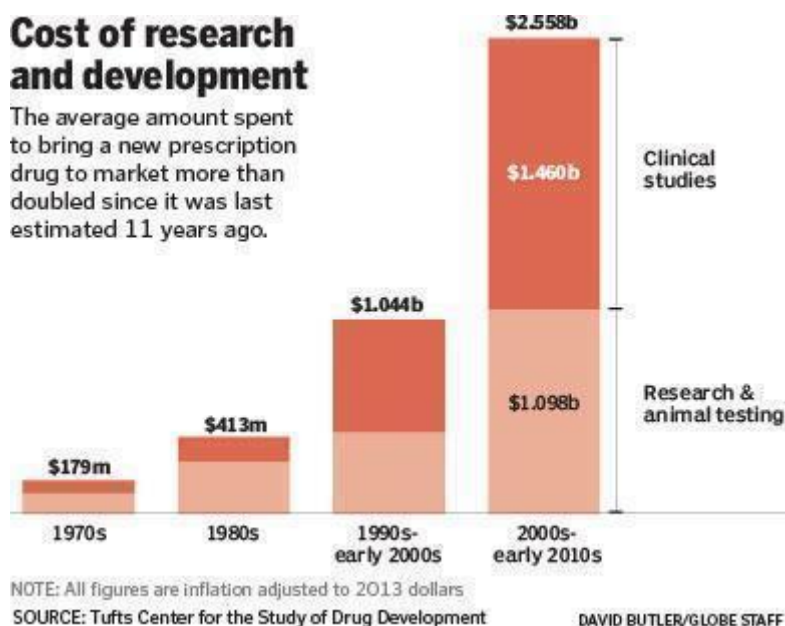


Fig 4 Increase in yearly cost of developing a new medicine to market

The previously independent and sequential steps taken in drug discovery and development was replaced by parallel, interdisciplinary workflows, (Fig 5) where Discovery scientists utilised the discipline of evaluating absorption, distribution, metabolism, excretion and toxicity (ADMET) to get an overall picture of the performance of the drug molecule which saves time and money with a possible improvement in the ratio of marketed drug to total expenditure.

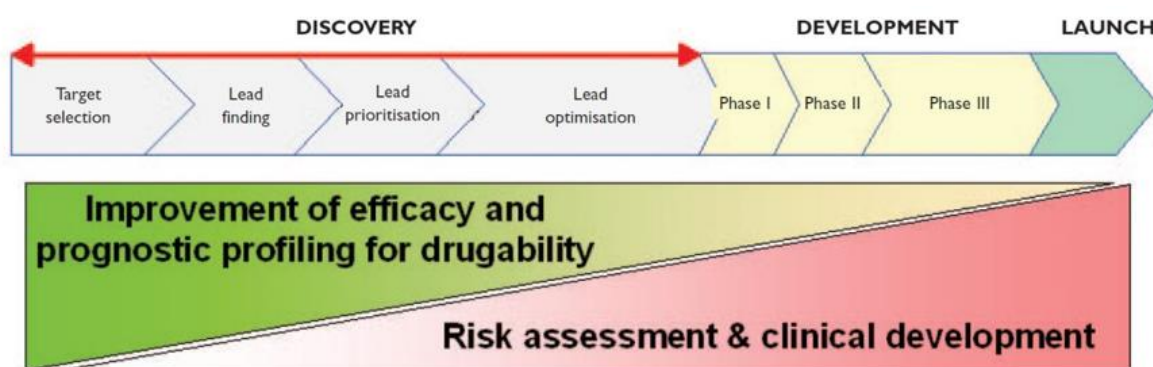


Fig 5 Taken from (Wang and Urban 2004) showing Modern strategy for Drug Discovery and Development where the optimisation of efficacy and drugability will be performed in parallel. The new strategy requires profiling of NCEs occurring in early discovery allowing for only all-around optimised candidates to be promoted to the subsequent development phase

1.2. Role of Pharmacokinetics in Drug Development

In promoting a molecule through the various stages of drug development, it is important to understand what the body does to the drug (Pharmacokinetics, PK) and conversely what the drug does to the body (Pharmacodynamics, PD). Pharmacokinetics introduces the concept of Absorption, Distribution, Metabolism and Excretion (ADME) of the drug molecule upon administration. Conversely, pharmacodynamics relates to the binding of the drug molecule to a target/receptor eliciting a response which may be of therapeutic benefit or one that causes undesired side effects with changes in expression of endogenous biomarkers, enzyme activity and body functions.

1.2.1. Absorption

Absorption refers to how the drug gets into the body and what extent. The most common routes of administration are oral (po), intravenous injection (iv) and inhalation (inh), each having its unique concentration-time profile but connected using a body plan schematic shown in Fig 6, which follows the flow of blood from the site of administration to the arterial circulation.

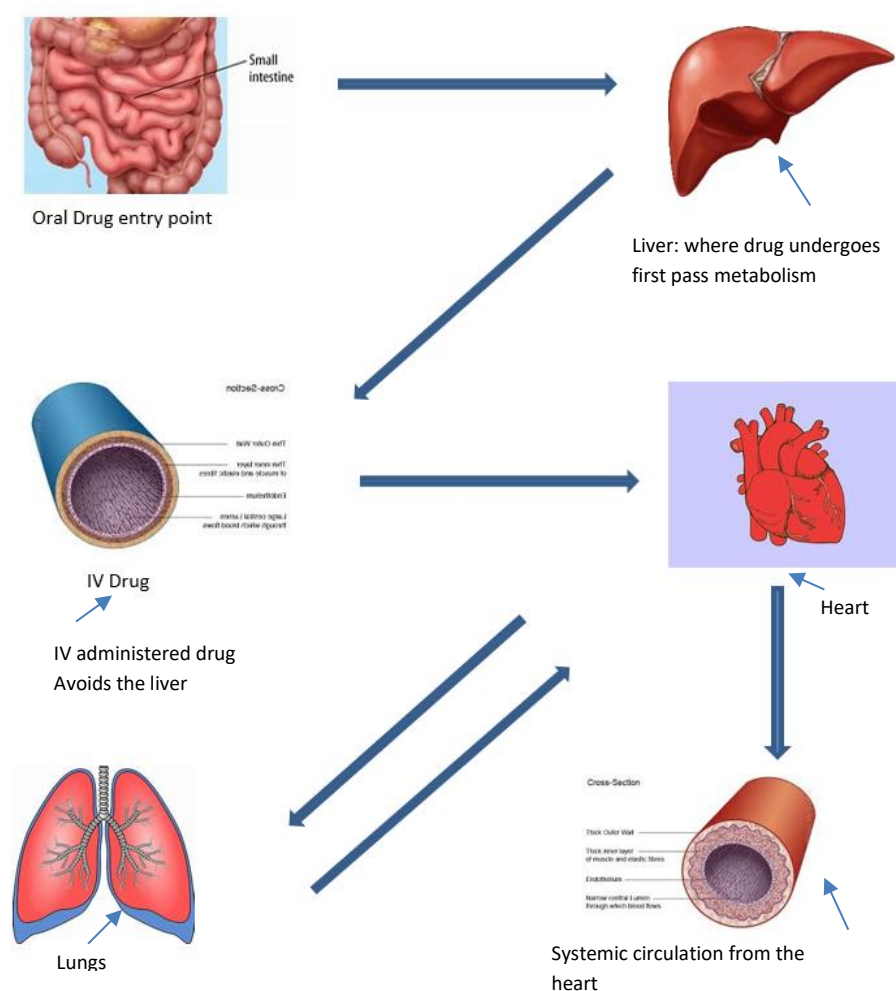


Fig 6 Body plan showing the direction of blood flow with different routes of drug administration.

Most orally administered drug is absorbed from the small intestine and passes into the liver *via* the hepatic portal vein. The blood flow exits the liver and travels into the right side of the heart, from where it goes into the lungs back to the heart before going into systemic circulation. Drugs that are highly cleared by the liver undergo substantial metabolism on their first transit through the liver and this is referred to as first-pass metabolism. Intestinal lymphatic system is another pathway that certain drug may follow prior to entering the systemic circulation thus avoiding hepatic first-pass metabolism. An intravenously administered drug passes into the right side of the heart *via* the venous system and bypasses the liver before transiting through the lungs, back into the heart and exits into the arterial circulation. Since the drug traverses a shorter path and there is no absorption phase, the maximum blood concentration is reached in less time than for a drug administered via any other route.

Inhaled drugs enter the lungs before going into arterial circulation *via* the heart. The maximum concentration is also achieved in less time than an orally dosed drug (Fig 7) because of a shorter absorption phase. The maximum concentration achieved is also greater for inhaled administration because of a larger percentage bioavailability compared with orally administered drug using the same dose. This has practical implications in Drug Development: for example, a drug may be given orally rather than intravenously if it has a potential toxicity and adverse side effect profile at high concentrations, or conversely, where a fast onset of action is required such as pain relief, the drug may be administered intravenously rather than orally.

From the drug concentration-time profile DMPK scientists can calculate several pharmacokinetic properties. These include the area under the concentration time curve (AUC (Area Under Curve)), which gives a measure of the total exposure of the drug within the measurement compartment, e.g., plasma. Assuming 100% bioavailability for intravenous administration, then relative total exposure can be determined by comparison of the AUC across different routes of drug administration. The half-life ($t_{1/2}$) of the drug can also be calculated using the concentration-time profile, which is the time taken for the drug concentration to fall by half. The half-life is a property of the drug molecule whose magnitude is determined by the extent of irreversible drug clearance (metabolism, excretion) and volume of distribution, but is not affected by route of administration. The two other important parameters that can be deduced from the concentration-time profile that are related to the route of administration and the rate and extent of absorption are the maximum concentration (C_{max}) achieved and the time taken to reach it (T_{max}).

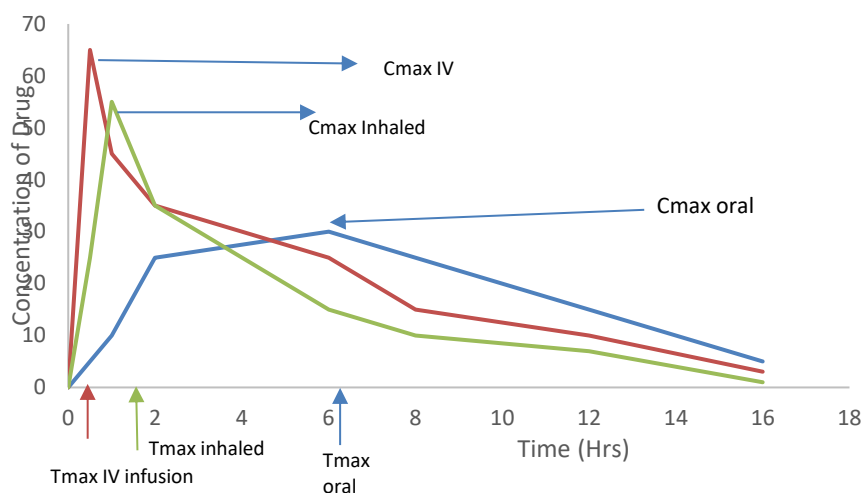


Fig 7 Graphical representation of the concentration-time profile of different routes of administration

1.2.2. Distribution

Once a drug is administered it is distributed amongst various fluid and tissue compartments throughout the body. The main compartments are defined as blood (plasma), lipids, extracellular and intracellular fluids (Fig 8). Molecules that are hydrophilic and therefore often poorly permeable through tissue membranes will be retained more in the blood compartment, whereas molecules that are hydrophobic are able to leave the blood and become more distributed through cellular barriers within the lipid compartments. The ability of the drug to move across the various compartments depends on its own physicochemical properties, the permeability of the individual compartments, the pH within the compartment and the binding capacity of the components within the compartments. These components are generally proteins (albumin) within the blood (plasma) and lipids in the tissue compartments. Drug molecules not bound to the plasma proteins (referred to as unbound or free drug) are available to cross cell membranes, bind to receptors (on-target and off-target) or non-specifically bind to general lipids or proteins in the tissue compartments. Eventually, equilibrium will be established between the free and bound drug contained within all these compartments, which is the process of drug distribution.

For a 70-kg male the total body fluid is approximately 42L, comprising plasma, intracellular fluid (ICF) and extracellular fluid (ECF). A small drug molecule residing largely in this total body would be characterised by a volume of distribution of roughly 0.6L/kg. A substantially larger V_d than 0.6L/kg would suggest that the drug has been sequestered into lipid and protein compartments in tissues by non-specific binding rather than in solely plasma water. Therefore, in dosing the drug molecule, the challenge is to get sufficient amounts of drug at the right place in the body where the therapeutic target resides, for the right amount of time, at the concentration to bind to the target, whilst minimizing side effects (which usually arise from distribution into compartments and subsequently off-target binding)..

Body Fluid Compartments of a 70-kg Adult Man

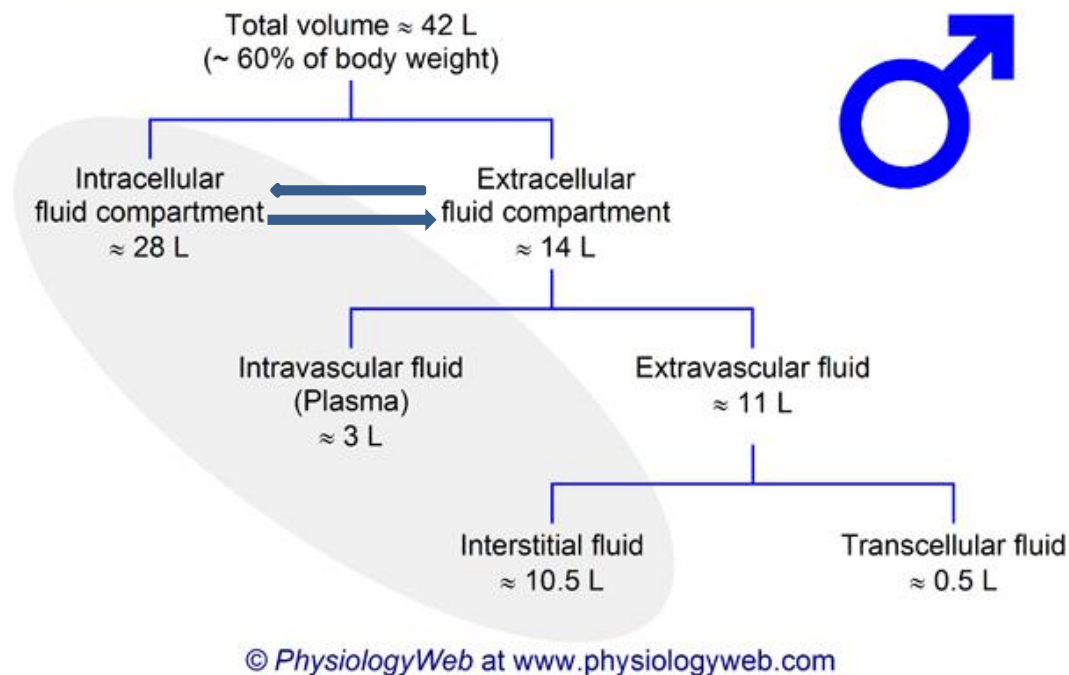


Fig 8.: Showing distribution of fluid in an adult male.

1.2.3. Metabolism

Getting the drug in and around the body are referred to as absorption and distribution. Elimination of the drug from the body is down to metabolism and excretion. Drug metabolism takes place predominantly in the liver through several processes including oxidation, hydrolysis facilitated by cytochrome P450 enzymes (Phase 1) and conjugation with endogenous biomolecules, often involving glucuronidation and sulphation enzymes (Phase 2). The process of metabolism results in increased hydrophilicity to facilitate excretion of drug-related products from the body in urine (Obach, Lombardo et al. 2008). Enhanced hydrophilicity is a consequence of an enzymatically catalysed chemical transformation of the drug into a metabolite, which inevitably influences its pharmacological activity. Generally, the transformation results in generating metabolites with reduced pharmacological/therapeutic activity, or even no activity at all. Since orally absorbed drugs pass directly through the liver, these metabolic processes can act on first-pass before unmodified drug can enter the general systemic circulation. If the extent of metabolism is very high, then first-pass metabolism would lead to a very low bioavailability. Glyceril trinitrate for the treatment of angina is a good example, as when given orally it undergoes rapid metabolism (Fig 9) to form its major metabolites glyceril dinitrate and glyceril mononitrate. This results in a high concentration of the metabolites but substantially lower concentrations of glyceril trinitrate active drug in the plasma (Hashimoto and Kobayashi 2003). Therefore, glyceril trinitrate is administered sublingually to have a more rapid onset of action.

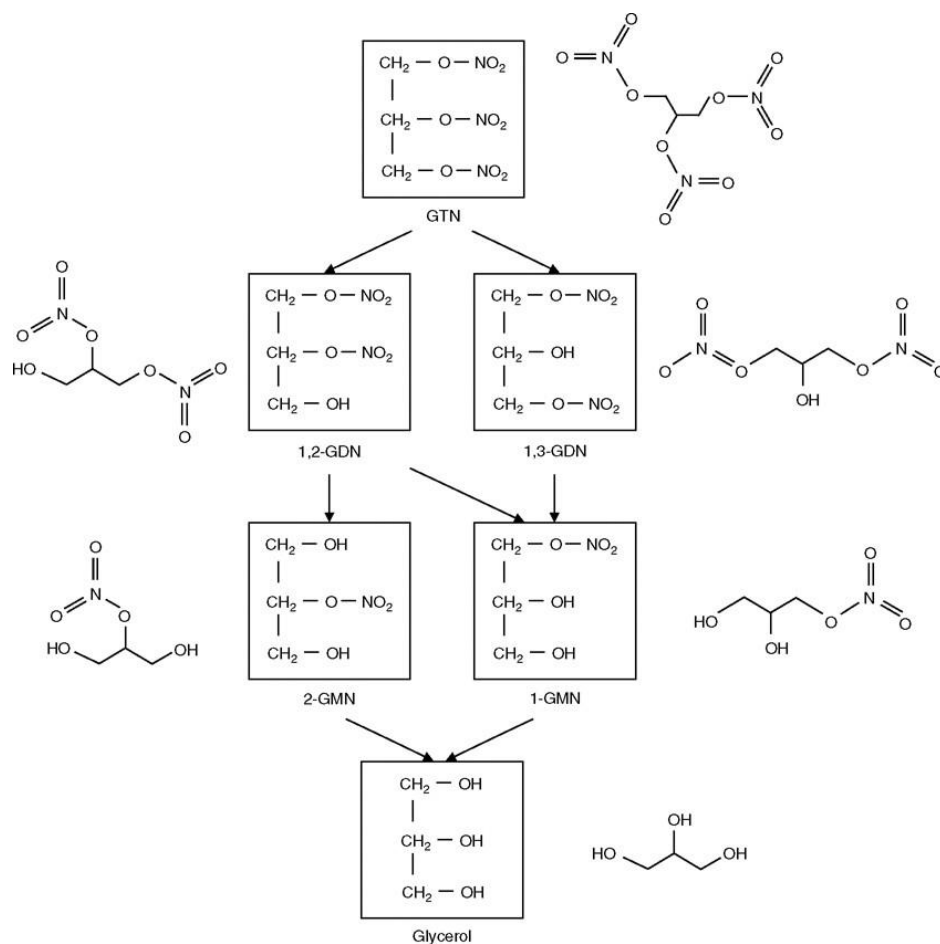


Fig 9 Metabolism of Glyceril trinitrate (GTN) in the liver reduces the amount of active drug in systemic circulation

First-pass metabolism can be utilised in drug development using pro-drug strategies. For example, the angiotensin converting enzyme (ACE) inhibitor enalaprilat has potent pharmacodynamic activity, but low bioavailability because of sub-optimal physicochemical properties that significantly reduce absorption from the small intestine. Enalapril is the more lipophilic pro-drug ester of enalaprilat, which has an improved absorption profile, but has poor pharmacodynamic activity. However, on first-pass through the liver, enalapril is rapidly metabolised to enalaprilat (Fig10) (Dickstein, Till et al. 1987), releasing the active drug into the circulation to engage with the target (ACE).



Fig 10. Metabolism of Enalapril in the liver leads to the formation of the active drug Enalaprilat

1.2.4. Drug Elimination

Drug elimination refers to the complete and irreversible removal of drug from the body. The two main routes of elimination are clearance *via* the hepatobiliary system (CL_H) or the kidney (CL_R). The overall clearance (C_T) is equal to the sum of all organ clearance process, so generally liver or bile for CL_H and the renally for CL_R. Usually, renal clearance is more important than biliary clearance although not for every small molecule drug. As an example,

the antibiotic rifamycin is excreted in the bile after a large first pass effect along with a proportion in urine (Acocella 1978). Most drugs however are excreted *via* the kidneys (Fig 11). For elimination *via* the kidney, drug present in the systemic circulation/plasma (C_p) is filtered through the nephron and a volume of urine (V_u) with a certain drug concentration (C_u) is produced at a specific rate. Movement of drug from the plasma into the kidney nephron involves filtration at the glomerular capillaries in the Bowman's capsule (Fig 11). Only free drug can be filtered from the plasma – drug bound to plasma proteins cannot be removed by filtration. Further drug can be removed from the plasma if it is a substrate for transporters in the cells lining the proximal convoluted tubule (PCT) further along the nephron. However, countering removal from the plasma is reabsorption of the drug from the nephron back into the plasma through the cells lining the distal convoluted tubule (DCT). The amount reabsorbed back into the plasma is related to the lipophilicity of the drug: the more lipophilic, the greater the tendency for reabsorption to reduce the amount excreted. The process of metabolism, which lowers the lipophilicity of the parent drug, has the effect of reducing reabsorption at the DCT, therefore increasing the proportion that can be excreted.

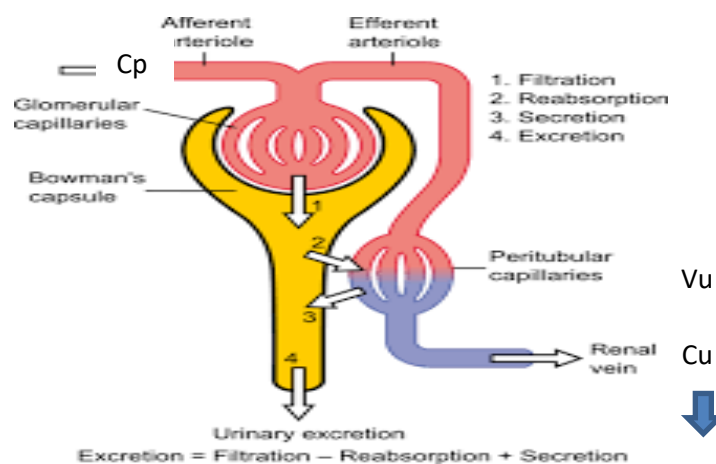


Fig 11. Elimination of drug molecule via the kidney (From Wikimedia Commons, the free media repository)

The clearance (CL) of a drug is the volume of fluid cleared of drug in unit time and is given by the equation $CL = (C_u * V_u) / C_p$. The reabsorption of drug into the plasma at the DCT reduces the amount of drug available to be cleared, whereas secretion of drug into the Bowman's capsule at the PCT results in more drug being cleared (Tucker 1981). The clearance of drug molecule via the kidney can be described mathematically (Eqn1);

$$C_u(\text{filtered into nephron}) + C_u(\text{secreted into nephron}) - C_u(\text{reabsorbed}) \quad \text{eqn. 1}$$

The concentration of drug in the plasma C_p is related to the dose that is administered and subsequently distributed. The volume of urine being produced is related to the glomerular filtration rate (GFR). Therefore, for individuals with lower GFR the concentration in the urine (C_u) will be lower than an otherwise healthy individual. As a result of the lower clearance this may cause accumulation and result in increased side effects and toxicity (Talbert 1994). Dose adjustments may be needed in these cases.

The pharmacokinetics of a drug molecule is therefore not only important in drug development but equally so in drug discovery. Understanding and optimization of the ADME properties

through the parallel interdisciplinary workflows that currently exist in drug discovery and development increases the probability of more drugs successfully reaching the clinic and thereby reducing attrition.

1.3. Free Drug Concentration: The Driving force for PK and PD

A major and important aspect of Drug Discovery and Development is the ability to measure the concentration of a drug molecule in a specific compartment. Quantification of drug levels is derived from its measurement in whole blood or blood constituents e.g., plasma, serum. Whole blood is in contact with all extracellular fluids of the various tissue compartments making it a convenient medium for sampling, measuring and determining drug levels in the body.

Drug molecules bind to plasma proteins (human serum albumin) and tissue proteins and lipids in cell membranes (Fig 12). The degree or extent of binding depends largely on the physicochemical properties of the drug, type and concentration of the endogenous plasma and tissue proteins and lipids. The proportion or amount of administered drug not bound to plasma and tissue components is described as the free or unbound drug. Conversely, the proportion of drug that non-specifically binds to plasma and tissue protein is described as bound drug. The unbound drug fraction can move between different compartments (if its physicochemical properties facilitate such movement) and is available for metabolism and excretion but can also engage with targets to drive PD efficacy or drug toxicity. Therefore, measurement of unbound drug concentrations is a very important parameter in the selection of drug candidates. In Drug Discovery, measuring the unbound concentration across species helps provide an early prediction of the human pharmacokinetics and dose. Modern DMPK focuses on the unbound concentration to refine PK/PD predictions, help interpret toxicology findings, and also assess safety risks for co-administered drugs (Bohnert and Gan 2013) or where changes in protein/lipid binding can impact PK, efficacy or safety (Roberts, Pea et al. 2013). Common examples include:

- Protein binding differences between species
- The variation of protein binding across a range of drug concentrations
- Drug-drug interactions which may potentially cause displacement from the binding site(s)
- Disease states (e.g., renal and hepatic) resulting in modification to the levels of plasma proteins and/or lipids

During Drug Discovery and Development DMPK scientists conduct plasma protein binding studies at various stages of drug development to aid study design, dosage, understand pharmacokinetic and pharmacodynamic outcomes and extrapolate pharmacological and toxicological data to humans.

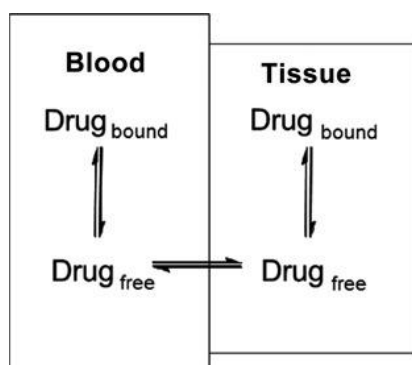


Fig 12 Drug binds to plasma and tissue proteins. At equilibrium the unbound drug concentration is the same in both blood and tissue medium (when passive diffusion is the governing process).

1.3.1. The Free Drug Hypothesis

The Free Drug Hypothesis states that it is the free drug concentration at the site of the receptor that elicits the pharmacological response (Du Souich, Verges et al. 1993) (Fig 13). If passive diffusion is the dominant process for unbound drug distribution, then at steady-state the unbound plasma concentration would reflect the unbound concentration in all extracellular fluid compartments. Transporters and intracellular pH can lead to modification of the unbound concentration in specific compartments; however, the free drug hypothesis still applies, clearly though additional information is needed to determine the unbound plasma concentration in this biophase (e.g., unbound plasma concentration is not a suitable surrogate). A few examples of the importance and role of the free drug hypothesis are described below.

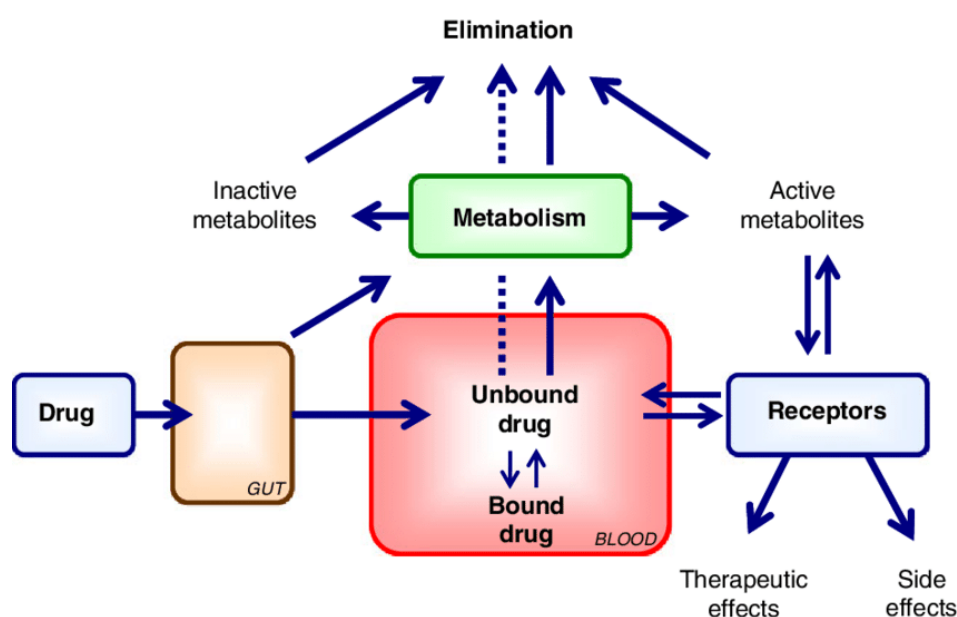


Fig.13 Diagram showing drug absorption, distribution, metabolism and elimination of drug molecules with the unbound parent drug and /or its metabolites responsible for the pharmacological effects. The broken arrow reflects drug that is not metabolised but still eliminated

1.3.2. Impact of Free Drug Hypothesis on CNS Drug Development

Although the Free Drug Hypothesis is now viewed as a good description of relating drug concentration to effect, this was not always as convincing as today because there was insufficient data to support the theory. Some believed that the total drug concentration (sum of bound and unbound drug) (Svensson, Woodruff et al. 1986) elicited the pharmacological effect. Indeed, this was a strong tenet held for CNS drugs where high brain-to-blood ratios were optimised on this premise because this meant more drug was present in the brain to drive efficacy. This led to an industry-wide error in calculating the extent of drug/CNS penetration (K_p) using the ratio of the total brain concentration/plasma concentration (Eqn2).(Jeffrey and Summerfield 2007).

$$\text{Brain } K_p = (AUC_{tot \text{ brain}}) / (AUC_{tot \text{ plasma}}) \quad \text{eqn. 2}$$

Alas high K_p (brain-to-plasma ratios) do not necessarily yield more therapeutically active CNS drugs. The limitation in using total drug concentration was highlighted in a review conducted by the same authors (Jeffrey and Summerfield 2010) which identified the need to consider the

role of free drug concentration at the active site in the brain and how this can be optimised given the influence and role of transporters, tight junctions, enzyme activity as well as permeability in influencing the PK and PD. Taking into account the nonspecific binding of drug molecules to plasma and brain tissue proteins led to the concept of unbound drug penetration K_{puu} (Reichel 2009)) where 'uu' refers to the use of unbound concentrations in both plasma and brain instead of total. Calculation of the drug penetration was therefore revised to:

$$\text{Brain } K_{p \text{ uu}} = AUC \text{ u brain} / AUC \text{ u plasma} \quad \text{eqn. 3}$$

At steady-state the equation can be further modified to describe the extent of drug penetration based on the free drug concentration in plasma and brain tissue, respectively.

$$\text{Brain } K_{p \text{ uu}} (\text{steady state}) = C \text{ u brain} / C \text{ u plasma} \quad \text{eqn. 4}$$

Consequently, the role of nonspecific binding was factored out and led to a better interpretation of the extent of drug penetration in the CNS and the amount available for receptor binding. For a drug undergoing passive diffusion, the free concentration is the same in the brain tissue and plasma at steady-state and therefore $K_{p \text{ uu}}$ would be equal to 1. A value of less than or greater than 1 indicates a component of active transport e.g., efflux (<1) or uptake transport (>1) in addition to any passive diffusion (Fig 14).

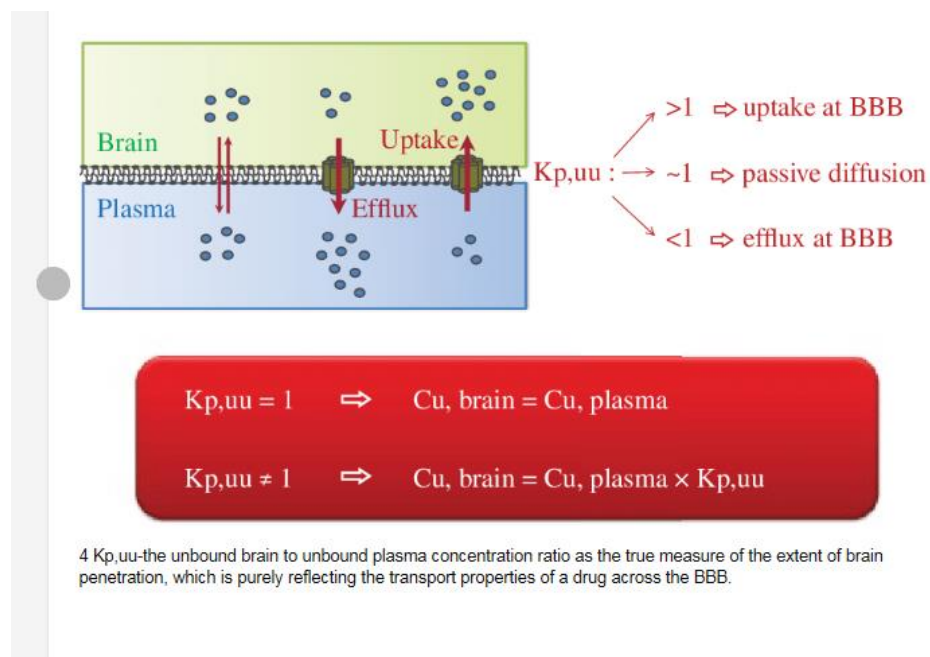


Fig 14 Showing the use the free drug hypothesis in explaining difference in the extent of drug penetration in the CNS

1.3.3. Impact of Free Drug Hypothesis in Relation to Drug Clearance

Clearance is the amount of drug that is removed from a known volume of blood in a specified time. Only the unbound drug can be removed and therefore clearance is driven by the free concentration (Butler and Begg 2008). The two major routes of clearance are via the liver and kidney, described as hepatic and renal clearance, respectively. The concept of the well stirred liver model was developed by (Wilkinson and Shand 1975) to provide a simplistic view of the liver as a one compartment model having inherent factors that influence hepatic clearance of drugs molecules.

In this model, the liver is likened to a cylinder (Fig 15) and assumed to be a homogenous mixture of plasma and tissue proteins to which drug molecules bind, have a unidirectional blood flow and contained within it, and have a single enzymatic action. After oral dosing and absorption from the gut, drug enters the liver via the hepatic portal vein at a certain concentration (C_{in}), which comprises both unbound and protein-bound drug. The degree of plasma protein binding varies according to the physicochemical properties of the compound and the level of plasma protein, which is dependent on age, disease state or where multiple drugs are dosed, on competition for the same binding site. Enzyme activity and liver blood flow can also have an influence. Within the liver, unbound drug bathes the enzyme (specific tissue binding) and is metabolised and then cleared from the system (hepatic clearance). This is referred to as first pass metabolism. Nonspecific tissue binding will also occur but is in dynamic equilibrium with the plasma protein binding. The concentration of free drug leaving the liver is referred to as C_{out} .

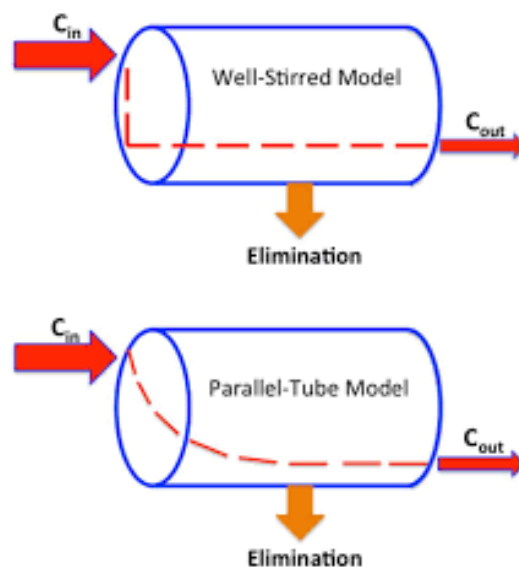


Fig 15 Well stirred and parallel tube models used to explain hepatic drug clearance

Using the well stirred liver model the extraction ratio (E) is defined by the equation

$$E = (C_{in} - C_{out}) \div C_{in} \quad \text{eqn 5}$$

From the equation when C_{out} approaches zero the extraction ratio approaches unity and so most of the drug is extracted through hepatic clearance and does not reach the systemic circulation. Where C_{out} approaches the value of C_{in} , the extraction ratio tends towards zero, clearance is lower and most of the drug goes into the systemic circulation. The clearance of a drug molecule can be defined by the liver blood flow(Q) and the extraction ratio(E) as follows.

$$Cl = Q \times E \quad \text{eqn. 6}$$

Using a liver blood flow of 90L/hr along with the predetermined extraction ratio obtained from an *in-vitro* experiment, the hepatic clearance in vivo can be predicted. This allows for dose adjustment to be made to affect the desired pharmacokinetic and pharmacodynamic outcome. The simplistic view of the well stirred model is not physiologically accurate and therefore other models e.g. parallel tube model (PTM) and dispersion model (DM) have been developed to better understand hepatic clearance (Sandy, Rang et al. 2019) (Fig 15).

Renal clearance refers to removal of drug via filtering through the kidney and is most commonly significant for polar drugs ($\text{LogD}_{7.4} < 1$) because of (1) very low plasma protein binding, (2) low passive permeability (and therefore poor reabsorption in the distal tubule), and finally (3) high expression of numerous transporter proteins in the kidney (e.g., OATs and OCTs). If passive diffusion is the dominant, then the renal clearance process is determined by two parameters the glomerular filtration rate (GFR) of plasma fluid into urine and the unbound drug fraction in plasma, f_u .

$$CL_r = GFR \times f_u \quad \text{eqn. 7}$$

In this instance renal clearance is generally well predicted across species and between individuals. However, when transporters are highly implicated in the renal clearance of drugs then the equation needs modifying to account for active secretion (CLs, which is still dependent on f_u) and the filtration rate of reabsorption (FR)

$$CL_r = f_u \times (GFR + CL_s)(1 - FR) \quad \text{eqn. 8}$$

Hence knowledge of the GFR and f_u alone are not sufficient to accurately predict interspecies or interindividual differences for compounds.

1.3.4. Free Drug Hypothesis Impacting Volume of Distribution

The Volume of Distribution at steady-state (V_{dss}) parameter accounts for the proportion of total drug dose not in plasma, e.g. distributed to tissues (Toutain and Bousquet-MÉLou 2004). Relative to body water for an average 70Kg human (42L), the value obtained for V_{dss} can be related to the molecular properties of a drug (e.g. lipophilicity, pK_a , permeability, solubility: Table 1) (Krishna and White 1996), (Shepherd, Hewick et al. 1977). In Drug Discovery, the volume of distribution is used to extrapolate preclinical (rat, dog) PK data to give an estimate of human PK data and enables the calculation of the required loading dose in order to achieve the desired concentration in plasma (McGinnity, Collington et al. 2007).

Table 1: Interpretation of volume of distribution values (V_D) relative to body water (42L).

	V_D	Comments
Warfarin	14L	Weak acid: low V_D reflects a high degree of plasma protein binding
Chloroquine	>7000L	Weak base: high log P - high V_D reflects sequestration of lipophilic compound into total body fat and extensive binding to a variety of tissues

Using a mass balance approach for an *in-vitro* system like equilibrium dialysis (as depicted in Fig 16), the volume of distribution at steady-state (V_{dss}) can be described in terms of the free drug fraction.

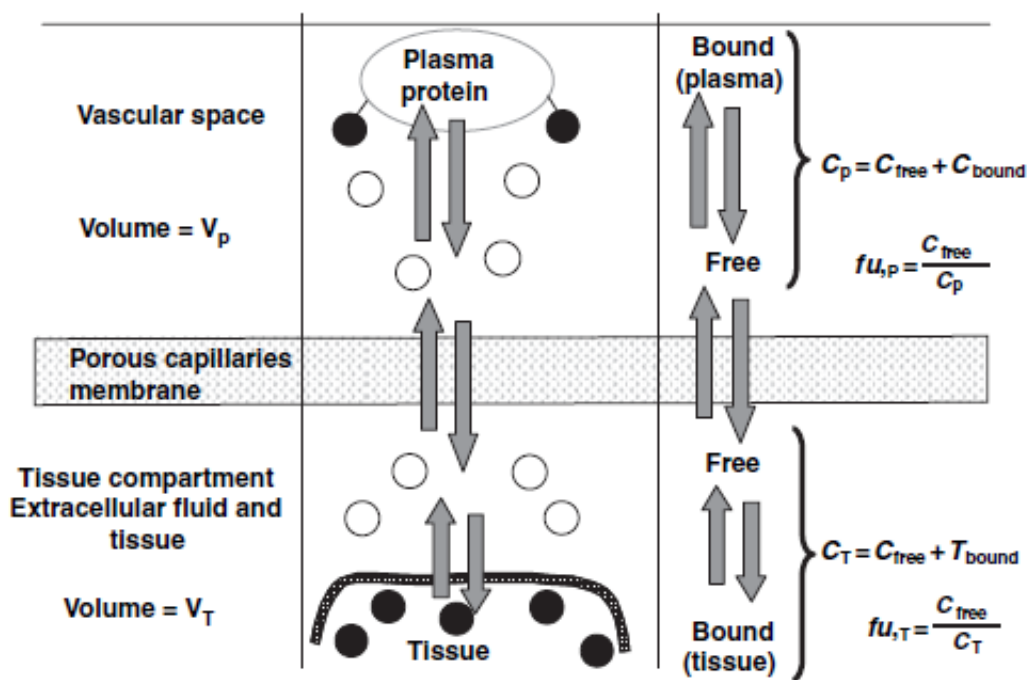


Fig 16: Partitioning of drug between plasma and tissue compartment (V_p is plasma volume, V_T is tissue volume, C_p is total drug concentration in plasma, C_T is total drug concentration in tissue, C_{free} is the free concentration, C_{bound} is drug concentration bound to plasma, T_{bound} is the drug concentration bound to tissue, fu_T is the free fraction in tissue, fu_p is the free fraction in plasma)

For drug molecules to bind tissue proteins, they must first transit through a porous or semipermeable membrane. At steady-state, the amount of drug within the plasma compartment is the product of the volume of the plasma (V_p) and the total concentration of drug within the plasma compartment (C_p), where the drug concentration can be determined directly by an appropriate bioanalytical method. Similarly, at steady-state, the amount of drug within the tissue compartment is the product of the volume of the tissue (V_t) and the total concentration of drug in the tissue compartment (C_t). The volume of distribution (V_{dss}) at steady state can be expressed as the sum of amounts in the respective compartments

$$V_{dss} C_p = (V_p \times C_p) + (V_t \times C_t) \quad \text{eqn. 9}$$

At equilibrium the free drug concentration (C_u) is the same in the plasma and organ tissue

$$C_u = f_{up} \times C_p = f_{ut} \times C_t \quad \text{eqn. 10}$$

Where f_{up} = fraction unbound in plasma and f_{ut} = fraction unbound in tissues.

$$V_{dss} = V_p + \left[V_t \times \left(\frac{f_{up}}{f_{ut}} \right) \right] \quad \text{eqn. 11}$$

The volume of distribution is therefore a measure of the ratio of the unbound fraction in plasma to the unbound fraction in tissue i.e.

$$V_{dss} \sim \left(\frac{f_{up}}{f_{ut}} \right) \quad \text{eqn. 12}$$

Acidic drug molecules generally exhibit stronger binding to plasma proteins to cationic binding sites and generally bind less effectively to tissue components, which leads to generally lower volume of distribution for acidic drugs (see warfarin in table 1), relative to bases and neutrals. Overall, this leads to a shorter plasma half-life for acidic drugs over the other two classes. Although this seems counterintuitive because of the generally higher plasma protein binding, the low sequestration into tissue means that most of the body burden of acidic drugs is localised to the plasma compartment and constantly exposed to passage through the liver. In turn this drives more opportunity for metabolism and/or active transport and hence low volume compounds tend to be characterised by shorter half-lives (this is also the case for bases and neutrals). Under these conditions, dose adjustment (amount administered and/or frequency) may be required to maintain the required therapeutic drug level at the site of action.

Conversely, lipophilic basic compounds generally exhibit weaker binding to plasma proteins (higher free fraction) but also more extensive binding to tissue components. The higher volumes distribution essentially sequesters a portion of drug into tissue away from the plasma and hence hepatic clearance is lower and the plasma half-life is longer (see chloroquine in table (1). Differences in the volume of distribution may not only be based on the physicochemical nature of a drug molecule but can also be affected by the changes in physiology (Klotz 1976). In the disease state, the protein concentration within the liver, kidneys and other organs can change resulting in alterations in plasma/tissue binding, thereby affecting the volume of distribution.

1.4. An Overview of *In-Vitro* Systems used to Determine the Binding Characteristics of Drug molecules to Plasma Protein

The desire and importance to provide fast, high quality and predictable free drug concentration and distribution data to support Drug Discovery and Development has led to significant investment in various high-throughput *in vitro* screening methods for determining plasma protein binding (Pacifici and Viani 1992). These methods include, but are not limited to, equilibrium dialysis, ultrafiltration, microdialysis, ultracentrifugation and immobilised artificial membranes. The technique used depends on the compound's physicochemical characteristics, ease of use, established processes and experience gained over time. A closer look at a number of these techniques, their methodologies, advantages and limitations are described in the following sections.

Direct measurement of the unbound drug concentration in a physiological system is analytically challenging (Nilsson 2013) due to the typically low concentrations involved and the low recoveries associated with techniques such as *in vivo* microdialysis (Lu, Liu et al. 2014). A more amenable approach is to determine the unbound concentration indirectly by measurement of the total concentration (e.g. bound and unbound) and then correcting for binding (using *in vitro* measurements) (Xu, Rose et al. 2014). A recent survey by the European Biological Forum (EBF) of member pharmaceutical companies, listed equilibrium dialysis as the most common technique (82%) used in plasma protein binding experiments (Buscher, Laakso et al. 2014). Equilibrium dialysis has been described as “the gold standard for determination of plasma protein binding”. However, this approach can be time consuming for multiple tissues (Xu, Rose et al. 2014). ThermoFisher Scientific, a multinational biotechnology company, has developed the next generation equilibrium dialysis system known as the Competitive Rapid Equilibrium Dialysis device or CRED. This new device enables protein-tissue binding to be determined in a multi-compartment parallel system for several proteins, lipids or tissue homogenates (as occurs *in-vivo*) simultaneously in order to meet the challenges of modern drug discovery and development. Parallel *in vitro* partition measurements with CRED offer the possibility to redefine and improve the prediction of *in-vivo* drug distribution and account for protein as well as lipid binding interactions in a medium-high throughput assay format using HPLC-MS/MS detection.

1.4.1. Microdialysis

Microdialysis, as a method of determining drug concentrations, came to the fore in the 1960s (Bito, Davson et al. 1966) when it was used in the determination of the free concentration of endogenous compounds, metabolites and xenobiotics in brain extracellular fluid of multiple species (Chefer, Thompson et al. 2001). Subsequently, the use of microdialysis has expanded to include the *in vivo* unbound concentration measurements in tissues organs such as skin, liver and kidney (Plock and Kloft 2005). The technique has been employed extensively by pharmaceutical companies in drug development as shown by the number of publications highlighted by (Bourne 2003) and documents (10,000) related to microdialysis that is available in ResearchGate.

The concept, methodology and principles that describe microdialysis are the same *in vitro* as they are *in vivo*, starting with the insertion of a probe into a matrix containing the analyte of interest. When performed *in vitro* the composition of the spiked matrix is reflective of the extracellular fluid concentration of the tissue homogenate or biological fluid under investigation. The probe is fitted with a semi permeable membrane that allows for the transfer

(or recovery) of free drug across a concentration gradient from the spiked matrix and into microdialysis perfusate, which flows through the probe (Fig 17). The collected dialysate is then analysed either online or offline using reversed phase chromatography and UV or HPLC MS/MS detection. The molecular weight cut-off of the semi-permeable membrane allows for the passive diffusion of free small molecular weight analytes but prevents the passage of large molecules into the perfusate. Passage of drug across the semi-permeable membrane follows Fick's Law, which states that molecules will diffuse across a membrane down a concentration gradient in the direction of the lower concentration towards equilibrium. Microdialysis as a method for determining the unbound drug concentration has several limitations that restricts its widespread applicability (Joukhadar and Müller 2005). Prior to measurement of the unbound drug concentration, the microdialysis probe needs to be calibrated in order to account for any non-specific binding losses occurring between the drug and the probe/tubing (e.g., determination of absolute recovery). Also, the tandem flow of perfusate and the periodic removal of dialysate (for analysis) makes it challenging to establish equilibrium and can lead to an underestimation of the free drug concentration (and likewise an overestimation of bound drug concentration and thus PPB). To counter this, low flow rate conditions are required (typically 1 μ l/min), although small sample aliquots may then lead to potential detection issues (due to lack of assay sensitivity). In addition, to adequately mimic *in vivo* drug binding using *in vitro* microdialysis, the probes need to be bathed in blood or an artificial surrogate adding to the complexity of the experimental setup. Despite these limitations, microdialysis continues to play a vital role in the pharmaceutical industry. Unlike equilibrium dialysis and ultrafiltration, microdialysis can be used directly *in vivo* to study the pharmacokinetics of drug distribution.

$$\text{Fick's Law: } J = S \times dC / T \quad \text{eqn. 13}$$

where J refers to the rate of diffusion, dC difference in concentration, S is the surface area and T is the membrane thickness.

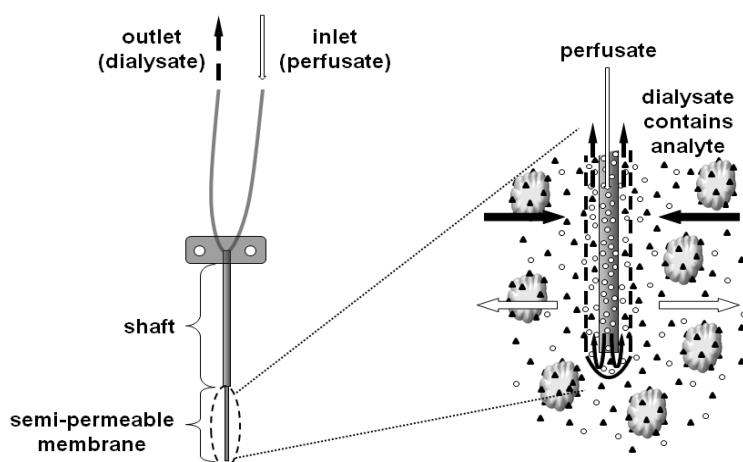


Fig 17: Microdialysis Representation (Ref: Images of microdialysis bing.com/images): A probe fitted with a semi permeable membrane is inserted in the tissue (or *in vitro* system) and connected to an inlet (perfusate) and outlet (dialysate) tubing. A concentration gradient allows the passive diffusion of drug molecules through the membrane into the dialysate for sampling and analysis.

1.4.2. Ultrafiltration

Ultrafiltration is another widely utilised technique for determining the fraction of unbound drug *in vitro* or *ex vivo*. The ultrafiltration device generally consists of an upper tube that is separated from the lower filtrate collection compartment by a semi permeable membrane. The membrane acts as a filter that only allows free molecules below a certain molecular size to permeate through while preventing larger molecules from doing so. The membrane is described as having a Molecular Weight Cut-Off (MWCO) value that excludes plasma proteins from passing between compartments, allowing only much lower molecular weight species to pass through (including the free analyte of interest). For *in vitro* experiments, plasma or (surrogate matrix) spiked with drug is first incubated for 10-15 min at physiological temperature (37°C) to attain equilibrium between the bound and unbound drug fractions. The sample is then loaded and secured in the upper tube. The filtrate is obtained by either the force of ultracentrifugation (Fig 18) or the application of a positive pressure.

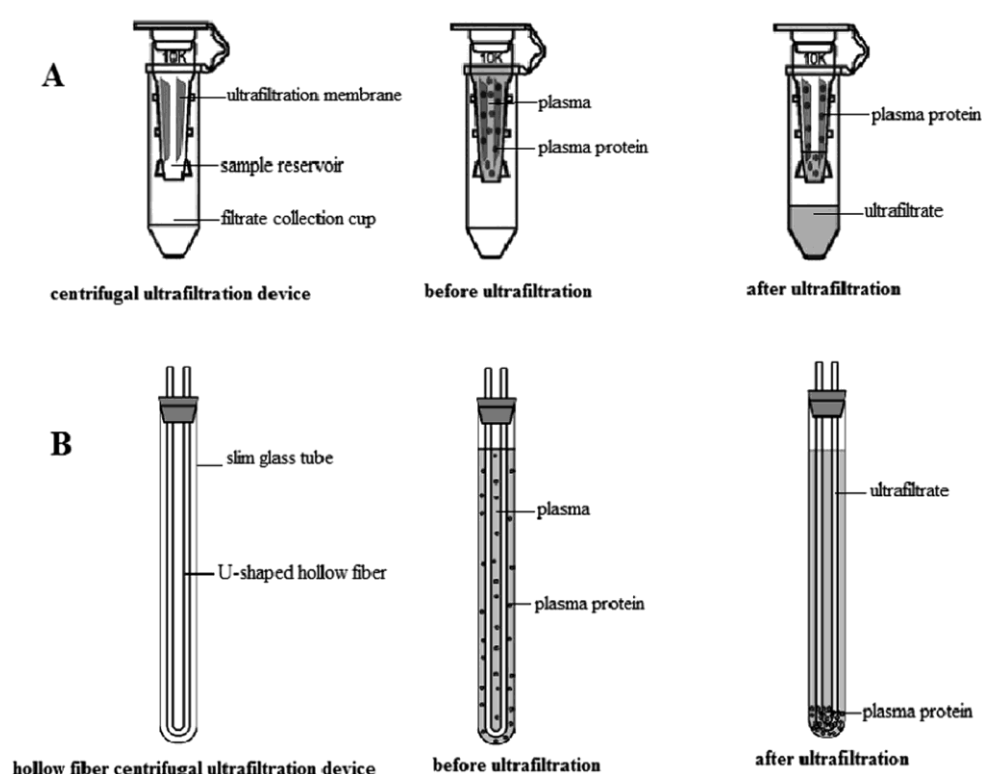


Fig 18: Schematic of the ultrafiltration process (Ref: Schematic of the ultrafiltration bing.com/images)

Analysis of the collected filtrate provides the unbound drug concentration while analysis of the original plasma (or surrogate matrix) provides the total concentration. The main advantage of using ultrafiltration is its speed, taking minutes to prepare the filtrate. However, the major disadvantage is the problem of non-specific binding to the tubes and filter bed (Lee, Mower et al. 2003). Excessive nonspecific binding leads to an underestimation of the fraction unbound and increases the need for a more sensitive detection instrument. In order to test whether nonspecific binding is an issue, it is necessary to conduct a preliminary experiment using drug-spiked phosphate buffered saline (PBS), as a surrogate for the extracellular fluid composition. Following ultracentrifugation, the concentrations can be compared between the original PBS solution and the filtered PBS.

The calculated recovery gives an indication whether nonspecific binding is significant enough to require correction of the final plasma protein binding calculations, or if an alternative method is more appropriate. A technique used to limit nonspecific binding is to passivate the filtration device by pre-treatment with 5% Tween 80 (TW 80) or 5% benzalkonium chloride (Lee, Mower et al. 2003), which blocks the binding sites on the ultrafiltration apparatus. Another disadvantage of ultrafiltration is having a low filtrate volume obtained for analysis.

Despite these disadvantages' ultrafiltration is still a widely used method because of its ease of use and speed of the experimental process, especially where compounds are found to be unstable over a short time period.

1.4.3. Immobilised Artificial Membranes

Another method of determining plasma protein binding of drug molecules is using column chromatography that incorporates immobilised artificial membrane (IAM) stationary phase technology. Human serum albumin (HSA) and artificial membrane (phospholipid) are individually immobilised onto a silica bed to form a stationary phase to which the drug binds (Fig 19). This mimics drug partitioning between HSA and tissue membrane respectively, as occurs *in vivo* (Valkó, Nunhuck et al. 2011). Free drug is injected onto the artificial membrane column and undergoes equilibrium between free and retained (via binding interactions) on transit down the column. In theory, higher retention times are quantitatively proportional to the extent of binding to the immobilised protein or lipid. The retention times of a test set of compounds with known % binding is determined, from which a calibration plot of % binding versus retention time can be constructed. The % binding of unknown compounds can then be interpolated from the calibration line as a function of their respective retention time.

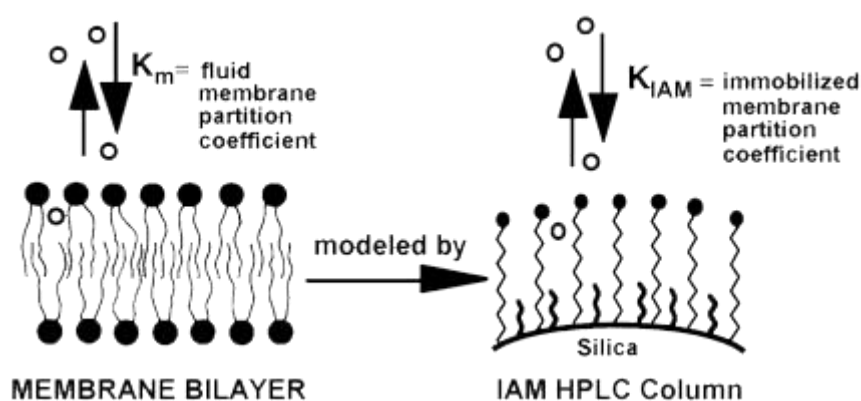


Fig 19: Showing membrane bilayer fused onto a silica backbone: Ref IAM Chromatography Columns, Regis Technologies

The main advantage of this technique is the speed of sample preparation and subsequent bioanalysis. However, the chemistry and composition of immobilised stationary phases may not allow access to all binding sites present in non-immobilised protein/lipid, but also these are very simple systems and replicate the interactions with only one protein/lipid per column. Furthermore, the bound HSA is conformationally modified and thus unable to reflect its natural three-dimensional structure. Although accuracy may be compromised, understanding binding

trends within a chemical series is still useful for Drug Discovery Medicinal Chemists. This is because IAM is a high throughput technique that matches the speed of compound development where potency, selectivity and PK properties are still being optimised.

1.4.4. Equilibrium Dialysis

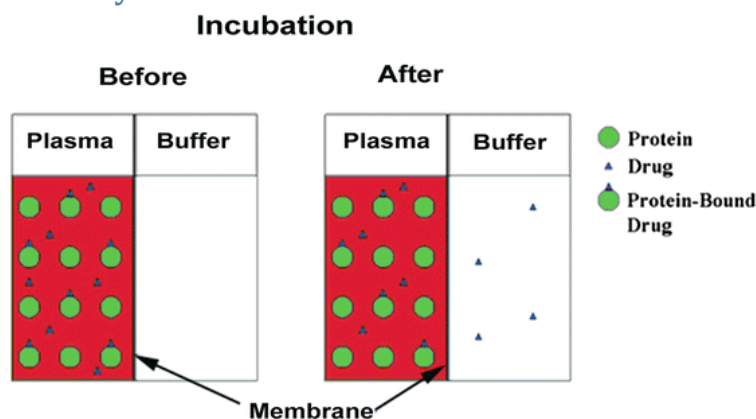


Fig 20: Showing the principal function of an equilibrium dialysis (Mukker, Singh et al. 2016)

In this model, drug molecules move from an initial high concentration in a sample compartment (representing drug bound to plasma or tissue homogenate) through a semi-permeable membrane to a second compartment (representing free drug). Like microdialysis, passive diffusion occurs according to Fick's First Law and is the principle on which equilibrium dialysis is based. At steady-state the unbound concentrations will be equivalent on both sides of the membrane and any nonspecific binding will also be equilibrated. Although described as the gold standard of measuring *in vitro* plasma protein binding, the major disadvantage of equilibrium dialysis is the time to reach equilibrium, which can vary between 6 to 24 hr (Taylor and Harker 2006), ((Buchanan and Eyberg 1974). Because of the time component, it is important to consider analyte stability to enzymes present in the biofluid under test.

The Rapid Equilibrium Dialysis (RED) approach was developed by Pierce Technologies and offers reduced equilibrium times of up 100 min with vigorous agitation, 3 to 4 hr with 200 rpm agitation and capability for automation as a high throughput screening system. The RED device consists of a Teflon base plate capable of holding 48 dialysis cells, each consisting of two side-by-side chambers separated *via* a vertical membrane and having a high surface to volume ratio and a molecular weight cut-off of 8kDa (Waters, Jones et al. 2008). This original RED device allows for drug partition to a single biofluid but does not adequately reflect the *in vivo* situation where drug partitions to multiple organs in parallel.

1.4.5. Competitive Rapid Equilibrium Dialysis (CRED)



Fig 21: Competitive Rapid Equilibrium Dialysis with multiple compartments

CRED is proposed to be the next generation of equilibrium dialysis device by enabling drug distribution to multiple biofluids and tissue homogenates in parallel. The base plate consists of compartmentalised chambers, which unlike the previous RED device, allows for the simultaneous analysis of drug interactions between multiple tissues. There are 4 different types of compartment designs; 4, 6, 8 and 16 (recommended sample volumes of 1.5, 2.5, 3.0 and 5.0mL respectively) capable of holding 2, 3, 4 and 8 dual inserts, respectively. Theoretically, CRED allows for the conduct of partition studies using 2-15 tissue homogenates and/or biofluids in concert. The selection of compartment geometry depends on the experimental study design. The re-usable base plate is in a standard 96-well format and is composed of chemically inert high-grade polytetrafluoroethylene (PTFE), which eliminates nonspecific binding and the risk of contamination. The CRED inserts consist of either one (single insert) or two (dual insert) dialysis chambers. The open end of the single insert provides a sampling site from the compartment without the need for disassembling. The molecular weight cut-off of the cellulose membrane is 12KDa. A base plate lid securely holds the inserts in place and allows for direct sampling from the top.

1.4.6. Aims and Objectives

- Validating a simple model of the competitive Rapid Equilibrium Dialysis
- Feasibility of the Competitive Rapid Equilibrium Dialysis in the Reduction, Refinement and Replacement of Animals in Scientific testing (3Rs)

- An Investigation into Increasing the Throughput of PPB using RapidSeparation Technology
- Competitive Rapid Equilibrium Dialysis Its Application in Liposome Technology: Proof of Concept

Chapter 2: Validating a Simple Model of the Competitive Rapid Equilibrium Dialysis

2.1. Creating an *in-vitro* Drug Distribution System using Surrogate Matrices

2.1.1. Introduction

In the *in vivo* environment, drug molecules may bind to protein and lipids in plasma, extracellular fluid or in tissues. It is the affinity of the drug for these proteins or lipids that dictates the extent of drug binding (Yata, Toyoda et al. 1990, Ghuman, Zunszain et al. 2005, Rodgers, Leahy et al. 2005). Human serum albumin is the major protein component within plasma whilst tissue cell membranes primarily consist of phospholipids, of which phosphatidylcholine is the major component. Using human serum albumin and phosphatidylcholine as competitive surrogate determinants to evaluate the extent of drug binding *in-vitro* therefore offers a mirror of *in-vivo* drug distribution (Dimitrova, Matsumura et al. 2000).

2.1.2. Tissue Composition with Respect to Drug Binding

Phospholipids play a very important role in cell permeability of exogenous as well as endogenous molecules through the formation of lipid bilayers around cell surfaces which can affect the pharmacokinetics of drug molecules (Dowhan 1994). Phosphatidylcholine (Fig 22) is the most abundant phospholipid in the cell membrane of tissues and accounts for nearly 60% of the overall phospholipid content. Across different organ tissues, phosphatidylcholine composition also varies (Choi, Yin et al. 2018) e.g. 55% of total phospholipid composition in rat liver compared to 39% in heart (Christie 1985). In this thesis, the relative amount of phosphatidylcholine in animal organ tissues was assumed to be the same in human. Phosphatidylcholine prepared at different concentrations in phosphate buffer were used to provide a physiologically relevant tissue surrogate for use in the CRED device. Phosphatidylserine, phosphatidylethanolamine, phosphatidylinositol are the other key components of lipid bilayers, but as they are present in much lower quantities, they were not investigated. Our hypothesis was that phosphatidylcholine micelles could act as a tissue surrogate to provide an assessment of drug molecule competitive binding (and hence distribution) for high throughput screening.

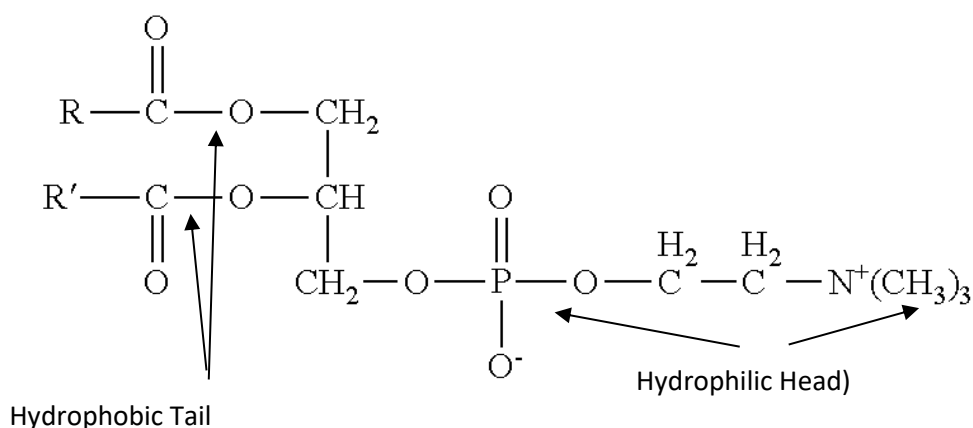


Fig 22. Structure of Phosphatidylcholine where R and R¹ represent acyl carbon chains

2.1.3. Plasma Composition with Respect to Drug Binding

Human plasma contains several types of proteins, including human serum albumin (HSA), alpha-1-acid glycoprotein, globulins, lipoprotein and fibrinogen in different concentrations. Human serum albumin is, however, the most abundant protein in plasma with a concentration of approximately 50g/l (molecular weight 66KDa) (Zhang, Xue et al. 2012) and therefore contributes significantly to plasma protein binding. The role and importance of HSA as a transporter molecule has been extensively studied (Curry 2002). The structure of HSA consists of three main domains for drug binding; i.e. Sudlows I, II and III sites (Figure 23), which are further divided in subdomains A and B (IA and 1B, IIA and IIB, and IIIA, IIIB) and provide high affinity binding sites for exogenous and endogenous drugs (Ascenzi, Di Masi et al. 2015). These high affinity binding sites overlap with endogenous ligand-binding sites with affinity driven by the shape and the distribution of basic and polar residues on the hydrophobic walls of HSA. Charge neutralization and hydrogen bonding of acidic or polar electronegative small molecule ligands (anionic compounds) therefore occurs preferentially (Ghuman, Zunszain et al. 2005). The high concentration of HSA with its multiple binding sites for various ligands underpins its importance in the pharmacokinetics of many drugs (Fasano, Curry et al. 2005) and makes HSA the most pertinent protein for performing high throughput *in vitro* drug partitioning experiments. HSA dissolved in phosphate buffer provides the ideal physiologically relevant plasma surrogate to mimic plasma protein binding *in vivo*.

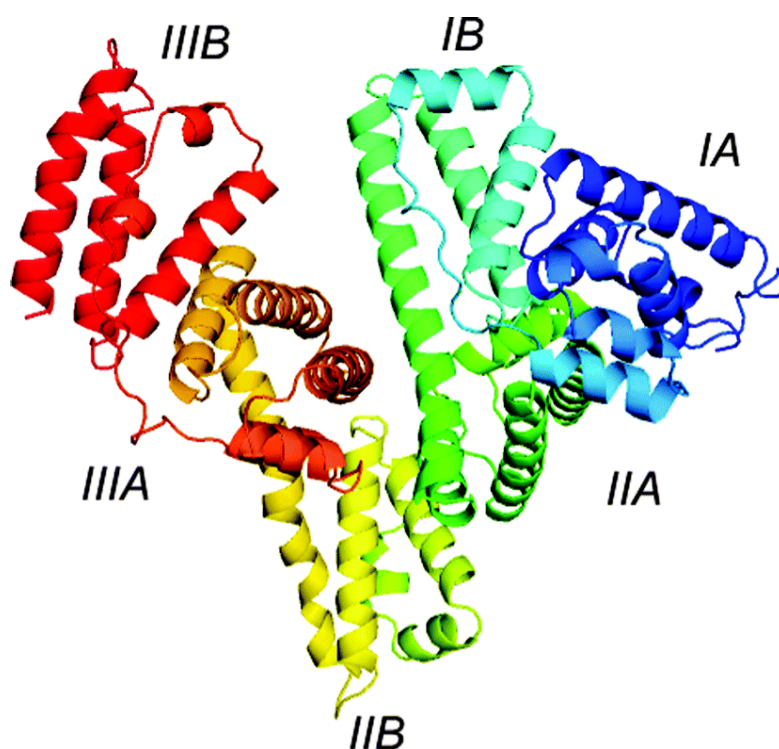


Fig 23. Helical structure of Human Serum Albumin

2.2. Factors Affecting Plasma Protein Binding Using Equilibrium Dialysis

2.2.1. Membrane Permeability

Partition membranes used in plasma protein binding experiments work as filters that selectively permit the passage of certain molecules whilst excluding the passage of others. The membrane inserts used in the CRED device consist of a vertical cellulose membrane with a molecular weight cut-off of 12kDa. A diffusion gradient facilitates the passage of the analytes of interest through the membrane from a high concentration (drug spiked in human serum albumin) to the tissues surrogates (unspiked phosphatidylcholine) and unspiked phosphate buffer saline according to Fick's 1st Law of mass transfer (Seddon, Casey et al. 2009). HSA has a molecular weight of approximately 66.5kDa and will therefore not cross the membrane. Phosphatidylcholine (lecithin) aggregates or micelles (31Kda) should also not be able to traverse the membrane (Asano, Izumi et al. 1993, Dua, Rana et al. 2012), otherwise their transfer in the phosphate buffer would lead to an overestimation of the unbound drug concentration in the buffer compartment (representing extracellular fluid). The CRED device inserts are also plugged at the non-sampling end and need careful handling so as not to create pockets through which volume shifts and hence liquid transfer can occur from one compartment to the next.

2.2.2. Time to Equilibrium

Within the multiplex format of the CRED device there is competition for binding of drug molecules to phosphatidylcholine (tissue surrogate) and human serum albumin (plasma surrogate). During the incubation period, drug partitions (diffuses) through the cellulose membrane from a high concentration (analyte spiked into human serum albumin only) to the lower concentration compartments (control tissue surrogates and phosphate buffer). Dynamic equilibrium or steady state is reached when the net flux or mass transfer over time through the cellulose membrane becomes zero i.e., when the total concentration (free and bound) within each tissue or plasma surrogate is maximised. The time at which steady-state is achieved is referred to as time-to-equilibrium and may vary under different conditions. It is therefore important that all the variables are well controlled and characterised including the concentrations of matrices used, the drug concentration, the incubation temperature, pH, buffer composition and the rate of shaking (Banker, Clark et al. 2003).

2.2.3. Stability of Compounds during Binding Studies

In order to provide physiologically meaningful data, it is important to establish ligand stability either during or prior to the incubation period. The analyte of interest should remain stable in the respective matrices used in the CRED device at the incubation temperature (37°C) and pH over the entire incubation period (minimum 6 hr). An acceptance criterion of $\pm 20\%$ was adopted based on department working practice for non-regulated experiments. This ensures that final drug concentrations in the respective compartments of the CRED device are not biased by ongoing degradation.

2.3 Methods and Experimental Procedures

2.3.1 Compound Selection, Reagents, and Instrumentation

The compounds (Table 2) were selected across acidic, basic and neutral series based on human serum albumin binding data obtained from the GSK repository KATE (Knowledgebase of Assays, Tests and Experiments). These compounds represent drugs marketed by GSK and other pharmaceutical companies as well as drugs in early discovery and development. Within each series a range of previously defined human serum albumin binding data obtained using HSA column chromatography conducted within GSK were selected. The plasma protein binding data obtained using the CRED device was used to calculate the volume of distribution at steady state (VD_{ss}). Comparison was then made between the volume of distribution and human serum albumin data obtained using the CRED device, column chromatography (Physchem Group) and observed literature values (for data that was found) for the series of compounds under investigation. Human serum albumin binding was determined and compared for a further 8 new chemical entities in parallel using both HSA column chromatography and CRED techniques to determine the correlation coefficient.

2.3.2. Reagents

Selected compounds across acidic, basic, and neutral series (Table 2) were ordered from the GSK compound Store (Harlow) and were received in a plate format as 150µL solutions

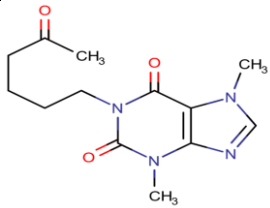
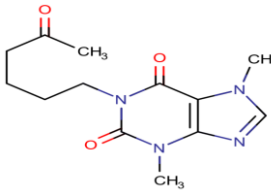
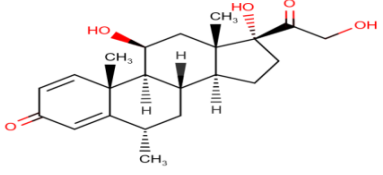
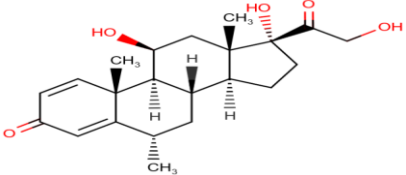
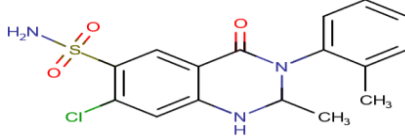
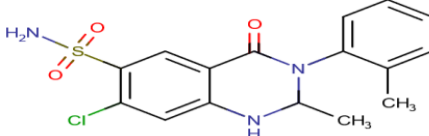
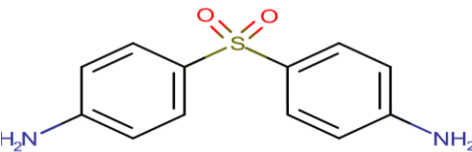
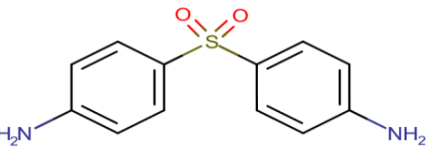
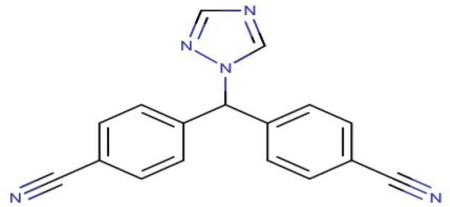
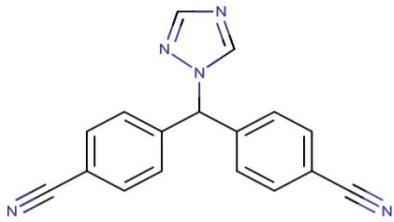
dissolved in DMSO at a concentration of 10mM, stored in a -80°C freezer. FeSSIF powder was purchased from Biorelevant.com (42 New Road London E1 2AX, United Kingdom). When dissolved in an aqueous medium (phosphate buffer) the FeSSIF powder, which also contains sodium taurocholate provides a physiologically relevant medium with a high concentration of phosphatidylcholine micelles to mimic tissues *in-vivo*. HSA lyophilized powder >= 97%, HPLC grade methanol, acetonitrile, propanol and ammonium formate were purchased from Sigma Aldrich (The Old Brickyard, New Road, Gillingham, Dorset, UK). PBS tablets and 1.4mL Micronics were obtained from Gibco-life technologies, Thermo Scientific (Stafford House, 1 Boundary Park, Hemel Hempstead, UK). Polypropylene graduated tubes (1.5 -1.7mL and 15 mL) were purchased from Fisher Scientific (Bishop Meadow Road, Loughborough, UK).

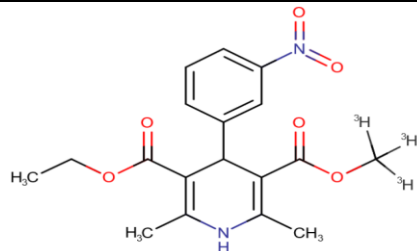
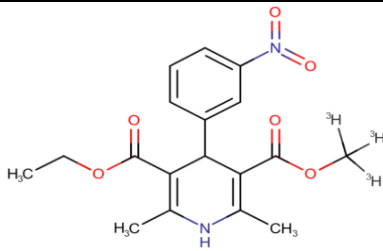
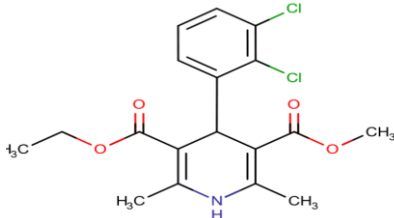
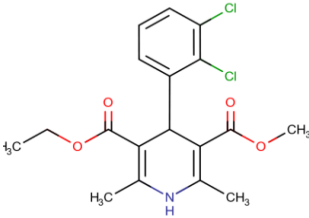
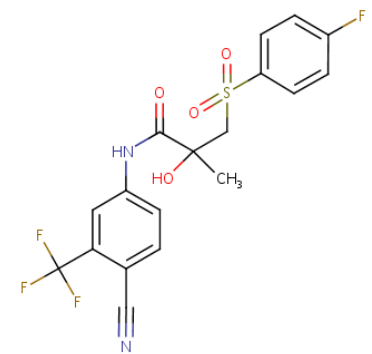
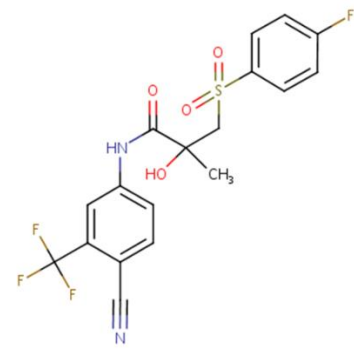
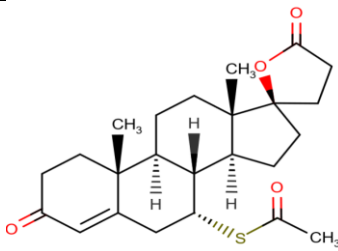
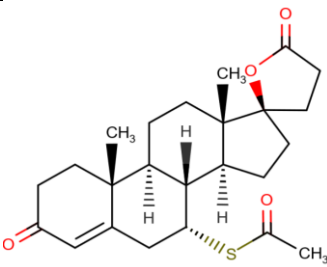
Table 2: Original Set of Compounds selected for evaluation using the CRED device. **Acids, bases, neutrals and zwitterions are depicted by red, green, blue and purple colour code respectively**

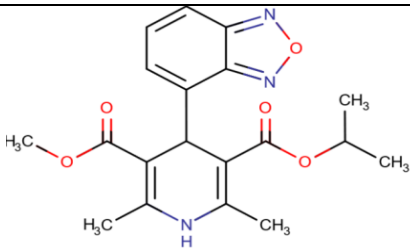
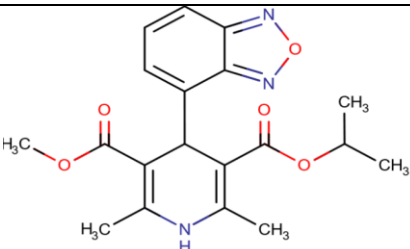
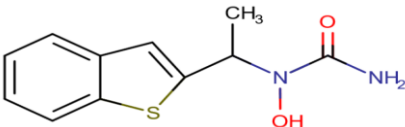
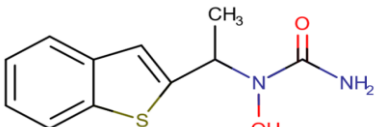
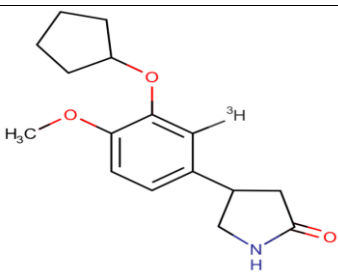
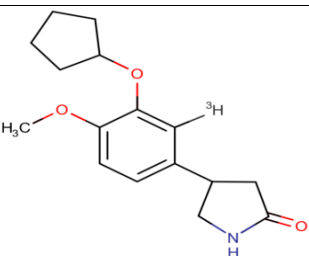
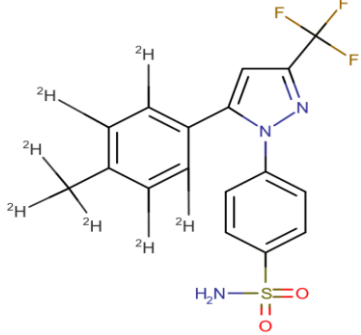
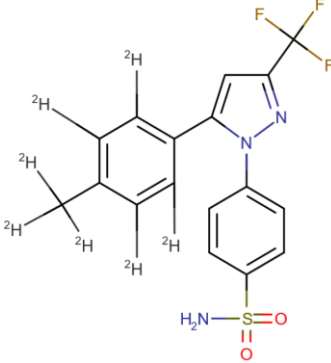
Compounds			
Acid	Base	Neutral	Zwitterion
CCI6817	CCI3993	GR91295X	GR99941A
GR62550X	SB731710	CC19371	GW300671A
GR87272X	CCI3748	CC122428	
GR138714X	GR30676X	GR104104X	
GR70487A	SKF95914	GF120403X	
CCI23760	GR189721X	GR78367X	
CCI120	GR192446A	GI115674X	
GR33000X	GR43175X	AH23463X	
BRL15541Q	GF120454X	GR33914X	
GW289865X	SB416332AA	GR38393X	
SB213421-Z	CC13839	GW388185X	
GI235401X	GR61317X	GR119497X	
CCI133	GR183544X	GW703803X	
GSK275458A	GW769340A	GR64334X	
GR118989X	CCI120557A	GI116108X	
AH22182X	CCI4001	GI99296X	
GR87036X	GR84804A		
GW622791X	GW787034X		
	GR77494A		
	GR35842A		

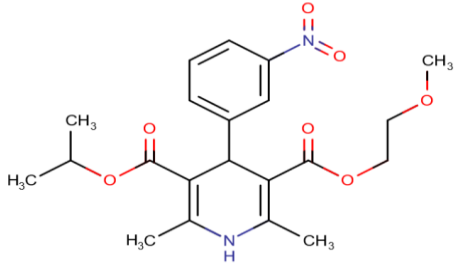
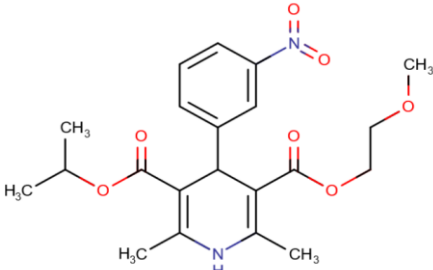
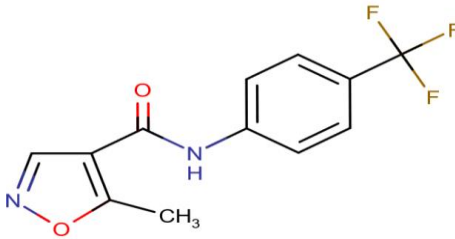
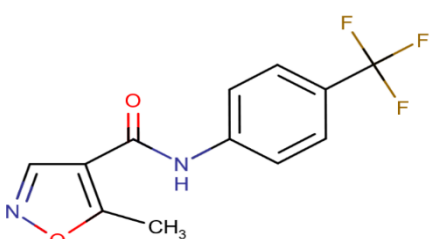
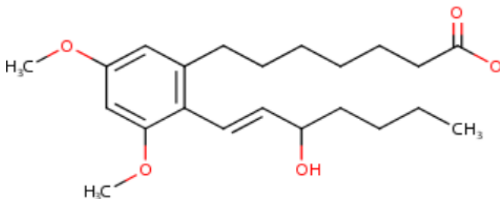
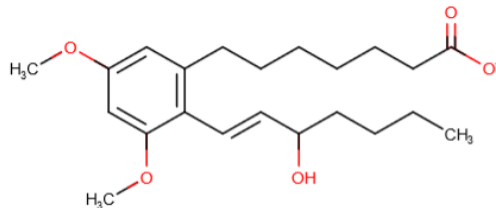
2.3.3. Physicochemical Properties and Structures of Tool Compounds.

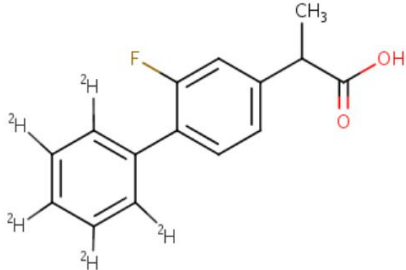
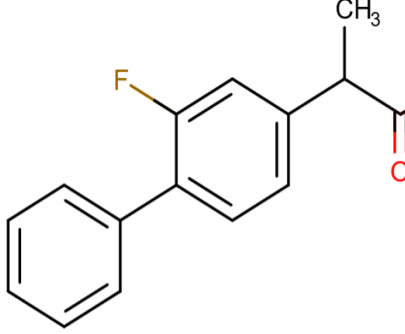
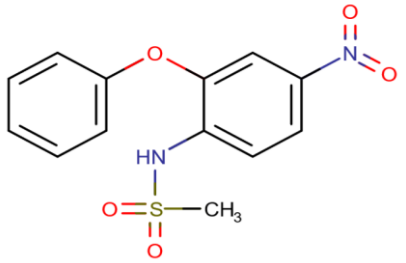
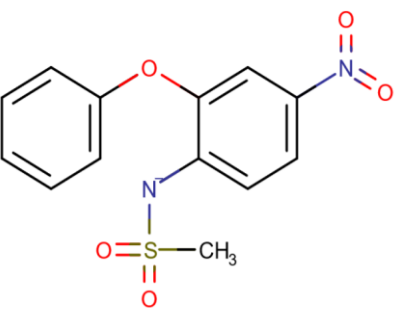
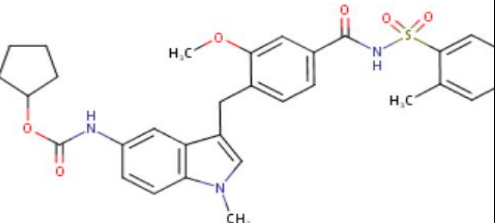
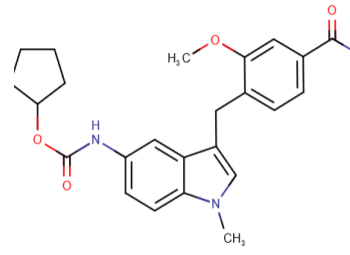
The structures and physicochemical properties of the compounds investigated were obtained using in house software packages Helium and Plexus Suite. The structures show the major microspecies at pH 7.4. The physchem descriptors Total Polar Surface Area (TPSA), Hydrogen Bond acceptor, Hydrogen Bond Donor and Lipophilicity (clogP and cLogD) will be used to evaluate the impact of the trend analysis with respect to Volume of Distribution at steady state (VDss).

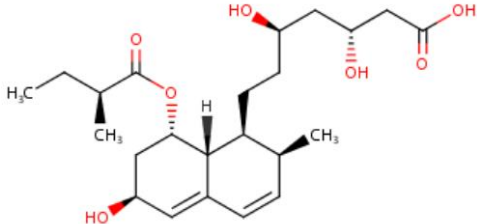
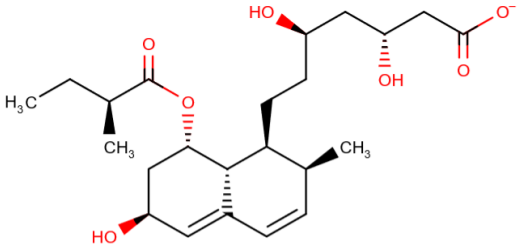
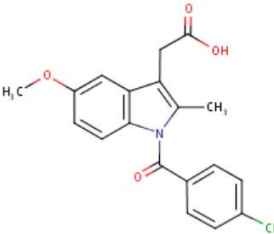
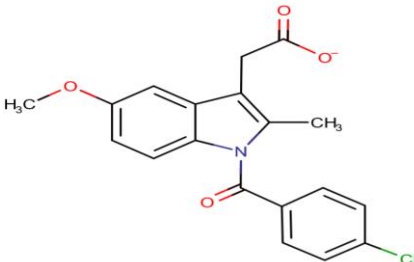
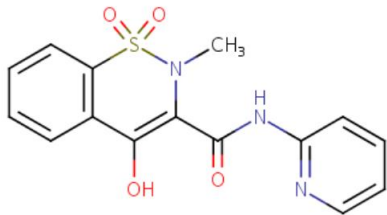
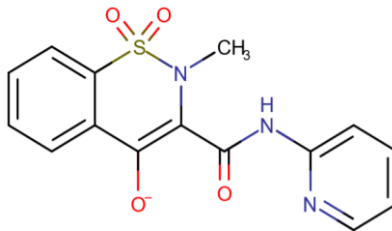
Compound	Compound Number	Structure	pKa	LogD	LogP	HBD	HBA	TPSA	Micro Species 1 at pH 7.4
GR91295	1		-1.2	0.1	0.13	7	0	75.5	
CCI22428	2		12.6	1.88	1.88	5	3	94.8	
GF120403	3		9.5	2.9	2.9	6	2	92.5	
AH23463	4		2.39	1.3	1.31	4	2	86.2	
GR119497	5		1.89	2.8	2.76	5	0	78.3	

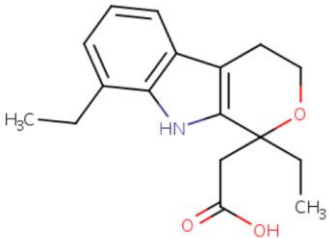
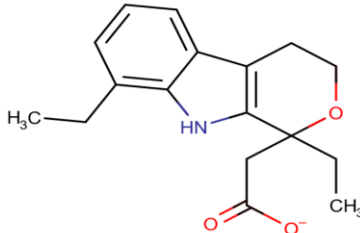
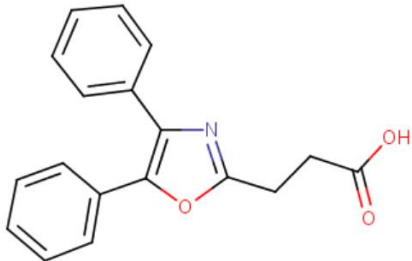
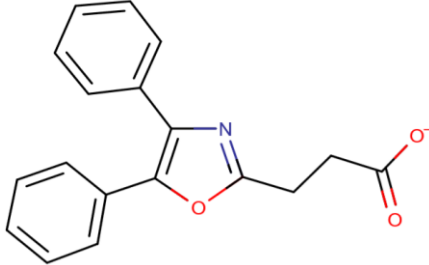
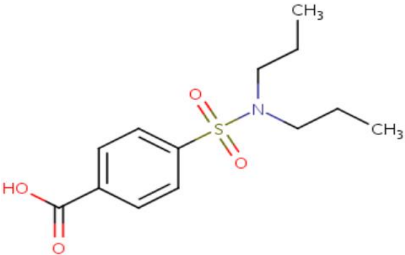
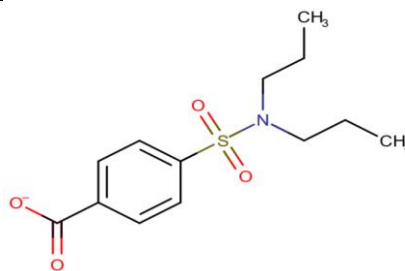
Compound	Compound Number	Structure	pKa	LogD	LogP	HBD	HBA	TPSA	Micro Species 1 at pH 7.4
GR38393	6		N/A	2.0	1.98	8	1	110.5	
GR64334	7		n/a	3.1	3.07	5	1	64.6	
GW708803	8		11.8	2.52	2.52	2	9	107.3	
CCI9371	9		No further microspecies	3.4	3.44	4	0	60.4	

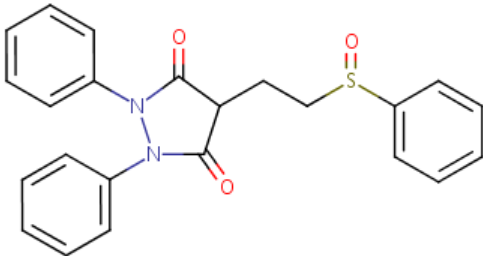
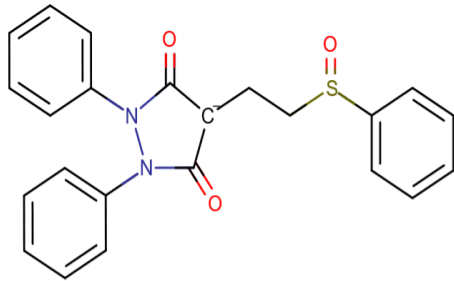
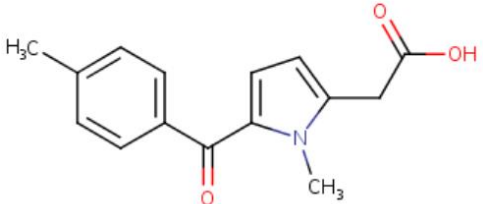
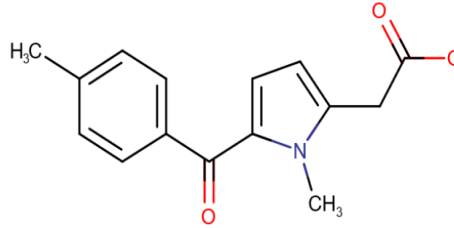
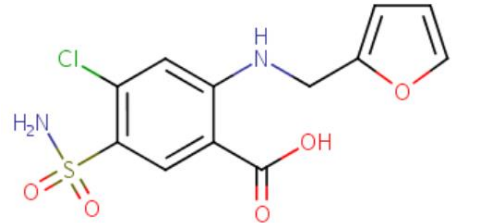
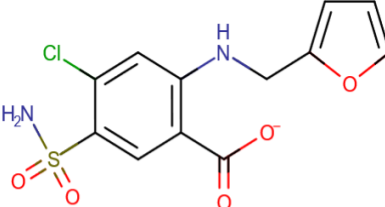
Compound	Compound Number	Structure	pKa	LogD	LogP	HBD	HBA	TPSA	Micro Species 1 at pH 7.4
GI116108	10		No further microspecies	2.1	2.07	8	1	103.6	
GR104104	11		8.84	1.8	1.82	4	2	66.6	
GI115674	12		n/a	1.69	1.66	4	1	47.6	
GW388185	13		10.6	3.8	3.83	5	1	77.9	

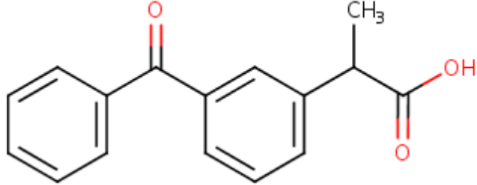
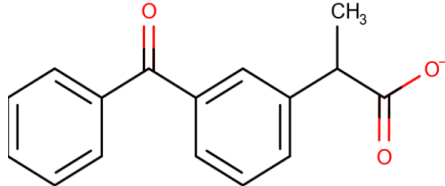
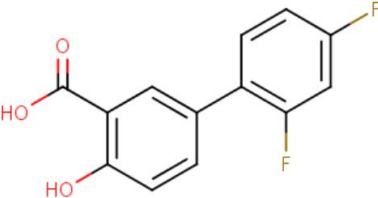
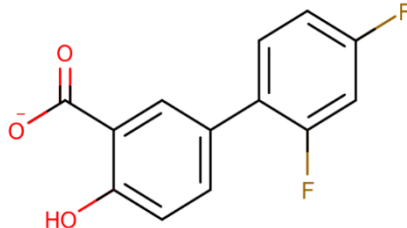
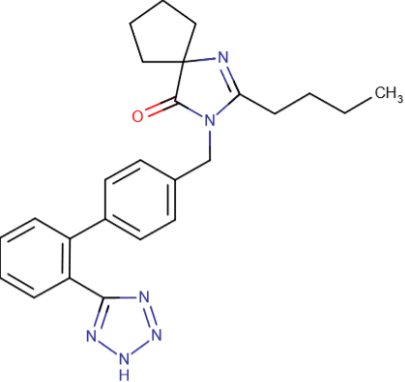
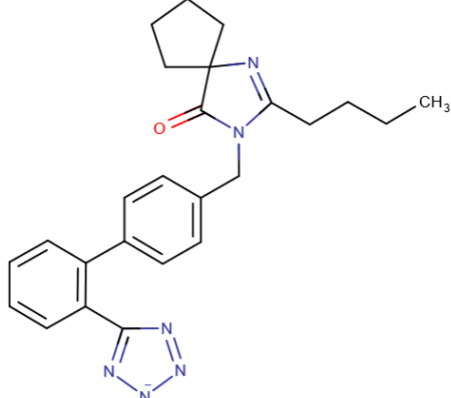
Compound	Compound Number	Structure	pKa	LogD	LogP	HBD	HBA	TPSA	Micro Species 1 at pH 7.4
GR33914	14		n/a	2.2	2.23	0	1	119.7	
GI99296	15		n/a	2.5	2.5	4	1	55.1	
CCI16817	16		4.31	1.8	4.77	5	2	78.8	

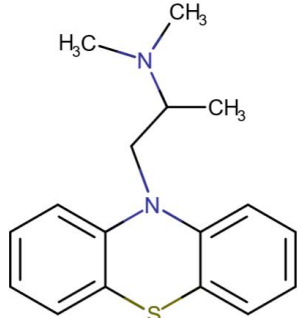
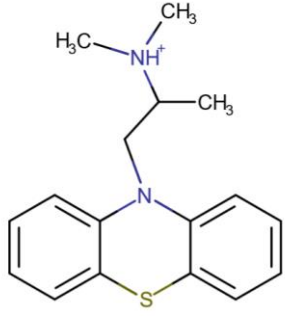
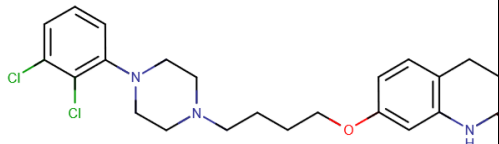
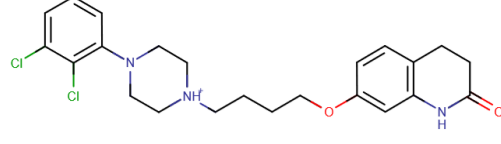
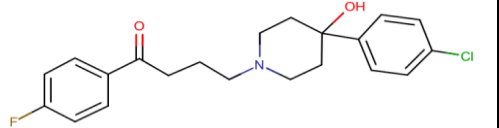
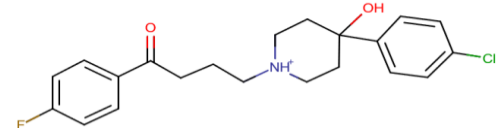
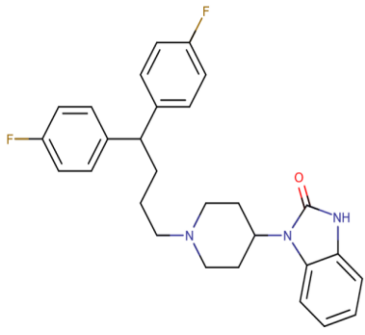
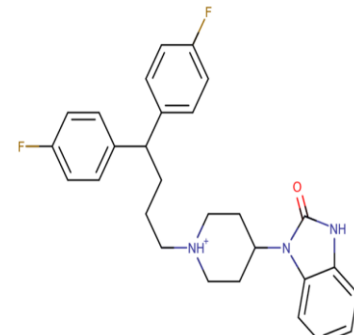
Compound	Compound Number	Structure	pKa	LogD	LogP	HBD	HBA	TPSA	Micro Species 1 at pH 7.4
GR62550	17		4.42	1.2	4.06	2	1	40.1	
GR87272	18		6.86	1.4	1.94	7	1	98.4	
GR138714	19		4.29	5.1	6.19	9	2	112.9	

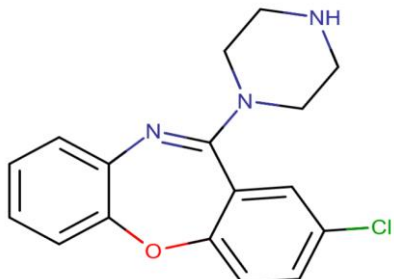
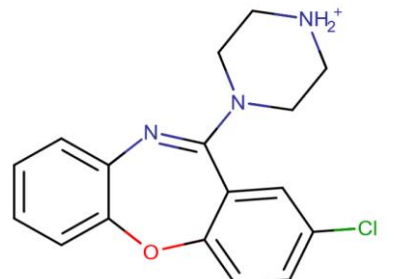
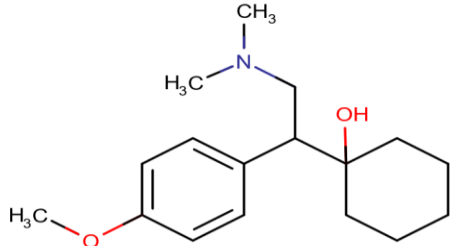
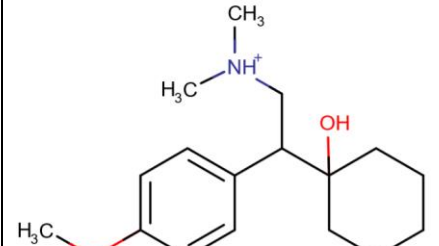
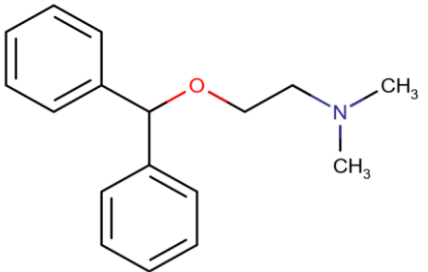
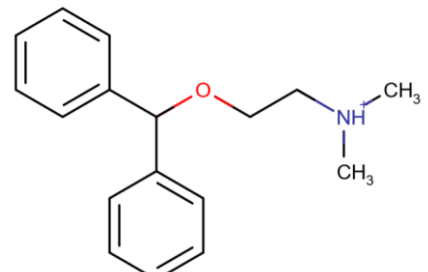
Compound	Compound Number	Structure	pKa	LogD	LogP	HBD	HBA	TPSA	Micro Species 1 at pH 7.4
GR70487	20		4.21	-1.8	1.27	7	4	127.1	
CCI120	21		3.79	0.0	3.31	5	1	71.4	
GR33000	22		4.8	-0.5	1.02	7	2	102.4	

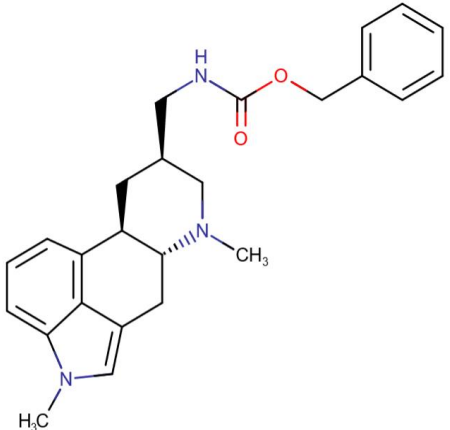
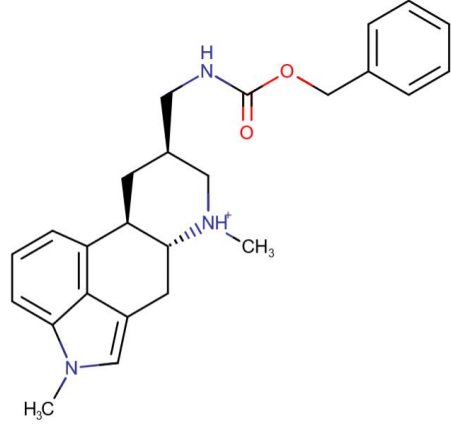
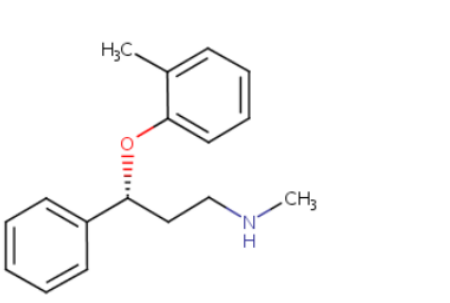
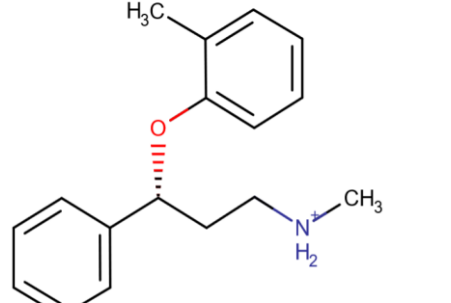
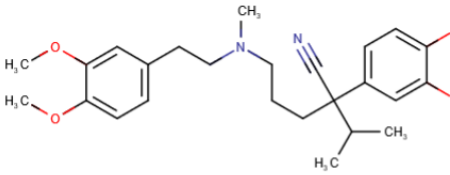
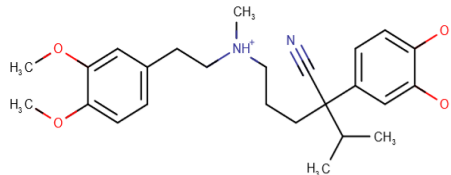
Compound	Compound Number	Structure	pKa	LogD	LogP	HBD	HBA	TPSA	Micro Species 1 at pH 7.4
GW289865	23		4.7	0.2	2.84	4	2	65.2	
GSK275458	24		4.95	1.1	3.54	4	1	66.2	
GR87036	25		3.53	-1.2	2.31	5	1	77.5	

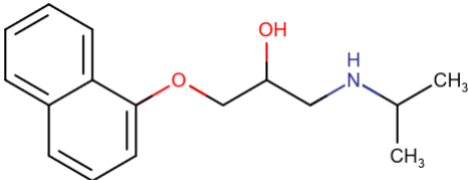
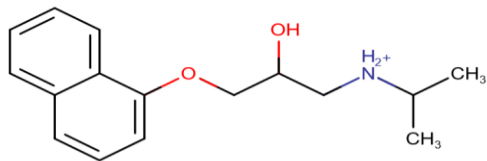
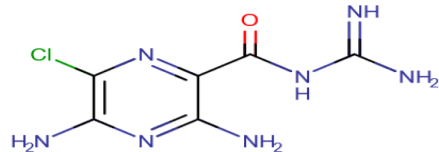
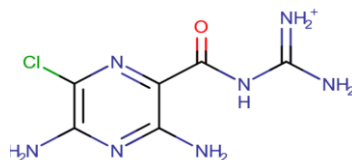
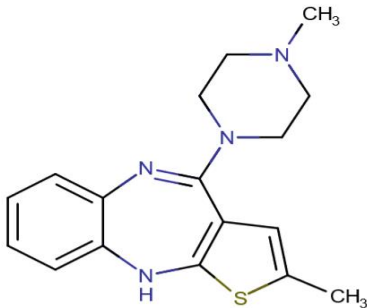
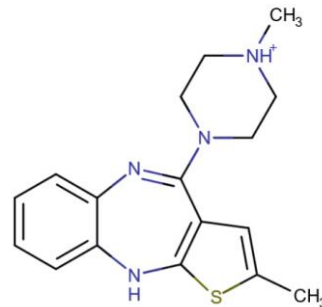
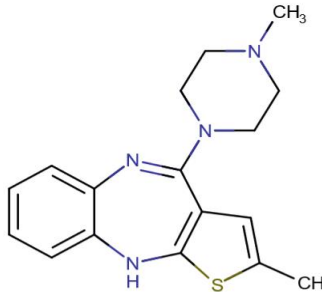
Compound	Compound Number	Structure	pKa	LogD	LogP	HBD	HBA	TPSA	Micro Species 1 at pH 7.4
AH22182	26		3.86, 12.86	1.2	3.3	5	0	57.7	
SB-213421	27		3.93	-1.1	2.15	4	1	62.1	
GR118989	28		4.25	-1.4	1.66	7	3	125.5	

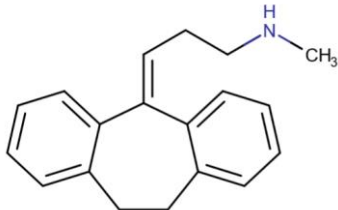
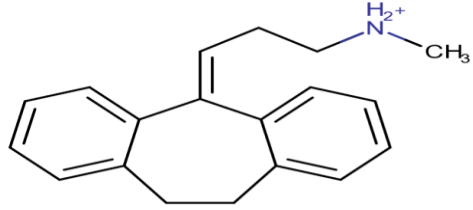
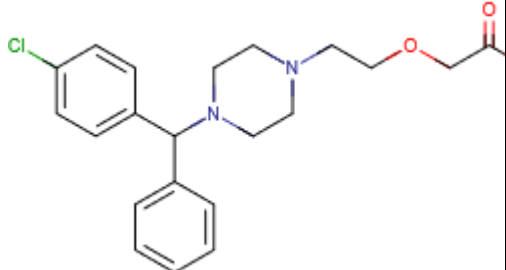
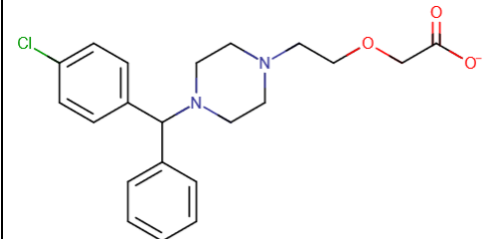
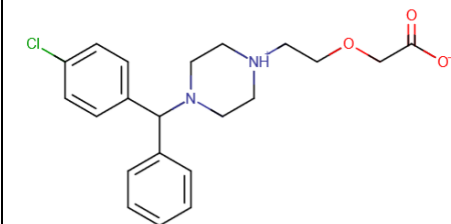
Compound	Compound Number	Structure	pKa	LogD	LogP	HBD	HBA	TPSA	Micro Species 1 at pH 7.4
BRL15541Q	29		3.88	0.2	2.76	3	1	57.2	
GI235401	30		2.69	0.2	3.89	3	2	60.4	
GW622791	31		4.12	3.2	5.74	7	1	84.2	

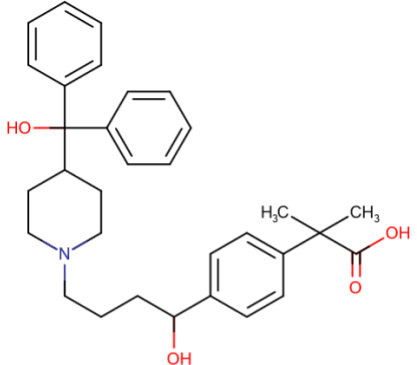
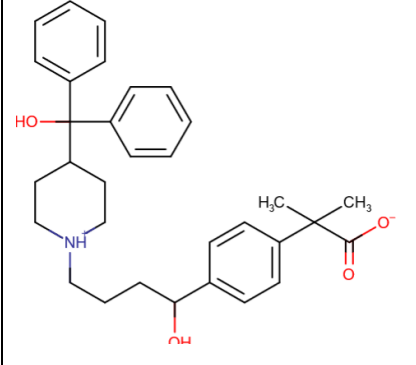
Compound	Compound Number	Structure	pKa	LogD	LogP	HBD	HBA	TPSA	Micro Species 1 at pH 7.4
CCI3993	32		9.05	2.7	4.4	11	4	150.9	
SB-731710	33		13.5	4.5	4.79	5	1	46.0	
CCI3748	34		13.9	2.3	3.08	3	1	41.7	
GR30676	35		12.9	5.4	6.4	4	1	36.8	

Compound	Compound Number	Structure	pKa	LogD	LogP	HBD	HBA	TPSA	Micro Species 1 at pH 7.4
GF120454	39		8.83	1.8	3.2	4	1	41.4	
SB-416332-AAA	40		8.91	0.7	2.25	3	1	33.9	
CCI3839	41		8.9	2.1	3.62	2	0	13.7	

Compound	Compound Number	Structure	pKa	LogD	LogP	HBD	HBA	TPSA	Micro Species 1 at pH 7.4
GR61317	42		8.22	3.2	4.08	5	1	47.7	
GW769340A	43		9.8	1.4	3.78	2	1	25.8	
CCI20557	44		8.7	2.3	4.55	6	0	65.2	

Compound	Compound Number	Structure	pKa	LogD	LogP	HBD	HBA	TPSA	Micro Species 1 at pH 7.4
CCI4001	45		9.7	0.2	2.5	3	2	46.1	
GR77494	46		11.4	-0.4	0.0	8	5	158.5	
GR189721	47		7.24	2.9	3.09	4	1	32.1	<p>Microspecies 3 at 41%</p>  <p>Microspecies 1 at 59%</p> 

Compound	Compound Number	Structure	pKa	LogD	LogP	HBD	HBA	TPSA	Micro Species 1 at pH 7.4
GR84804	48		10.5	1.6	4.57	1	1	16.6	
GR99941	49		3.59	0.2	3.48	1	5	57.04	<p>MICROSPECIES 1</p>  <p>MICROSPECIES2</p> 

Compound	Compound Number	Structure	pKa	LogD	LogP	HBD	HBA	TPSA	Micro Species 1 at pH 7.4
GW300671	50		4.04	2.5	5.68	3	5	85.03	

2.3.4. Instrumentation

The Competitive Rapid Equilibrium Dialysis was purchased from Thermo Scientific (Stafford House, 1 Boundary Park, Hemel Hempstead, UK), comprising base plates made of high-grade polytetrafluoroethylene (PTFE), 50 pack of dual inserts comprising (40 dual membrane and 10 single membrane inserts with molecular weight cut-off (MWCO) of 12KDa). Stuart microlite plate shaker SSM5 with high-speed vibrational mixing for four plates simultaneously and a variable agitation speed (250 to 1,250 rpm). Eppendorf Centrifuge 5810R: high centrifugation speed of up to $20,913 \times g$ (14,000 rpm) and temperature range from -9 °C to 40 °C.

2.3.5. Matrix Effects

The analysis of biological samples using mass spectrometry (MS) results not only in the ionization of the analyte of interest but also of the biological components within the complex matrix. The ions produced from the endogenous matrix components compete with the analyte ions for charge and space. This may result in lower analyte signal or ion suppression (Jessome and Volmer 2006). Where the concentrations of the biological components are high this may also result in the saturation of the MS detector leading to reduced analyte signal. Ion suppression can therefore affect reproducibility, linearity, bias and precision and is therefore of major concern in mass spectroscopy. There are several ways to reduce or eliminate ion suppression such as solid phase extraction for sample clean-up and gradient modification to prevent coelution of analyte of interest with endogenous sample components. Differences in the concentration and type of matrices used simultaneously in the six well compartment of the CRED device may result in matrix and ion suppression effects leading to inaccurate and unreliable data comparison of the drug affinity binding properties. To normalise the matrix and ion suppression effects post incubation, the overall sample composition needs to be equal for all samples prior to extraction or alternatively read from individually constructed calibration curves. This ensures accurate comparison and validity of data generated. The matrix “total matrix match” used for the preparation of calibration samples is made by pooling equal volumes of 1% (w/v) phosphate buffer, human serum albumin at 50 g/L and phosphatidylcholine at 25.5 mg/10mL (PC1), 50.9 mg/10mL (PC2) and 76.4 mg/10mL(PC3), respectively. Post incubation, a specific matrix “partial matrix match” is added to the samples aliquoted from the dialysis based on its composition to create a sample matrix that is identical to the “total matrix match” used in the preparation of calibrants. This normalises the matrix and ion suppression effects between sample aliquots from the dialysis and the calibration samples. For normalising matrix, the sequence below was applied.

- For 10µl 1% (w/v) phosphate buffer aliquot added to 40µl “partial matrix match” made from a pool of equal volumes of (control HSA+ control PC1 +control PC2 +control PC3)
- For 10µl HSA aliquot added to 40µl “partial matrix match” made from a pool of equal volumes of (control Buffer+ PC1 + PC2+ PC3)
- For 10µl PC1 sample added to 40µl “partial matrix match” made from a pool of equal volumes of (control HSA+ control Buffer +control PC2+control PC3)
- For 10µl PC2 sample added to 40µl “partial matrix match” made from a pool of equal volumes of (control HSA+ control PC1 +control Buffer+ control PC3)

- For 10µl PC3 sample added to 40µl “partial matrix match” made from a pool of equal volumes of (control HSA+ control PC1 +control Buffer+ control PC2)

2.4. Experiments and Results to Aid Preliminary Assessments:

2.4.1. Membrane Permeability

The efficiency of the cellulose membrane to block the transfer of micelles (phospholipids) was ascertained using known multiple reactions monitor (MRM) transitions for phospholipids (524 to 184, 496 to 184). As a preliminary experiment to test membrane permeability (post incubation), 50µL of buffer and phosphatidylcholine samples were pipetted from the inserts and extracted individually using 200 µL of acetonitrile/methanol/water (ratio 85/10/5) containing an in-house generic internal standard [^2H $^{13}\text{C}_3$]-SB243213. Samples were then briefly mixed and centrifuged for 10 minutes at 3000 rpm, followed by injection onto the HPLC-MS/MS system.

The semi-permeable membrane with a molecular weight cut-off of 12kDa is to prevent the passage of proteins from one compartment to the other. Breakage of the membrane would lead to migration of protein and drug-protein complexes into the buffer. The presence of phosphatidylcholine in the tissue surrogate compartment but absent from the phosphate buffer (Fig 24 (a) and (b)) indicated that the semi-permeable membrane of the CRED inserts prevented the passage of phospholipid between compartments and would therefore provide an accurate and reliable measurement of free drug concentration.

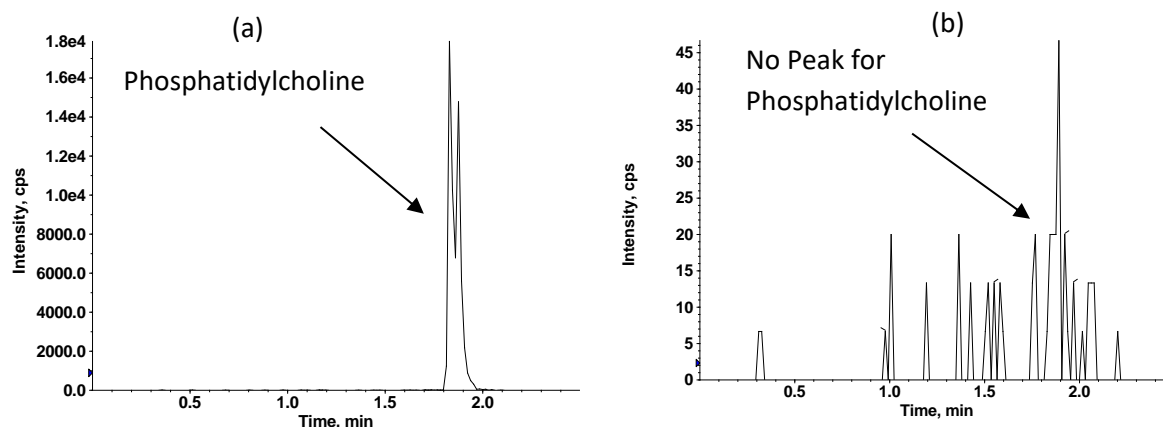


Fig 24: Extracted tissue surrogate and phosphate buffer showing the presence (a) and absence (b) of phosphatidylcholine.

2.4.2. Time to Equilibrium

In order to establish the time to equilibrium, a 20 μL aliquot of stock compound AH23463X (initial concentration of 10 mM) was spiked into 980 μL human serum albumin in order to realise a concentration of 200 μM . This was followed by a 10-fold dilution (300 μL of 200 μM spiked human serum albumin added to 2700 μL control human serum albumin to give a final volume of 3mL. To the 6-well compartment of the CRED device was added 2500 μL of spiked human serum albumin. FeSSIF powder containing phosphatidylcholine was weighed to give 100 mg/10mL and 200 mg/10mL of which 200 μL was added to the CRED inserts placed within the well. The CRED device was placed on a shaker within an incubator set at 37 °C and 20 μL aliquots were taken from the 100 mg/10mL and 200 mg/10 mL weighed FeSSIF powder at 4 hr, 6 hr and 24 hr and extracted using 200 μL of acetonitrile/methanol/water (ratio 85/10/5) containing an in-house generic internal standard [^2H $^{13}\text{C}_3$]-SB243213. Samples were then briefly mixed and centrifuged for 10 minutes at 3000 rpm and injected onto the HPLC-MS/MS. Analyte peak area was plotted against time to give an indication of time to equilibrium.

A plot of the analyte peak area of compound AH23463X incubated at 37°C with time (Fig 25) indicates that the mean analyte peak area increased by between 8.0% and 5.4% between 6 and 24h, for aliquots taken from the 100 mg/10mL and 200 mg/10 mL, respectively i.e., approximately 0.4% change every hour (Table 3). The minimal change in analyte peak area after 6 hr led to the minimum time-to-equilibrium using the CRED device system being set at 6h for the series of compounds under investigation.

Table 3: Variation of analyte peak area over time during incubation at 37 °C

Time (h)	Analyte Peak Area (100 mg/10 mL)	Analyte Peak Area (200 mg/10 mL)
4	88470.8	110806.9
6	1126484.4	1290018.1
24	1216640.2	1362824.9

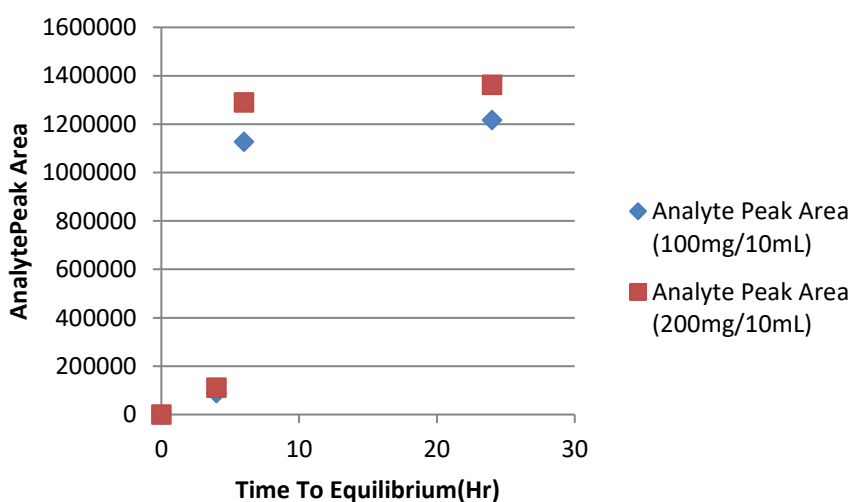


Fig 25: Plot of analyte peak area versus sampling time during incubation

2.4.3. Stability of Compounds during Binding Studies

To assess compound degradation across the compound series (acids, bases and neutrals), 2µL aliquots of each analyte (10 mM stock solutions) were spiked into 998µL of HSA (50 g/L) and 1% phosphate buffered saline (PBS) to realise final concentrations of 20 µM. Both matrices were incubated for 5 min in order to attain 37 °C prior to spiking in drug. Aliquots (50µL) were extracted immediately in replicates of 6 and the remainder subjected to incubation for at least 6hr at 37°C. Extraction was performed using 200 µL of acetonitrile/methanol/water (volume ratio 85/10/5) containing an in-house generic internal standard [²H ¹³C₃]-SB243213. Post incubation, replicate samples were extracted and injected onto the HPLC system along with replicates that were immediately extracted upon spiking. The analyte peak area ratio immediately upon spiking (zero hours) was compared to analyte peak area ratio post incubation (six hours) and the percentage difference calculated. In cases where the internal standard response was not consistent the analyte peak area was used to calculate the percentage difference.

Data showing stability of the series of compounds in 1% PBS and in 50 g/L HSA are listed in appendix 1. The percentage difference for basic compounds, SKF95914 and GR43175X in HSA were calculated as -63.2 and 304.9, respectively. The values obtained were attributed to variability in the internal standard at the 6hr sample injections. In PBS, the values obtained were -6.32 and -8.13, respectively therefore both compounds were included in the final test set. Compound (CCI133) from the acidic series was found to be unstable in both HSA and PBS with percentages differences of -66.4 and -30.5, respectively and was therefore excluded. Neutral compound GI99296X had a percentage difference of 27.2% in HSA but was stable in PBS (-12.4%). Using analyte peak area, the percentage difference was 4.5% in HSA and therefore was included in the final test set. For the neutral compound GR78367, a single chromatographic peak was observed at 0 hr in both HSA and PBS. Double/split chromatographic peaks were observed after 6 hr incubation in both HSA and PBS; the analyte was therefore not selected as part of the test set. The percentage difference for neutral compounds GR64334X and GR33914X were -26.0, -27.1 respectively in PBS and 1.15%, 9.83% respectively in HSA suggesting instability in PBS. Further examination of the injection of replicate samples for GR33914X showed a lower internal standard peak area at 0h compared to 6h which resulted in a reduced peak area ratio at 6h. The percentage difference in PBS was attributed to the internal standard performance at the start of the run and therefore the compound was included. GR64334X was selected as part of the investigative set as the internal standard performance was inconsistent for the replicate injections at 0 and 6 hr in PBS. Basic compound, SKF1498A showed stability in HSA but not in PBS. Peak area was used to calculate the stability in PBS (-10.7%) due to variation in the internal standard at the 6hr time point and therefore SKF1498A was included. Compound SB213421 was 28.4 and 17.6% respectively in HSA and PBS using peak area ratio. Using analyte peak area, the stability in HSA was 17.2%. The percentage difference in HSA and PBS were within ±15% for the remaining compounds across the acidic, basic and neutral series

2.4.4. Feasibility Study

CRED investigative experiments were conducted using a total subset of 12 compounds, across acid, base, neutral and zwitterion series. The pilot study was carried out in triplicate in order to assess the experimental variability and the assay methodology is described below.

Results from HSA binding determinations of the initial test set of 12 compounds are presented in Table 4. Results for binding to phosphatidylcholine, the unbound fractions in HSA and unbound concentration in PBS for the individual compounds are presented in Appendix 3. The mean %HSA binding ranged as follows; acids (70.5 to 99.75%), bases (21.5 to 96.9%), neutral (55.9 to 97.0%) and zwitterion was 74.9%. The standard deviation of the analytical measurements of HSA binding (n=3) within each subset of compound series ranged from 0.37 to 6.0, 0.9 to 9.1, 1.7 to 11.7 and 5.4 for the acids, bases, neutrals and zwitterion, respectively. Across the subset series, the standard deviation of the analytical measurements of HSA binding ranged from 0.37 to 3.5 and 3.0 to 11.7 for compounds with >90% HSA and <90% binding, respectively. Overall, the standard deviation across the series of compounds tested in the pilot study ranges from 0.37 to 11.7%.

The feasibility study showed that the experimental procedure is robust, reproducible and can deliver HSA binding data across a wide range of values (21.5% to 99.75%) for a variety of compounds. The coefficient of variation (%CV) was $\leq 15\%$ for at least 75% of compounds done in triplicate and provided confidence that accurate and credible data can be obtained from a single assay per compound rather than being done in triplicate. This saves on extraction and processing time. In summary data shows consistency and provides confidence to proceed with the main study with an experimental design using single measurements.

Table 4: The average measured % HSA binding values and their experimental standard deviations obtained from n=3 measurements of 12 research compounds

	Acidic Subset			
	CC16817	GW622791X		G1235401X
% HSA Bound_1	72.5	93.4		99.96
% HSA Bound_2	75.2	94.6		99.96
% HSA Bound_3	63.8	88.6		99.32
Mean ±SD	70.5 ± 6.0	92.2 ± 3.2		99.75 ± 0.37
% CV	8.5	3.4		0.4
	Basic Subset			
	CC13839	GR77494A	SB416332	GR613617
% HSA Bound_1	41.6	32.2	16.1	96.6
% HSA Bound_2	42.7	35.6	26.5	96.1
% HSA Bound_3	32.2	18.5	22.0	97.9
Mean ± SD	38.8 ± 5.7	28.8 ± 9.1	21.5 ± 5.2	96.9 ± 0.9
% CV	14.9	31.5	24.2	1.0
	Neutral Subset			
	GR119497	GW703803	GI116108	AH23463
% HSA Bound_1	59.7	92.3	97.4	56.2
% HSA Bound_2	65.2	95.5	98.5	60.4
% HSA Bound_3	42.8	88.6	95.1	*
Mean ±SD	55.9 ± 11.7	92.1 ± 3.5	97.0 ± 1.7	58.3 ± 3.0
% CV	20.9	3.7	1.8	5.1
	Zwitterion			
	GR99941			
% HSA Bound_1		69.9		
% HSA Bound_2		74.2		
% HSA Bound_3		80.6		
Mean ±SD		74.9 ± 5.4		
% CV		7.2		

*AH23463 was used extensively in the initial stages of testing, establishing protocol and was insufficient to conduct a third analysis. However, as part of the earlier investigation into setting up of an analytical methodology and using the CRED device

the %HSA binding of AH23463 was determined as 62%. This is documented in the Appendix. The overall feasibility data obtained across the series establishes the robustness of the CRED device.

2.5. Simple Model: Drug Distribution within the CRED using Surrogate Phosphatidylcholine as the lipid component of Cell membrane:

Previously established time to equilibrium, stability of compounds during incubation and the robustness of the method to accurately reproduce binding data allows for further investigation and optimisation of the CRED design using surrogate matrices to better mimic the in-vivo situation, enabling the calculation and comparison of drug distribution parameters (PPB, VDss) and understanding the effect of physicochemical properties on binding.

2.5.1. Preparation of Buffer

Phosphate buffer was prepared by dissolving a 5g tablet of phosphate buffered saline in 500ml of water to give a final concentration of 1% phosphate buffered saline. Within the CRED device, the use of 1% phosphate buffer both as a dialysate as well as diluent in the preparation of the plasma (human serum albumin) and tissue (phosphatidylcholine) surrogates was included to maintain pH control over the incubation period. During incubation, a seal covering the lid of the CRED base plate prevented evaporation and protected the system from external factors which could influence pH changes. Phosphate buffer, tissue and plasma surrogates gave pH readings of 7.3 ± 0.1 , 7.4 and 7.2, respectively when tested pre- and post-incubation at 37°C; indicating that the pH is maintained adequately during incubation.

2.5.2. Preparation of Tissue Surrogate

Fed State Simulated Intestinal Fluid (FeSSIF) powder in the form of lecithin was used as the source of phosphatidylcholine. FeSSIF powder was weighed and dissolved in 1% phosphate buffered saline to give 25.5, 50.9 and 76.4 mg/10 mL, respectively.

2.5.3. Preparation of Plasma Surrogate

Plasma surrogate was prepared by dissolving a weighed amount of Human Serum Albumin lyophilized powder in 1% PBS to give a final concentration of 50g/litre.

2.5.4. Preparation of Analyte concentration (2µM) in Plasma Surrogate

To attain a final concentration 2 µM of individually spiked compounds in 50 g/L HSA, a two-step serial dilution was carried out. Initially, a 2 µL aliquot of stock compound at a concentration of 10 mM was spiked into 998 µL HSA (50 g/L) to give a concentration of 20 µM. This was followed by a 10-fold dilution i.e., 300 µL of 20 µM spiked HSA added to 2700 µL control HSA to give a final volume of 3 mL.

2.5.5. Preparation of Base Plate

Prior to and after each experiment, the base plate of the CRED device was (1) soaked for 20 min in 20% ethanol (aq) under ultrasonication, (2) rinsed with water and allowed to bathe in water for a further 10 min and then (3) rinsed with water before drying on blotting paper.

2.5.6. Preparation of Samples within CRED Device Prior to Incubation

Using the 6-chamber format of the CRED device, 2.5 mL of 2µM individually spiked HSA was added to the well. The plate lid was then secured onto the base plate and loaded with 2 dual and a single membrane insert. The inserts were loaded with 200 µL of 100 mg/10 mL, 200 mg/10 mL, 300 mg/10 mL, a duplicate 200 mg/10 mL tissue surrogate and 1% PBS,

respectively. An adhesive sealing tape was then placed over the entire plate lid in order to prevent evaporation during incubation. The appropriately labelled CRED device was then placed onto an orbital shaker at 600 rpm in the incubator set at 37°C. Incubation was allowed to take place for a minimum 6 hr up to 24hrs to reach equilibrium. Post equilibrium dialysis, 10 µL aliquots were taken from each insert along with a 10 µL aliquot of spiked HSA sampled from the open end of the single membrane insert. In order to normalise matrix and suppression effects as with the matrix used to prepare calibration standards, 40 µL of individually prepared “partial matrix” to achieve total matrix match was added to the relevant 10 µL aliquot (outlined in Matrix Effects section 2.2.1). Samples were extracted by addition of 200 µL of acetonitrile/methanol/water (volume ratio 85/10/5) containing an in-house generic internal standard [^2H $^{13}\text{C}_3$]-SB243213. Samples were then briefly mixed and centrifuged for 10 min at 3000 rpm after which they are ready for injection onto the HPLC-MS/MS system for analysis.

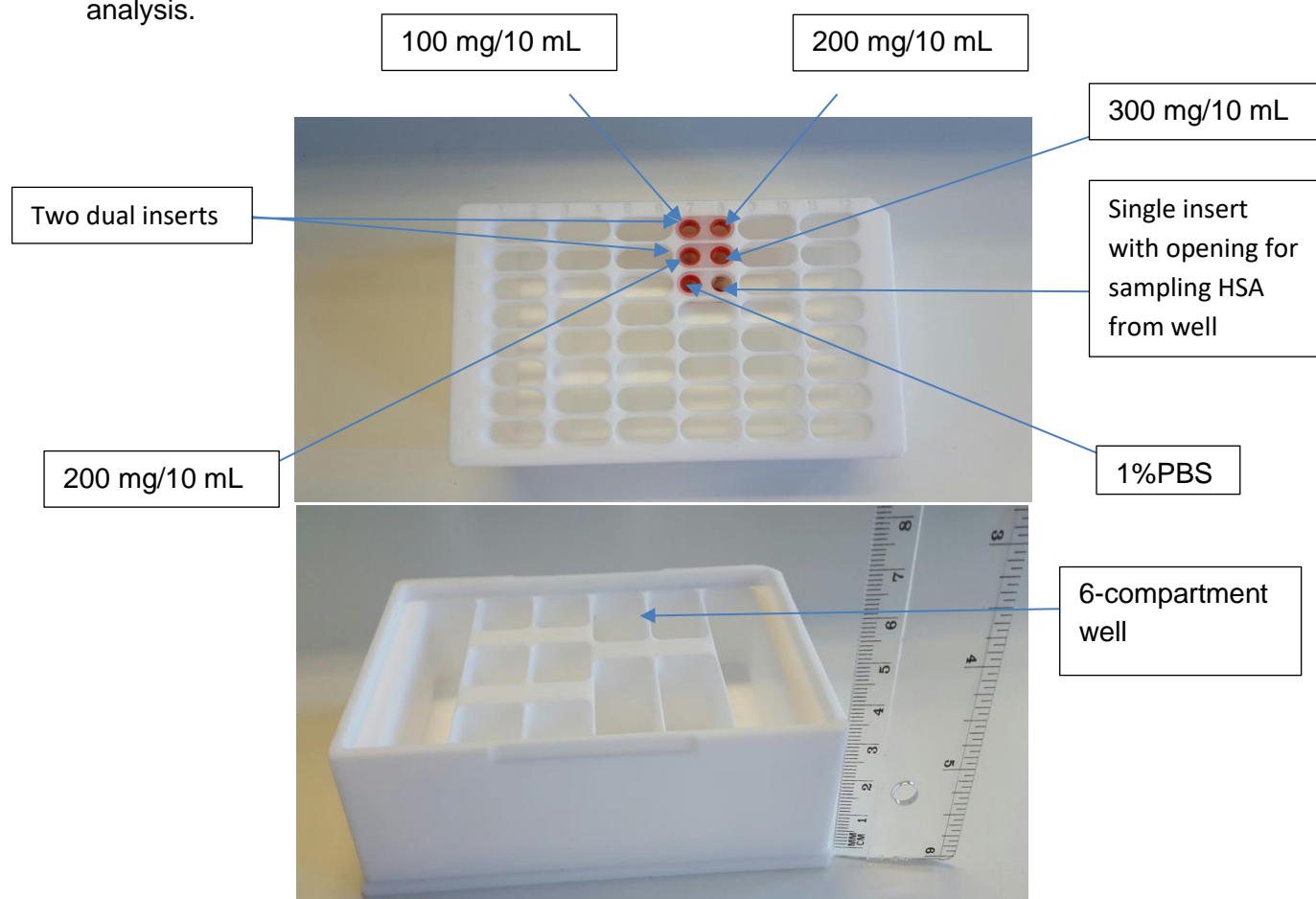


Fig 26: Standard base plate of the CRED device and a 6-compartment design with 2 dual and a single CRED insert

2.5.6. Preparation of Calibrations standards

Working solutions were prepared by initially adding 5 µL (10 mM stock) of 4 individual analytes to 180 µL acetonitrile/water 50/50 (v/v) to give individual concentrations of 250 µM. This allowed for the preparation of calibration standards and the quantification of 4 compounds per CRED experimentation using 2 base plates, each containing 2 of the 6 compartments well model. Using 10-fold serial dilutions, additional working solutions in acetonitrile/water were prepared to realise concentrations of 25, 2.5 and 0.25 µM, respectively. An assay range of

0.005 to 5 μM was prepared for each analyte by addition of no more than 5% volume of working solutions to previously prepared “total matrix” to give calibrations standards of 0.005, 0.01, 0.02, 0.1, 0.5, 1.0, 4.0 and 5 μM , respectively. “Total matrix” was prepared by mixing equal volumes of 1% phosphate buffered saline, control human serum albumin at 50 g/L, 100, 200 and 300 mg/10 mL of FeSSIF powder, respectively. Protein precipitation was carried out by extracting 50 μL duplicate aliquots of each standard using 200 μL of acetonitrile/methanol/water (volume ratio 85/10/5) containing an in-house generic internal standard [$^2\text{H}^{13}\text{C}_3$]-SB243213. Samples were then briefly mixed and centrifuged for 10 min at 3000 rpm after which there are ready for injection onto the HPLC-MS/MS system for analysis.

2.5.6. Chromatographic and Mass Spectroscopy Conditions

A Perkin Elmer Sciex API4000 Mass Spectrometer using TurbolonSpray™ source in Multiple Reaction Monitoring was used for chromatographic peak detection. Generic HPLC gradient conditions were achieved with an Acquity C18 UHPLC column (50 x 2.1 mm, 1.7 μm) equilibrated to 40 °C (Waters Corporation Ltd). Data was acquired over a run time of 2.5 min. The organic mobile phase (B) was acetonitrile while the aqueous mobile phase (A) used was based on the ionization state of the compound. For analytes that were negatively charged at the physiological pH of 7.4 (acids), an aqueous mobile phase of 10 mM ammonium formate was preferred in negative acquisition mode, whilst 0.1% formic acid was used for positively charged compounds (bases) in positive acquisition mode. The generic HPLC condition used were 0.0 to 0.2 min at 5% acetonitrile, 0.2 to 1.5 min organic phase change 5 to 95% B, 1.5 to 2.0 min held at 95% B and 2.0 to 2.5 min back to the initial starting conditions. Where necessary, modification to resolve the analyte of interest from any endogenous peaks was applied. An example was seen for the acidic compound GR62550 where the analyte of interest is unresolved (Fig 28 (a)). Separation was achieved by a reduction in the organic composition between 1.5 to 2.0 min from 95% to 65% B ensuring better selectivity (Fig 28 (b)). A Waters Acquity UPLC system was used to drive the mobile phases (flow rate of 0.7 mL/min in partial loop injection mode). The injection volume ranged from 5 to 15 μL depending on analyte sensitivity. Eluent from the column was diverted from the mass spectrometer up to 0.3 min and after 2.0 min to keep the mass spectrometer clean.

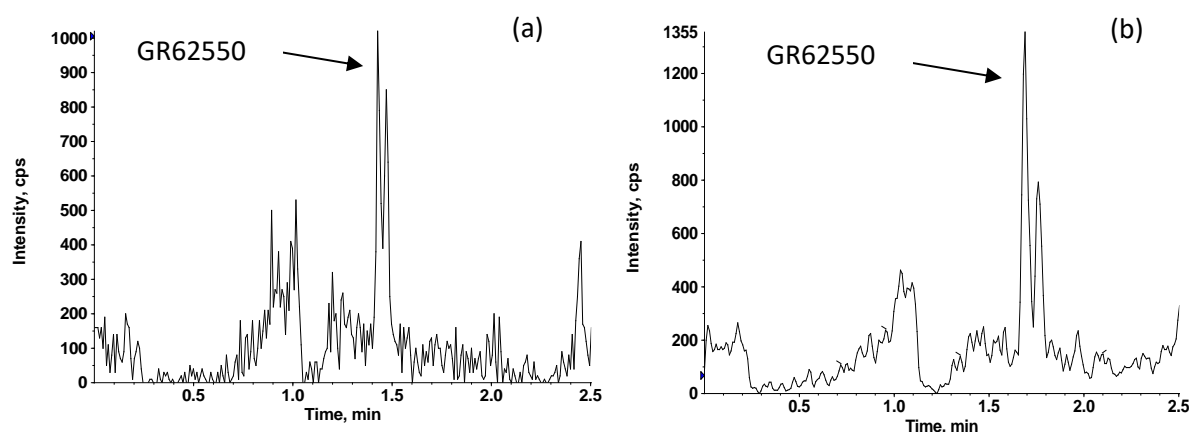


Fig 27. (a) analyte of interest unresolved from endogenous peak using generic gradient, (b) analyte of interest resolved from endogenous peak using modified gradient

2.5.7. Data Acquisition and Processing

HPLC-MS/MS data were acquired and processed (integrated) using the proprietary software application Analyst™ (Version 1.4.2, Applied Biosystems/MDS Sciex, Canada). Calibration

plots of analyte/internal standard peak area ratio versus individual analyte concentration were constructed and a weighted $1/x^2$ linear regression applied to the data. Where necessary (due to high sensitivity) a weighted $1/x$ quadratic regression applied to the data. Concentrations of analytes were determined from the appropriate calibration line in “total matched matrix”.

2.6. Calculations:

2.6.1. Percentage Bound

The amount of drug bound to human serum albumin or phosphatidylcholine tissue surrogate at steady state is calculated using the formula below:

$$\%Bound = (C_t - C_u) \div C_t \times 100 \quad Eqn\ 14$$

Where C_t = total concentration (bound plus unbound) in human serum albumin or phosphatidylcholine tissue surrogate and C_u = free (unbound) concentration obtained from the analysis of drug in 1% PBS.

2.6.2. Fraction unbound

The fraction of drug unbound in HSA or phosphatidylcholine tissue surrogate at steady-state is calculated using the formula below:

$$Fraction\ Unbound\ (F_u) = C_u \div C_t \quad Eqn15$$

Where F_u can be further defined as fraction unbound in HSA F_{up} (plasma surrogate) and fraction unbound in phosphatidylcholine F_{ut} (tissue surrogate).

2.6.3. Tissue Dilution

Matrix dilution results in a reduction in the concentration of available receptor binding to HSA or phosphatidylcholine, which in return alters unbound concentration present in the diluted matrix. In order to accurately determine *in-vivo* drug distribution from *in-vitro* binding parameters, this dilution effect must be accounted for (Kalvass, Maurer et al. 2007).

The relationship between the binding component concentration $[B]$ and the unbound fraction (f_u) in the tissue is given by the equation. Where K_d is referred to as the dissociation constants

This can be rearranged to give $K_d = f_u [B] / 1 - f_u \quad Eqn16$

Where there are two different concentrations of binding receptor $[B1]$ and $[B2]$ with corresponding free fractions f_{u1} (in undiluted tissue as *in-vivo*) and f_{u2} (measured *in vitro* using diluted tissue) the following equation is true

$$1 = f_{u1}[B1](1 - f_{u2}) / f_{u2}[B2](1 - f_{u1})$$

Defining $[B1] / [B2]$ as a dilution factor D and simplifying gives

$$fu1 \text{ (Undiluted free fraction)} = (1/D) / \left(\frac{1}{fu} - 1 \right) + \frac{1}{D} \quad Eqn17$$

2.6.4. Determination of Tissue Dilution Factor

The liver is the largest solid internal organ in the human body (Molina and DiMaio 2012) and was assumed to contain the highest levels of phospholipids. The total phospholipid content in wet liver was determined as 2.7 g/100 g of wet liver (Hood, Gustafson et al. 1961). The average weight of liver in human is 1.5 kg per body weight. Therefore, the total phospholipids content in wet liver is 40.5 g. Phosphatidylcholine accounts for nearly 60% of total phospholipid i.e. 24.3 g. Liver volume is on average 1500 mL (Hausken, Leotta et al. 1998). The endogenous concentration of phosphatidylcholine under normal physiological conditions was therefore estimated to be 162 mg/10 mL (Hausken, Leotta et al. 1998). The total phospholipid content is therefore calculated as 270 mg/10 mL. The actual concentration of phosphatidylcholine in 100 mg/10 mL, 200 mg/10 mL and 300 mg/10 mL of weighed FeSSIF powder is 25.5, 50.9 and 76.4 mg/10 mL. The dilution factor (D) therefore is the ratio of total phospholipid content to the individual concentration of phosphatidylcholine used within the CRED device i.e., 10.6, 5.3 and 3.5, respectively (Table 5). The *in-vitro* fraction unbound in HSA was not normalised as a physiological concentration of 50 g/L representing the amount of HSA *in vivo* was used in the experimentation.

Table 5: Levels of Sodium taurocholate, Lecithin (PC) based on Biorelevant protocol*

		PC1	PC2	PC3
	112 mg/10 mL *	100 mg/10 mL	200 mg/10 mL	300 mg/10 mL
Sodium taurocholate (mM)	15	14.4	28.8	34.2
Lecithin (mM)	3.75	3.35	6.7	10.05
Lecithin (mg/10 mL)	28.5	25.5	50.9	76.4
Dilution Factor (D)	-	10.6	5.3	3.5

2.6.5. *In-vivo* Volume of Distribution (V_{dss})

The volume of distribution *in-vivo* is calculated using the equation below:

$$V_{dss} = \text{Mean} \sum \frac{F_{up}}{F_{ut}(\text{undiluted})} \quad \text{Eqn18}$$

Where *F_{ut} (undiluted)* is the scaled tissue fraction unbound that mimics the *in-vivo* situation based on the endogenous levels of phosphatidylcholine in a healthy adult. The mean of the individual volumes of distributions for each concentration of phosphatidylcholine tissue surrogate used in the CRED device therefore gives the overall volume of distribution at steady-state *in-vivo* for comparison with the *in-vivo* volume of distribution obtained from the GSK repository (KATE database) and observed literature values

2.7. Discussion of Preliminary studies

One of the major limitations in conducting plasma protein binding studies is obtaining comparable and accurate data across different labs using various techniques (Kratochwil, Huber et al. 2002). Therefore, rigorous preliminary experiments were conducted to ensure the CRED device is suitable to perform optimally and generate reliable, consistent binding data. There was no evidence suggesting phosphatidylcholine micelles cross the semipermeable cellulose membrane. This was tested periodically throughout the study using

aliquots of the phosphate buffer samples (PBS) post incubation and were negative in all instances e.g. (Fig 24) indicating that there was no impact on the calculated unbound concentration. This was also evident from visual examination of the precipitated sample. Buffer Extracted using acetonitrile as organic solvent was clear but precipitated tissue surrogate sample was cloudy indicating the presence of phospholipid. This provided confirmation of the molecular weight cut-off efficiency of the semipermeable cellulose membrane used in the CRED device.

To assess the stability of the compounds in HSA and 1%PBS during incubation at 37°C for 6hr a $\pm 15\%$ percentage difference between the analyte peak area ratio obtained immediately upon spiking (zero hours) and the analyte peak area ratio post incubation was used as the default acceptance criteria. This was based on in house Standard Operating Procedures (SOP) for acceptance of analyte stability in the matrix of interest. Further examination of internal standard performance, sample injection variability and the use of analyte peak area were also employed as necessary to define compound stability. Of the 56 compounds tested, 50 (Table 6) were selected for evaluation of their binding parameters using the CRED device and represents a set of structurally diverse drugs. Stability experiments were not performed in phosphatidylcholine tissue surrogate solutions as data from HSA and PBS stability experiments were assumed to be indicative of analytes that are unstable and subject to degradation. From the conduct of the feasibility study, low data variability, especially for the high binders shows that the methodology, sample extraction and analysis procedures were consistent and robust. This provided the added confidence that the data quality and system performance are reliable. Conducting single analysis of each compound in the main study was therefore deemed enough to validate the CRED system as a tool for evaluating the biomimetic parameters of the series of compounds under investigation.

2.7.1 Results Simple Model: Drug Distribution within the CRED using Phosphatidylcholine as the major lipid component of Cell membrane

Table 6: HSA Binding of Acidic, Basic, Neutral and Zwitterion Series using the Competitive Rapid Equilibrium Dialysis

Acidic Series	CRED %HSA Binding	Basic Series	CRED %HSA Binding	Neutral Series	CRED %HSA Binding	Zwitterion	CRED %HSA Binding
CCI6817	76.1	CCI3993	74.7	GR91295X	11.4	GR99941A	67.7
GR62550X	99.7	SB731710	92.1	CCI9371	80.2	GW300671A	59.0
GR87272X	97.8	CCI3748	57.0	CCI22428	58.2		
GR138714X	99.92	GR30676X	97.1	GR104104X	82.02		
GR70487A	37.3	SKF95914	99.0	GF120403X	90.2		
CCI120	99.2	GR35842A	40.2	GI115674X	63.4		
GR33000X	96.2	GR43175X	11.0	AH23463X	48.5		
GW289865X	97.5	GF120454X	68.5	GW388185X	99.6		
GSK275458A	99.8	SB416332AAA	9.6	GR119497X	51.8		
GR87036X	88.8	CC13839	31.9	GR33914X	98.3		
AH22182X	98.5	GR61317X	97.2	GR38393X	99.1		
SB213421Z	99.4	GW769340A	64.5	GR64334X	74.1		
GR118989X	96.9	CCI20557A	35.9	GW703803X	94.6		
BRL15541QQ	98.0	CCI4001	47.4	GI116108X	97.3		
GI235401X	99.1	GR84804A	70.5	GI99296X	99.3		
GW622791X	91.9	GR77494A	40.4				
		GR189721X	30.1				

Results for the determination of the HSA binding across the acidic, basic and neutral series obtained using the CRED device are presented in Table 6. For the series of compounds investigated, the % HSA binding ranged from 37.3 to 99.92, 9.6 to 99.0 and 11.4 to 99.6, for acids, bases, and neutrals, respectively. The %HSA binding for GR99941 and GW300671 (zwitterions) were 67.7% and 59.0%, respectively. The overall %HSA binding ranged from 9.6 to 99.92% showing that the CRED device could be a powerful PPB binding technique capable of delivering a wide range of HSA binding values across a variety of compounds. Across the tool compound set the overall extent of HSA binding decreases from acids, neutrals to bases (Fig 28). The data shows that for the overall series of compounds investigated, HSA had the highest binding capacity for the acids.

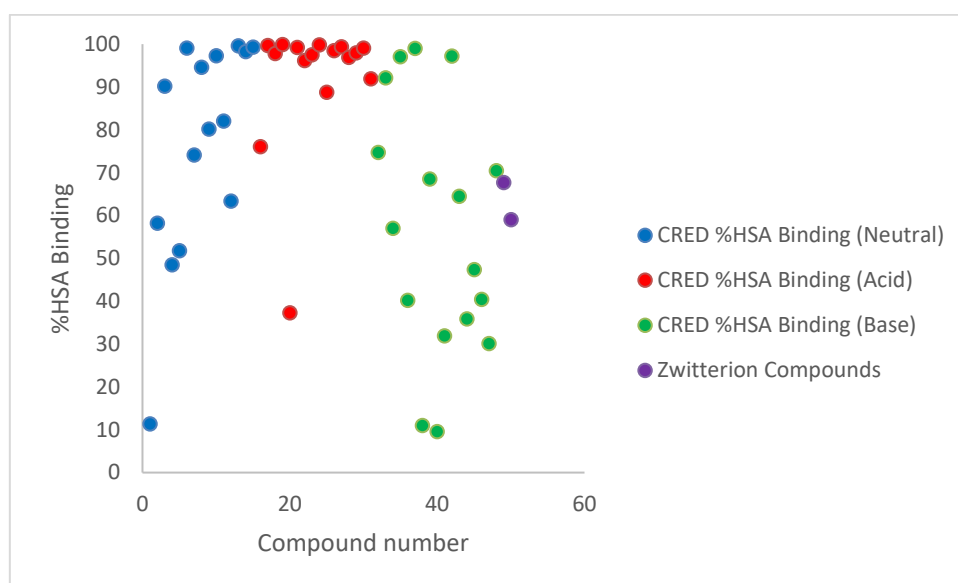


Fig 28: Variation of HSA binding across series using the CRED

HSA binding data across the acidic, basic, neutral (and zwitterion series) obtained using the CRED device are presented along with the existing HSA binding data obtained by the Physchem Group using column chromatography in (Table7). The linear correlation coefficients obtained were 0.9616, 0.6068 and 0.8619 for acids, bases and neutrals, respectively (Fig 29). The combined linear coefficient for the series of compounds investigated was 0.6953 (Fig 29 (d)). Due to insufficient data a plot for the zwitterions was not pursued.

Table 7: %HSA Binding Across All Series of Compounds using the Competitive Rapid Equilibrium Dialysis compared to HSA binding using column Chromatography. * Indicates Zwitterions

Acidic Series		Basic Series		Neutral Series	
Compound_ Chromatographic %HSA Binding	CRED %HSA Binding	Compound_ Chromatographic %HSA Binding	CRED %HSA Binding	Compound_ Chromatographic %HSA Binding	CRED %HSA Binding
CCI6817_77.6	76.1	CCI3993_92.5	74.7	GR91295_25.9	11.4
GR62550_98.6	99.7	SB731710_97.8	92.1	CCI9371_86.7	80.2
GR87272_98.0	97.8	CCI3748_90.4	57.0	CCI22428_71.9	58.2
GR138714_98.8	99.92	GR30676_98.6	97.1	GR104104_91.2	82.02
GR70487_40.3	37.3	SKF95914_98.7	99.0	GF120403_83.8	90.2
CCI120_98.6	99.2	GR35842_86.1	40.2	GI115674_79.1	63.4
GR33000_97.3	96.2	GR43175_28.0	11.0	AH23463_80.6	48.5

GW289865_95.6	97.5	GF120454_88.4	68.5	GW388185_97.1	99.6
GSK275458_98.7	99.8	SB416332_35.0	9.6	GR119497_59.3	51.8
GR87036_95.4	88.8	CC13839_68.7	31.9	GR33914_92.0	98.3
AH22182_97.2	98.5	GR61317_96.0	97.2	GR38393_93.9	99.1
SB213421_95.0	99.4	GW769340_87.5	64.5	GR64334_95.9	74.1
GR118989_89.7	96.9	CC120557_88.1	35.9	GW703803_96.8	94.6
BRL15541_97.6	98.0	CCI4001_72.7	47.4	GI116108_94.4	97.3
GI235401_98.8	99.1	GR84804_86.2	70.5	GI99296_92.6	99.3
GW622791_96.1	91.9	GR77494_38.6	40.4	*GW300671A_74.1	59.4
		GR189721_86.2	30.1	*GR99941A_92.0	67.6

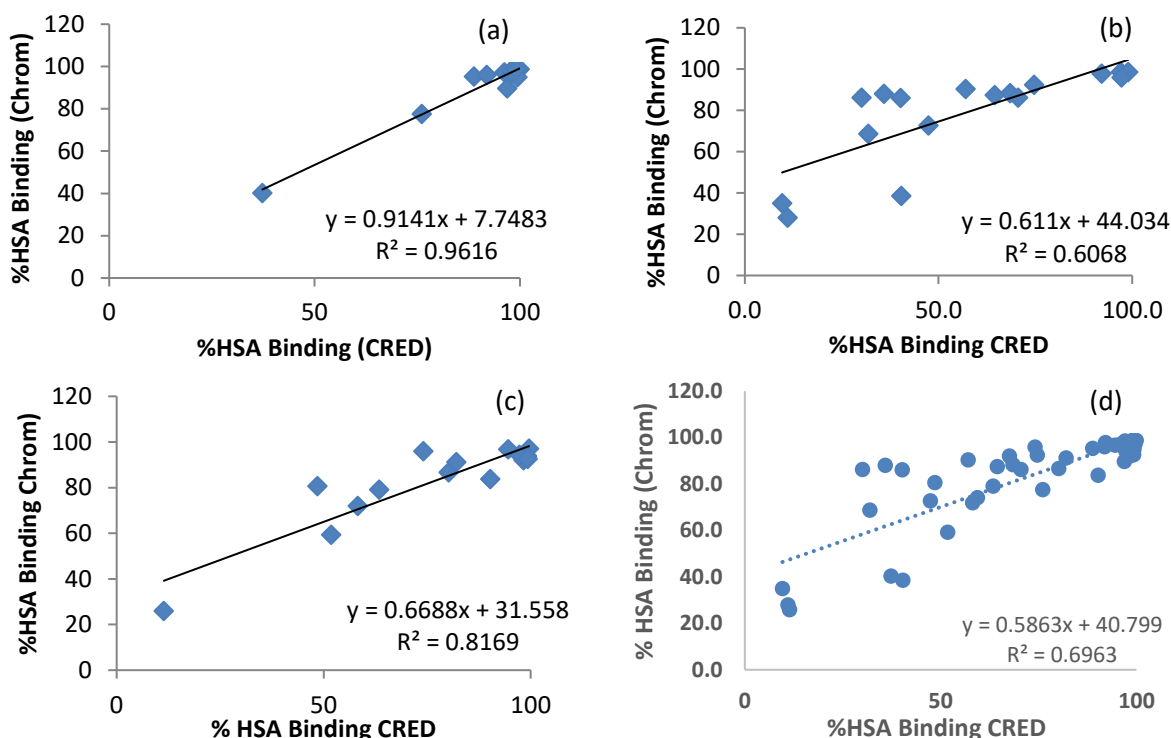


Fig 29: Linear plot of the chromatographic HSA binding data as a function of the CRED HSA binding for (1a) acidic series, (b) basic series, (c) neutral series and (d) combined

HSA binding data across selected acidic, basic, neutral compounds using the CRED device are presented along with the observed literature plasma protein binding data in Table 8. The linear correlation coefficients obtained were 0.862, 0.641 and 0.737 for acids, bases and neutrals, respectively (Fig 30). The combined linear coefficient for the selected series of compounds investigated was 0.647 (Fig 30 (d)). A replot of the basic series excluding outliers CCI3839 and CCI20557 gave a correlation coefficient of 0.807 (Fig 30 (e)) and a subsequent combined linear coefficient of 0.765 (Fig 30 (f)).

Table 8: %HSA Binding using the Competitive Rapid Equilibrium Dialysis compared to Observed Literature Plasma protein binding for compounds where data were found. * Denotes data not found (DNF)

Acidic Series		Basic Series		Neutral Series	
Observed Literature %PPB Binding	CRED %HSA Binding	Observed Literature %PPB Binding	CRED %HSA Binding	Observed Literature %PPB Binding	CRED %HSA Binding
CCI6817_94	76.1	CCI3993_91	74.7	GR91295_DNF*	11.4
GR70487_50	37.3	SB731710_99	92.1	CCI22428_77	58.2
CCI120_90	99.2	CCI3748_92	57.0	GF120403_95	90.2

GR87036_87	88.8	GR30676_96.2	97.1	AH23463_75	48.5
AH22182_98.3	98.5	GR35842_DNF*	40.2	GR119497_59	51.8
GR118989_98.8	96.9	GR43175_17	11.0	GR33914_98.4	98.3
BRL15541_99.2	98.0	SB416332_27	9.6	GR38393_98	99.1
GI235401_99.84	99.1	CC13839_81	31.9	GR64334_99.64	74.1
GW622791_90	91.9	GW769340_98	64.5	GI116108_96	97.3
		CC120557_90.7	35.9		
		CCI4001_87	47.4		
		GR84804_88	70.5		

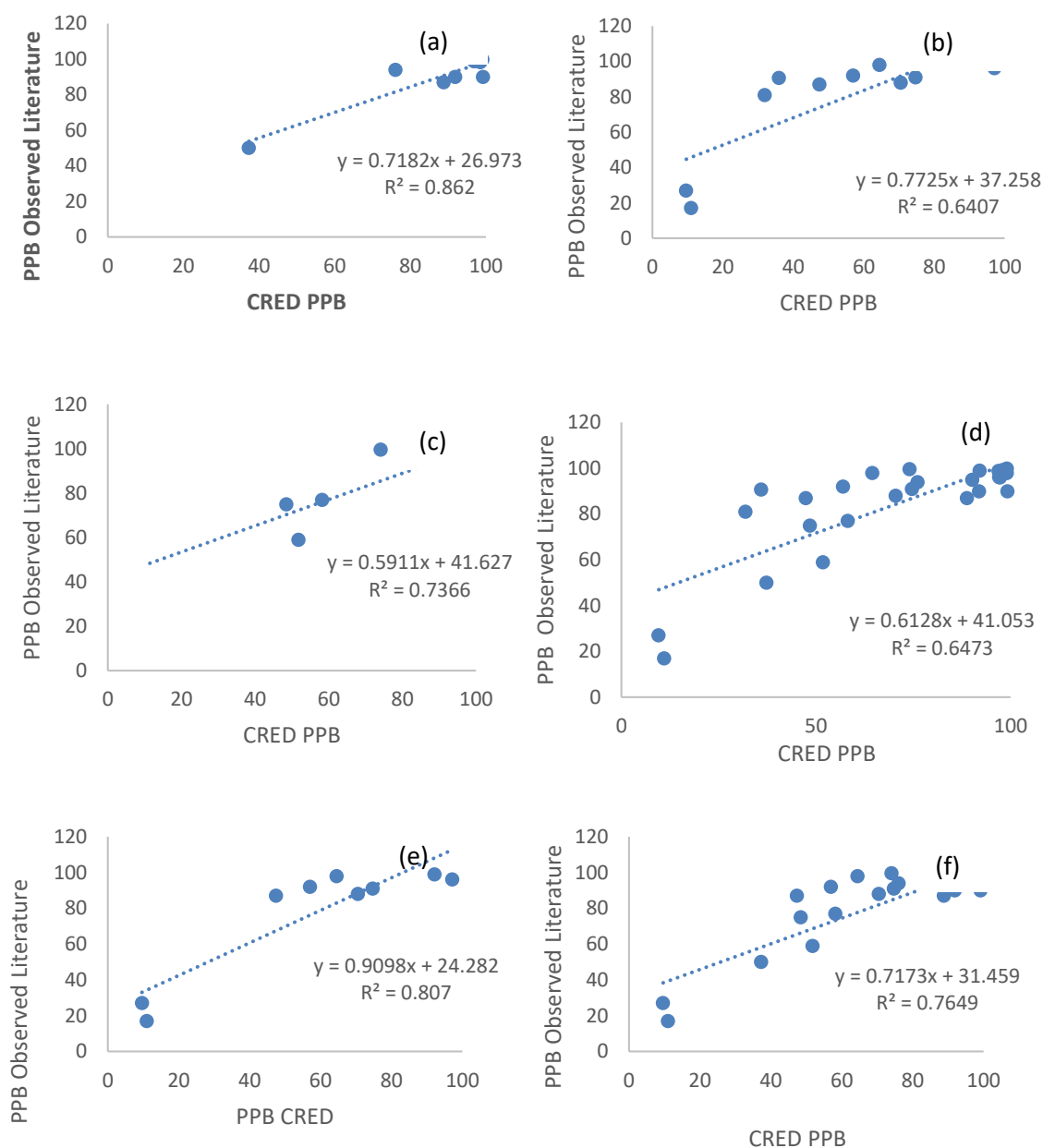


Fig 30: Linear plot of the Observed Literature binding data found as a function of the CRED HSA binding for (1a) acidic series, (b) basic series, (c) neutral series, (d) combined, removal of outliers from basic series (e) and combined excluding outliers (f)

HSA binding data across selected acidic, basic, neutral compounds using the data obtained from HSA column chromatography are presented along with the observed literature plasma protein binding data in Table 9. The linear correlation coefficients obtained were 0.798, 0.938 and 0.899 for acids, bases and neutrals, respectively (Fig 31). The combined linear coefficient for the selected series of compounds investigated was 0.886 (Fig 30 (d)).

Table 9: %HSA Binding using Column Chromatography compared to Observed Literature Plasma protein binding for compounds where data were found.

Acidic Series		Basic Series		Neutral Series	
Observed Literature %PPB Binding	Compound_Chromatographic %HSA Binding	Observed Literature %PPB Binding	Compound_Chromatographic %HSA Binding	Observed Literature %PPB Binding	Compound_Chromatographic %HSA Binding
CCI6817_94	77.6	CCI3993_91	92.5	GR91295_*	
GR70487_50	40.3	SB731710_99	97.8	CCI22428_77	71.9
CCI120_90	98.6	CCI3748_92	90.4	GF120403_95	83.8
GR87036_87	95.4	GR30676_96.2	98.6	AH23463_75	80.6
AH22182_98.3	97.2	GR35842_*		GR119497_59	59.3
GR118989_98.8	89.7	GR43175_17	28	GR33914_98.4	92
BRL15541_99.2	97.6	SB416332_27	35	GR38393_98	93.9
GI235401_99.84	98.8	CC13839_81	68.7	GR64334_99.64	95.9
GW622791_90	96.1	GW769340_98	87.5	GI116108_96	94.4
		CC120557_90.7	88.1		
		CCI4001_87	72.7		
		GR84804_88	86.2		

*: Literature value not found

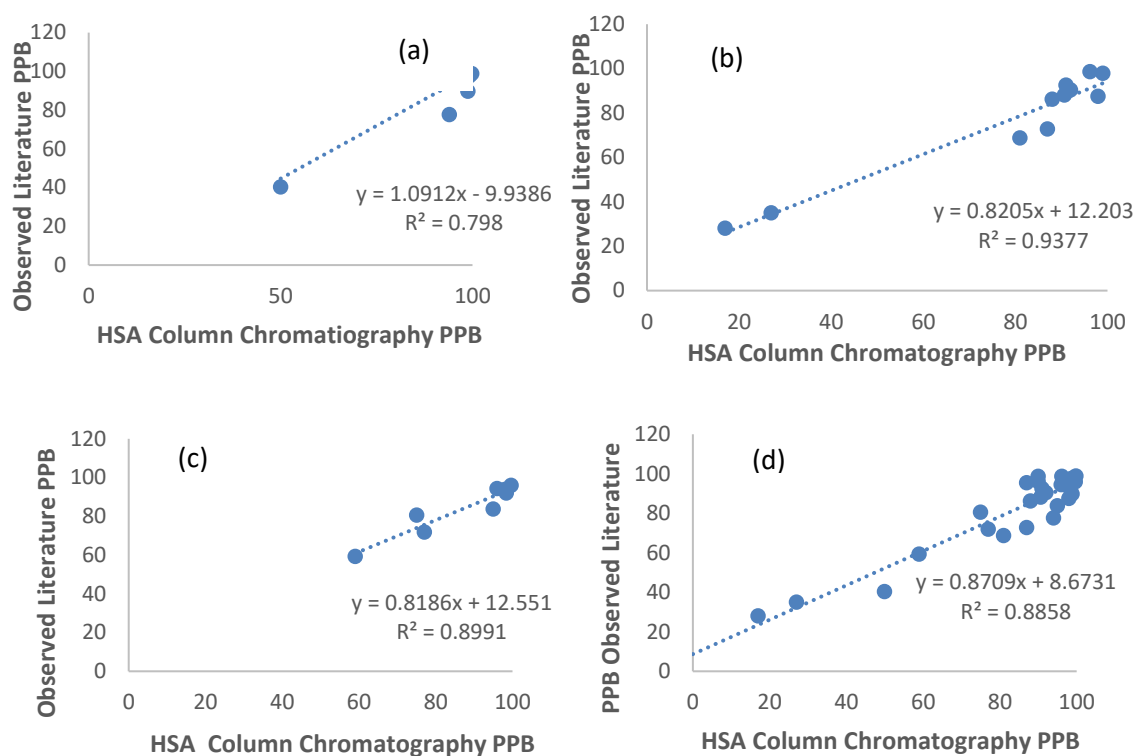


Fig 31: Linear plot of the Observed Literature binding data found as a function of the Column Chromatography HSA binding for (1a) acidic series, (b) basic series, (c) neutral series and (d) combined

Results for the determination of the free concentration (μM) across the acidic, basic and neutral series obtained using the CRED device are presented in Table 10. Across the acidic, basic and neutral series, the free concentrations ranged from 0.002 to 1.159, 0.008 to 1.320 and 0.004 to 1.630, respectively. The free concentration for GR99941 and GW300671 (zwitterions) were 0.524 and 0.833, respectively. There was generally an increase in free concentration going from acids, neutrals to bases (Fig 32). This is expected as where there is an increase in %HSA binding from bases to neutrals to acids, there is a corresponding a reduction in the unbound concentration.

Table 10: Free Concentration of Acidic, Basic, Neutral and Zwitterion Series using the Competitive Rapid Equilibrium Dialysis

Acidic Series	Unbound Conc. (μM)	Basic Series	Unbound Conc. (μM)	Neutral Series	Unbound Conc. (μM)
CC16817	0.492	CCI13993	0.136	GR91295X	1.630
GR62550X	0.006	SB731710	0.209	CC19371	0.444
GR87272X	0.056	CCI3748	0.358	CC122428	0.624
GR138714X	0.002	GR30676X	0.042	GR104104X	0.252
GR70487A	1.159	SKF95914	0.008	GF120403X	0.181
CCI120	0.017	GR35842A	0.472	GI115674X	0.571
GR33000X	0.084	GR43175X	1.224	AH23463X	0.947
GW289865X	0.050	GF120454X	0.833	GW388185X	0.009
GSK275458A	0.003	SB416332AAA	1.320	GR119497X	0.483
GR87036X	0.254	CC13839	1.074	GR33914X	0.036
AH22182X	0.028	GR61317X	0.068	GR38393X	0.036
SB213421Z	0.011	GW769340A	0.291	GR64334X	0.496
GR118989X	0.052	CCI120557A	0.784	GW703803X	0.108
BRL15541QQ	0.034	CCI4001	0.621	GI116108X	0.053
GI235401X	0.022	GR84804A	0.127	GI99296X	0.004
GW622791X	0.158	GR77494A	0.542		
		GR189721X	0.080		
Zwitterion	Unbound Conc. (μM)				
GR99941A	0.524				
GW300671A	0.833				

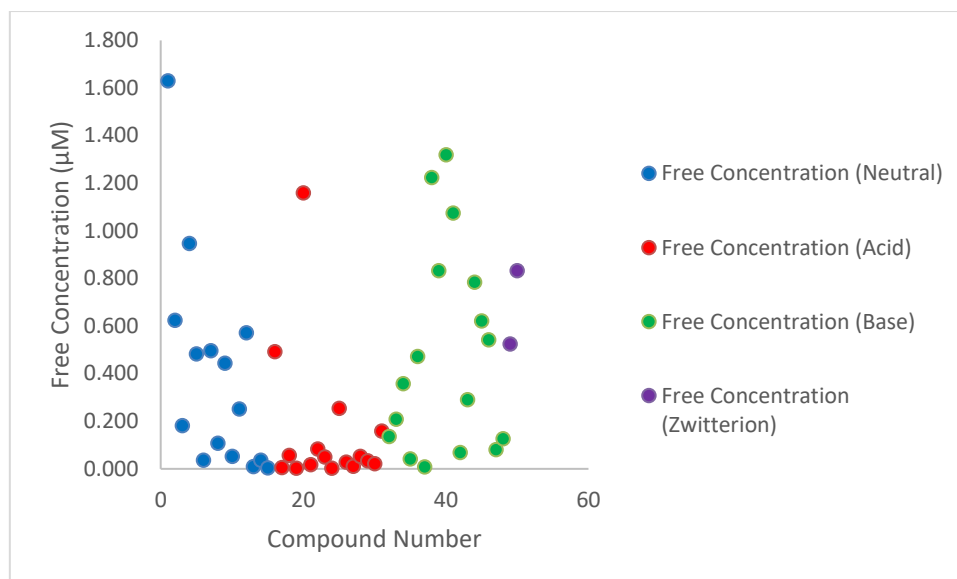


Fig 32: Variation of Free Concentration across series using the CRED

The % PC binding of drugs across the acidic, basic and neutral series are presented in Tables 11, 12 and 13, respectively. For zwitterions GR99941 and GW300671 the %PC binding are presented in Table 14. There was a general increase in %PC binding with increasing phosphatidylcholine concentration from 25.5, 50.9 and 76.4mg/10mL, PC1, PC2 and PC3, respectively. Where duplicate samples were analysed as in the case of PC2 (50.9mg/10mL) the mean %PC binding value was calculated. For the series of compounds investigated the overall %PC binding was largest for the basic compounds and lowest for acidic compounds.

The experimental data for % HSA binding, % PC binding, free fractions (in human serum albumin, phosphatidylcholine), free concentrations in buffer, stability in phosphate buffer and HSA will be included in the appendices of the final thesis.

Table 11: Binding of acidic drug, molecules to phosphatidylcholine tissue surrogate

Compound	%Binding PC1	%Binding Mean PC2	%Binding PC3
CCI16817	14.0	27.2	38.8
GR62550	0.0	2.70	0.00
GR87272	44.8	63.0	76.3
GR138714	85.5	93.8	93.4
GR70487	0.0	5.30	5.60
CCI120	37.3	74.2	96.9
GR33000	0.00	9.05	9.00
GW289865	28.4	50.8	63.6
GSK275458	86.7	84.6	99.4
GR87036	0.0	43.85	18.2
AH22182	27.5	27.35	51.6
SB213431	23.5	31.7	55.8
GR118989	24.5	37.35	89
BRL15541	22.0	5.3	5.2
GI235401	96.5	85.7	91.6
GW622791	34.1	63	64.8

Table 12: Binding of basic drug, molecules to phosphatidylcholine tissue surrogate

Compound	%Binding PC1	%Binding Mean PC2	%Binding PC3
----------	--------------	-------------------	--------------

CCI13993	91	93.85	94.4
SB731710	37.5	35.2	35.2
CCI3748	73.5	86.45	88.5
GR30676	93.6	93.85	94
SKF95914	83.1	78.3	79.5
GR35842	65.7	82.9	88.3
GR43175	3.3	17.25	10.6
GF120454	84.8	85.85	86.3
SB416332	19.6	35.2	45.4
CC13839	46.7	64.5	72.6
GR61317	94.3	95.7	96.3
GW769340	83.1	88.1	91.3
CCI120557	62.9	73.65	81.3
CCI4001	75.1	87.7	89
GR84804	93.1	95.05	95.4
GR77494A	25.2	34.6	48.2
GR189721	29.5	23.95	85.4

Table 13: Binding of neutral drug, molecules to phosphatidylcholine tissue surrogate

Compound	%Binding PC1	%Binding Mean PC2	%Binding PC3
GR91295X	0.00	0.00	0.00
CC19371	60.7	71.1	77.5
CC122428	42.4	58.1	64.9
GR104104X	66.9	77.35	80.5
GF120403X	29.1	40.8	50.5
GI115674X	22.2	42.75	51.1
AH23463X	20.8	41.2	50.5
GW388185X	71.4	76.0	78.1
GR119497X	28.4	41.6	51.9
GR33914X	95.1	95.5	95.9
GR38393X	93.4	94.45	94.7
GR64334X	0.00	0.00	0.00
GW703803X	90.1	92.9	91.8
GI116108X	90.6	92.9	93.3
GI99296X	91.3	96.5	97.6

Table 14: Binding of zwitterionic molecules to phosphatidylcholine tissue surrogate

Compound	%Binding PC1	%Binding Mean PC2	%Binding PC3
GR99941	50	67.55	78
GW300671	28.5	44.2	55.9

The VDss across the acidic, basic and neutral series is presented in tables 15 to 17. The values obtained ranged from 0.003 to 0.753, 0.270 to 31.202 and 0.073 to 3.747 for acids, bases and neutrals respectively. The VDss for zwitterions GR99941A and GW300671A were 0.599 and 0.349 respectively as shown in Table 18. Overall, the VDss was highest for the bases and lowest for the acids and can be shown using a plot of LogVDss as a function of the %HSA binding (Figure 33).

Table 15: Volume of Distribution (VDss): acidic compounds (ratio of free fractions HSA to undiluted tissue surrogate)

Compound Number	CRED VDss	CRED Log VDss
-----------------	-----------	---------------

CC16817	0.713	-0.147
GR62550X	0.003	-2.523
GR87272X	0.227	-0.644
GR138714X	0.041	-1.387
GR70487A	0.753	-0.123
CCI120	0.593	-0.227
GR33000X	0.051	-1.292
GW289865X	0.158	-0.801
GSK275458A	0.089	-1.051
GR87036X	0.166	-0.780
AH22182X	0.059	-1.229
SB213421Z	0.025	-1.602
GR118989X	0.132	-0.879
BRL15541QQ	0.025	-1.602
GI235401X	0.306	-0.514
GW622791X	0.533	-0.273

Table 16: Volume of Distribution (VDss): basic compounds (ratio of free fractions HSA to undiluted tissue surrogate)

Compound Number	CRED VDss	CRED Log VDss
CCI13993	21.004	1.322
SB731710	0.357	-0.447
CCI3748	13.783	1.139
GR30676X	2.717	0.434
SKF95914	0.270	-0.569
GR43175X	1.555	0.192
GR35842A	15.286	1.184
GF120454X	11.767	1.071
SB416332AAA	3.453	0.538
CC13839	7.137	0.854
GR61317X	3.548	0.550
GW769340A	12.888	1.110
CCI120557A	10.742	1.031
CCI4001	18.416	1.265
GR84804A	31.202	1.494
GR77494A	2.522	0.402
GR189721X	5.285	0.723

Table 17: Volume of Distribution (VDss): neutral compounds (ratio of free fractions HSA to undiluted tissue surrogate)

Compound Number	CRED VDss	CRED Log VDss
GR91295X	0.886	-0.053
CCI9371	3.057	0.485
CC122428	3.464	0.540
GR104104X	3.437	0.536
GF120403X	0.491	-0.309
GI115674X	1.705	0.232
AH23463X	2.293	0.360
GW388185X	0.073	-1.137
GR119497X	2.358	0.373
GR33914X	2.191	0.341
GR38393X	0.889	-0.051
GR64334X	0.259	-0.587
GW703803X	3.747	0.574
GI116108X	1.969	0.294
GI99296X	0.990	-0.004

Table 18: Volume of Distribution (VDss) for zwitterion compounds obtained from the ratio of free fraction in HSA to undiluted free fraction in tissue surrogate showing similarity on average to neutral molecules.

Compound Number	CRED VDss	CRED Log VDss
GR99941A	3.970	0.599
GW300671A	2.200	0.342

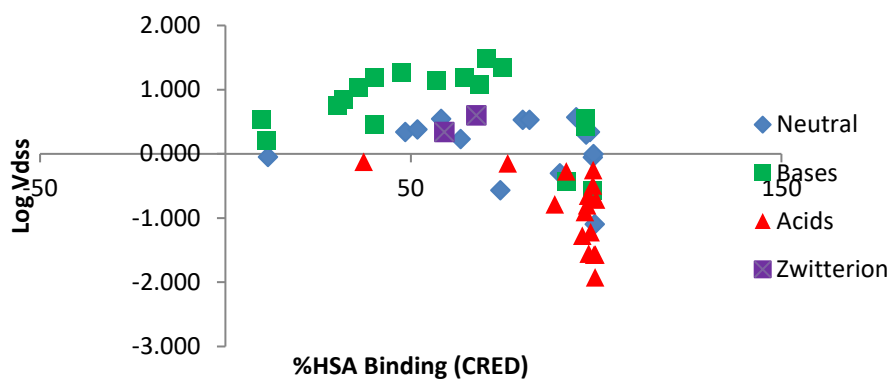


Fig 33: CRED Log VDss as a function of %HSA binding across acidic, basic, neutral series and Zwitterion

Data showing the VDss obtained using the CRED device, HSA column chromatography and observed literature value are presented in Tables 19 to 22. A linear plot of HSA column chromatography log VDss for the acidic, basic, neutral and zwitterion series as a function of the CRED Log VDss gave correlation coefficient of 0.549 (Fig 34(a)). For the series of compounds investigated using the CRED device 81.3%, 86.7% and 41.2% of the calculated Log VDss representing acids, bases and neutrals respectively were within 3-fold of the value obtained using HSA column chromatography. Of the two zwitterions one was within 3-fold of the VDss HSA column chromatography value. On average 64.7% of the VDss data calculated using the CRED device was within 3-fold of the values obtained from HSA column chromatography data.

A linear plot of observed literature log VDss for the acidic, basic and neutral series of compounds as a function of the CRED Log VDss gave correlation coefficient of 0.5158 (Figure 34(b)). For the 27 compounds 66.7%, 77.8% and 22.2% of the calculated Log VDss representing acids, bases and neutrals respectively were within 3-fold of the value obtained using observed literature VDss. On average 55.6% of the VDss data calculated using the CRED device was within 3-fold of the values obtained from the observed literature data.

Table 19: Volume of Distribution data for the Acidic Series from CRED, HSA Column Chromatography and Observed Literature

Compound Number	CRED Log VDss	HSA Column Chromatography Log VDss	Observed Literature Log VDss
CC16817 (Diazoxide)	-0.147	-0.135	-0.678
GR62550X (Flurbiprofen)	-2.523	-1.022	-
GR87272X (Nimesulide)	-0.644	-0.759	-
GR138714X (Zafirlukast)	-1.387	-0.253	-
GR70487A (Pravastatin)	-0.123	-0.013	-0.337
CCI120 (Indomethacin)	-0.227	-0.876	-1.018
GR33000X (Piroxicam)	-1.292	-0.848	-
GW289865X (Etodolac)	-0.801	-0.402	-
GSK275458A (Oxaprozin)	-1.051	-1.032	-
GR87036X (probenecid)	-0.780	-0.701	-0.886
AH22182X (Sulfinpyrazone)	-1.229	-0.742	-0.921
SB213421Z (tolmetin)	-1.602	-0.790	-
GR1189894X (Furosemide)	-0.879	-0.435	-0.921
BRL15541QQ (Ketoprofen)	-1.602	-1.013	-0.886
GI235401X (Diflunisal)	-0.514	-0.860	-1.013
GW622791X (Irbesartan)	-0.273	-0.604	-0.027

Table 20: Volume of Distribution data for the Basic Series from CRED, HSA Column Chromatography and Observed Literature

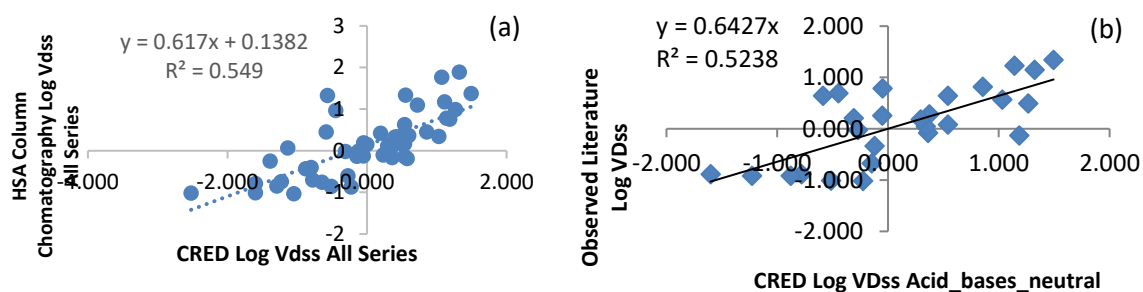
Compound Number	CRED Log VDss	HSA Column Chromatography Log VDss	Observed Literature Log VDss
CCI3993 (Promethazine)	1.322	1.891	1.146
SB-731710 (Aripiprazole)	-0.447	0.961	0.690
CCI3748 (Haloperidol)	1.139	0.781	1.230
GR30676X (Propafenone)	0.434	0.591	0.342
SKF-95914 (Ebastine)	-0.569	1.207	-
GR35842A (Procyclidine)	1.184	0.756	-0.131
GR43175X (Sumatriptan)	0.192	0.417	0.230
GF120454X (Amoxapine)	1.071	1.766	-
SB-416332-AAA (Venlafaxine)	0.538	0.623	0.643
CCI3839 (Orphenadrine)	0.854	0.358	0.813
GR61317X (Metergoline)	0.550	1.332	-
GW769340A (Tomoxetine)	1.110	1.176	-0.071
CCI20557A (Verapamil)	1.031	0.338	0.568
CCI4001 (Propranolol)	1.265	0.991	0.491
GR84804A (Nortriptyline)	1.494	1.371	1.342
GR77494A (Amiloride)	0.402	0.326	
GR189721X (Olanzapine)	0.723	1.097	

Table 21: Volume of Distribution data for the Neutral Series from CRED, HSA Column Chromatography and Literature

Compound Number	CRED Log VDss	HSA Column Chromatography Log VDss	Observed Literature Log VDss
GR91295X(Pentoxifylline)	-0.053	-0.125	0.255
CCI9371(Spironolactone)	0.485	0.173	-
CC122428(Methylprednisolone)	0.540	0.167	0.079
GR104104X (Zileuton)	0.536	-0.171	-
GF120403X(Metolazone)	-0.309	-0.019	0.204
GI115674X(Rolipram)	0.232	-0.102	-
AH23463X(Dapsone)	0.360	-0.165	-0.081
GW388185X(Celecoxib)	-1.137	0.064	-
GR119497X(Letrozole)	0.373	0.167	0.279
GR33914X(Nimodipine)	0.341	0.057	0.041
GR38393X(Nitrendipine)	-0.051	0.190	0.785
GR64334X(Felodipine)	-0.587	0.447	0.643
GW703803X(Bicalutamide) Casodex	0.574	-0.190	-
GI116108X(Isadipine)	0.294	0.114	0.176
GI99296X(Leflunomide)	-0.004	0.152	-

Table 22: Volume of Distribution data for the Zwitterion Series from CRED, HSA Column Chromatography and Observed Literature

Compound Number	CRED Log VDss	HSA Column Chromatography Log VDss	Observed Literature Log VDss
GR99941A	0.599	0.362	-
GW300671A	0.342	0.407	-

**Fig 34:** Linear plot of HSA Column Chromatography (a) and Observed Literature (b) Log VDss as a function of CRED Log VDss across acidic, basic and neutral series.

2.7.2. Trend Analysis of the Volume of the Distribution obtained using the CRED across calculated Molecular Descriptors obtained using in-house Plexus Suite software for acids, bases, neutrals and Zwitterions. Bases are denoted with a blue colour, acids in red and neutrals in green.

Table23: - Variation of VDss obtaining using CRED with the Total Polar Surface Area (TPSA) across acid, base and neutral

Compound	TPSA	Phase 1_CRED Log VDss
GR91295X	75.51	-0.053
CC122428	94.83	0.540
GF120403X	92.5	-0.309
AH23463X	86.18	0.360
GR119497X	78.29	0.373
GR38393X	110.45	-0.051
GR64334X	64.63	-0.587
CCI9371	60.44	0.485
GI116108X	103.55	0.294
GR104104X	66.56	0.536
GI115674X	47.56	0.232
GW388185X	77.98	-1.137
GW703803x	107.3	0.574
GR33914X	119.68	0.341
GI99296X	55.13	-0.004
CC16817	78.82	-0.147
GR62550X	40.13	-2.523
GR87272X	98.42	-0.644
GR138714X	112.93	-1.387
GR70487A	127.12	-0.123
CCI120	71.36	-0.227
GR33000X	102.43	-1.292
GW289865X	65.15	-0.801
GSK275458	66.16	-1.051
GR87036X	77.51	-0.780
AH22182X	57.69	-1.222
SB213421Z	62.13	-1.602
GR11898X	125.46	-0.879
BRL15541Q	57.2	-1.602
GI235401	60.36	-0.514
GW622791	84.23	-0.273
CCI13993	150.98	1.322
SB-731710	46.01	-0.447
CCI3748	41.74	1.139
GR30676	36.78	0.434
GR35842	24.67	1.184
SKF95914	30.74	-0.569
GR43175X	66.4	0.192
GF120454X	41.44	1.071
SB-416332-AAA	33.9	0.538
CCI3839	13.67	0.854
GR61317X	47.7	0.550
GW769340A	25.84	1.110
CCI20557A	65.15	1.031
CCI4001	46.07	1.265
GR84804A	16.61	1.494
GR77494A	158.5	0.402
GR189721X	32.07	0.723

GR99941	57.04	0.599
GW300671	85.03	0.342

Table 24: - Variation of VDss obtaining using CRED with the Partition Coefficient (Log P) across acid, base, neutral and Zwitterion

Compound	Log P	Phase 1_ CRED Log VDss
GR91295X	0.13	-0.053
CC122428	1.88	0.54
GF120403X	2.92	-0.309
AH23463X	1.31	0.36
GR119497X	2.76	0.373
GR38393X	1.98	-0.051
GR64334X	3.07	-0.587
CCI9371	3.44	0.485
GI116108X	2.07	0.294
GR104104X	1.82	0.536
GI115674X	1.66	0.232
GW388185X	3.83	-1.137
GW703803X	2.52	0.574
GR33914X	2.23	0.341
GI99296X	2.5	-0.004
CC16817	4.77	-0.147
GR622550X	4.06	-2.523
GR87272X	1.94	-0.644
GR138714	6.19	-1.387
GR70487A	1.27	-0.123
CCI120	3.31	-0.227
GR33000X	1.02	-1.292
GW289865	2.84	-0.801
GSK275458	3.54	-1.051
GR87036X	2.31	-0.780
AH22182X	3.3	-1.222
SB213421Z	2.15	-1.602
GR11898X	1.66	-0.879
BRL155410Q	2.76	-1.602
GI235401X	3.89	-0.514
GW622791X	5.74	-0.273
CCI13993	4.4	1.322
SB-731710	4.79	-0.447
CCI3748	3.08	1.139
GR30676	6.4	0.434
SKF95914	6.74	-0.569
GR35842	3.27	1.184
GR43175X	1.01	0.192
GF120454X	3.2	1.071
SB-416332-AAA	2.25	0.538
CCI3839	3.62	0.854
GR61317X	4.08	0.55
GW769340	3.78	1.11
CCI20557A	4.55	1.031
CCI4001	2.5	1.265
GR84804A	4.57	1.494
GR77494A	-0.090	0.402
GR189721X	3.09	0.723
GR99941	3.48	0.599
GW300671	5.68	0.342

Table 25: - Variation of VDss obtaining using CRED against Distribution Coefficient (Log D) across acid, base, neutral and Zwitterion

Compound	Log D	Phase 1_CRED Log VDss
GR91295X	0.1	0.608
CC122428	1.88	0.659
GF120403X	2.9	0.043
AH23463X	1.3	0.298
GR119497X	2.8	0.653
GR38393X	2	-0.135
GR64334X	3.1	0.136
CCI9371	3.4	2.048
GI116108X	2.1	0.135
GR104104X	1.8	0.536
GI115674X	1.69	0.232
GW388185X	3.8	-1.137
GW703803	2.52	0.574
GR33914X	2.2	0.341
GI99296X	2.5	-0.004
CCI16817	1.8	-0.147
GR622550X	1.2	-2.523
GR87272X	1.4	-0.644
GR138714	5.1	-1.387
GR70487A	-1.8	-0.123
CCI120	0.0	-0.227
GR33000X	-0.5	-1.292
GW289865	0.2	-0.801
GSK275458	1.1	-1.051
GR87036X	-1.2	-0.780
AH22182X	1.2	-1.222
SB213421Z	-1.1	-1.602
GR11898X	-1.4	-0.879
BRL15541Q	0.2	-1.602
GI235401	0.2	-0.514
GW622791	3.2	-0.273
CCI13993	2.7	1.322
SB-731710	4.5	-0.447
CCI3748	2.3	1.139
GR30676	5.4	0.434
SKF959514	5.7	-0.569
GR35842	1.2	1.184
GR43175X	-1.1	0.192
GF120454X	1.8	1.071
SB-416332-AAA	0.7	0.538
CCI3839	2.1	0.854
GR61317X	3.2	0.55
GW769340A	1.4	1.11
CCI20557A	2.3	1.031
CCI4001	0.2	1.265
GR84804A	1.6	1.494
GR77494A	-0.4	0.402
GR189721X	2.9	0.723
GR99941	0.2	0.599
GW300671	2.5	0.342

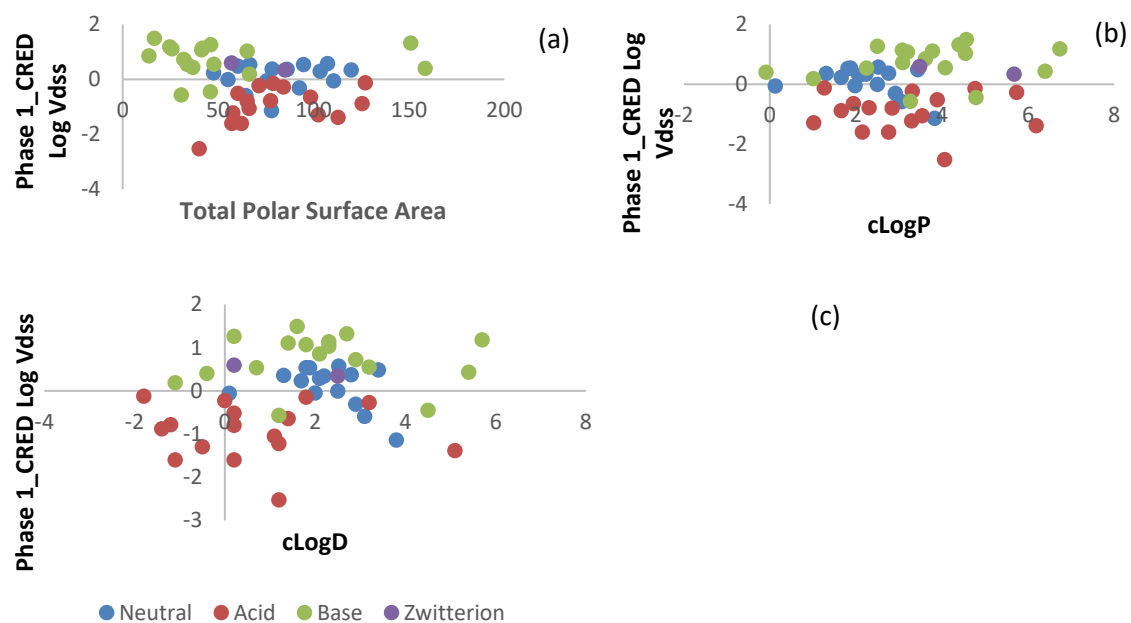


Fig 35: Trend Analysis showing Variation of VDss obtained using CRED with the Total Polar Surface Area (a), cLogP (b) and cLogD (c) across acid, base, neutral and Zwitterion.

Table: 26 - Variation of VDss obtaining using CRED against HB acceptor, donor and total number of hydrogen bond across acid, base, neutral and zwitterion

Compound	HB acceptor	HB donor	Total HB	Phase 1_CRED VDss
GR91295X	7	2	7	-0.053
CC122428	5	3	8	0.54
GF120403X	6	2	8	-0.309
AH23463X	4	2	6	0.36
GR119497X	5	0	5	0.373
GR38393X	8	1	9	-0.051
GR64334X	5	1	6	-0.587
CCI19731	4	0	4	0.485
GI116108X	8	1	9	0.294
GR104104X	4	2	6	0.536
GI115674X	4	1	5	0.232
GW388185X	5	1	6	-1.137
GW703803	2	9	11	0.574
GR33914X	0	1	1	0.341
GI99296X	4	1	5	-0.004
CC16817	5	2	7	-0.147
GR622550X	2	1	3	-2.523
GR87272X	7	1	8	-0.644
GR138714	9	2	11	-1.387
GR70487A	7	4	11	-0.123
CCI120	5	1	6	-0.227
GR33000	7	2	9	-1.292
GW289865	4	2	6	-0.801
GSK275458	4	1	5	-1.051
GR87036	5	1	6	-0.780
AH22182	5	0	5	-1.222
SB213421	4	1	5	-1.602
GR11898X	7	3	10	-0.879
BRL15541Q	3	1	4	-1.602
GI235401	3	2	5	-0.514
GW622791	7	1	8	-0.273
CCI13993	11	4	15	1.322
SB-731710	5	1	6	-0.447
CCI3748	3	1	4	1.139
GR30676	4	1	5	0.434
SKF95914	3	0	3	-0.569
GR35842	2	1	3	1.184
GR43175X	5	2	7	0.192
GF120454X	4	1	5	1.071
SB-416332-AAA	3	1	4	0.538
CCI3839	2	0	2	0.854
GR61317X	5	1	6	0.55
GW769340A	2	1	3	1.11
CCI20557A	6	0	6	1.031
CCI4001	3	2	5	1.265
GR84804A	1	1	2	1.494
GR77494A	8	5	13	2.048
GR189721X	4	1	5	0.723
GR99941	1	5	6	0.599
GW300671	3	5	8	0.342

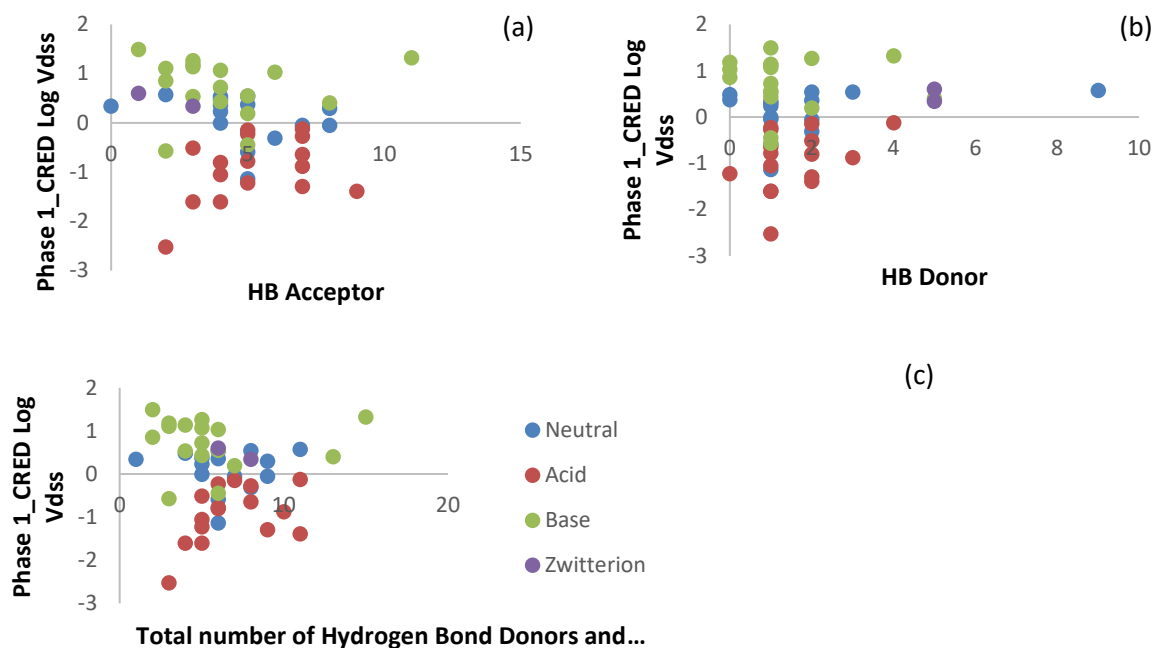


Fig 36:- Trend Analysis showing Variation of VDss obtaining using CRED against HB acceptor (a), HB donor (b) and total number of hydrogen bond donors and acceptors (c) across acid, base, neutral and Zwitterion.

Table 27: Variation of VDss against pKa of hydrogen bond across acid, base, neutral and zwitterion obtained using CRED

Compound	pKa	Phase 1_CRED VDss
Neutrals		
GR91295X	-1.2	-0.053
CCI22428	12.6	0.659
GF120403X	9.54	0.043
AH23463X	2.39	0.36
GR119497X	1.89	0.373
GR38393X	1.89	-0.051
GR64334X	3.07	-0.587
CCI9371	3.44	0.485
GI116108X	2.07	0.249
GR104104X	8.84	0.536
GI115674X	-1.93,14.28	0.232
GW388185X	-0.41,10.60	-1.137
GW703803X	11.78	0.574
GR33914X	2.23	0.341
GI99296X	-0.45,13.72	-0.004
Acids		
CCI16817	4.31	-0.147
GR62550X	4.42	-2.523
GR87272X	6.86	-0.644
GR138714X	4.29	-1.387
GR70487A	4.21,	-0.123
CCI120	3.79	-0.227
GR33000X	4.76,	-1.292
GW289865X	4.73	-0.801
GSK275458	4.95	-1.051
GR87036X	3.53	-0.780
AH22182X	3.86	-1.222
SB213421Z	3.93	-1.602
GR118989X	4.25	-0.879
BRL15541Q	3.88	-1.602
GI235401	2.69	-0.514
GW622791	4.12	-0.273
Bases		
CCI3993	9.05	1.322
SB-731710	7.45	-0.447
CCI3748	8.05	1.139
GR30676	8.38	0.434
GR35842	9.45	1.184
SKF95914	8.43	-0.569
GR43175X	9.54	0.192
GF120454X	8.83	1.071
SB-416332-AAA	8.91	0.538
CCI3839	8.87	0.854
GR61317X	8.22	0.55
GW769340A	9.80	1.11
CCI20557A	8.68	1.031
CCI4001	9.67	1.265
GR84804A	10.47	1.494
GR189721X	7.24	0.723
GR77494A	11.43	0.402

2.7.3. Validation Study Conducted in Parallel using analytical techniques CRED and Column Chromatography

In order to assess both methods in parallel a selection of 8 untested compounds was sent to the Ware site for CRED analysis, with only their plate position as reference. The experimental procedure, analysis and calculations were out carried as described previously. The named compounds were added post data analysis. The results obtained using both methods are shown below Table 28. The linear correlation coefficient obtained was 0.7857 (Fig 37 (a)). Exclusion of the data point for compound GSK3782748A which had the largest difference between the two methods gave a linear correlation coefficient of 0.9742 (Fig 37(b)).

Table 28: HSA Binding data using CRED analysis and HSA column chromatography for NCEs

Compound Unknown	HSA Binding CRED	HSA Binding Data Phychem Group (% HSA)
GSK3782748A	26	75.84
GSK3782776A	63.1	81.85
GSK3787507A	71.6	81.33
GSK3782743A	49.6	69.27
GSK3780469A	79.1	92.62
GSK3780771A	17.1	33.16
GSK3781631A	90.9	95.12
GSK3780440A	15.6	32.9

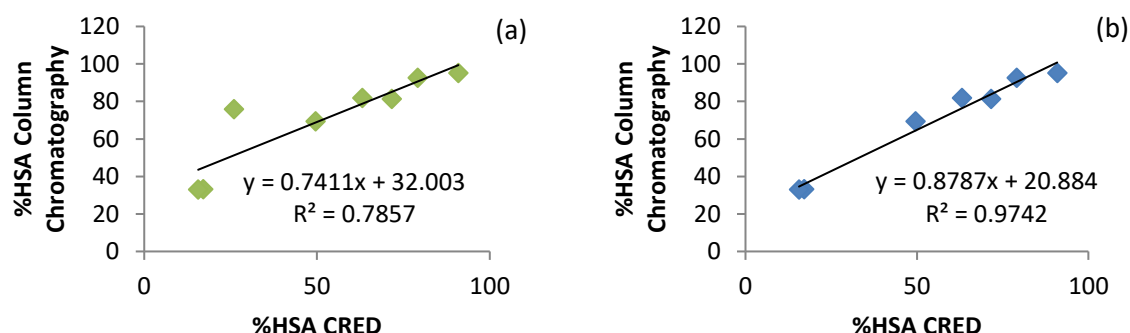


Fig 37: The linear plot of the chromatographic HSA binding data as a function of the CRED HSA binding for NCEs with (a) and without (b) the outlier.

2.7.4. Discussion: Simple Design Model of the CRED

The %HSA binding and LogVDss data shows the capability of the CRED device to deliver a wide range of values 9.6% to 99.2% (Table 6) and -2.523 to 1.494 (Tables 15 to 18) respectively, across a variety of compounds in a competitive and fluid environment that is a more realistic representation of the *in-vivo* situation.

PLEXUS Suite software was used to access the compound database and generate physicochemical properties across the series of compounds investigated. Set at the experimental physiological pH of 7.4 along with the calculated pKa values (the degree of ionization) the corresponding structure of the major microspecies were generated (pages 35 to 55). Of the 16 acid molecules investigated 14 were 100% ionised at physiological pH,

GW622791 was 97% ionised and GR87272 was 78% ionised. At pH values higher than the pKa, acids are deprotonated and therefore exists largely in the ionised (anionic negatively charged) state (Manallack, Prankerd et al. 2013). Most of the acids (12 out of 16) were greater than 95% bound to HSA highlighting the effect of the negatively charged molecules on plasma protein binding (Table 6). There were however a few exceptions (GW622791, GR70487, GR87036 and CCI16817) that were less than 95% bound even though they were in the ionised form.

Of the 15 basic molecules investigated 10 were over 95% ionised. At pH values lower than the pKa, bases are protonated and therefore exists largely in the ionised (cationic, positively charged) state (Manallack, Prankerd et al. 2013). Most of the bases (12 out of 15) were less than 95% bound to HSA showing a reverse effect of positively charged molecules on plasma protein binding. A few exceptions (GR30676, SKF95914 and GR61317) were more than 95% bound even though they were 91%, 92% and 87% respectively, in the ionised form at the physiological pH. This could be as a result of structural rearrangement which changes the molecules into a more uncharged state increasing its lipophilicity and therefore binding to HSA.

For the neutral compounds 6 of the 17 showed %HSA binding over 95% while most of the remaining molecules were between 40 and 80%. As expected, the binding to HSA decreased as follows acids > neutrals > zwitterions > bases. This is in keeping with the general a rule of thumb (Gleeson 2008) that the negatively charged acids will preferential bind to the alkaline protein (HSA) (Spector 1975). Bases on the other hand are generally positively charged at pH of 7.4, have stronger electrostatic interactions with the negatively charged phosphate group of phospholipids and therefore binds less to the HSA.

However, the binding of drug molecules to plasma proteins is very complex as acids and bases may bind to specific proteins in plasma. Acids tend to bind more to HSA than bases, whereas the latter are also more likely to bind to lipoprotein and alpha 1-acid glycoprotein (AGP). HSA also has various binding sites which accounts for the highest enantioselectivity and therefore enantiomers can show differences in binding data. From the HSA data generated using the CRED device (Table 8) the differences in correlation coefficients were 0.862, 0.640, 0.7366 and 0.798, 0.9377, 0.8991 for the acids, bases and neutrals respectively Fig 30 (a), (b), (c) and Fig 31 (a), (b), (c). The overall correlation coefficient obtained between HSA binding using the CRED and observed literature PPB compared to HSA binding using column chromatography and observed literature PPB were 0.6473 and 0.8858 respectively, Fig 30 (d,) and Fig 31(d). The data highlights the complex nature of binding. The basic compounds contributed largest to the lower overall correlation coefficient. For the basic compounds the HSA binding was generally lower for CRED compared to the HSA column chromatography and observed literature PPB. The largest difference was for compounds CCI3839 (Orphenadrine), CCI120557A (Verapamil) 31.9% and 35.9% respectively as against 81.0% and 90.7% for observed literature. The corresponding data for HSA binding using column chromatography was similar to the observed literature.

In order to investigate the discrepancy in binding data for CCI3839 and CCI120557A (Table 8) a literature search was conducted. Plasma proteins are highly selective in binding drug molecules and can therefore show differences in binding due to enantiodifferentiation. The binding enantio-differentiation of 4 antihistamines including CCI3839 (Orphenadrine) to HSA was done by (Martínez-Gómez, Villanueva-Camañas et al. 2007) and showed that CCI3839 (Orphenadrine) has the highest enantioselectivity with binding values of between 24 to 38%

for one enantiomer and 82 to 85% for the other. In another study (Gross, Heuer et al. 1988), Verapamil (CCI120557), the free fractions of the enantiomers were different based on binding to either HSA or alpha 1-acid glycoprotein (AGP). The free fraction was roughly 0.6 for the (-) form and was unaffected by change in drug concentration when bound to HSA. Whereas the free fraction varied between 0.12 and 0.37 with increasing concentration drug concentration when bound to a1-acid glycoprotein (AGP). Data therefore suggest that Verapamil (CCI120557) is roughly 40% bound to HSA and 63 to 88% bound to a1-acid glycoprotein (AGP). The HSA binding values obtained using the CRED were 31.9% and 35.9% respectively for CCI3839 and CCI120557 and reflected the enantio-differentiation that occurs in PPB. Assigning the HSA data of both compounds as outliers improved the correlation coefficient when compared to observed literature from 0.640 to 0.807 for the bases Fig 30(b) and Fig 30(e) and the overall correlation coefficient from 0.6473 to 0.7649 Fig 30(d) and Fig 30(f).

Apart from the %HSA binding the VDss also takes in account the relative binding to PC. From the series of compounds investigated, the positively charged bases have relatively lower %HSA binding (higher unbound fraction) compared to higher %PC binding (lower unbound fraction) resulting in relatively higher VDss compared to the acids and neutrals (Fig 33). However, other physicochemical descriptors e.g. the logarithm of the partition coefficient (logP) which gives a measure of the lipophilicity, the logarithm of the distribution (logD) which gives a measure of the hydrophobicity of the uncharged portion only of the drug molecule at pH 7.4, total polar surface area (TPSA), total number of hydrogen bonds and number of hydrogen bond acceptors may play a role in plasma protein binding and VDss (Pajouhesh and Lenz 2005). Basic compounds GR30676, SKF95914 and GR61317 as mentioned previously binds strongly to HSA. This is attributed to relatively larger logD values of 5.4, 5.7 and 3.2 respectively (Table 25) which shows that hydrophobicity dominates binding instead of the charged state.

As the total polar surface area of the bases increases the VDss decreases (Fig 35 (a)). From Fig 35 (b) a variation in logP does not appear to influence VDss of acids. However in keeping with (Lobell and Sivarajah 2003) it does appear from the data generated that as the logP increases it generally leads to an increase VDss for bases and neutrals. The complex nature of predicting VDss is highlighted by basic compounds SB731710 and SKF-95914 which although having relatively high lipophilicity 4.79 and 6.74 respectively, have low VDss. Variation of logD also does not appear to influence VDss across acids but may influence bases and to a lesser extent neutral (Fig 35 (c)). Neutral compound GW388185 although not in a negative charge state is 99.6% bound to HSA which could be attributed to a logD of 3.83 and correspondingly a low VDss (-1.137).

In general, as the number of hydrogen bond acceptors of the bases increases the VDss decreases (Fig 36 (a)). This may be due to a less lipophilic characteristic and therefore a reduction in tissue binding i.e. to PC resulting in a higher fraction unbound and therefore a reduction in VDss (Obach, Lombardo et al. 2008). As the number of total polar surface area and hydrogen bond acceptors of the acids increases the relative VDss within the group increases (Fig 35 (a) and 36 (a)). From the graphs, neutrals are not affected by changes in the number of hydrogen bond acceptors and total polar surface. The number of hydrogen bond donors does not appear to have any effect on the VDss for the series of compounds investigated (Fig 36 (b)).

There was a general increase in the %PC binding (Table 11 to 13) as the phosphatidylcholine concentration increases highlighting the importance of phospholipids in the distribution of (Li, Wang et al. 2015) and potential use as a transport medium for low solubility and low bioavailability of drug molecules. This could also be used to identify, rank the order of binding to different organs *in vivo* and provide a valuable decision tool for drug progression or termination due to on or off target engagement. The free concentration data (Table 10) obtained between and within the series of compounds could be used to compare, enhance and influence study design in early discover to better predict dosing frequency to achieve the desired therapeutic concentration or understand toxicity issues.

In order to obtain robust, accurate and reliable data a search of publicly available human clinical pharmacokinetic data was conducted for comparison of observed literature VDss against the experimental CRED VDss data. The research paper (Obach, Lombardo et al. 2008) was used as the single source of information regarding human VDss and plasma protein binding for consistency. Of the 50 compounds investigated 27 were identified within this paper for comparison with the VDss and HSA binding obtained using CRED device.

The correlation coefficient (R^2) of the VDss between HSA column chromatography, observed literature against CRED were 0.55 and 0.52, Fig 34 (a) and (b), respectively showed equal comparison. The VDss for three compounds SB731710(base), GR64334(neutral) and AH23463(neutral) which were common to all 3 methods contributed largely to the resulting correlations. SB731710 has a low VDss (-0.447_CRED) suggesting that the drug resided mostly in the systemic compartment while higher VDss (0.961_HSA column chromatography and 0.690_Observed literature) suggest it resides mainly in the tissues (PC). GR64334 had a low VDss (-0.587_CRED) shows that the drug resided mostly in the systemic compartment while higher VDss (0.447_ HSA column chromatography and 0.643_ Observed literature) suggest it resides mainly in the tissues (PC). AH23463 had a higher VDss (0.360) shows that the drug resided mostly in the tissue while lower VDss (-0.165 and -0.081) suggest it resides mainly in the HSA (plasma).

The calculation of VDss *in-vitro* can be difficult as mechanism other than passive diffusion occurs *in vivo*. Other factors (Yap and Chen 2005), (Giacomini, Huang et al. 2010) e.g. functional groups (primary-secondary-tertiary amines, fluorine), nonspecific binding sites, spatial conformation, size, active transport and/or a combination of these factors can also affect drug partitioning between plasma and tissue proteins. Individual physicochemical properties or their combinations may dominate and drive the direction of drug binding and therefore the VDss. In terms of a qualitative assessment however there was a strong agreement (Table19) between all 3 methods in terms of the VDss of the acids i.e. molecules reside in the systemic (HSA4) compartment (low VDss). The VDss of the bases and neutrals were 75% and 44% in agreement across all 3 methods.

The ability to deliver accurate HSA and tissue protein binding data has been established with this simple experimental model of the CRED device. Additional benefits include the ability to generate free concentration data across a series of compounds. As a qualitative assessment of the VDss the results are encouraging with the VDss for neutrals being clearly the bottle neck. The current design of CRED device includes phosphatidylcholine as a tissue surrogate. Although phosphatidylcholine is the major phospholipid of tissue cell membrane other

phospholipids are present and may have varying affinity for drug molecules potentially impacting the VDss. The other major phospholipids are phosphatidylserine, phosphatidylinositol and phosphatidylethanolamine. The unionised form of drug molecules will have greater affinity for phosphatidylcholine a neutral phospholipid (Small, Gardner et al. 2011) while the acidic phospholipids phosphatidylserine, phosphatidylinositol which are ionised at the physiological pH have strong electrostatic interactions with the partly ionised and ionised basic compounds effecting a change in the VDss. In order to better represent the in-vivo situation an investigation of the impact that other major phospholipids has on the VDss particularly across the neutral series of compounds will be carried out using a modified design.

2.8. Investigation in Improving the Drug Distribution between Human Serum Albumin and the major phospholipids to better mimic the in-vivo situation:

To further characterise the CRED and better simulate *in vivo* drug distribution, the competitive binding between human serum albumin (HSA) and phospholipids *in-vitro* was further investigated by the addition of phosphatidylethanolamine (PE), phosphatidylinositol (PI) and phosphatidylserine (PS) individually (Fig 39) and combined (Fig 40) within the six-compartment model. These experiments are described as Phase 2 and Phase3, respectively. In the previous experimental design Phase 1 (Fig 38) phosphatidylcholine, a neutral lipid at various concentrations was utilised. The addition of phosphatidylethanolamine, phosphatidylserine and phosphatidylinositol with different physico-chemical properties (e.g phosphatidylserine is an acidic lipid) may alter the partitioning of the analyte across the semi-permeable membrane and therefore its VDss (Murakami, Yumoto et al. 2011). Comparing the VDss (CRED) from phase 2 and 3 against literature values and with the previous data set from phase1 will enable the assessment of potential impact of the different designs on the VDss with respect to observed literature data.

PC1	PC2
PC2	PC3
Buffer	Open well for sampling HSA

Fig 38: Simplified view of Phase 1 design: PC at 100mg/mL, 200mg/10mL and 300mg/10mL

PC	PI
PS	PE
Buffer	Open well for sampling HSA

Fig 39: Simplified view of Phase 2 design: Individual compartments containing PC, PE, PI and PS at 83.2, 24.05, 13.5 and 2.7mg/10mL, respectively.

PCEIS	PCEIS
PCEIS	PCEIS
Buffer	Open well for sampling HSA

Fig 40: Simplified view of Phase 3 design: Combined phospholipids to mimic in-vivo concentration of 162, 67.5, 13.5 and 2.7mg/10mL, respectively

2.8.1. Physiological Concentration of Major Phospholipids

In terms of total lipid composition in liver tissue, phosphatidylethanolamine accounts for approximately 25% (10.125g in wet liver), followed by phosphatidylinositol 5% (2.025g in wet liver). The concentration of phosphatidylserine is negligible and was given a value of 1% (0.405 g in wet liver) of total lipid composition for simplicity. Other simple lipids e.g. cholesterol, triglycerols make up the rest of the total phospholipid composition but were not included. The physiological concentration of phosphatidylethanolamine, phosphatidylinositol and phosphatidylserine were therefore estimated to be 67.5mg/10mL, 13.5mg/10mL and 2.7mg/10mL, respectively, based on a liver volume of 1500mL.

2.8.2. Compound Selection and Reagents

A subset of the original set of 50 compounds (Table 29) for which observed literature values of VDss were obtained from the research paper by (Obach, Lombardo et al. 2008) were selected for Phases 2 and 3 investigation looking at the partition of drug molecules between HSA and phosphatidylcholine, phosphatidylethanolamine, phosphatidylinositol and phosphatidylserine.

Table29: List of compounds for which observed literature VDss data was found

Neutrals	Acids	Bases
GR91295X	GR70487	SB-731710
CC122428	CCI120	CCI3748
GF120403	GR11898	SB-416332-AAA
AH23463	GI235401	CCI4001
GR119497	GW622791	GR84804A
GR38393X		
GR64334		
GI116108		
GR35842		

The selected compounds (acids, bases and neutrals) were ordered from the GSK compound Store (Harlow) and were received in a plate format as 150µL solutions dissolved in DMSO to give a concentration of 10mM and stored in a -80°C freezer. FeSSIF powder was purchased from Biorelevant.com (42 New Road London E1 2AX, United Kingdom). Phosphatidylethanolamine, phosphatidylserine and phosphatidylinositol were obtained from Sigma as Phosphatidylethanolamine (from egg yolk), 1,2-Diacyl-sn-glycero-3-phospho-L-serine, and L-α-Phosphatidylinositol sodium salt from (soya bean). Human serum albumin lyophilized powder >= 97%, HPLC grade methanol, acetonitrile, propanol and ammonium formate were purchased from Sigma Aldrich (The Old Brickyard, New Road, Gillingham, Dorset, UK). PBS tablets and 1.4mL Micronics were obtained from Gibco-life technologies, Thermo Scientific (Stafford House, 1 Boundary Park, Hemel Hempstead, UK). Polypropylene graduated tubes (1.5 -1.7mL and 15 mL) were purchased from Fisher Scientific (Bishop Meadow Road, Loughborough, UK)

2.8.3. Preparation of Samples within CRED Device Prior to Incubation

Phosphatidylethanolamine (PE), phosphatidylserine (PS) and phosphatidylinositol (PI) were obtained as 25mg, 25mg and 10mg powders respectively and dissolved in 1% phosphate buffered saline (PBS) to give concentrations of 48.1mg/10mL, 2.7mg/10mL and

13.5mg/10mL, respectively. Phosphatidylcholine (PC) was dissolved in 1% phosphate buffered saline (PBS) to give concentrations of 83.2mg/10mL. Dilution factors of 1.4, 1.0, 1.0, and 1.9 will be considered when calculating the fraction of the tissue unbound undiluted (fu undiluted) for phosphatidylethanolamine, phosphatidylserine, phosphatidylinositol and phosphatidylcholine based on endogenous levels of 67.5mg/10mL, 2.7mg/10mL, 13.5mg/10mL and 162mg/10mL respectively. Using the 6-chamber format of the CRED device, 2.5 mL of 2µM individually spiked drug molecule in HSA (50g/l) is added to the well. The inserts were loaded with 200 µL of control phosphatidylethanolamine, phosphatidylserine, phosphatidylinositol, phosphatidylcholine and 1% PBS, respectively. An adhesive sealing tape was then placed over the entire plate lid to prevent evaporation during incubation. The appropriately labelled CRED device was then placed onto an orbital shaker at 600 rpm in the incubator set at 37°C. Incubate for a minimum 4hr to reach equilibrium. Post equilibrium dialysis, 10µL aliquots were taken from each insert along with a 10µL aliquot of spiked HSA sampled from the open end of the single membrane insert. In order normalise matrix and suppression effects, 40 µL of individually prepared “partial matrix” to achieve total matrix match was added to the relevant 10 µL aliquot. Samples were extracted by addition of 200 µL of acetonitrile/methanol/water (volume ratio 85/10/5) containing an in-house generic internal standard [²H ¹³C₃]-SB243213. Samples were then briefly mixed and centrifuged for 10 min at 3000 rpm after which there are ready for injection onto the HPLC-MS/MS system for analysis.

2.8.4. Preparation of Calibrations standards

Working solutions were prepared by adding 5 µL (10 mM stock) of 4 individual analytes to 180 µL acetonitrile/water 50/50 (v/v) to give individual concentrations of 250 µM. Using 10-fold serial dilutions, additional working solutions in acetonitrile/water were prepared to realise concentrations of 25, 2.5 and 0.25 µM, respectively. An assay range of 0.005 to 5 µM was prepared for each analyte by addition of no more than 5% volume of working solutions to previously prepared “total matrix” to give calibrations standards of 0.005, 0.01, 0.02, 0.1, 0.5, 1.0, 4.0 and 5 µM, respectively. “Total matrix” was prepared by mixing equal volumes of 1% PBS, control HSA at 50 g/L, PE (48.1mg/10mL), PS (2.7mg/10mL), PI (13.5mg/10mL) and PC (83.2mg/10mL), respectively. Protein precipitation was carried out by extracting 50 µL duplicate aliquots of each standard using 200 µL of acetonitrile/methanol/water (volume ratio 85/10/5) containing an in-house generic internal standard [²H¹³C₃]-SB243213. Samples were then briefly mixed and centrifuged for 10 min at 3000 rpm after which there are ready for injection onto the HPLC-MS/MS system for analysis

2.8.5. Volume of Distribution (Vdss) *In-vivo*

The Vdss *in-vivo* is calculated using the equation below, where *F_{up}* refers to the fraction unbound in HSA, *F_{ut}*(undiluted) is the undiluted fraction unbound in phospholipids. The summation of the individual Vdss within each compartment gives the overall Vdss within the system. Values obtained are then compared with the observed literature data.

For phase 2 a factor was applied to the calculated Vdss for PC, PE, PI and PS individually, based on their relative physiological concentrations in vivo to normalise the binding effect.

Factors applied were 0.6,0.25,0.05 and 0.01 based on the relative abundance in vivo of 60, 25, 5 and 1% respectively. In the case of phase 1 and 3 this normalisation factor was not applied as the phospholipids were either of the same type within the device or combined. The correlation between the VDss of different phases of CRED design, normalised(N) and non-normalised (NN) against the observed literature data provide an indication of the predictability of in vivo drug distribution.

$$Eqn18: Vdss = Total \Sigma \frac{Fup}{Fut(undiluted)}$$

2.8.6. Results

Table 30: Phase1: Volume of Distribution across neutrals, acids and bases for Observed Literature and CRED

	Compound	Observed Literature Log VDss	Phase 1_CRED Total Log VDss
Neutral	GR91295	0.255	0.549
	CC122428	0.079	1.049
	GF120403	0.204	0.209
	AH23463	-0.081	0.898
	GR119497	0.279	0.905
	GR38393	0.785	0.429
	GR64334	0.643	0.112
	GI116108	0.176	0.774
Acid	GR70487	-0.337	0.449
	CCI120	-1.018	0.157
	GR11898	-0.921	-0.561
	GI235401	-1.013	-0.252
	GW622791	-0.027	0.024
Bases	SB-731710	0.69	0.022
	CCI3748	1.23	1.554
	GR35842	-0.131	1.673
	SB-416332-AAA	0.643	1.001
	CCI4001	0.491	1.678
	GR84804	1.342	1.903

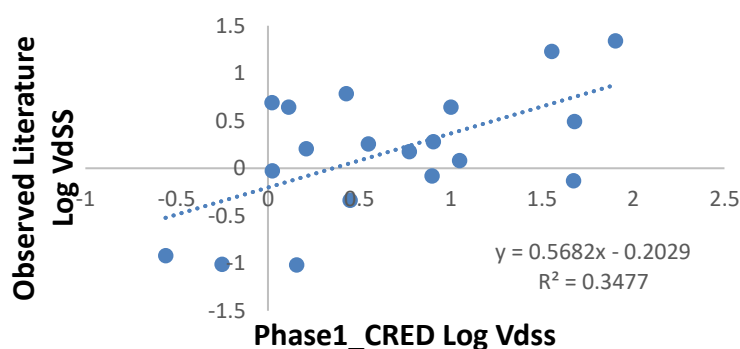


Fig 41: Phase 1: Plot showing Comparison of Vdss CRED against observed literature using phosphatidylcholine at different concentrations

Table 31: -Phase2: Normalised(N) Volume of Distribution across neutrals, acids and bases for Observed Literature and CRED

	Compound	Observed Literature Log VDss	N-Phase 2_CRED Log Total VDss
Neutral	GR91295	0.255	0.036
	CC122428	0.079	0.088
	GF120403	0.204	-0.352
	AH23463	-0.081	-0.345
	GR119497	0.279	0.101
	GR38393	0.785	-0.450
	GR64334	0.643	-0.299
	GR35842	-0.131	1.473
	GI116108	0.176	-0.394
	GR70487	-0.337	-0.333
Acids	CCI120	-1.018	-2.102
	GR11898	-0.921	-1.282
	GI235401	-1.013	-1.457
	GW622791	-0.027	-0.907
Bases	SB-731710	0.69	-0.210
	CCI3748	1.23	0.698
	GR35842	-0.131	1.473
	SB-416332-AAA	0.643	0.220
	CCI4001	0.491	0.801
	GR84804	1.342	0.722

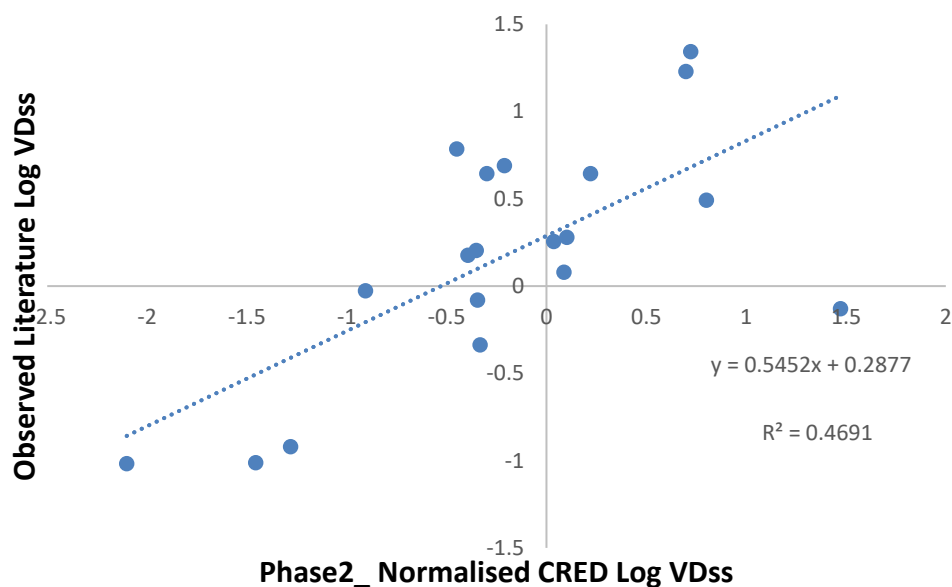


Fig 42 Phase 2: Plot showing Comparison of Normalised(N) Vdss CRED against observed literature using phosphatidylcholine, phosphatidylethanolamine, phosphatidylinositol and phosphatidylserine individually in separate compartments

Table 32: -Phase2: Non-Normalised (NN) Volume of Distribution across neutrals, acids and bases for Observed Literature and CRED

	Compound	Observed Literature Log VDss	NN-Phase 2_CRED Log Total VDss
Neutral	GR91295	0.255	0.608
	CC122428	0.079	0.659
	GF120403	0.204	0.043
	AH23463	-0.081	0.298
	GR119497	0.279	0.653
	GR38393	0.785	-0.135
	GR64334	0.643	0.136
	GI116108	0.176	0.135
Acid	GR70487	-0.337	0.246
	CCI120	-1.018	-1.640
	GR11898	-0.921	-0.731
	GI235401	-1.013	-1.046
	GW622791	-0.027	-0.454
Base	SB-731710	0.69	0.435
	CCI3748	1.23	1.251
	GR35842	-0.131	2.048
	SB-416332-AAA	0.643	0.787
	CCI4001	0.491	1.278
	GR84804	1.342	1.336

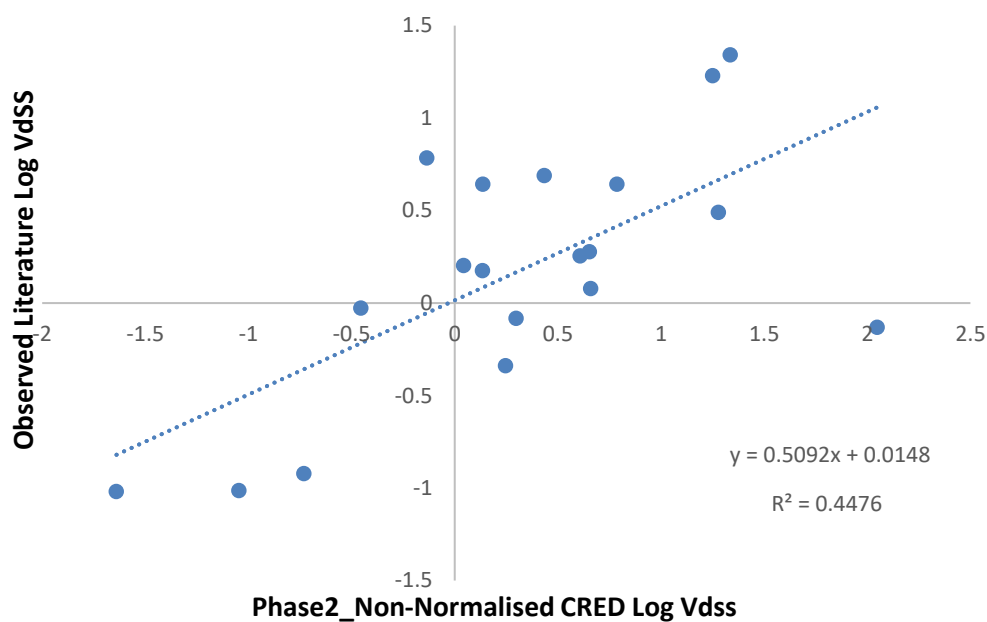


Fig 43: Phase 2: Plot showing Comparison of Non-Normalised (NN) Vdss CRED against observed literature using phosphatidylcholine, phosphatidylethanolamine, phosphatidylinositol and phosphatidylserine individually in separate compartments

Table 33: -Phase3: Non-Normalised (NN) Volume of Distribution across neutrals, acids and bases for Observed Literature and CRED

	Compound	Observed Literature Log VDss	NN-Phase 3_CRED Log Total VDss
Neutral	GR91295	0.255	0.635
	CC122428	0.079	0.740
	GF120403	0.204	0.128
	AH23463	-0.081	0.575
	GR119497	0.279	0.664
	GR38393	0.785	0.125
	GR64334	0.643	0.073
	GI116108	0.176	0.464
Acid	GR70487	-0.337	0.634
	CCI120	-1.018	-0.699
	GR11898	-0.921	-0.261
	GI235401	-1.013	-0.82
	GW622791	-0.027	0.019
Base	SB-731710	0.69	0.379
	CCI3748	1.23	1.722
	GR35842	-0.131	1.474
	SB-416332-AAA	0.643	0.995
	CCI4001	0.491	1.806
	GR84804	1.342	2.057

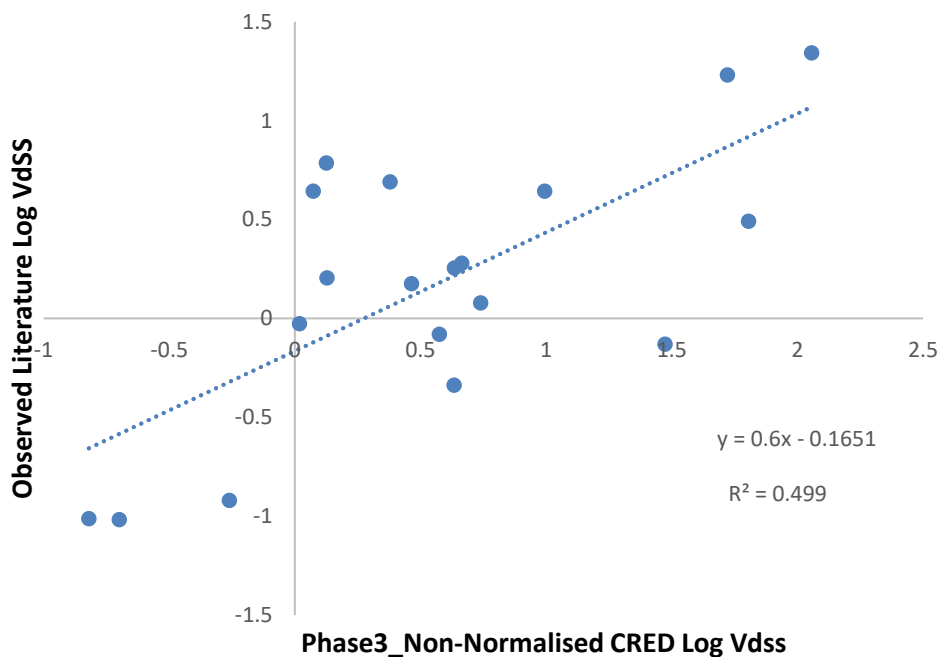


Fig 44 Phase 3: Comparison of Non-Normalised (NN) Vdss CRED against observed literature using phosphatidylcholine, phosphatidylethanolamine, phosphatidylinositol and phosphatidylserine combined.

2.8.7. Trend Analysis of VDss with Physico-chemical descriptors

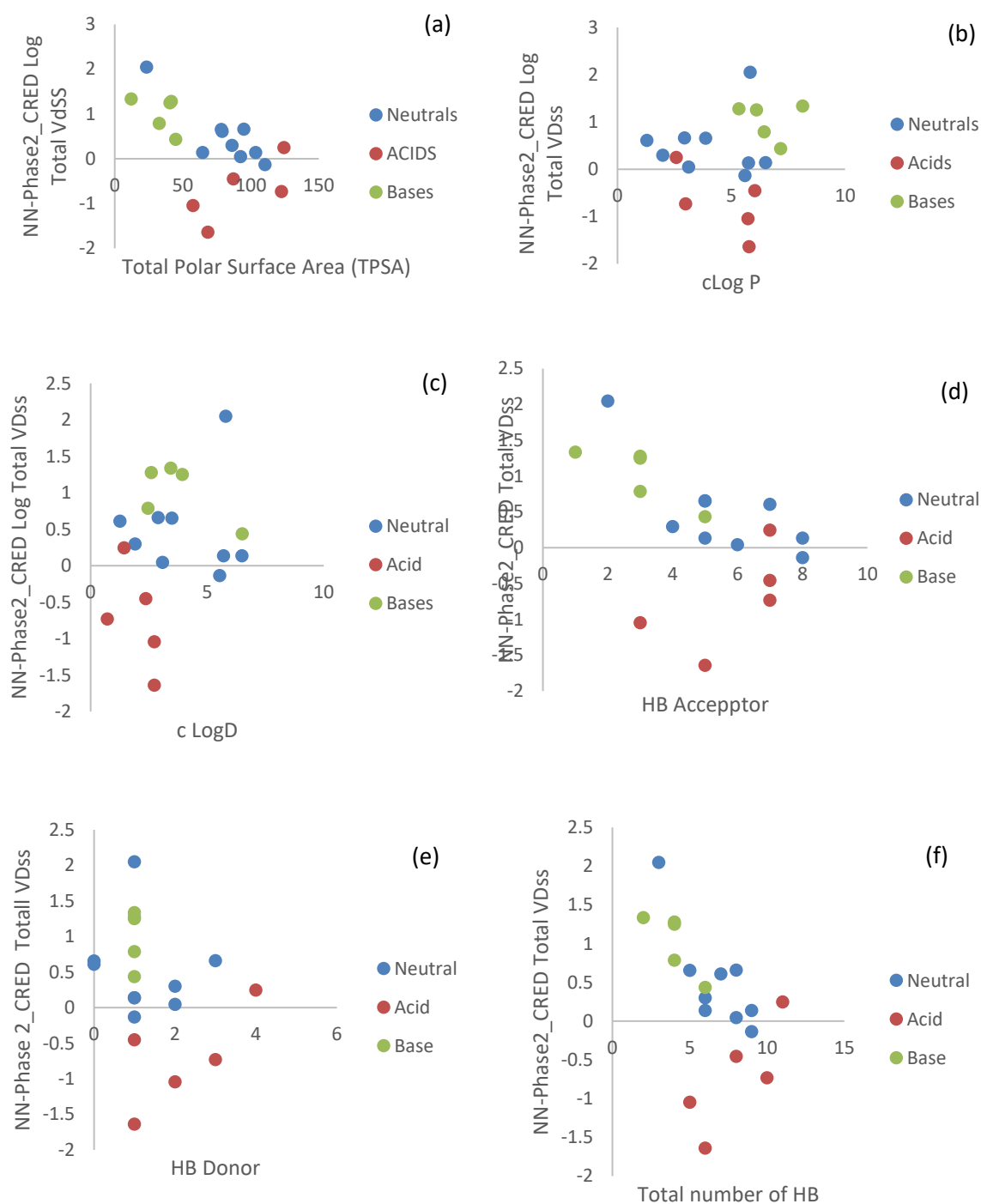


Fig 45. Trend Analysis showing the relationship between Phase 2 non-normalised Volume of distribution (VDss) and physicochemical descriptors: Total Polar Surface Area (a), cLogP (b) which represents the Lipophilicity, cLogD (c) which represents Dissociation, number of hydrogen bond acceptors (d), number of hydrogen bond donors (e) and the total number of hydrogen bonds which is the sum of the hydrogen bond acceptors and donors (f).

2.8.8. Variation of VDss Across Different CRED Designs Compared to the Observed Literature VDss as Standard

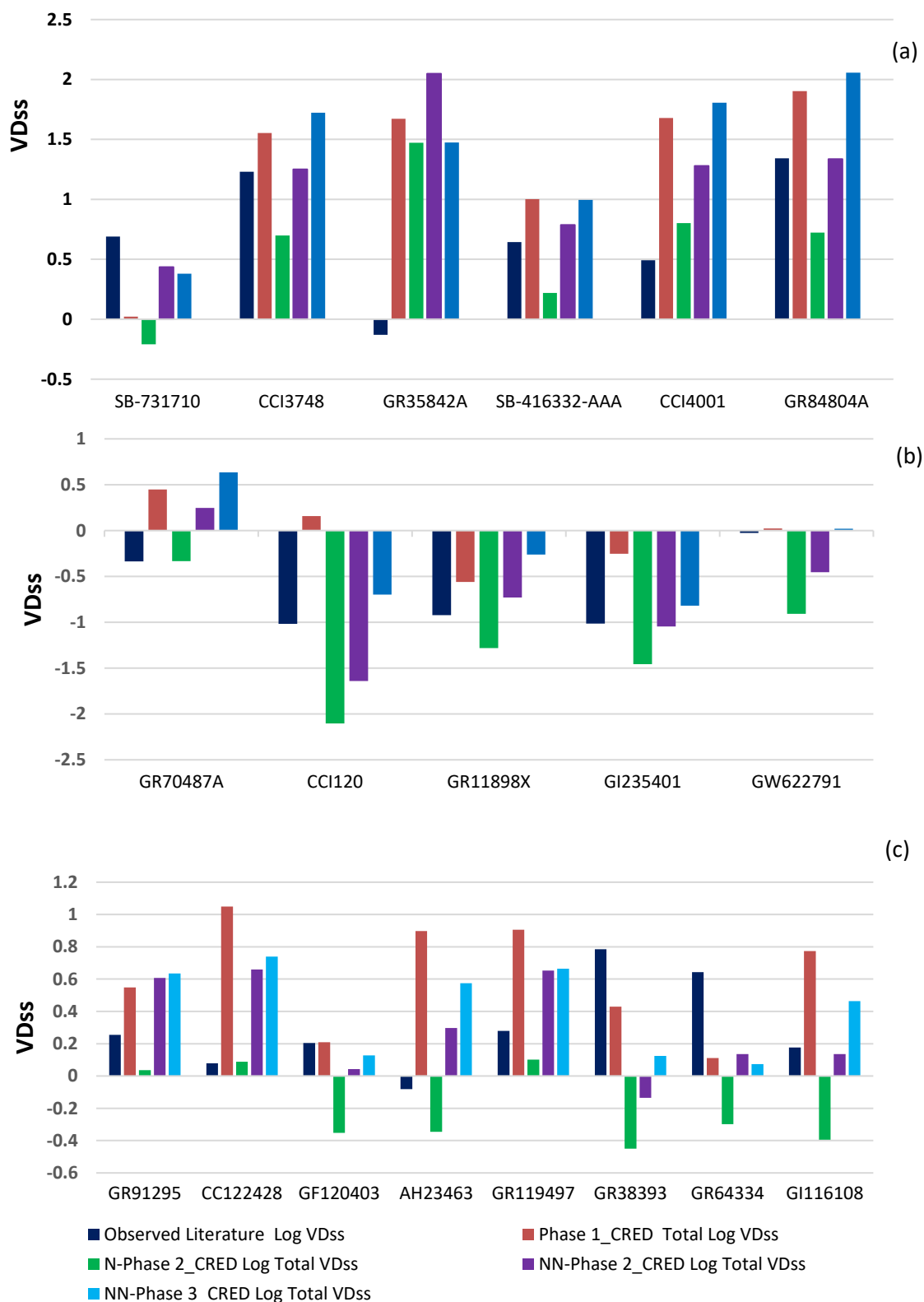


Fig 46: VDss of the observed literature relative to the CRED various processes for bases (a), acids (b) and Neutral (c) compounds

2.8.9. Replot of Volume of Distribution across neutrals, acids and bases for Observed Literature and CRED Excluding Outliers

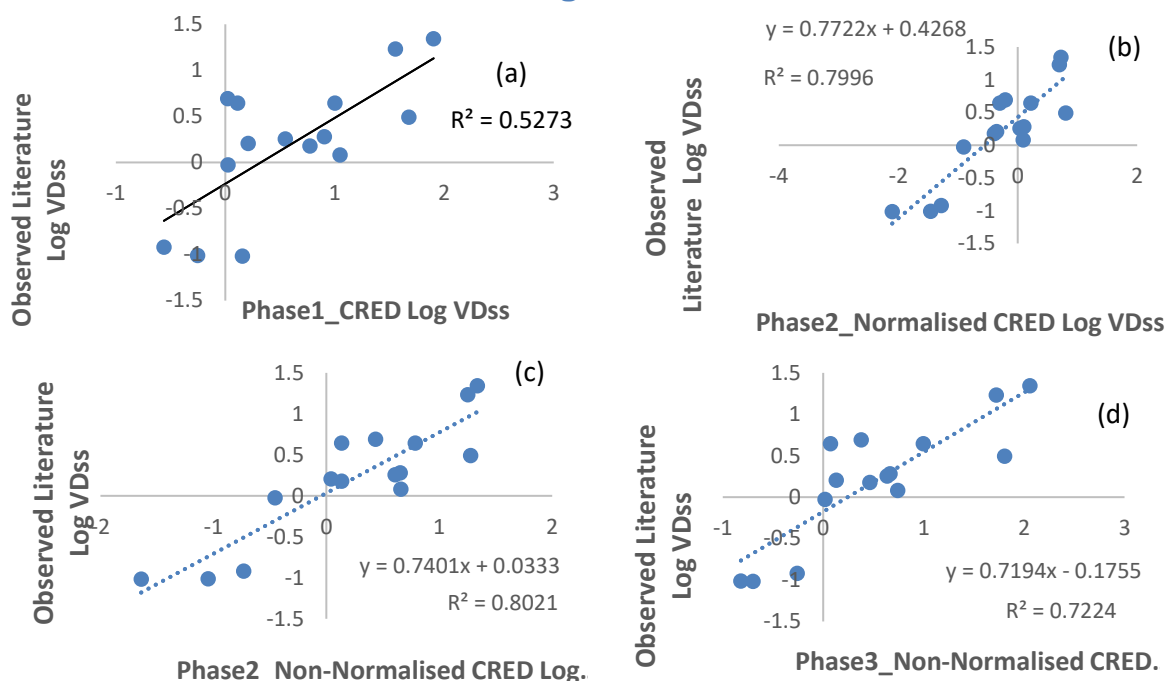


Fig 47: Plot showing Comparison of Vdss CRED against observed literature over the 3 phases excluding outliers

2.9. Data summary

Modifications to the original phase1 CRED design were carried out in phases 2 and 3 to assess the impact on the VDss by including phosphatidylethanolamine, phosphatidylserine and phosphatidylinositol (other major phospholipids) either individually or combined.

For phase 2 project design where PC, PE, PI and PS were in separate compartments, normalisation factors based on their relative amounts in vivo were applied individually to the calculated VDss (non-normalised) to give a normalised VDss (Table 31). Comparison of normalised and non-normalised VDss (Table 32) was used to assess whether applying a rating or weight has an impact on the VDss compared to observed literature. Where a single phospholipid type was used as in the case of study design in phase 1 (Table 30) or combined as in phase 3 (Table 33) this factor was not applied. The method of extraction and analysis were the same irrespective of the study design.

2.10. Discussion

The linear correlation coefficients (R^2) obtained were 0.3477, 0.4691, 0.4476 and 0.499 for the VDss obtained from phase1, 2 (normalised), 2 (non-normalised) and phase 3, respectively when compared to the VDss observed literature (Fig 41, 42, 43 and 44). This would suggest an improvement of around 10% from phase 1 to phases 2 and 3 in relation to the observed literature. There was no difference between normalised and non-normalised for the compounds tested (0.4691 and 0.4476).

From the trend analysis showing the variation of the VDss with physicochemical descriptors (Fig 45) it was reaffirmed that a drug molecule with lower TPSA, higher lipophilicity (cLogP), lower HB acceptor and lower total HB is more likely to have a higher VDss. This structure-VDss relationship is already well understood- and applied by scientist in drug development to predict drug distribution *in-vivo*. The trend analysis of the VDss with molecular descriptors TPSA, cLogP, HB acceptor and total HB agrees with the research paper “Trend Analysis of a Database of Intravenous Pharmacokinetic Parameters in Humans for 670 Compounds.

A graphical and qualitative assessment of the varying designs across acids, bases and neutrals (Fig 46) was performed in order to view the relative bias and therefore identify which compounds are outliers irrespective of the CRED experiment performed. An outlier analysis to establish which compounds were to be excluded based on the different experimental designs and processes to give the best predictive model *in-vivo*. A criterion was adopted whereby if two or more of the processes or designs used within the CRED device generated a VDss that was of a different bias to the observed literature value these compounds were categorised as outliers. Compounds GR35842A, GR70487A and AH23443 were therefore classified as outliers and the stats regenerated to give linear correlation coefficients (R^2) of 0.5273, 0.7996, 0.8021 and 0.7224 for the VDss obtained from phase1, 2(normalised), 2(non-normalised) and phase3 respectively, when compared the observed literature data. The revised plots are shown in Fig 47. The observed literature VDss for GR35842A had a negative bias compared to the other basic compounds investigated across the different CRED design types (Fig 46 (a)). This suggest that GR35842A has a low VDss *in vivo* and is mostly located with the plasma compartment. GR35842 is positively charged at pH 7.4 suggesting it is a basic compound more likely to have a higher VDss. The data from the CRED device is relevant to passive diffusion as transfer mechanism *in vivo*. Therefore, GR35842 may be subjected to another transport mechanism *in vivo* besides passive distribution that occurs in the CRED device. GR70487A and AH23443 may also be subjected to another transport mechanism other than passive diffusion, enantioselectivity or structural rearrangement *in vivo*.

Altering the design of the CRED through the inclusion of phosphatidylethanolamine, serine, and inositol (other major phospholipids) either individually or combined has improved the VDss relative to the observed literature. The application of the normalisation factor does not appear to impact the VDss in the cases tested due to the major impact that phosphatidylcholine has on the overall binding effect compared to the lower concentrations of PE, PS and PI. The concentrations used was based on the relative amounts in the liver with PC accounting for a larger percentage of the total phospholipids. However, the concentration of PE in the brain, heart and kidney is larger than PC (Choi, Yin et al. 2018) and therefore, may have a greater effect on the distribution of the drug molecule. The CRED is a passive system during which distribution across a semi-permeable membrane is based on an existing concentration gradient. The VDss data generated shows the impact and importance of passive drug distribution *in-vivo* with a correlation of around 0.8. As a passive system the CRED does not include transporter or clearance mechanisms and therefore is limited by its application to accurately predict the VDss based on the observed literature which is assumed to be correct. However, in most cases tested the CRED device provides a qualitative assessment of the where the drug molecule may reside based on its physicochemical properties and the VDss generated. There is also potential to create a model using the results of the molecules in

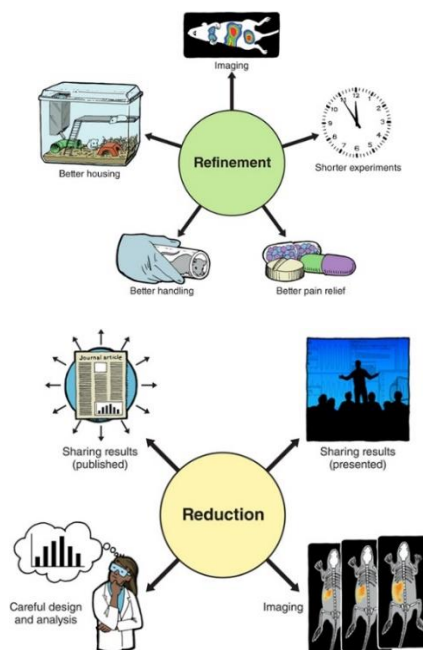
phases 2 and 3 and their molecular descriptors as a set of tool compounds (except for outliers) to predict the VDss of an unknown drug.

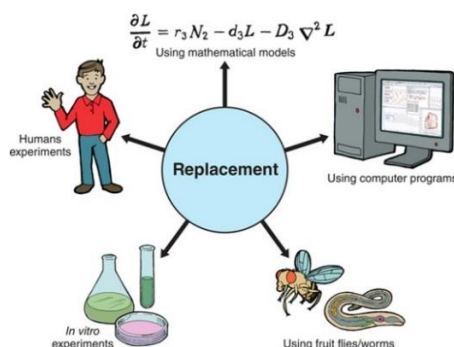
Chapter 3: Feasibility of the Competitive Rapid Equilibrium Dialysis in the Reduction, Refinement and Replacement of Animals in Scientific testing (3Rs)

3.1. An Investigation into Plasma protein Binding of Different Species in Parallel using the CRED.

The 3Rs refers to the refinement, reduction, and replacement of animals in scientific testing. This concept was put forward by Russell and Burch in their book “*The Principles of Humane Experimental Technique*” and was first published in 1959. They proposed and challenged the scientific community to identify and adopt policies and procedures that would improve the treatment of laboratory animals without compromising the integrity and quality of the scientific studies. By utilizing the 3Rs it minimizes the potential for animal pain and distress in scientific research that uses animals.

So far in this research the CRED has been used to determine plasma protein binding (PPB), free concentration (Cu), Volume of Distribution (VD), using Human Serum Albumin (as surrogate for human plasma) with competitive binding against phosphatidylcholine (surrogate for tissue cell membranes) in the first instance and also a more complex system involving other major phospholipids thereafter. Using the compartmentalized system of the CRED device may offer valuable insight into whether there is potential for its use as an *in-vitro* system to aid in the 3Rs during scientific testing by investigating binding across various species.





Plasma protein binding is important in drug development as it influences the amount of free drug that is available to go to the site of action and elicit a pharmacological response. Drug molecules are therefore optimized to gain a better understanding of the relationship between fraction of drug unbound and the pharmacodynamic effect. Comparison of plasma protein binding from various matrices e.g., rat, dog, mouse and human are used to predict and account for differences in PK and PD data. The determination of PPB from various species is usually done individually *in-vitro* (Påhlman and Gozzi 1999). The CRED provides a novel platform to investigate and compare PPB from various species simultaneously. An initial investigation using GSK compound GSK2485680 (novel GSK compound for which a bioanalytical method was being developed at the time, but for which the project was terminated, structure not provided) to assess PPB across different species in parallel rather than individual assays was conducted with a view to explore the possibility of reducing animal usage. Plasma protein binding was investigated at 100 and 1000ng/mL GSK2485680 using the CRED on 3 separate occasions in triplicate.

3.1.1. Method

Control rat, dog, mouse plasma was obtained from Marshall Bioresource, healthy pooled human plasma was obtained from GSK. Phosphatidylcholine (PC) used as a surrogate for tissue cell membrane was obtained from biorelevant and dissolved in 1% phosphate buffered saline (PBS) to give an endogenous concentration of 162mg/10ml. Compound GSK2485680 was obtained from SHANGHAI STA, China and dissolved in acetonitrile/water to give a concentration of 1mg/mL. Phosphate buffer saline was spiked with GSK2485680 to give 100 and 1000ng/mL, respectively. Using the 6-chamber format of the CRED device, 2.5 mL of 100 and 1000ng/mL GSK2485680 in 1%PBS was added individually to separate wells. Each well was loaded with inserts containing 200µL of rat, dog, human, mouse plasma and phosphatidylcholine, respectively. This allows for the parallel distribution of the drug between the various matrices. An adhesive sealing tape was then placed over the entire plate lid to prevent evaporation during incubation. The CRED device was then placed onto an orbital shaker at 600 rpm in the incubator set at 37°C. Post equilibrium dialysis, 10µL aliquots were taken from each insert along with a 10µL aliquot of spiked phosphate buffer sampled from the open end of the single membrane insert. In order normalise matrix and suppression effects, 40 µL of individually prepared “partial matrix” to achieve total matrix match was added to the relevant 10 µL aliquot. Samples were extracted by addition of 200 µL of acetonitrile/methanol/water (volume ratio 85/10/5) containing an in-house generic internal

standard [$^2\text{H } ^{13}\text{C}_3$]-SB243213. Samples were then briefly mixed and centrifuged for 10 min at 3000 rpm after which they were ready for injection onto the HPLC-MS/MS system for analysis.

Rat Plasma	Dog Plasma
Human Plasma	Mouse Plasma
Phosphatidylcholine	Open well for sampling Buffer

Layout of the CRED to investigate PPB to rat, dog, human, mouse plasma and phosphatidylcholine simultaneously.

3.1.2. Preparation of Calibrations standards

Working solutions were prepared by adding 50 μL (1.0 mg/mL stock) to 450 μL acetonitrile/water 50/50 (v/v) to give 0.1 mg/mL. Using 10-fold serial dilutions, additional working solutions in acetonitrile/water were prepared to realise concentrations of 0.01, 0.001 and 0.0001 mg/mL, respectively. An assay range of 1 to 1000 ng/mL was prepared by addition of no more than 5% volume of working solutions to previously prepared “total matrix” to give calibrations standards of 1, 2, 5, 30, 100, 400, 800 and 1000 ng/mL, respectively. “Total matrix” was prepared by mixing equal volumes of 1% PBS, control rat, dog, human plasma and phosphatidylcholine (162 mg/10 mL), respectively. Protein precipitation was carried out by extracting 50 μL duplicate aliquots of each standard using 200 μL of acetonitrile/methanol/water (volume ratio 85/10/5) containing an in-house generic internal standard [$^2\text{H } ^{13}\text{C}_3$]-SB243213. Samples were then briefly mixed and centrifuged for 10 min at 3000 rpm after which there are ready for injection onto the HPLC-MS/MS system for analysis

3.1.3. Chromatographic and Mass Spectroscopy Conditions

A Perkin Elmer Sciex API5000 Mass Spectrometer using TurbolonSpray™ source in Multiple Reaction Monitoring was used for chromatographic peak detection. Generic HPLC gradient conditions were achieved with an Acquity C18 UHPLC column (50 x 2.1 mm, 1.7 μm) equilibrated to 50 °C (Waters Corporation Ltd). Data was acquired over a run time of 2.5 min. The organic mobile phase (B) was acetonitrile while for the aqueous mobile phase (A) 0.1% formic acid was used in positive acquisition mode. The generic HPLC condition used were 0.0 to 0.2 min at 5% acetonitrile, 0.2 to 1.5 min organic phase change 5 to 35% B, 1.5 to 2.0 min held at 95% B and 2.1 min back to the initial starting conditions. A Waters Acquity UPLC system was used to drive the mobile phases set to a flow rate of 0.5 mL/min in partial loop injection mode with an injection volume of 1 μL . Eluent from the column was diverted from the mass spectrometer up to 0.3 min and after 2.0 min to keep the mass spectrometer clean.

3.1.4. Data Acquisition and Processing

HPLC MS/MS data were acquired and processed (integrated) using the proprietary software application -Analyst™ (Version 1.4.2, Applied Biosystems/MDS Sciex, Canada). Calibration plots of analyte/internal standard peak area ratio versus individual analyte concentration were constructed and a weighted $1/x^2$ linear regression applied to the data. Concentrations of analytes were determined from the calibration line in “total matched matrix”.

3.2. Experimental Data obtained from Plasma protein Binding of Different Species in Parallel using the CRED

3.2.1. Experiment 1: Concentration of GSK248560 Post CRED using Protein Precipitation

Table 34: 1 % Phosphate Buffer spiked initially at 100ng/mL

Compound Number	Concentration of GSK2485680 (ng/mL)					
	Rat Plasma	Dog Plasma	Human Plasma	Mouse Plasma	Buffer	PC
Rep 1	77.5	80.4	83.1	60.6	42.2	66.1
Rep 2	75.0	78.7	91.3	61.2	44.7	61.6
Rep 3	77.8	78.7	87.3	60.2	42.3	63.9
Mean	76.7	79.3	87.2	60.7	42.0	63.9
SD	1.566	0.993	4.08	0.506	0.320	2.225
CV	2.0	1.3	4.7	0.8	0.8	3.5
Free Concentration (ng/mL)					42.0	
% Binding	45.2	47.0	51.8	30.7		34.2

Table 35: 1 % Phosphate Buffer spiked initially at 1000ng/mL

Compound Number	Concentration of GSK2485680 (ng/mL)					
	Rat Plasma	Dog Plasma	Human Plasma	Mouse Plasma	Buffer	PC
Rep 1	489.8	593.0	693.5	493.3	365.1	482.0
Rep 2	520.9	607.6	722.2	482.8	387.5	466.1
Rep 3	535.9	648.5	690.2	503.6	379.4	515.3
Mean	515.5	616.3	701.9	493.2	377.3	487.8
SD	23.5	28.8	17.6	10.4	11.3	25.2
CV	4.6	4.7	2.5	2.1	3.0	5.2
Free Concentration (ng/mL)					377.3	
% Binding	26.8	38.8	46.2	23.5		22.6

3.2.2. Experiment 2: Concentration of GSK248560 Post CRED using Protein Precipitation

Table 36: 1 % Phosphate Buffer spiked initially at 100ng/mL

Compound Number	Concentration of GSK2485680 (ng/mL)					
	Rat Plasma	Dog Plasma	Human Plasma	Mouse Plasma	Buffer	PC
Rep 1	97.9	109.2	164.4	56.6	41.9	47.8
Rep 2	81.8	114.6	176.9	57.3	37.0	48.6
Rep 3	85.9	119.6	166.5	62.5	39.8	55.5
Mean	88.5	114.5	169.3	58.8	39.5	50.6
SD	8.4	5.2	6.7	3.2	2.4	4.2
CV	9.4	4.5	3.9	5.5	6.1	8.4
Free Concentration (ng/mL)					42.0	
% Binding	55.3	65.5	76.6	32.8		21.9

Table 37: 1 % Phosphate Buffer spiked initially at 1000ng/mL

Compound Number	Concentration of GSK2485680 (ng/mL)					
	Rat Plasma	Dog Plasma	Human Plasma	Mouse Plasma	Buffer	PC
Rep 1	1005.5	1165.3	1651.2	558.6	400.5	511.6
Rep 2	960.0	1135.7	1563.5	542.7	400.0	525.4
Rep 3	965.0	1183.25	1604.0	601.4	531.4	495.8
Mean	976.8	1161.4	1606.2	567.5	444.0	510.9
SD	24.9	23.9	43.9	30.3	75.7	14.8
CV	2.6	2.1	2.7	5.3	17.0	2.9
Free Concentration (ng/mL)					444.0	
% Binding	54.6	61.8	72.4	21.8		13.1

3.2.3. Experiment 3: Concentration of GSK248560 Post CRED using Protein Precipitation

Table 38: 1 % Phosphate Buffer spiked initially at 100ng/mL

Compound Number	Concentration of GSK2485680 (ng/mL)					
	Rat Plasma	Dog Plasma	Human Plasma	Mouse Plasma	Buffer	PC
Rep 1	87.4	112.1	158.3	58.3	37.8	48.9
Rep 2	87.0	122.1	161.3	58.0	37.1	49.5
Rep 3	89.4	129.2	175.7	57.6	35.3	48.9
Mean	87.9	121.1	169.3	58.0	36.7	49.1
SD	1.30	8.6	6.7	0.351	1.27	0.334
CV	1.5	7.1	3.9	0.6	3.5	0.7
Free Concentration (ng/mL)					36.7	
% Binding	58.3	69.7	77.8	36.7		25.2

Table 39: 1 % Phosphate Buffer spiked initially at 1000ng/mL

Compound Number	Concentration of GSK2485680 (ng/mL)					
	Rat Plasma	Dog Plasma	Human Plasma	Mouse Plasma	Buffer	PC
Rep 1	953.2	1139.9	1698.9	628.6	372.1	571.1
Rep 2	952.5	1164.7	1805.2	595.3	397.4	511.0
Rep 3	911.9	1207.2	1748.0	621.3	382.8	538.7
Mean	939.2	1170.6	1750.7	615.1	384.1	540.3
SD	23.7	34.0	53.2	17.5	12.7	30.1
CV	2.5	2.9	3.0	2.9	3.3	5.6
Free Concentration (ng/mL)					384.1	
% Binding	59.1	67.2	78.1	37.6		28.9

3.2.4. Results

Parallel plasma protein binding values ranged from 30.7 to 36.7%, 45.2 to 58.3%, 47.0 to 69.7% and 51.8 to 77.8% in mouse, rat, dog and human plasma respectively, with 1% PBS initially spiked at 100ng/mL (Tables 34,36,38). At 1000ng/mL spiked in 1% PBS plasma protein binding ranged from 21.8 to 37.6%, 26.8 to 59.1%, 38.8 to 67.2% and 46.2 to 78.1% in mouse, rat, dog and human plasma respectively. (Tables 35,37,39).

The mean plasma protein binding in parallel across all 3 experiments were 33.4, 52.9, 60.7 and 68.7% for mouse, rat, dog and human respectively with 1%PBS initially spiked at 100ng/mL. The mean plasma protein binding in parallel across all 3 experiments were 27.6, 46.8, 55.9 and 65.6% for mouse, rat, dog and human respectively with 1%PBS initially spiked at 1000ng/mL.

Across all the species investigated the mean plasma protein binding with 1%PBS spiked at 100ng/mL were within 6% of the corresponding value spiked at 1000ng/mL in 1% PBS. Overall, there was no difference in PPB for the individual species across the two concentrations and a proportional 10-fold increase in free drug concentration with a 10-fold increase drug concentration was observed showing spiking proportionality. The free concentrations from the 3 experiments at 100ng/ml spiked PBS were 42.0, 39.5 and 36.7ng/mL respectively. The free concentrations at 1000ng/ml were 377.3, 444.0 and 384.1ng/mL. The mean free concentrations were 39.4 and 401.8ng/mL, respectively.

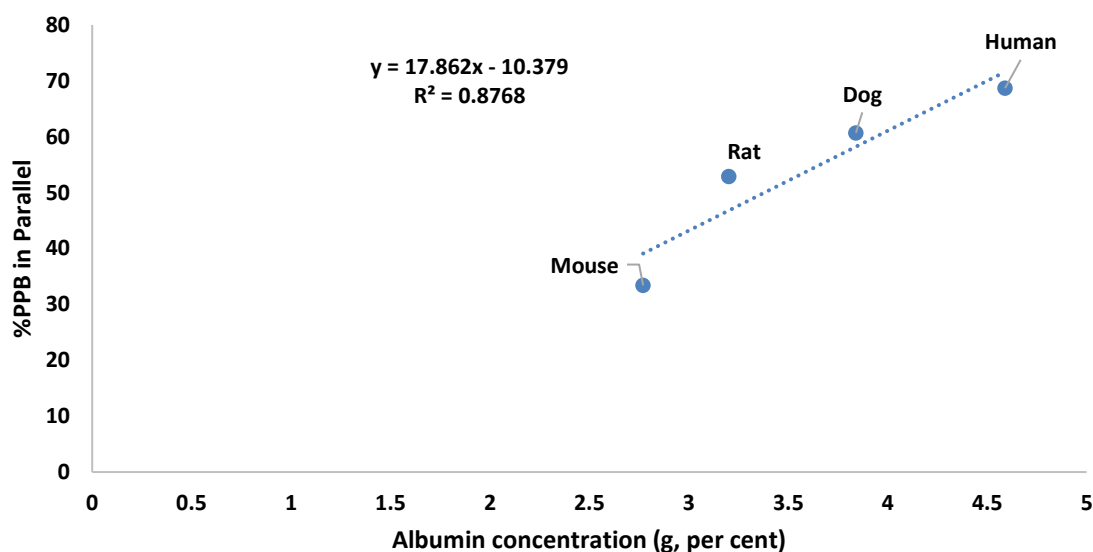


Fig 48 Variation of %PPB in Parallel using the CRED against Albumin concentration

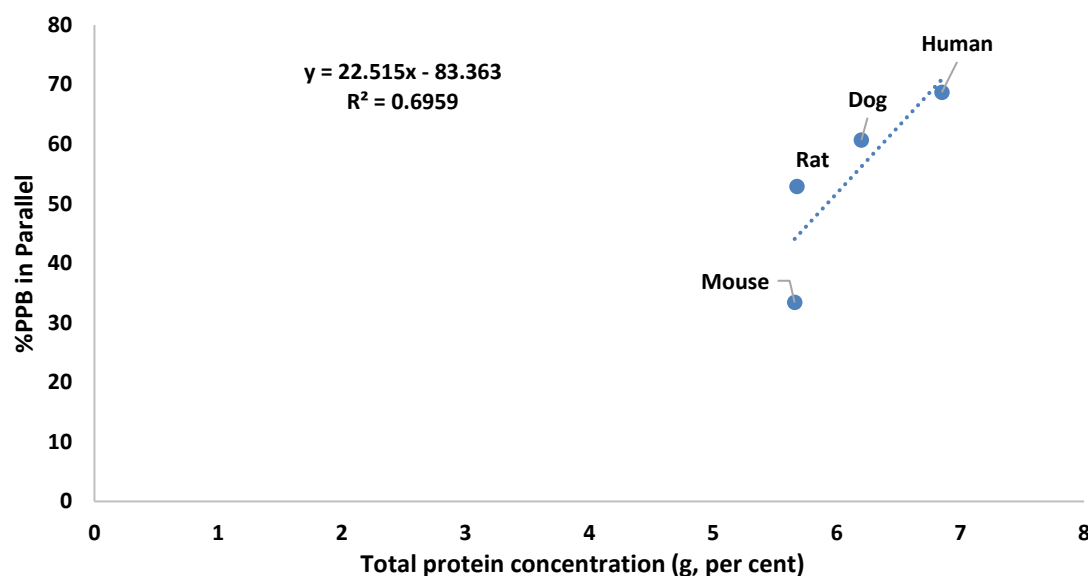


Fig 49: Variation of %PPB in Parallel using the CRED against Total Protein concentration

3.2.5. Discussion

Parallel PPB across species shows that there are differences in the order mouse <rat<dog <human for compound GSK2485680. This experiment follows the trend highlighted in research paper (Colclough, Ruston et al. 2014) where compounds tend to be more bound to human plasma proteins than to plasma proteins from preclinical species. The pharmacological effect is driven by the free drug concentration and therefore understanding the effects of differences in plasma protein binding across species is important in connecting and understanding the effects in human. Free drug concentration would therefore be expected to decrease in the order mouse > rat > dog > human for compound GSK2485680. The differences in plasma protein binding between mouse, rat, dog compared to human plasma using the CRED was less than 2.5-fold and therefore a good fit for predictability of PPB in the preclinical species from the human PPB data would be assumed.

The difference seen in the PPB *in-vitro* using the CRED where a competitive environment exist may be explained by the relative amount of albumin and total protein concentration present in each matrix. Using the concentration of albumin in mouse, rat, dog, and human plasma as 2.77, 3.2, 3.84 and 4.59g. per cent respectively (Morris and Courtice 1955), a plot of the % PPB in parallel versus albumin (g. per cent) gave a correlation coefficient of 0.8768 (Fig 48). Using the concentration of total protein in mouse, rat, dog, and human plasma as 5.66, 5.68, 6.20 and 6.85g per cent respectively (Morris and Courtice 1955), a plot of the % PPB in parallel versus total protein (g. per cent) gave a correlation coefficient of 0.6959 (Fig 49). As the albumin and protein content increased so does the PPB. The total protein content comprises AGP as and well as other proteins however the data suggest that the PPB is driven by binding to HSA. Therefore equation ($y = 17.862(x) - 10.379$) was used to predict the PPB of the individual matrix using their respective total albumin content. The predicted values in mouse, rat, dog, and human plasma were calculated as 39.0, 46.8, 58.2 and 71.6, respectively

A comparison of the mean HSA column binding for GSK2485680 obtained from the HELIUM software (A GSK repository of molecular descriptors for various compounds) and the mean PPB of the CRED (using the CRED device with matrices from different species in parallel spiked in 1%PBS at 100 and 1000ng/mL) were 66.5% (range 54.5 to 72.7%), 68.7% (range 51.8 to 77.8%) and 65.6% (46.2 to 78.1%), respectively. The data therefore suggest that for GSK2485680, HSA binding can also be obtained using the CRED from multiple species in parallel.

Cross species differences in PPB for GSK2485680 was obtained using the CRED device and was attributed to their relative albumin and total protein concentration with binding to serum albumin being dominant. This interpretation would allow for the use of diluted human serum albumin to mimic the concentration in the individual preclinical species to be used potentially replacing the traditional individual PPB assays involving preclinical species. This would contribute to the 3Rs and enable high throughput within drug discovery setting where human plasma is readily available. The use of preclinical species to study and interpret the pharmacodynamics and pharmacokinetics of drug molecules is however important in understanding the efficacy and toxicological effects for translation and prediction in humans. Therefore, as compounds progress PPB studies may need to be conducted individually in the relevant species. GSK2485680 is a single compound with low PPB (<98%) and therefore further investigation using a variety of molecules with various physiochemical properties is needed for further evaluation in replacing, reducing, and refining the use of preclinical species in plasma protein binding studies.

3.3. Further Investigation into Plasma protein Binding Across Different Species in Parallel using subset of tool Compounds

The PPB data obtained across multiple species in parallel using test compound GSK2485680 follows the trend highlighted by (Colclough, Ruston et al. 2014) where it was concluded that drug molecules are more bound to human plasma proteins than to plasma proteins from preclinical species. This was argued as a potential to reduce the requirement for multiple assays across individual species and therefore prediction of PPB across preclinical species can be drawn using data from the human *in-vitro* experiment.

To further assess the relative binding across various species in parallel using the CRED device a subset of the tool compounds across acids, bases and neutrals were also evaluated. The resulting data are presented (Tables 40, 41 and 42). The PPB data for individual compounds within each series was plotted against the albumin concentration of the different species (Figures 50, 51 and 52) to further evaluate binding predictability across species.

3.3.1. Results

Table 40: %PPB across mouse, rat, dog, and human for a subset of acid compounds (structures on pages 36,37 and 39)

Species	Albumin (g percent)	PPB CRED Acid				
		LIPO680	CCI120	GR70487	GR87036	GI235401
Mouse	2.77	33.4	94.3	6.6	43.9	96.3
Rat	3.2	52.9	96.3	24.8	59.3	97.5
Dog	3.84	60.7	96.1	19.2	52.3	97.5
Human	4.59	68.7	96.0	30.8	84.2	98.1

Species	Albumin (g percent)	PPB CRED Acid			
		AH22182	BRL15541	GW622791	GR118989
Mouse	2.77	76.6	85.9	83.1	72.7
Rat	3.2	86.3	91.5	85.8	65.4
Dog	3.84	85.3	91.80	89.8	86.1
Human	4.59	88.7	92.8	89.3	90

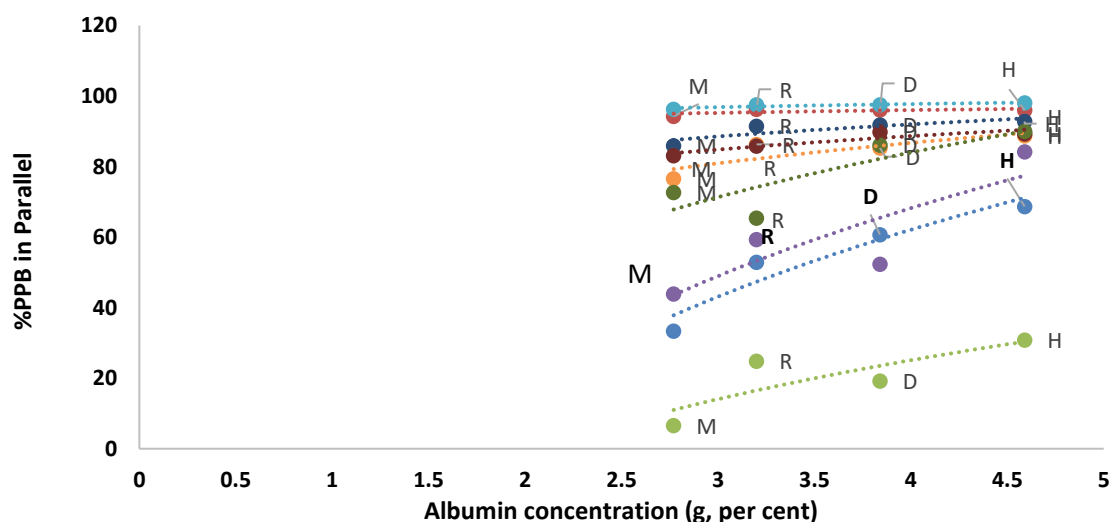


Fig 50. Plots showing the variation of PPB with albumin concentration across species for a subset of acid compounds

Table 41: %PPB across mouse, rat, dog, and human for a subset of basic compounds (structures on pages 39,40,42 and 43)

Species	Albumin (g percent)	PPB CRED Base			
		SB731710	SB416332	CCI3748	CCI4001
Mouse	2.77	51.2	32	91.3	78
Rat	3.2	45.0	25.4	86.6	78.1
Dog	3.84	41.8	11.6	87.3	76.1
Human	4.59	48.9	26.6	89.6	68.6
Species	Albumin (g percent)	PPB CRED Base			
		CCI3993	GR84804	CC13839	CCI120557A
Mouse	2.77	95.8	93.3	67.9	83.7
Rat	3.2	93.2	88.4	56.6	81.7
Dog	3.84	94.8	89.6	65.90	82.3
Human	4.59	96.3	87.7	73.9	86.9

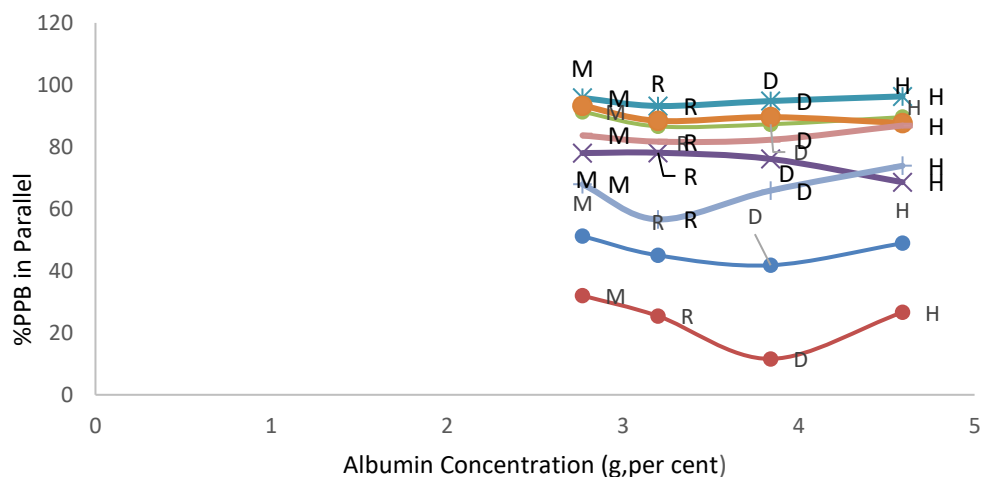
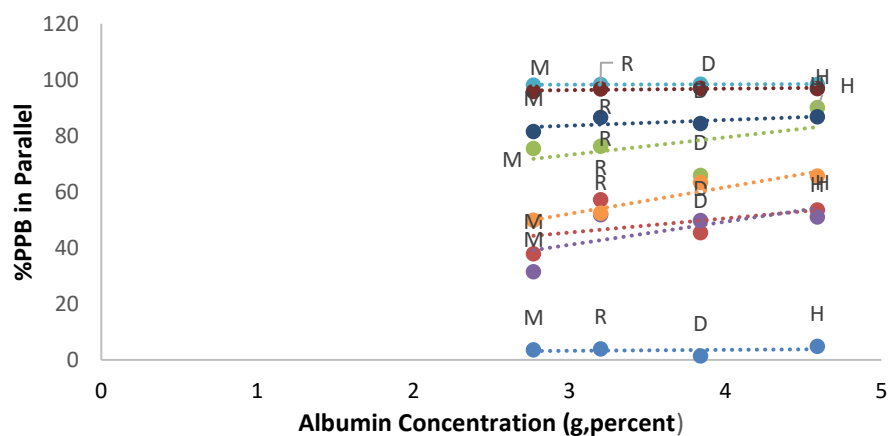


Fig 51. Plots showing the variation of PPB with albumin concentration across species for a subset of basic compounds

Table42: %PPB across mouse rat, dog and human for a subset of neutral compounds (structures on pages 30,31,32 and 33)

Species	Albumin (g percent)	Mean PPB CRED Neutral			
		GR33914	GI116109	GR119497	GR38393
Mouse	2.77	98.1	81.6	49.9	95.8
Rat	3.2	98.4	86.6	52.4	96.8
Dog	3.84	98.5	84.4	63.4	97.0
Human	4.59	98.4	86.8	65.7	96.9

Species	Albumin (g percent)	Mean PPB CRED Neutral			
		GR91295	CC122428	GF120403	AH23463X
Mouse	2.77	3.6	37.9	75.5	31.5
Rat	3.2	3.9	57.2	76.3	51.8
Dog	3.84	1.4	45.4	65.9	49.7
Human	4.59	4.9	53.5	90.1	51.0



Fig

52. Plots showing the variation of PPB with albumin concentration across species for a subset of neutral compounds

3.3.2. Discussion

For the acidic and neutral series of compounds evaluated there was a general increase in PPB from the preclinical species to human with an increase from mouse to rat to dog (Fig 50 and 52). For the basic series of compounds there are noticeable differences in PPB across the species that does not follow the general expectation of PPB increasing from mouse to rat to dog to humans (Fig 51). In fact, for several of the basic compounds investigated the binding decreased from human to dog to rat but increased in mouse plasma which accounted for the highest binding percentage like human (Fig 51, compounds SB416332, SB731710 and CCI3839). Across the series of compounds investigated the majority PPB values were within 2-fold of the human data. It has been established that the binding of drugs to albumin increases from bases to neutrals to acids. This is due to the dominant attraction of acidic compounds to the binding sites within albumin and highlights the major impact that differences in albumin content and concentration have on the binding of drug to plasma. However, other plasma proteins example AGP which binds more to basic compounds may dominate or have a major impact on PPB. Using this information predictability of PPB in preclinical species using human data may show more correlation for basic compound in mouse rather than rat and dog. Likewise, predictability of PPB in preclinical species using human data may show more correlation for acidic compound in rat and dog rather than mouse. The extent of PPB also has an impact on the level of predictability between human and preclinical species. For highly bound compounds >98% there is minor difference across the species highlighting that the physiochemical properties dominate rather than the difference in level of albumin concentration e.g. (basic compound GR33914). For highly bound compounds therefore the predictability of PPB using human data can be done for preclinical species with a large degree of certainty. For low binding acidic compound eg GSK2485680 and GR80736 the trend is more evident. As the percentage PPB increases within each series the difference and trend between species is less evident e.g., neutral compounds GR119497 and GR38393. Overall although there was a general increase in PPB from preclinical species to human the data suggest this may not always be the case as variation may occur across a specific series of compound.

Chapter 4: An Investigation into Increasing the Throughput of PPB using RapidSeparation Technology

4.1. Introduction

The need for high throughput screening in drug discovery is of vital importance in the selection of suitable molecules from a large pool of potential drug candidates for specific biological targets. Similarly, in bioanalysis the use of automation and improved workflows enables the faster generation of data critical for use in analysing biological data, enabling faster decision-making processes while maintaining regulatory integrity and predefined acceptance criteria in supporting PKPD studies. The need for faster analysis times whilst maintaining accuracy and precision is always a moving target in drug development as slower processes and systems have several potential disadvantages. These include lack of instrument availability, increased solvent use, delay in data generation and decision making.

The workflow of competitive rapid equilibrium dialysis has several steps. They are mainly sample incubation at 37°C for minimum 4hrs, sample extraction and HPLC analysis. Incubation is a critical step which allows for the time to equilibrium to be achieved and therefore there is very little to do by way of reducing the time using this system. The LC-MS/MS analysis of samples post extraction utilises a generic gradient with a run time of approximately 3mins per sample injection using gradient profile A shown below.

Time (mins)	Flow Rate mL/min	%A	%B
0	0.8	60	40
0.10	0.8	60	40
2.00	0.8	40	60
2.50	0.8	5	95
3.00	0.8	5	95
3.10	0.8	60	40
3.50	0.8	60	40

Gradient Profile A: Standard LC: Mobile Phase A=0.1% formic Acid, B=Acetonitrile

Rapid Separation (RapidSep) offers a novel alternative to the conventional LC for fast sample throughput. It utilises a short 10x1.0mm column with a C18 stationary phase attached directly to the MS source (Fig 53). It utilises a fast gradient (Gradient profile B) of <1min cycle time which is advantageous in improving and creating a faster overall workflow.

Time (mins)	Flow Rate mL/min	%A	%B
0.00	1.0	90	10
0.40	1.0	10	90
0.50	1.0	10	90
0.51	1.0	90	10
0.6	1.0	90	10

Gradient Profile B: RapidSEP: Mobile Phase A=0.1% formic Acid, B=Acetonitrile



Fig 53: RapidSep column directly attached to the mass spectrometer source

Comparison of PPB across different species using conventional HPLC and RapidSep was investigated using a set of tool compounds to test the reliability of the RapidSep to generate credible data faster. PPB was initially performed across mouse, rat, dog and human species in parallel using the CRED and samples injected onto the two chromatographic systems. Values obtained were then compared to determine whether the PPB value obtained from both systems were comparable and therefore using RapidSep provides faster analysis and data generation which speeds up the workflow.

In addition to testing increased throughput using the RapidSep compared to conventional HPLC for individual compounds, PPB was also determined using cassettes containing 3 to 4 compounds. Therefore, coupled cassette and RapidSep has the potential to have greater impact on the turnaround times and workflow in generating PPB using the CRED.

4.2. Material and Methods

The Competitive Rapid Equilibrium Dialysis was purchased from Thermo Scientific (Stafford House, 1 Boundary Park, Hemel Hempstead, UK), comprising base plates made of high-grade polytetrafluoroethylene (PTFE), 50 pack of dual inserts comprising (40 dual membrane and 10 single membrane inserts with molecular weight cut-off (MWCO) of 12KDa).

Stuart microlite plate shaker SSM5: Features high-speed vibrational mixing for 4 plates simultaneously with a built-in digital timer or continuous operation, supplied with a highly effective non-slip mat, the mat will securely hold in place up to four microtitre plates. Agitation speed is variable from 250 to 1,250 rpm and is easily set via the digital display in 10 rpm increments.

Eppendorf Centrifuge 5810R: Plate rotors for centrifugation of Deepwell Plates, high centrifugation speed of up to $20,913 \times g$ (14,000 rpm) and temperature range from -9°C to 40°C .

Selected compounds across acidic, basic and neutral series (Table 43) were ordered from the GSK compound Store (Harlow) and were received in a plate format as $150\mu\text{L}$ solutions dissolved in DMSO at a concentration of 10mM and stored in a -80°C freezer. FeSSIF powder was purchased from Biorelevant.com (42 New Road London E1 2AX, United Kingdom). HPLC grade methanol, acetonitrile and ammonium formate were purchased from Sigma Aldrich (The Old Brickyard, New Road, Gillingham, Dorset, UK). Phosphate Buffered Saline (PBS) tablets

and 1.4mL Micronics were obtained from Gibco-life technologies, Thermo Scientific (Stafford House, 1 Boundary Park, Hemel Hempstead, UK). Polypropylene graduated tubes (1.5 - 1.7mL and 15 mL) were purchased from Fisher Scientific (Bishop Meadow Road, Loughborough, UK). Control mouse, rat, and dog plasma were obtained from Marshall Bioresource, healthy pooled human plasma was obtained from GSK.

Table 43. List of compounds across acids, bases and neutrals for which plasma protein binding was determined following injection using the RapidSep and Conventional HPLC (structures on pages 30 to 43)

Neutral	Base	Acid
GR91295	SB731710	GR70487
CCI22428	SB416332	CCI120
GF120403X	CCI3748	GR87036
GR33914X	CCI4001	GI235401
GI116108X	CCI3993	BRL155541
GR119497X	GR84804	AH22182X
GR38393X	CC13839	GW622791
AH23463X	CCI120557A	GR118989

4.2.1. Preparation of Buffer

Phosphate buffer was prepared by dissolving a 5g tablet of phosphate buffered saline in 500ml of water to give a final concentration of 1% phosphate buffered saline. Within the CRED device the use of 1% phosphate buffer both as a dialysate as well as diluent in the preparation tissue (phosphatidylcholine) surrogate helps to maintain pH control over the incubation period. During incubation a seal covers the lid of the CRED base plate preventing evaporation and helps to protect the system from external factors which could influence pH changes.

4.2.2. Preparation of Tissue Surrogate

Fed State Simulated Intestinal Fluid (FeSSIF) powder in the form of lecithin was used as the source of phosphatidylcholine. When dissolved in an aqueous medium (phosphate buffer) the FeSSIF powder which also contains sodium taurocholate provides a physiologically relevant medium with a high concentration of phosphatidylcholine micelles to mimic tissues *in-vivo* to give an endogenous concentration of 162mg/10mL

4.2.3. Preparation of Analyte concentration (2µM) in Phosphate Buffer

To obtain a cassette of up to four compounds having final individual concentrations of 2µM in 1%Phosphate buffered saline, a two-step serial dilution was carried out. Initially, a 2µL aliquot of each stock compound (8µL total) at a concentration of 10 mM was spiked into 992µL of 1%Phosphate buffered saline to give individual concentrations of 20µM. This was followed by a 10-fold dilution i.e., 300µL of 20µM spiked 1%Phosphate buffered saline added to 2700µL control 1%Phosphate buffered saline to give a final volume of 3mL

4.2.4. Preparation of Base Plate

Prior to and after each experiment the base plate of the CRED device was (1) soaked for 20 min in 20% ethanol (aq) under ultrasonication, (2) rinsed with water and allowed to bathe in water for a further 10 min and then (3) rinsed with water before drying on blotting paper.

4.2.5. Preparation of Samples

Using the 6-chamber format of the CRED device, 2.5 mL of the cassetted compounds in phosphate buffer saline was added to the well. The plate lid was then secured onto the base plate and loaded with 2 dual and a single membrane insert. The inserts were loaded with 200 µL of control mouse, rat, dog, human plasma and 1% PBS, respectively. This allows for the parallel plasma protein binding (PPPB) of the drug between the various matrices. An adhesive sealing tape was then placed over the entire plate lid to prevent evaporation during incubation. The appropriately labelled CRED device was then placed onto an orbital shaker at 600 rpm in the incubator set at 37°C. Incubation took place for a minimum 4 hr to reach equilibrium. Post equilibrium dialysis, 10 µL aliquots were taken from each insert along with a 10 µL aliquot of spiked phosphate buffer sampled from the open end of the single membrane insert. To normalise matrix and suppression effects, 30 µL of individually prepared “partial matrix” to achieve total matrix match was added to the relevant 10 µL aliquot. Samples were extracted by addition of 120 µL of acetonitrile/methanol/water (volume ratio 85/10/5) containing an in-house generic internal standard [$^2\text{H } ^{13}\text{C}_3$]-SB243213. Samples were then briefly mixed and centrifuged for 10 min at 3000 rpm after which there are ready for injection onto the RapidSep and the conventional HPLC-MS/MS systems, respectively.

4.2.6. LC-MS/MS Quantitative Analysis

The analytical run was analysed initially using our conventional chromatography and then using a rapid sub one-minute chromatography approach.

Chromatographic separation was achieved using an Acquity UPLC system (Waters, MA, USA) equipped with a sample manager, sample organizer, a binary solvent manager and column oven. Mobile phases used were deionised water containing 0.1% formic acid (mobile phase A) and 100% acetonitrile (mobile phase B). Analytes were separated initially using an Acquity C18 BEH column 50 x 2.1 mm i.d., 1.7 µm particle-size (Waters, MA, USA) kept at 50°C and a gradient elution applied, this will be referred to as conventional chromatography. The analytical runs were then reanalysed using a rapid chromatography approach using a HALO™ C18 column 10 x 1.0 mm i.d., 5 µm particle-size (Advanced materials technology, DE, USA) kept at ambient temperature and a gradient elution applied. The column cartridge was fitted into a HALO™ column holder installed directly into the MS/MS nebuliser. A generic gradient approach using rapid chromatography was employed, gradient B.

MS detection was achieved using an API-5000 tandem quadrupole mass spectrometer (AB Sciex, USA) equipped with TurbolonSpray™ interface. The analysis was performed using multiple reaction monitoring (MRM) mode. The instrument was operated with the source temperature set at 650°C and an ion spray voltage of 4.5 kV. All gases used were nitrogen and unit resolution were applied to both Q1 and Q3. The dwell time of 100ms was employed for ion monitoring for the conventional analysis which was reduced to 10ms for the subsequent RapidSep chromatography, this was due to the significantly reduced peak widths and to enable accurate peak quantification by having enough data points across the peaks. HPLC-MS/MS data were acquired and processed (integrated) using Analyst software (v1.6.1 Applied Biosystems/MDS Sciex, Canada)

4.3. Results

Chromatographic Separation obtained using the conventional HPLC and RapidSep are shown below. Analytes are more retained using conventional HPLC and less retained using RapidSep. Symmetrical peaks are obtained across the different platforms and provide for ease of integration and quantification of the peaks of interest.

4.3.1. Examples of Chromatographic Profiles obtained using Conventional HPLC and RapidSep Technology

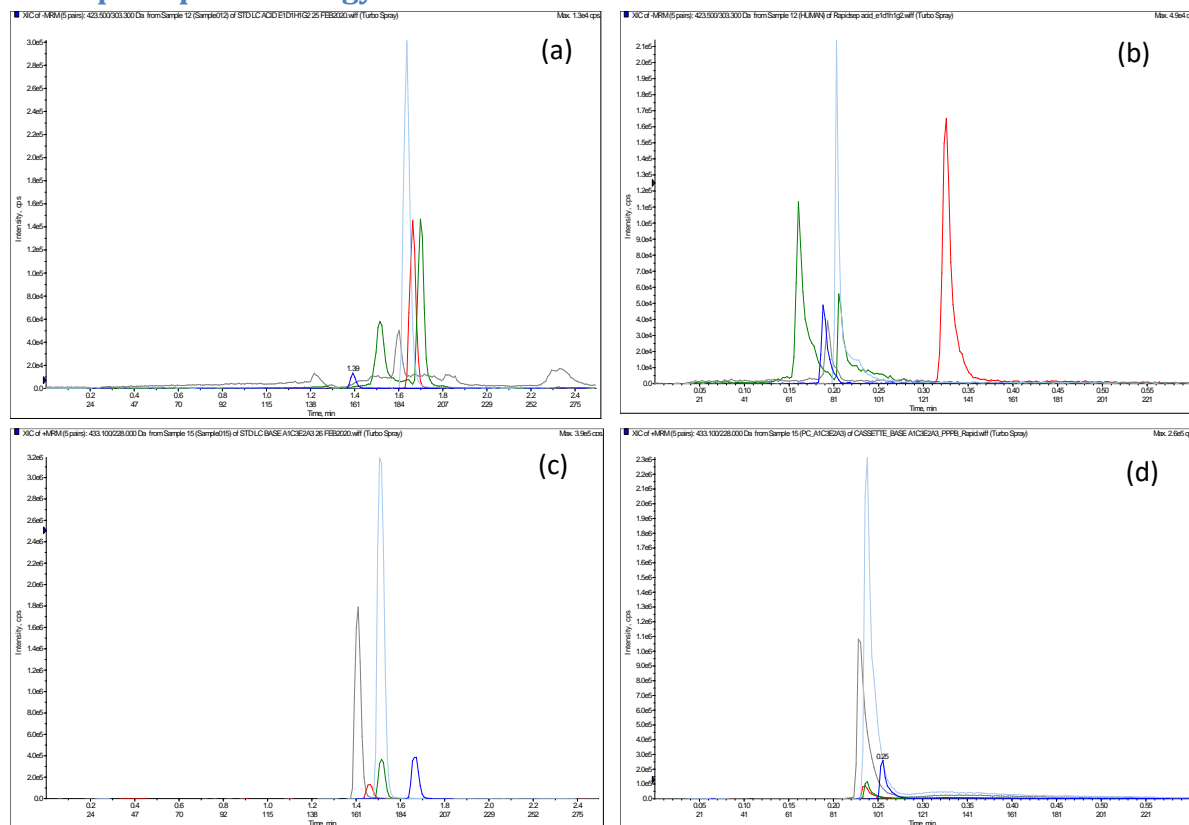


Fig 54: Representative Chromatographic Separation of a Cassette of Acidic compounds using Conventional LC system and RapidSep (a), (b) respectively and of a Cassette of Basic compounds using Conventional LC system and RapidSep, (c) and (d) respectively.

4.3.2. Comparison of Human Plasma Protein Binding Obtained using RapidSep and Conventional Liquid Chromatographic System

Tables 44 to 46 shows the plasma protein binding values of the basic, neutral and acid compound set that were generated from CRED measurements and subsequently analysed with a conventional LC-MS run time (2.5 mins) or RapidSep (0.6 mins). Figures 55 to 57 the correlation coefficients are high (0.871 to 0.9783), the slopes are close to unity and the Y-intercept is low, showing that there is no significant bias introduced by analysing the samples with a significantly faster LC method. This is similarly highlighted in composite result (Fig 58) across all the compounds.

Table 44. Data of Parallel Plasma Protein Binding (PPPB) in Human Plasma for a cassette of basic compounds using RapidSep and Conventional Liquid Chromatography

	Basic Compounds	PPPB%_RapidSep	PPPB%_Conventional LC
Cassette 1	SB731710	63.4	72.9
	SB416332	31.5	28.0

	CCI3748	88.6	92.2
	CCI4001	62.7	66.4
Cassette 2	CCI3993	94.4	96.3
	GR84804	89.6	92.8
	CC13839	77.1	81.0
	CCI120557A	88.7	88.8

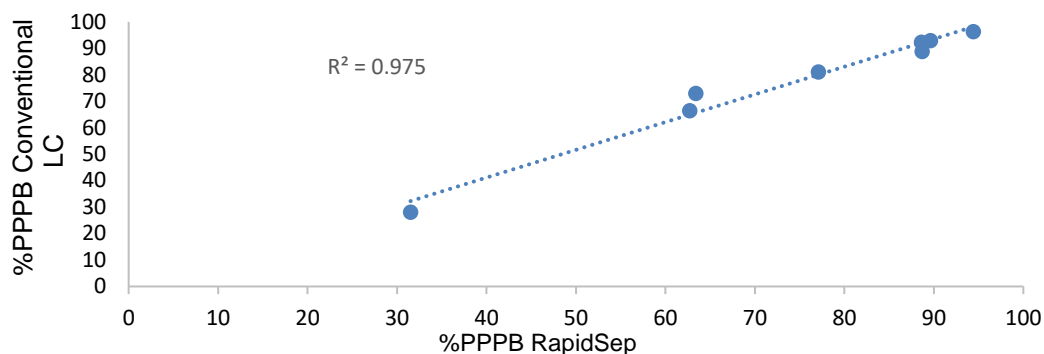


Fig 55. Comparison of %Parallel Plasma Protein Binding (PPPBB) in Human Plasma for Basic compounds between RapidSep and Conventional Liquid Chromatography

Table 45 Data of Parallel Plasma Protein Binding (PPPBB) in Human Plasma for neutral compounds using RapidSep and Conventional Liquid Chromatography

	Neutral Compounds	PPPBB%_RapidSep	PPPBB%_Conventional LC
Cassette 1	GR91295	7.90	8.80
	CCI22428	62.1	54.5
	GF120403X	84.4	56.2
Cassette 2	GR33914X	88.0	88.8
	GI116108X	91.8	90.8
	GR119497X	54.9	56.5
	GR38393X	84.6	84.2

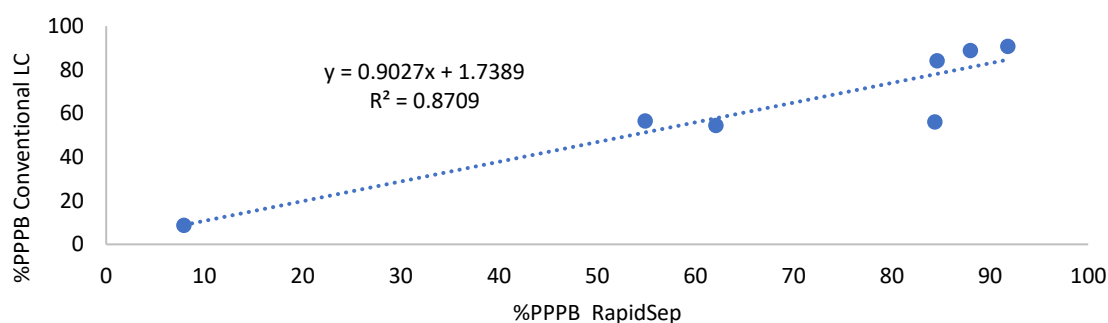


Fig 56 Comparison of Parallel Plasma Protein Binding (PPPBB) in Human Plasma for neutral compounds obtained using RapidSep against Conventional Liquid Chromatography

Table46. Data of Parallel Plasma Protein Binding (PPPBB) in Human Plasma for acid compounds using RapidSep and Standard Liquid Chromatography

	Acid Compounds	PPPBB%_RapidSep	PPPBB%_Conventional LC
Cassette 1	GR70487	34.3	31.5
	CCI120	95.7	94.5
	GR87036	90.6	82.9

	GI235401	97.1	97.2
Cassette 2	BRL155541	85.6	78.8
	AH22182X	95.3	89.6
	GW622791	93.7	91.5
	GR118989	92.6	93.2

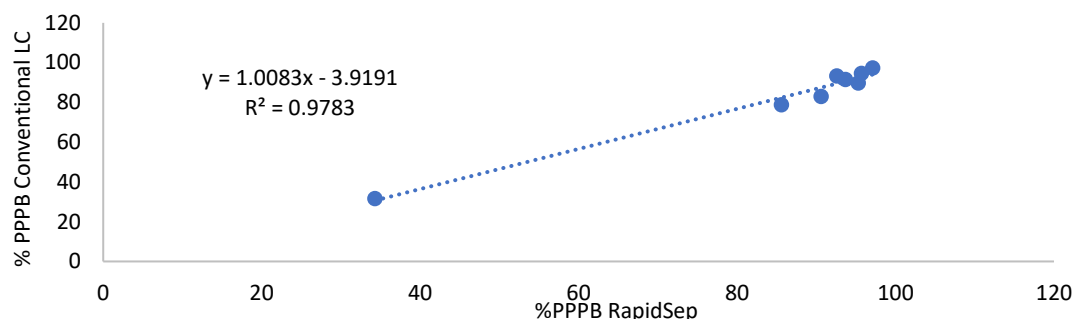


Fig 57. Comparison of Parallel Plasma Protein Binding (PPPBB) in Human Plasma for acid compounds obtained using RapidSep against Conventional Liquid Chromatography

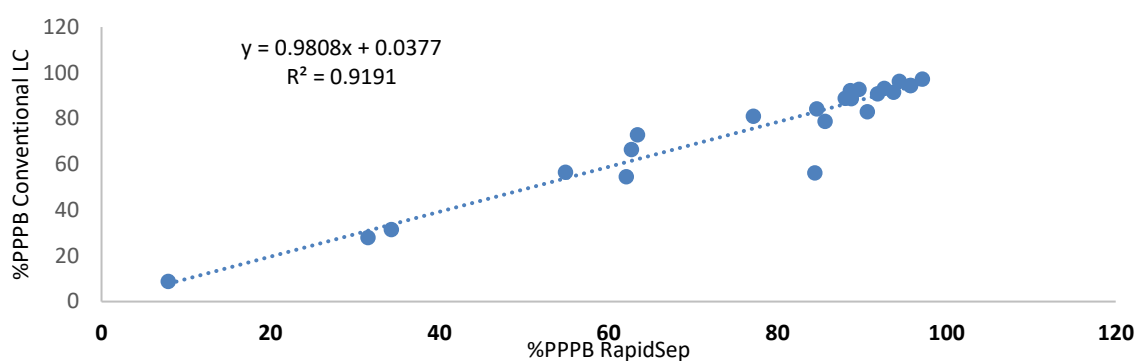


Fig 58. Comparison of Parallel Plasma Protein Binding (PPPBB) in Human Plasma across acids, bases and neutral series using RapidSep against Conventional Liquid Chromatography

4.3.3. Comparison of Mouse Plasma Protein Binding of RapidSep with Conventional LC system

Tables 47 to 49 shows the plasma protein binding values of the basic, neutral and acid compound set that were generated from CRED measurements and subsequently analysed with a conventional LC-MS run time (2.5 mins) or RapidSep (0.6 mins). From Figures 59 to 61 the correlation coefficients are high (0.892 to 0.9759), the slopes are close to unity and the Y-intercept is low, showing that there is no significant bias introduced by analysing the samples with a significantly faster LC method. This is similarly highlighted in the composite result (Fig 62) across all the compounds

Table 47. Data of Parallel Plasma Protein Binding (PPPBB) in Mouse Plasma for basic compounds using RapidSep and Conventional Liquid Chromatography

	Basic Compounds	PPPBB%_RapidSep	PPPBB%_Conventional LC
Cassette 1	SB731710	65.8	75.2
	SB416332	30.7	24.6
	CCI3748	88.7	92.4
	CCI4001	81.7	75.2
Cassette 2	CCI3993	94.6	96.3

	GR84804	95.5	96.3
	CC13839	74.7	75.4
	CC1120557A	87.1	88.5

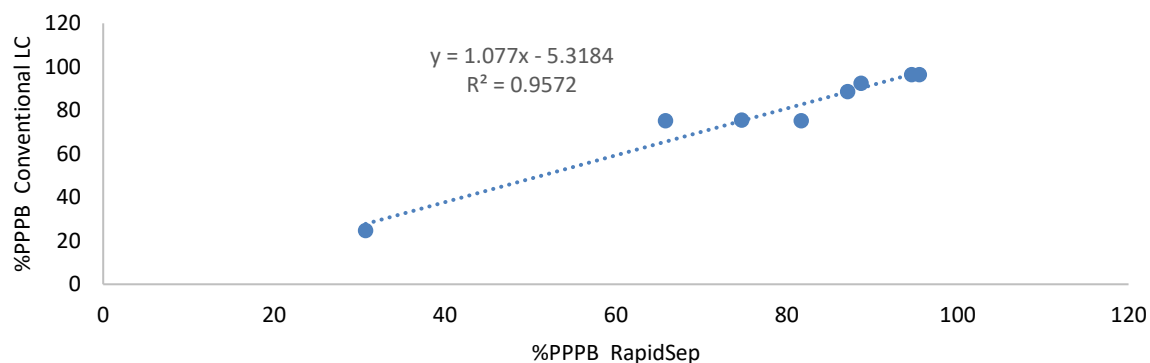


Fig 59. Comparison of Parallel Plasma Protein Binding (PPPB) in Mouse Plasma for basic compounds obtained using RapidSep against Conventional Liquid Chromatography

Table 48. Data showing Parallel Plasma Protein Binding (PPPB) in Mouse Plasma for neutral compounds obtained using RapidSep and Conventional Liquid Chromatography

	Neutral Compounds	PPPB%_RapidSep	PPPB%_Conventional LC
Cassette 1	GR91295	15.9	2.60
	CC122428	59.2	48.1
	GF120403X	78.0	74.0
Cassette 2	GR33914X	88.2	88.5
	GI116108X	90.2	90.7
	GR119497X	48.1	50.8
	GR38393X	81.2	83.4

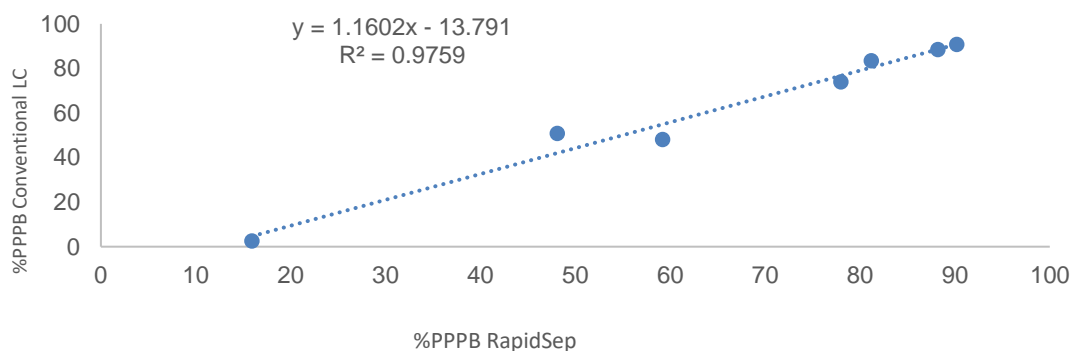


Fig 60. Comparison of Parallel Plasma Protein Binding (PPPB) in Mouse Plasma for neutral compounds obtained using RapidSep against Conventional Liquid Chromatography

Table 49. Comparison of Parallel Plasma Protein Binding (PPPB) in Mouse Plasma for acid compounds obtained using RapidSep against Conventional Liquid Chromatography

	Acidic Compound	PPPB%_RapidSep	PPPB%_Conventional LC
Cassette 1	GR70487	16.1	16.0
	CC1120	94.6	95.2
	GR87036	68.6	44.2
	GI235401	95.9	95.7
Cassette 2	BRL155541	62.3	44.8

AH22182X	95.8	86.0
GW622791	92.9	90.7
GR118989	83.4	87.6

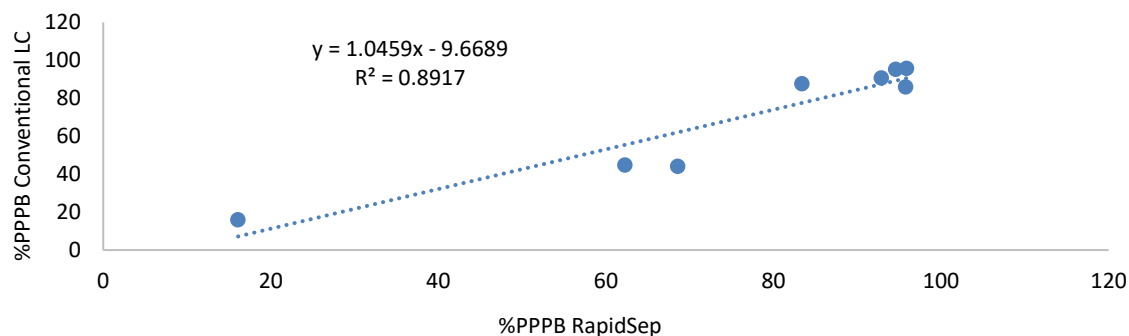


Fig 61. Comparison of Parallel Plasma Protein Binding (PPPBB) in Mouse Plasma for acid compounds obtained using RapidSep against Conventional Liquid Chromatography

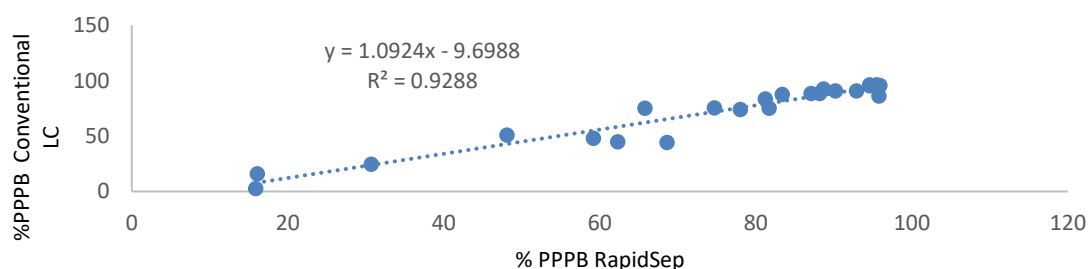


Fig 62. Comparison of Parallel Plasma Protein Binding (PPPBB) in Mouse Plasma across acids, bases and neutral series of compounds obtained using RapidSep against Conventional Liquid Chromatography

4.3.4. Comparison of Rat Plasma Protein Binding of RapidSep with Conventional LC system

Tables 50 to 52 shows the plasma protein binding values of the basic, neutral and acid compound set that were generated from CRED measurements and subsequently analysed with a conventional LC-MS run time (2.5 mins) or RapidSep (0.6 mins). From Figures 63 to 65 the correlation coefficients are high (0.9477 to 0.9728), the slopes are close to unity and the Y-intercept is low, showing that there is no significant bias introduced by analysing the samples with a significantly faster LC method. This is similarly highlighted in the composite result (Fig 66) across all the compounds.

Table 50. Data of Parallel Plasma Protein Binding (PPPB) in Rat Plasma for Basic compounds obtained using RapidSep and Conventional Liquid Chromatography

	Basic Compounds	PPPB%_RapidSep	PPPB%_Conventional LC
Cassette 1	SB731710	65.2	75.6
	SB416332	35.4	27.6
	CCI3748	87.8	92
	CCI4001	86.9	85.2
Cassette 2	CCI3993	94.6	96
	GR84804	95.5	96.2
	CCI3839	69.7	74.8
	CCI120557A	90.8	90.1

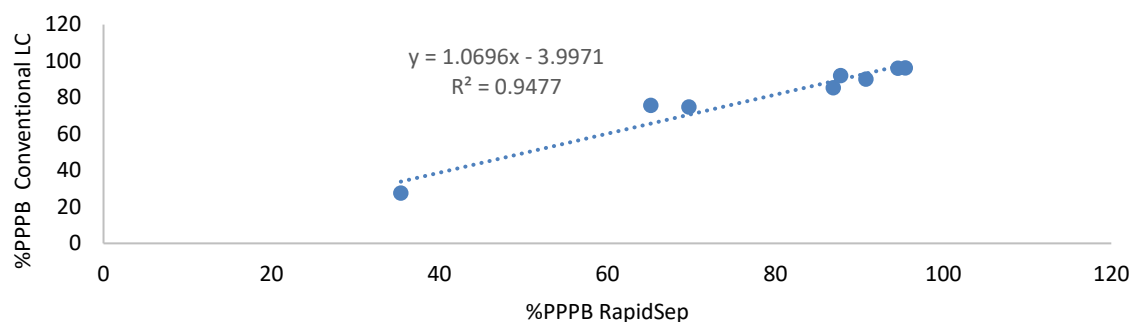


Fig 63. Comparison of Parallel Plasma Protein Binding (PPPB) in Rat Plasma for Basic compounds obtained using RapidSep against Conventional Liquid Chromatography

Table 51: Data showing Parallel Plasma Protein Binding (PPPB) in Rat Plasma for neutral compounds obtained using RapidSep and Conventional Liquid Chromatography

	Neutral Compounds	PPPB%_RapidSep	PPPB%_Conventional LC
Cassette 1	GR91295	6.2	2.1
	CCI22428	61.5	56.5
	GF120403X	71.5	67.4
	GR33914X	89.8	89.7
Cassette 2	GI116108X	92.0	92.0
	GR119497X	42.1	52.2
	GR38393X	84.5	85.9

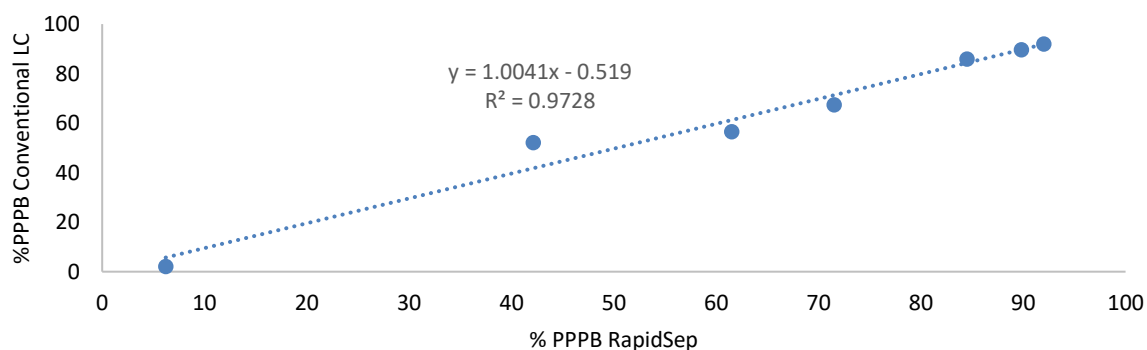


Fig 64. Comparison of Parallel Plasma Protein Binding (PPPB) in Rat Plasma for Neutral compounds obtained using RapidSep against Standard Liquid Chromatography

Table 52. Data showing Parallel Plasma Protein Binding (PPPB) in Rat Plasma for acidic compounds obtained using RapidSep and Conventional Liquid Chromatography

Compound	Cassette_Rat PPPB%_RapidSep	Cassette_Rat PPPB%_Conventional LC
GR70487	16.2	20.6
CC1120	95.7	95.2
GR87036	84.3	74.6
GI235401	96.7	97.0
BRL155541	83.0	74.0
AH22182X	96.1	89.7
GW622791	95.8	94.1
GR118989	92.4	93.4

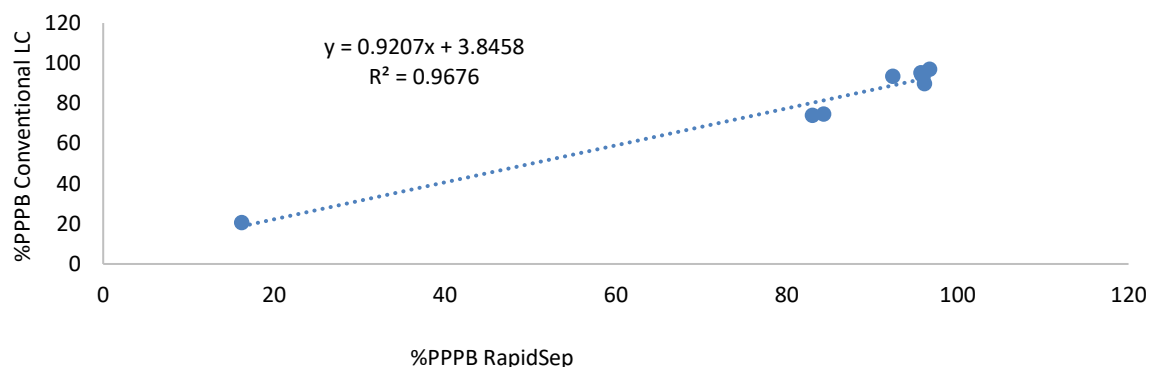


Fig 65. Comparison of Parallel Plasma Protein Binding (PPPB) in Rat Plasma for acid compounds obtained using RapidSep against Conventional Liquid Chromatography

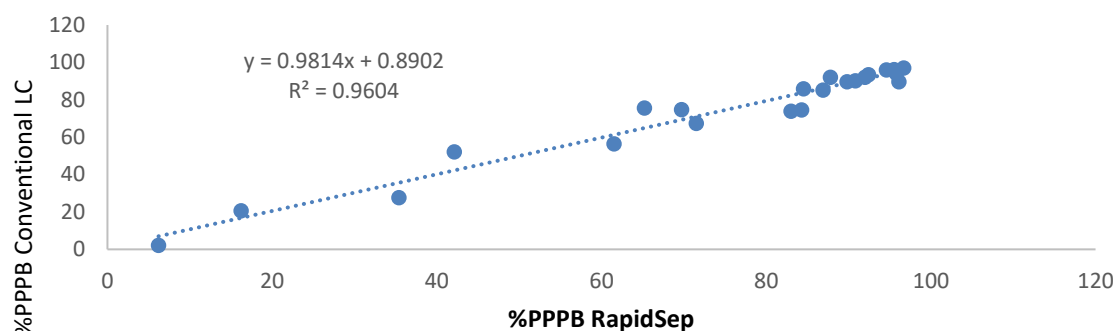


Fig 66. Comparison of Parallel Plasma Protein Binding (PPPB) in Rat Plasma across acids, bases and neutral series of compounds obtained using RapidSep against Conventional Liquid Chromatography

4.3.5. Comparison of Dog Plasma Protein Binding of RapidSep with Conventional LC system

Tables 53 to 55 shows the plasma protein binding values of the basic, neutral and acid compound set that were generated from CRED measurements and subsequently analysed with a conventional LC-MS run time (2.5 mins) or RapidSep (0.6 mins). From Figures 67 to 69 the correlation coefficients are high (0.9244 to 0.9669), the slopes are close to unity and the Y-intercept is low, showing that there is no significant bias introduced by analysing the samples with a significantly faster LC method. This is similarly highlighted in the composite result (Fig 70) across all the compounds

Table 53. Data showing Parallel Plasma Protein Binding (PPPB) in Dog Plasma for Basic compounds obtained using RapidSep and Conventional Liquid Chromatography

	Compound	Cassette_Dog PPPB%_RapidSep 0.6min	Cassette_Dog PPPB%_Conventional LC
Cassette 1	SB731710	65.5	74.1
	SB416332	38.5	28.9
	CCI3748	92.8	89.3
	CCI4001	83.7	85.2
Cassette 2	CCI3993	94.5	96.5
	GR84804	93.5	95.6
	CC13839	73.0	76.5
	CCI120557A	88.1	88

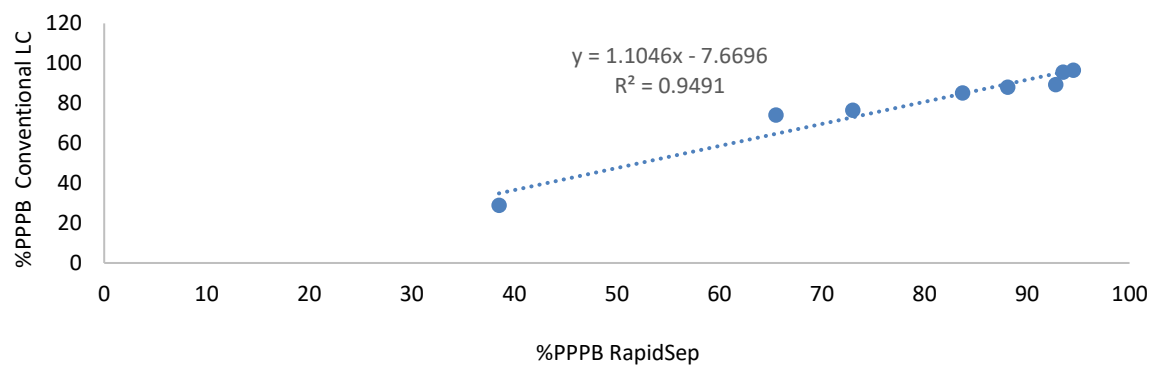


Fig 67. Comparison of Parallel Plasma Protein Binding (PPPB) in Dog Plasma for basic compounds obtained using RapidSep against Conventional Liquid Chromatography

Table 54. Data showing Parallel Plasma Protein Binding (PPPB) in Dog Plasma for neutral compounds obtained using RapidSep and Conventional Liquid Chromatography

	Compound	Cassette_Dog PPPB%_RapidSep 0.6min	Cassette_Dog PPPB%_Conventional LC
Cassette1	GR91295	10.1	8.2
	CCI22428	41.1	54.3
	GF120403X	60.0	57.6
	GR33914X	91.2	90.3
Cassette 2	GI116108X	92.3	91.4
	GR119497X	56.1	54.9
	GR38393X	85.5	85.3

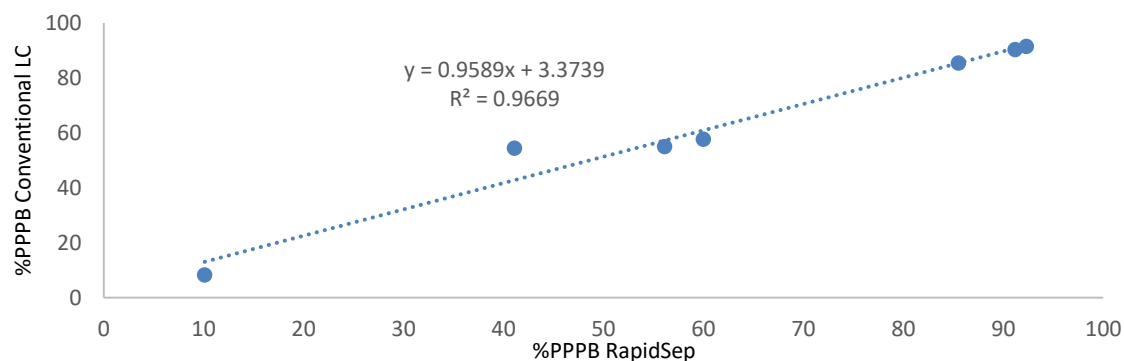


Fig 68. Comparison of Parallel Plasma Protein Binding (PPPB) in Dog Plasma for Neutral compounds obtained using RapidSep against Conventional Liquid Chromatography

Table 55. Data showing Parallel Plasma Protein Binding (PPPB) in Dog Plasma for acidic compounds obtained using RapidSep and Conventional Liquid Chromatography

		Cassette_Dog PPPB% RapidSep 0.6min	Cassette_Dog PPPB% Conventional LC
Cassette 1	GR70487	18.3	14.4
	CCI120	94.9	90.9
	GR87036	71.1	48.9
	GI235401	96.7	96.9
Cassette 2	BRL155541	74.7	62.8
	AH22182X	91.8	90.0
	GW622791	94.1	91.7
	GR118989	78.4	81.1

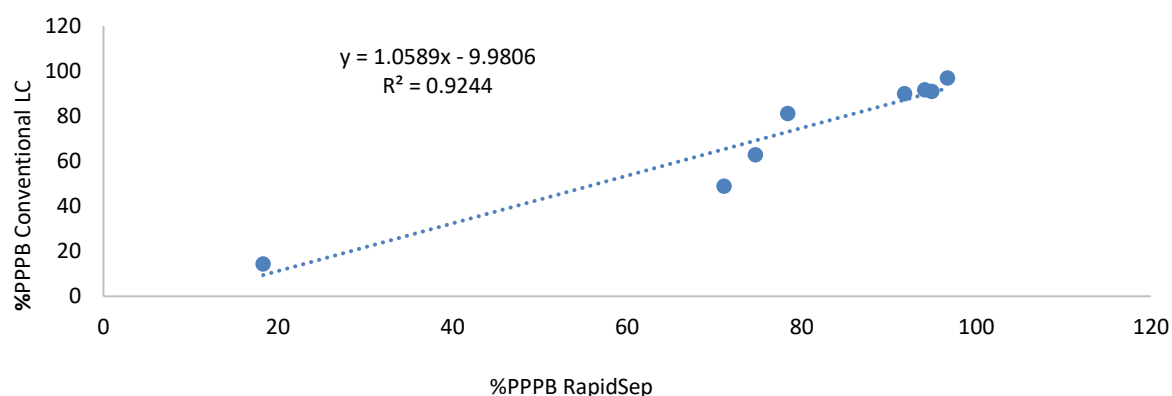


Fig 69. Comparison of Parallel Plasma Protein Binding (PPPB using RapidSep against Conventional Liquid Chromatography) in Dog Plasma for acid compounds

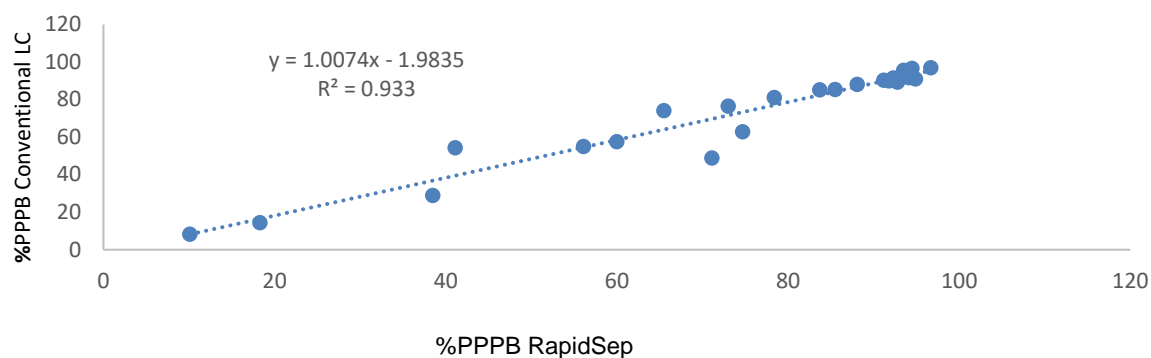


Fig 70. Comparison of Parallel Plasma Protein Binding (PPPBB) using RapidSep against Conventional Liquid Chromatography in Dog Plasma across acids, bases and neutral series of compounds

The overall correlation coefficient is high, accounting for 93% of the variance (Fig 71), with the slope approaching unity and intercept low showing that there is no significant bias between the conventional HPLC and RapidSep.

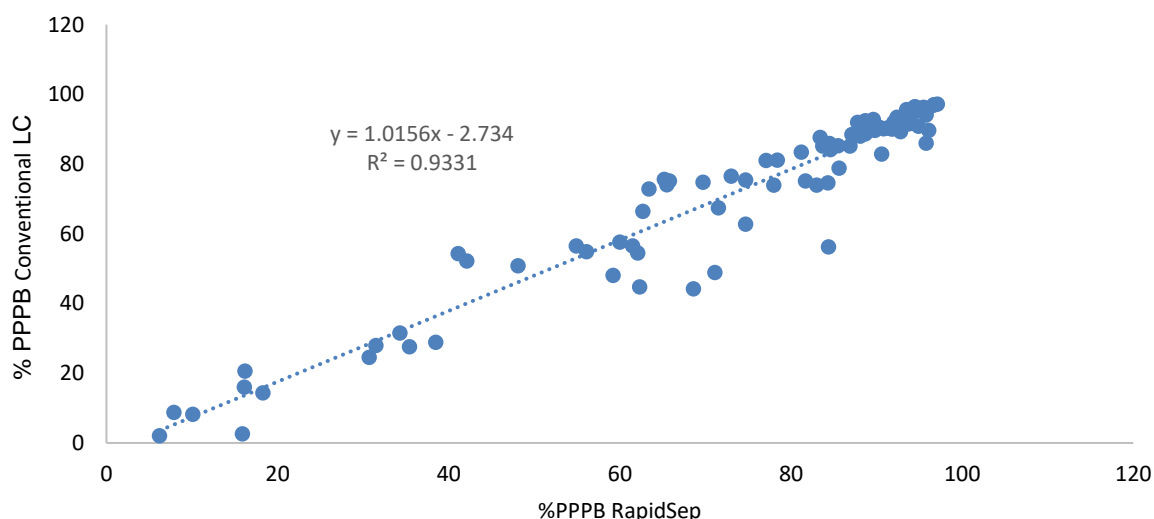


Fig 71. Comparison of Parallel Plasma Protein Binding across mouse, rat, dog and human plasma using RapidSep against Conventional Liquid Chromatography for a series of acids, bases and neutral compounds.

4.3.6. Discussion

In drug discovery fast screening of drug molecules is essential and therefore identification of ways to reduce the turnaround time in using the CRED device would be advantageous. One of the areas where data turnaround can be improved is faster chromatographic separation. Comparison of chromatographic separation between RapidSep and the conventional LC systems are shown in Fig 54. Chromatographic plots of the acids and bases are shown as they exhibit greater change in column retention time. Symmetrical peaks were obtained across both systems enabling peak integration and therefore quantification of drug concentration to be performed accurately. The PPB values obtained using the two chromatographic systems were all within 2-fold of each other (Tables 44 to 55) across all the species and series of compounds. The correlation coefficient in human, mouse, rat and dog plasma across the series of compounds were better than 0.8709, 0.8917, 0.9477 and 0.9244

respectively (Figs 56, 61, 63 and 69). A correlation coefficient ($R^2=0.9331$) for the series of cassetted compounds investigated in rat, mouse, dog and human plasma was obtained (Fig 71) when comparing PPB data via RapidSep versus conventional LC system. With retention times between 0.15 to 0.35s as against 1 to 2.5mins for conventional LC separation using the RapidSep provides an advantageous, reliable, alternative method to enhance the workflow while maintaining chromatographic integrity. This result along with the use of cassetted as against single compound experimentation allows for increased assay throughput, faster data turn around and screening of drug molecules in different species across compounds of varying modalities to aid drug development.

Chapter 5: Competitive Rapid Equilibrium Dialysis Its Application in Liposome Technology: Proof of Concept

5.1. Introduction

Liposomes are one of the first and most successful nanocarrier drug delivery systems with the potential to enhance therapeutic efficacy and reduce off target toxicities exhibited by conventional medicines (Fan and Zhang 2013). Liposomes were first described by Bangham in 1961 and since then have become the most well-established lipid-based nanomedicines with the first liposomal drug being approved by the FDA in 1995 (Bulbake, Doppalapudi et al. 2017). Liposomes are spherical vesicles formed spontaneously when lipids are dispersed in aqueous media. Once immersed in water the hydrophilic “heads” are attracted to water and the hydrophobic “tails” repel and orientate towards each other. This side-by-side alignment forms a phospholipid bilayer which extends itself to form a sheet which then curl into a liposome (Fig 72).

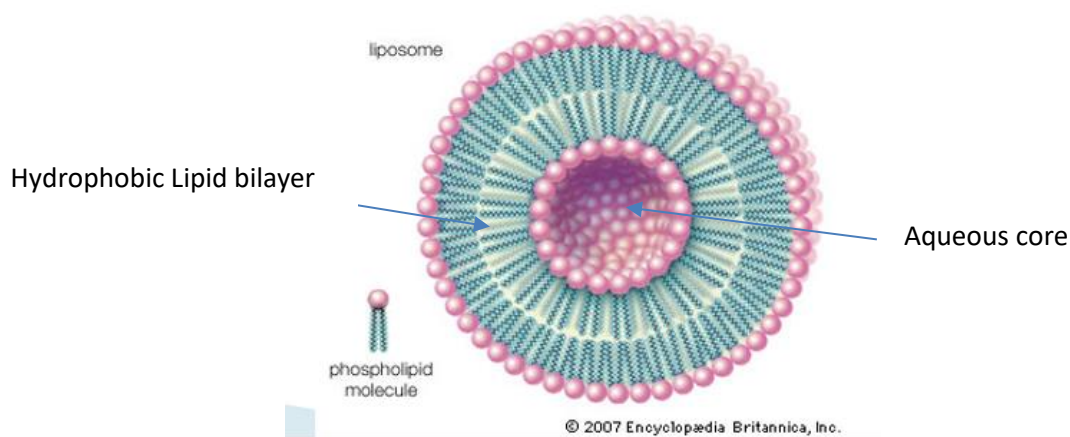


Fig 72: Structure of a liposome showing hydrophobic region and an aqueous core

The ability to encapsulate water soluble molecules within the aqueous interior and entrap lipid soluble molecules in the lipid bilayer enables liposome to act as a carrier for all types of molecules. The liposomes are therefore described as nanocarriers and represents a novel way of drug delivery in nanomedicine. This has implications in terms of drug distribution and pharmacokinetics. Encapsulation reduces the amount of free drug, increases the half-life of the drug in liposomes, reduces toxicity where otherwise there may be a safety concern. (Rahman, Yusuf et al. 2007). Using liposomes as a drug delivery system is important in drug development as it protects and therefore influences the amount of free drug that can be released or delivered directly to the site of action causing a desired pharmacological response. Liposome formulations are therefore tested and compared to enhance drug deliver efficiency and reduce cytotoxicity.

5.2. Comparison of the Distribution of Doxorubicin Loaded Liposome Formulations Using the Competitive Rapid Equilibrium Dialysis.

Doxil/Caelyx is one of the most successful liposomal drugs and contains the anticancer drug Doxorubicin. The measurement of the free drug, drug encapsulated, and drug bound to protein

are 3 of the more important physicochemical markers to fully characterize drug bound to liposomes in nanomedicine (Mehn, Capomaccio et al. 2020). The CRED provides a novel platform to evaluate liposome formulations. Only the free drug is able cross the semipermeable membrane and therefore measurement of the amount over various time intervals will allow us to rank, compare, select/deselect, and characterise the various formulations. Armed with this knowledge optimization and modification can occur to provide the desired effect and design.

In this investigation 3 liposome formulations were tested, 2 containing Distearoylphosphatidylcholine (DSPC) and 1 containing Dipalmitoylphosphatidylcholine (DOPC). The 2 formulations composed of DSPC were produced using 2 different manufacturing parameters, Flow Rate Ratios (FRR 1:1 and 3:1) that resulted in different particle sizes being produced. Both DSPC and DOPC contain 18 carbons, however DSPC is completely saturated whereas DOPC is unsaturated (Figure 73). Due to this difference in saturation both of these lipids have very different transition temperatures (the temperature at which the lipids within the bilayer exist in a more fluid phase) with DSPC having a transition temperature of 55°C and DOPC having a transition temperature of -17°C (Li, Wang et al. 2015). The presence of double bonds in DOPC affects the permeability of the lipid bilayer as the double bonds create space between the tightly backed lipid tails (Monteiro, Martins et al. 2014). Therefore, when DSPC is incorporated into liposomes it provides a much more rigid phospholipid bilayer resulting in more stable structure and prolonged release of the payload (Monteiro, Martins et al. 2014, Li, Wang et al. 2015).

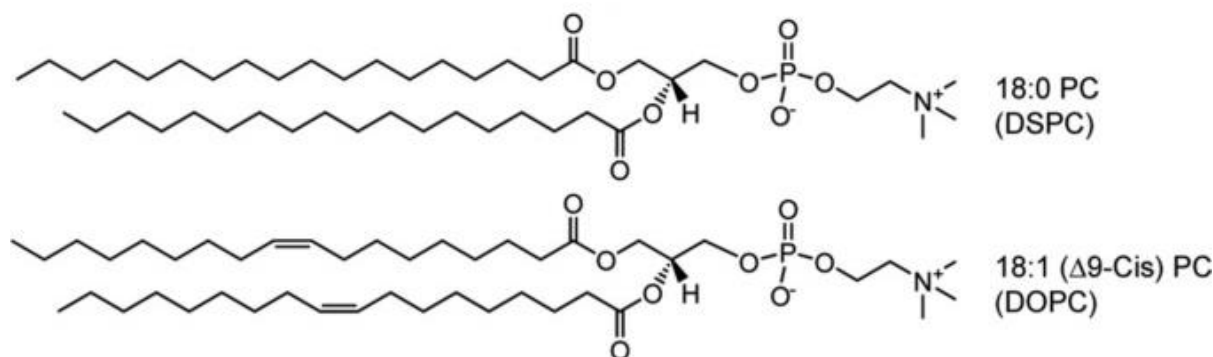


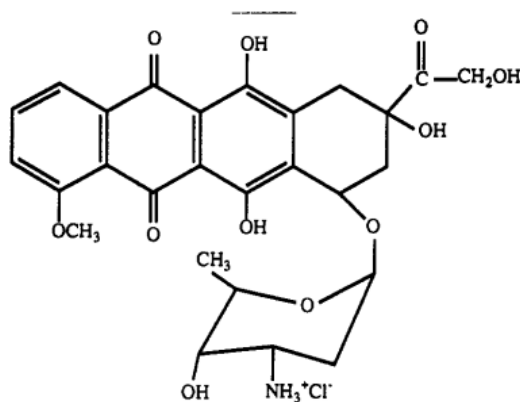
Fig 73: Chemical structures of DSPC and DOPC. Image cropped and taken from (O'Leary, Jiang et al. 2018)

Doxorubicin loaded within liposome formulations of different designs is therefore evaluated using competitive rapid equilibrium dialysis to understand its potential distribution in-vivo by binding to phosphatidylcholine and human serum albumin as tissue and plasma surrogates, respectively. Creating a concentration-time profile of each formulation provides direct comparison of the relative stability doxorubicin in the different formulations. Determination and comparison of the PPB and volume of distribution of Doxorubicin with observed literature data will also be carried out to validate the proof of concept of the CRED as a system to qualitatively and quantitatively assess drug liposome bound distribution.

5.2.1. Method

Doxorubicin loaded liposome formulations of 3 different designs were prepared and shipped by Sarah Lindsay, PhD student from the Strathclyde Institute of Pharmacy and Biomedical

Sciences, Strathclyde University, Glasgow. They are described as liposome 1, 2 and 3 in the experimentation and were loaded with 0.492, 0.582 and 0.3mg/ml Doxorubicin giving a % encapsulation of 78.6, 92.9 and 48.0% respectively (Table 56). Phosphatidylcholine (PC) used as a surrogate for tissue cell membrane was obtained from biorelevant and dissolved in 1% phosphate buffered saline (PBS) to give an endogenous concentration of 162mg/10ml (640mg of Fessif powder in 10ml of 1% phosphate buffered saline). Concentrations of 126.5mg/10ml and 101.25mg/10ml (500 and 400mg of Fessif powder in 10ml of 1% phosphate buffered saline, respectively were also included). They are described as PC640, PC500 and PC400 in this investigation. Plasma surrogate was prepared by dissolving a weighed amount of Human Serum Albumin lyophilized powder in 1% PBS to give a final concentration of 50g/litre. Human serum albumin was spiked with Doxorubicin to give 0.626mg/ml assuming 100% encapsulation. Doxorubicin HCL (10mg) was obtained from Merck Millipore and supplied by VWR international.



Structure of Doxorubicin

Using the 6-chamber format of the CRED device, 2.5 mL HSA was added to each well. Each well was loaded with inserts containing 200µL of Doxorubicin loaded liposome, 1% phosphate buffered saline, phosphatidylcholine at the different concentrations, respectively.

PC640	PC500
Doxorubicin Loaded liposome /HSA Spiked	HSA (Open-ended insert)
PC400	Buffer

Layout of the CRED to investigate distribution of Doxorubicin loaded liposomes.

This allows for the distribution of the drug between the various matrices. An adhesive sealing tape was then placed over the entire plate lid to prevent evaporation during incubation. The CRED device was then placed onto an orbital shaker at 600 rpm in the incubator set at 37°C. At 15mins, 1hr, 2hrs, 4hrs and 6hrs periods 10µL aliquots were taken from each insert along with a 10µL aliquot of HSA sampled from the open end of the single membrane insert. In order to normalise matrix and suppression effects, 40 µL of individually prepared “partial matrix” to achieve total matrix match was added to the relevant 10µL aliquot. Samples were extracted by addition of 150 µL of acetonitrile containing an in-house internal standard. Samples were then briefly mixed and centrifuged for 10 min at 3000 rpm and injected onto the HPLC-MS/MS system for analysis.

Table 56. Data showing liposome measured characteristics using a microplate reader (Bio-rad Laboratories)

Liposome Formulation		Particle Size (d.nm)	Lipid Type	Flow Rate Ratio	% Encapsulation
1	Pre-Loading	61.7	DSPC	FRR 3:1	78.6
	Post-Loading	107.7			
2	Pre-Loading	131.5	DSPC	FRR 1:1	92.9
	Post-Loading	134.7			
3	Pre-Loading	37.8	DOPC	FRR 3:1	48.0
	Post-Loading	44.0			

5.2.2. Preparation of Calibrations standards

Doxorubicin was received as a 10mg powder and dissolved in 2mL of acetonitrile/water 50/50 v/v to give a 5mg/mL stock solution. Working solutions were prepared by adding 100µL (5.0 mg/mL stock) to 150 µL acetonitrile/water 50/50 (v/v) to give 2mg/mL. Using 10-fold serial dilutions, additional working solutions in acetonitrile/water were prepared to realise concentrations of 0.2 and 0.02 mg/mL, respectively. An assay range of 100 to 100,000ng/mL was prepared by addition of no more than 5% volume of working solutions to previously prepared “total matrix” to give calibrations standards of 100, 200, 1000, 5000, 20000, 50000, 80000 and 100000ng/mL, respectively. “Total matrix” was prepared by mixing equal volumes of 1% PBS, HSA (50g/litre), PC640, PC500 and PC400, respectively. Protein precipitation was carried out by extracting 50 µL duplicate aliquots of each standard using 150 µL of acetonitrile containing an in-house internal standard. Samples were then briefly mixed and centrifuged for 10 min at 3000 rpm after which there are ready for injection onto the HPLC-MS/MS system for analysis.

5.2.3. Chromatographic and Mass Spectroscopy Conditions

A Waters TQS using TurbolonSpray™ source in Multiple Reaction Monitoring was used for chromatographic peak detection. Generic HPLC gradient conditions were achieved with a Waters Corporation Ltd Acquity BEH phenyl column (150 x 2.1 mm, 1.7µm) equilibrated to 50 °C. Data was acquired over a run time of 5.0 min. The organic mobile phase (B) was acetonitrile while for the aqueous mobile phase (A) 0.1% formic acid was used in positive acquisition mode. The HPLC condition used was 0.0 to 0.2 min at 20% acetonitrile, 0.2 to 2.5 min organic phase change 20 to 35% B, 2.5 to 4.0 min organic phase change 35 to 60% B,

4.0 to 4.2 min organic phase change 60 to 95% B, held at 95% B up to 4.7min and at 4.75 min back to the initial starting conditions. A Waters Acquity UPLC system was used to drive the mobile phases set to a flow rate of 0.4 mL/min in partial loop injection mode with an injection volume of 1 μ L.

Mass spectrometer parameters (capillary, cone, and source offset voltages) were set at 3.50, 45 and 50 respectively. Desolvation temperature, collision and nebulizer gas were 600°C, 25 and 7(bar), respectively. Desolvation and cone gas flows were 1200 and 150 (L/Hr), respectively.

Parent and daughter transitions (m/z) were 543.8 and 361.1, respectively with a dwell time of 0.080 ms.

5.2.4. Data Acquisition and Processing

HPLC MS/MS data were acquired and processed (integrated) using the proprietary software application-MassLynx 4.1 SCN843). Calibration plots of analyte/internal standard peak area ratio versus individual analyte concentration were constructed and a weighted 1/x² quadratic regression applied to the data. Concentrations of analytes and peak areas were determined from the calibration line in “total matched matrix.

5.3. Result

Chromatographic Separation of Doxorubicin from endogenous peaks was obtained. An example is shown below Fig 72.

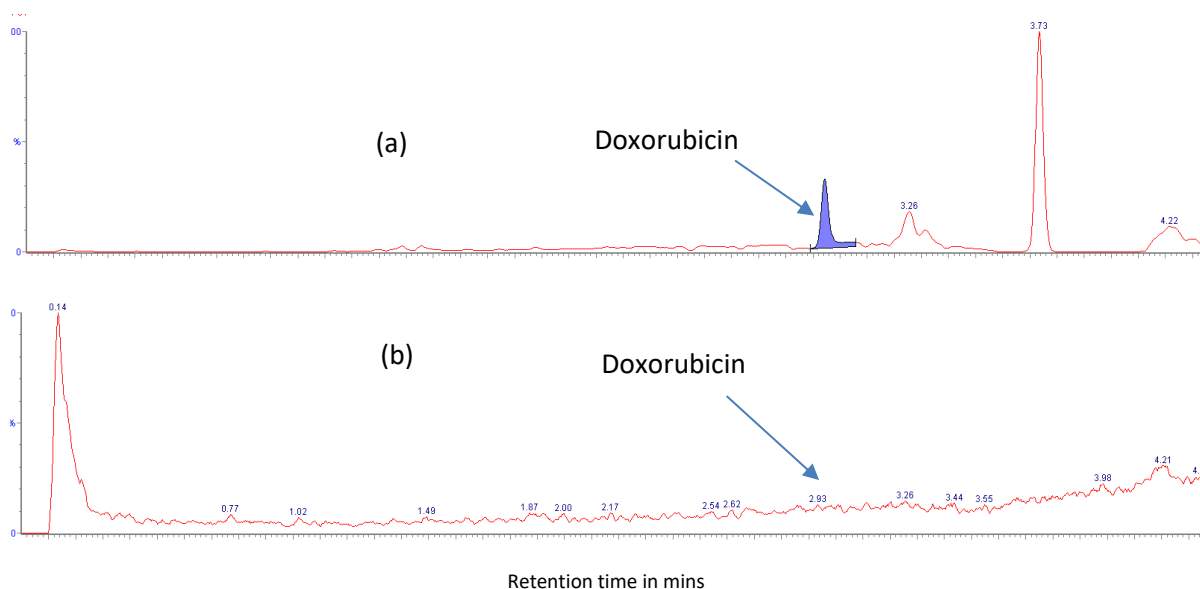


Fig 72. Chromatography showing analyte of interest (a) and a total blank sample (b).

Data obtained from the analysis of aliquots of Doxorubicin from the various compartments over time are presented below table 57 and 58. Prior to the start of the experiments the concentration of the individually loaded liposomes and HSA spiked at 0.626mg/ml was determined using the extraction procedure described above i.e., 40µL of “partial total matrix” was added to 10µL aliquot of sample and extracted with 150µL acetonitrile containing an in-house internal standard. This gave concentration at zero hours. The values obtained were 0.237, 0.384, 0.213, 0.477 mg/ml for L1, L2, L3 and HSA spiked doxorubicin, respectively. Plasma protein binding values for Doxorubicin were calculated (Eqn19) using peak areas instead of concentrations as the values were largely unquantifiable across the different timepoint for the L1 and L2. There was a 71.9% drop from 0.25hrs to 6hrs for HSA spiked doxorubicin (Table 57) whereas the drop in Doxorubicin loaded liposomes varied between 5.2 and 11.7%. The drop in Doxorubicin loaded liposomes were calculated using the highest and lowest concentration obtained for each liposome over the 6hr incubation period. The drop in concentration was 5.2%, 11.5% and 11.7% respectively for Liposome 2, 1 and 3 respectively (Table 57).

$$\%Bound = (Peak\ Area(HSA) - Peak\ Area\ (buffer)) \div Peak\ Area\ (HSA) \times 100 \quad Eqn\ 19$$

Table 57. Data showing variation in Doxorubicin concentration levels of the different liposome designs, HSA spiked and the corresponding change in HSA binding and free Doxorubicin concentration over a 6hr incubation period using the CRED

Time (Hrs)	Liposome 1 Concentration (mg/mL)	Liposome1 HSA (Peak Area)	Buffer (Peak Area)	HSA (Conc) ng/mL	Buffer (Conc) ng/mL	PPB (%) Using Peak Area
0.25	0.233	0	0	0	0	
1	0.228	0	0	0	0	
2	0.250	0	0	0	0	
4	0.256	1981.3	790.9	0	0	60.1
6	0.226	3150.1	788.2	0	0	75.0
Time (Hrs)	Liposome 2 Concentration (mg/mL)	Liposome 2 HSA (Peak Area)	Buffer (Peak Area)	HSA (Conc) (ng/mL)	Buffer (Conc) (ng/mL)	PPB (%) Using Peak Area
0.25	0.401	0	0	0	0	
1	0.399	0	0	0	0	
2	0.380	0	0	0	0	
4	0.385	2222.4	586.6	0	0	73.6
6	0.383	2178.8	660.7	0	0	69.7
Time (Hrs)	Liposome 3 Concentration (mg/mL)	Liposome 3 HSA (Peak Area)	Buffer Peak Area	HSA (Conc) (ng/mL)	Buffer (Conc) (ng/mL)	PPB (%) Using Peak Area
0.25	0.207	0	0	0	0	
2	0.199	7228.3	1596.9	0	0	77.9
4	0.200	15318.7	4009.3	0	0	73.8
6	0.183	27651.6	8626.8	1509.9	234	68.8
Time (Hrs)	HSA Spiked Concentration (mg/mL)	HSA_HSA (Peak Area)	Buffer Peak Area	HSA (Conc) (ng/mL)	Buffer (Conc) (ng/mL)	PPB (%) Using Peak Area
0.25	0.549	2684.6	462.4	0	0	82.8
2	0.286	142016.1	26354.7	10673.5	1753.1	81.4
4	0.248	202954.8	68910.7	16771.6	5239.7	66.0

6	0.154	233247.1	90769.6	17846.9	6800.4	61.1
---	-------	----------	---------	---------	--------	------

The PPB at 6hrs varied from 61.1 to 75% for the series of experiments conducted. The individual values were 75, 69.7, 68.8 and 61.1% for liposome 1, liposome 2, liposome 3 and HSA spiked respectively. The PPB at 4hrs varied from 60.1 to 73.8%. The individual values were 60.1, 73.6, 73.8 and 66.0% for liposome 1, liposome 2, liposome 3 and HSA spiked respectively. The PPB could only be determined at 2hrs for liposome 3 and HSA spiked experiments. The values obtained were 77.9 and 81.4% respectively.

Table 58. Data showing the variation of peak Area of Doxorubicin at equilibrium across the matrix components. The ratio of the free fraction in HSA to the free fraction in PCs gives a measure of the volume of distribution at steady state.

	Liposome 1				
Matrices	PC 640	PC500	PC 400	PBS	HSA
Peak Area	2801.2	2612.9	1993.9	788.1	3150.1
% Protein Binding	71.9	69.8	60.5		75.0
Fu	0.281	0.302	0.395		0.250
fu (undiluted)	0.281	0.252	0.290		
VDss(mean)	0.914				
	Liposome 2				
Matrices	PC 640	PC500	PC 400	PBS	HSA
Peak Area	2550.2	1804.9	1067.9	660.7	2178.8
% Protein Binding	74.1	63.4	38.1		69.7
Fu	0.259	0.366	0.619		0.303
fu (undiluted)	0.259	0.311	0.503		
VDss(mean)	0.916				
	Liposome 3				
Matrices	PC 640	PC500	PC 400	PBS	HSA
Peak Area	16738.3	17341.8	15624.3	6626.8	27651.6
% Protein Binding	60.4	61.8	57.6		76.0
Fu	0.396	0.382	0.424		0.239
fu (undiluted)	0.396	0.326	0.315		
VDss (mean)	0.700				
	HSA Spiked				
Matrices	PC 640	PC500	PC 400	PBS	HSA
Peak Area	195245.5	207023.9	218648.6	90769.6	233247.1
% Protein Binding	53.5	56.2	58.5		61.1
Fu	0.465	0.438	0.415		0.389
fu (undiluted)	0.465	0.379	0.307		
VDss (mean)	1.04				

Plots comparing the variation in concentration of doxorubicin spiked in L1, L2, L3 and HSA at various timepoints are shown below Fig 73. The corresponding Doxorubicin peak areas in

unspiked HSA as a result of distribution across the semipermeable membrane are shown in Fig 74.

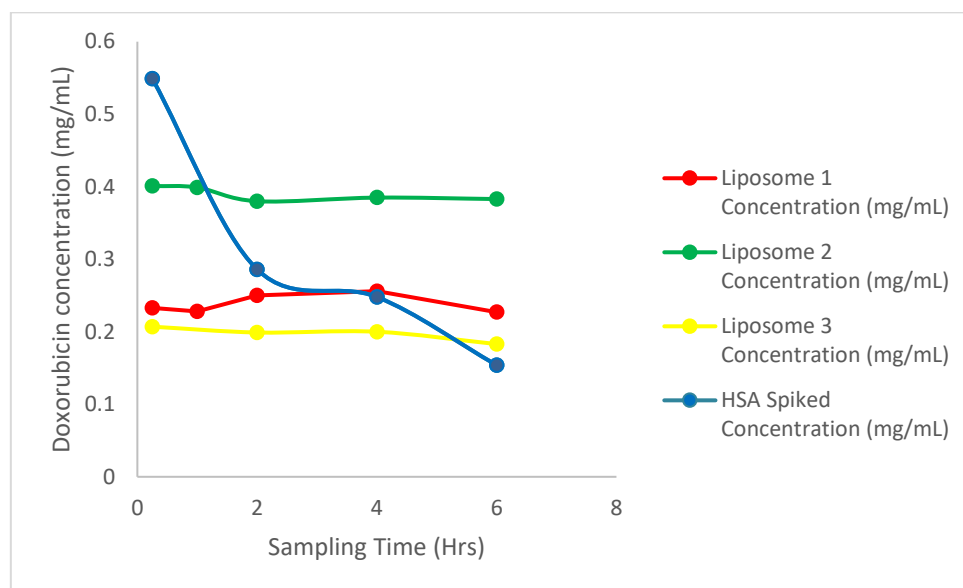
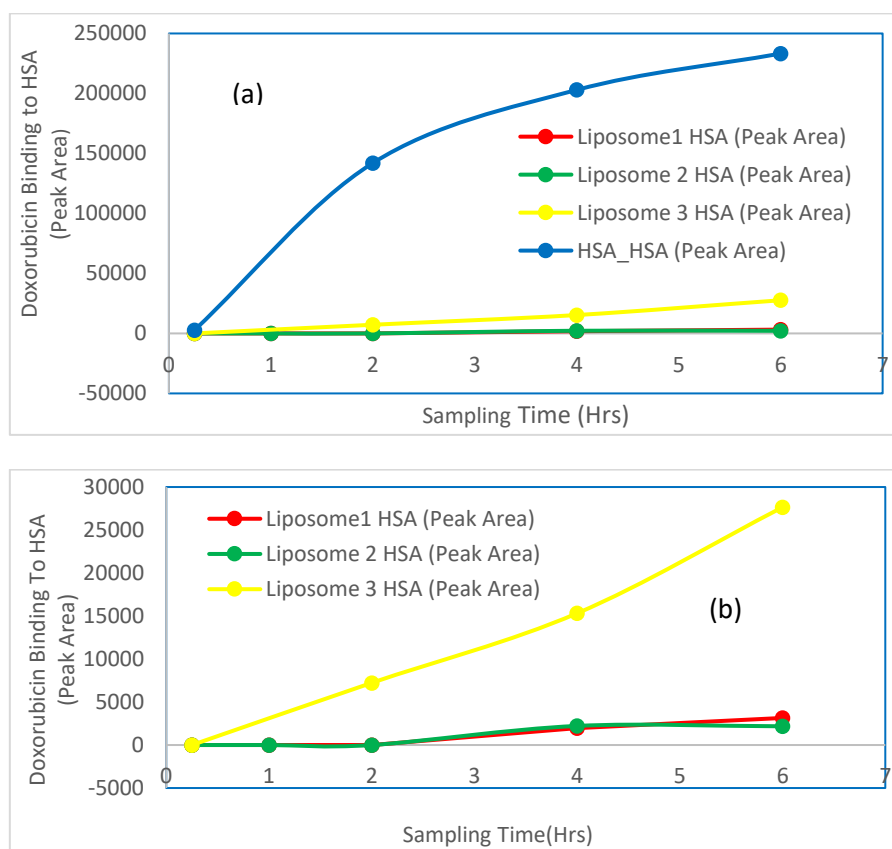


Fig 73. Plot of showing the variation of Doxorubicin loaded liposome and HSA spiked concentration over 6hrs incubation using CRED



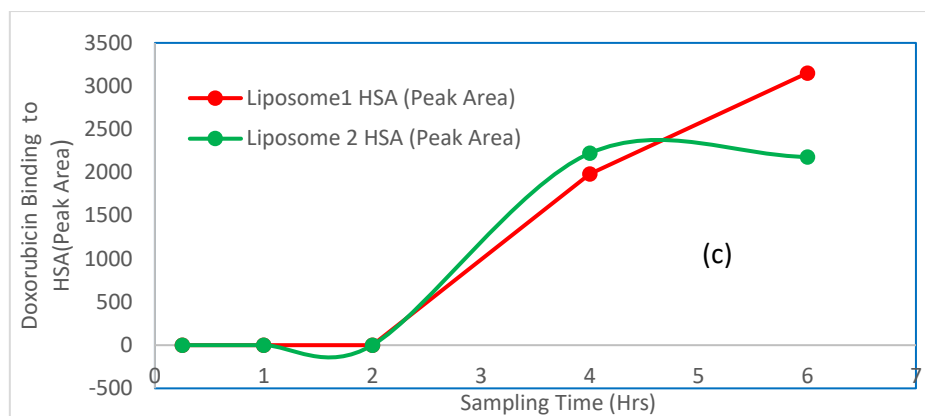


Fig 74. Plot showing the levels of Doxorubicin in terms of peak area binding to drug free HSA over 6hrs incubation using CRED. Fig 74 (a) comparing leakage of L1, L2, L3 and HSA respectively, Fig 74 (b) comparing leakage of L1, L2 and L3 respectively, Fig 74 (c) comparing leakage of L1 and L2 respectively.

From Fig 74(a) Doxorubicin spiked in HSA, L1, L2 and L3 is distributed over time across the semipermeable membrane of the CRED inserts into the drug free HSA compartment. The increase in peak area gives a measure of the efficiency of the various matrices to hold onto its payload. Drug leakage is highest for the non-liposome HSA spiked Doxorubicin compared to L1, L2 and L3 as expected. Figure 74(b) shows a comparison of Doxorubicin drug leakage from L1, L2 and L3- with the DOPC loaded L3 having a higher drug leakage due to its lower transition temperature, unsaturated less rigid structure compared to L1 and L2 with higher transition temperature, saturated DSPC which are more rigid and therefore greater carrier efficiency. Figure 74(c) compares L1 and L2 both DSPC loaded liposomes but with different particle sizes. Liposome 1 was prepared using a flow rate ratio (FRR) of 3:1(aqueous to solvent) having an average particle size of 80nm, while L2 was prepared using a FRR of 1:1 with an average particle size of 132nm. The drug leakage is similar suggesting the difference in particle size has little impact on drug carrier efficiency.

5.4. Discussion

From the investigational work of drug distribution of liposomes loaded DOPC and DSPC using the CRED it is evident that Doxorubicin loaded DOPC leaks quicker than DSPC. This is in keeping with and matches the observation in vivo (Monteiro, Martins et al. 2014, Li, Wang et al. 2015). From the data of the 3 liposomes tested, the 2 formulations (L2 and L1) which are composed of DSPC but having different particle sizes, the differences in stability and rigidity of both liposomes to hold unto Doxorubicin was marginal and therefore particle size showed no real effect. There was however a notably difference between the DSPC and DOPC (L1 and 2 vs L3). The L3 was made using DOPC which resulted in unsaturated C18 chain. This difference in saturation causes transition temperatures of 55°C and -17°C for DSPC and DOPC respectively (Li, Wang et al. 2015). The presence of double bonds in DOPC affects the permeability of the lipid bilayer as the double bonds create space between the tightly backed lipid tails (Monteiro, Martins et al. 2014). As a proof of concept using the CRED, distinction was made between DSPC and DOPC incorporated into liposomes with DSPC resulting in more stable structure and prolonged release of the payload. The data

therefore shows that the release of drug from the various liposomes were more influenced by the saturation and therefore transition temperature rather than particle size.

Peak areas from drug distributed into the unspiked HSA was highest for HSA spiked Doxorubicin. For liposome loaded Doxorubicin peak areas from drug distributed into the unspiked HSA was highest for liposome 3 and lowest for liposome 2. The trend was also reflected in the change in concentration of the buffers. This highlights the ability of the liposome loaded Doxorubicin to hold onto its payload and exert a controlled release when compared to Doxorubicin spiked in HSA.

From the ratio of free fraction in HSA to free fraction in PCs the VDss were calculated as 0.700, 0.914, 0.916 and 1.04 for liposome 3, 1, 2 and HSA spiked respectively (Table 58). The observed literature volume of distribution of Doxorubicin at steady state is 18l/kg (Mross, Mayer et al. 1990) which suggest the drug has a high uptake in the tissues. Using a 0.6l/kg (VDss in total body water) as baseline the data suggest that the drug loaded liposome are less likely to have high uptake in the tissues than drug spiked in HSA. This suggest that there is less likelihood of drug accumulation leading to off target toxicity for the liposome loaded Doxorubicin (Fan and Zhang 2013). However precise target engagement is the function of the liposome delivery system to allow for accumulation in tumor tissues (Charrois and Allen 2004), exert better bioavailability and then release the active drug. It is important to exercise care in this interpretation of VDss as against bioavailability.

From the unspiked HSA and corresponding buffer concentrations PPB can then be calculated. With an experimental assay range 100 to 100000 ng/ml however values below 100ng/ml were not quantifiable. Further method development would therefore be required to reduce the lower limit of quantification. Analyte peak areas were therefore used where it was verified from the chromatograms that it represented a parent peak and not background noise. The plasma protein binding of doxorubicin (Thies, Cowens et al. 1990) ranges from 50 to 90% in keeping with the values obtained. The ability to determine PPB after 2hrs incubation is worth further investigation across various compounds as there is potential to reduce incubation time to 2hrs.

The data also shows the ability to differentiate between the free, HSA bound, and drug bound to liposome which can be applied *in vivo* and is important in understanding the pharmacokinetics and toxicity of liposomal drugs (Thies, Cowens et al. 1990). As a preliminary study the CRED has shown its potential as a system to provide invaluable pharmacokinetic parameters for liposome loaded doxorubicin. The rate at which drug is distributed between HSA and tissue compartments also enables a better understanding of liposome load drug disposition and prediction *in vivo*. The experiment conducted is a proof of the concept which can be applied and tested using a wide variety of drug loaded liposomal formulations.

5.5. Conclusion

The use of the CRED to investigate liposomal formulations is a novel way of comparing and exploring drug release efficiency. This has implications regarding efficacy, toxicity and stability of liposomal formulations. From the data generated the CRED has shown the capacity to correctly distinguish between liposome formulations DSPC and DOPC in keeping with *in vivo* data. Faster leakage of Doxorubicin loaded unsaturated DOPC with its lower transition temperature was observed in contrast to the more stable saturated liposome. Only

free drug can permeate the semipermeable membrane of the CRED device and therefore authenticates the dynamic process that is occurring within the liposomes where drug is moving from a high concentration within the liposome to a low concentration in its surrounding environment. A classification system can then be applied with HSA spiked Doxorubicin having a fast release rate, liposome 3(DOPC) a medium release rate and liposome 1&2 (DSPC) comparable low release rate using HSA as the baseline. Furthermore, the compartmentalised design of the CRED allows not only for comparison of drug release from liposome formulations but, in tandem allows for the calculation of other important drug distribution parameters such as plasma protein binding, free concentration, and a qualitative measure of the volume of distribution. As new technology to continuously improve liposomes as drug delivery systems evolves, the CRED provides a platform with the capability for complimenting the selection of the most appropriate formulation to support clinical trials with a view of reducing side effects, improving efficacy, and reducing accumulation.

Chapter 6: Improving in vitro prediction of *in-vivo* drug distribution using the Competitive Rapid Equilibrium Dialysis

6.1. Discussion

Plasma protein and tissue binding plays a pivotal role in Drug Discovery Development as it enables a greater understanding between the pharmacokinetics and pharmacodynamics of a drug molecule because unbound drug is the fraction available for drug distribution, elimination, and target binding. It is important therefore, to measure the extent of protein/tissue binding accurately, reliably, and reproducibly at sufficient throughput. Equilibrium dialysis has been established as the gold standard of measuring drug binding to biofluids and tissue homogenates. Comparison of PPB data between in house technique (HSA column chromatography) and the next generation rapid equilibrium dialysis (CRED) across a series of 50 compounds gave a good linear correlation of 0.7011 accounting for most of the variance. The most significant differences were observed in PPB values related to a small portion of compounds namely bases and neutral where there were discrepancies in binding data between the CRED and the observed literature. This could be attributed to a variation in PPB with drug concentration, not having the correct literature value (form of the drug that was dosed may be different) and/or analysis of a different form of the compound i.e a specific enantiomer. The steady-state volume of distribution (VD_{ss}) is a measure of where the drug mostly resides within the body, such as the blood or tissues. The VD_{ss} obtained using the CRED for a subset of the compounds gave a correlation coefficient of approximately 0.5 when compared to observed literature values. CRED relies on passive diffusion of drug and hence the calculated VD_{ss} values represents the passive diffusion component *in vivo*. The correlation of CRED VD_{ss} and literature values would be expected to be strongest when a drug molecule is not subject to extensive active transport into organs and/or tissues. Even so, for drugs undergoing active transport the correlation is sufficient to demonstrate that the drug physicochemical properties are suitable for tissue penetration. A qualitative assessment of the values obtained gave a measure of where drug has a propensity to reside and differentiates this based on acidity or basicity. From the CRED basic compounds had a higher VD_{ss} than acids in line with scientific literature. The inclusion of other major phospholipids at their physiological concentrations improved this correlation from a R² value of 0.5 to 0.8 ((as seen from a subset of the compounds with the outliers removed (Fig 47)). The significance of the compartmentalised design of the CRED to accommodate more complex *in vitro* experiments is therefore advantageous. The remaining 20% of the variance unaccounted for in a R² of 0.8 may be due to the impact of (1) transporters on the distribution of these test compounds, (2) interactions with phospholipids or proteins that are not included as part of the CRED test system or (3) the effect of pH differences that occur on a sub cellular level not accounted for *in vitro*.

By performing a single rather than multiple assays across various species in parallel the CRED device also shows its versatility in better understanding PPB across different species. As shown the PPB increases from preclinical species to human for certain compounds and is related to the protein load. But also, the importance of the physicochemical properties in PPB irrespective of the protein load (highly bound compounds show little difference across species). Therefore, utilising the CRED in *in-vitro* studies may help in understanding dose-toxicity relating to disease state where protein load is compromised (lower protein e.g.in disease state could result in increased free drug concentration and potential toxic effect).

One of the drawbacks in determining plasma protein/tissue binding by means of equilibrium dialysis is the time to reach equilibrium. CRED offer some advantage here over preceding setups and so incubation can be completed in as little as 4hrs to attain equilibrium through

diffusion (as opposed to a full day for say the traditional Dianorm device). The Initial set-up was to determine PPB from a single drug molecule spiked in HSA. Use of 2 CRED devices simultaneously allowed for a maximum of 2 individually spiked experiments to be done at a time. This has progressed to using a cassette of 4 compounds for which PPB was determined simultaneously. Coupled with the use of the RapidSep this drastically reduces the turnaround time and increases the throughput. This is especially useful in the drug discovery environment where fast, reliable data generation is required. Reduction of assay run time from 2.5 minutes per sample to 0.6 minutes means that a full 96-well plate could be analysed under 1 hour (as opposed to 4 hours). The entire time of the incubation and analysis is now around 5 hours given sufficient time in normal working day for the initial set-up and LC-MS data integration. Equilibrium dialysis determines the extent of protein binding while the soluble protein is in its native state and not bound to chromatographic phase where some binding sites may be hindered, or protein conformation may be compromised.

For example, a screen of 50 compounds would utilise 25 CRED units each having available two 6-compartment sections, taking 100 hours (2 compounds per device, each device undergoing 4hrs incubation) to dialyse to equilibrium. This would produce 3000 samples (samples in replicates of 6, calibrants and washes) for LC-MS that would take 125hrs to analyse (2.5mins per injection) compared to using the cassette approach assuming 4 analytes per cassette, then only 28hrs incubations would be required across a smaller number of CRED plates (7 plates) generating 868 samples. RapidSep analysis would realise an LC-MS run time of 8.7 hours (0.6min per injection), so the overall experimental time is reduced by 188.3hrs.

Extraction of samples from the buffer and HSA compartments for calculation of PPB in singlet rather than replicates of 6 would produce 392 injections (2 separate buffer samples, 2 separate HSA samples, 32 calibrants, 20 washes multiplied by 7 plates). Total run time using the RapidSep would then be 3.9hrs. By comparison, analysis of 50 compounds by HSA column chromatography would take approximately 8 hours (6.5minute run time per sample in singlet and including calibrants and quality control samples). The overall analysis time would therefore be 31.9hrs and 8hrs using the CRED and HSA column chromatography, respectively. Using a cassette of compounds along with the RapidSep provides quality data in an environment which better reflects the *in vivo* situation where HSA is not attached to the column which may shield some binding sites. The conformation of HSA (in column chromatography) might be affected by the presence of organic in the elution buffer and therefore affect the binding, hence the use of dialysis as gold standard for PPB determination. The incorporation of Hi-Res MS would further simplify the methodology as the MS/MS conditions would not need optimising on individual compounds, only the accurate mass of the analytes would be needed for the MS method.

6.2. Conclusion

The purpose of this project was to determine whether the CRED could lead to an improvement in the understanding of drug distribution to better aid *in-vitro* prediction by providing a compartmentalised system that better mimics drug distribution *in vivo*. This study used a set of tool compounds across acids, bases, neutrals and zwitterions with human serum albumin and phosphatidylcholine acting as surrogates for human plasma and tissue membrane

respectively. HSA binding, volume of distribution measurements, free drug concentration, free and bound fractions can be determined with a relative certainty of 80% or better. As an initial project greater thought around design, methodology and experimentation can enhance this capability. Evidence of the stereo-selectivity of enantiomers to bind to HSA has been found from the data generated for Orprenadrine(CCI3839) and Verapamil(CCI20557A) and therefore this can be utilised to better understand drug distribution of stereoisomers which can affect the pharmacokinetic of the drug molecule causing side effect and toxicity *in vivo*. The use of different matrices and species enhanced the understanding of the distribution and binding relationship of drug molecules having different physicochemical properties. This enables the effect of modification of drug molecules to achieve a desired outcome to be performed within the CRED. The CRED therefore allows not only for a high throughput but can also facilitate a more in-depth investigation in molecules that progress to improve drug candidates and better predict their pharmacokinetics *in-vivo*. The CRED therefore can complement faster PPB techniques, add diversity to study support for the progression of drug molecules and reduce attrition. Other techniques like column chromatography are available, however, the measurement only provide one element that is important (e.g., HSA binding) and additional factors such as phospholipid binding require separate and additional experiments e.g column based Immobilised artificial membrane. CRED brings all the necessary measurements into a single workflow that is relatively rapid to perform when incubation and analysis times are optimised. Why is this important? Medicinal Chemistry tend to identify lead series with sufficient potency and selectivity to merit further optimisation. Provide measured data back before the next cycle of synthetic experiments means that unpromising lead series can be deprioritised and there is no reliance on *in silico* estimates of physchem properties. Often the importance of this latter point is often underplayed as Medicinal Chemistry is searching for novelty that is patentable. This means the structures being synthesised may be novel and differentiated from those used in the *in silico* test set to build the predictive model. Measured data is therefore superior if it can be generated with sufficient experimental haste.

In terms of Drug Development, CRED would be valuable to probe the binding characteristics to specific proteins or lipids within a single experiment. Rather than screening for potent and tractable leads, Drug Development is looking to understand what drives the distribution of drug and where major accumulation occurs. The variation in protein and phospholipids content across tissue could be explored via CRED and analysed rapidly. Although dialysis cannot by itself account for the component of active transport associated with the distribution of a drug, it can determine how important passive diffusion is relative to transport. If measured VDss is substantially different from the *in vitro* measurement in CRED, then this is a strong indicator that processes other than passive diffusion needed to be investigated and understood further. All in all, CRED is superior to the current approaches available to Drug Discovery and Development scientists, and if adopted widely, would provide better data for better decision making.

6.3. Further Work

The experiments performed using the CRED are not exhaustive and more can be done to improve the predictability *in vivo*. Although improvements have been demonstrated to the overall workflow time, the major bottleneck remains time to equilibrium in the dialysis device. As seen in large molecule analysis a protocol for fast digest has been implemented to speed

up protein extraction (Switzar, Giera et al. 2013) from overnight to within minutes. Similarly, ways of reducing the time to equilibrium within the CRED needs to be explored which can help increase the throughput. Increasing the rate of diffusion is challenging (1) a higher temperature is feasible and simple but this may affect the extent of drug binding to protein, (2) additional agitation could be implemented provided the liquid cells do not overspill and cross contaminate, (3) use of ultrasound to enhance diffusion with a view to ensuring any heat is dissipated effectively. Even a modest gain would be useful because reducing the incubation time from 4 hours to 3 hours would enable 2 incubation runs per day. Increasing the cassette size from 4 to 6 or 8 could potentially reduce the analytical portion of the high throughput method by 1-5- to 2-fold.

As a closed system a way of including or involving drug clearance can also be explored to better mimic the *in vivo* situation. This would reduce two experiments into one and mimic an *IV* dose in a single *in vitro* experiment, e.g., by measuring intrinsic clearance from incubating liver microsomes in parallel to assessing distribution. To fully utilise the CRED in understanding drug distribution organ tissue matrices could be used for e.g., liver, kidney, lung homogenates. Alpa-1-acid glycoprotein is another major protein present in human plasma and therefore may have an impact on the PPB especially for basic drug molecules. In fact, any plasma protein or lipid could be studied if it were believed to be implicated in a specific binding interaction. Experiments involving AGP or a combination of AGP and HSA could therefore be performed with the CRED to investigate whether there is an impact on drug distribution due to enantio-differentiation. The CRED can also be used to investigate whether the binding to HSA differs for enantiomers.

As liposome technology evolves to provide a drug delivery system which reduces toxicity and improves efficacy the CRED device can provide a pivotal role in enhancing this capability. Load efficiency of various formulations can be explored, compared and modified to enhance the *in vivo* prediction.

The use of high-resolution MS as previously mentioned would also simplify the detection and quantification aspects of the analytes instead of the use of Multiple Reaction Monitoring on a triple quad. HR-MS would reduce the instrument set up time as there is no longer a need to optimise the MS/MS conditions for each compound, only the exact mass of the molecular ion is necessary. Another area worth exploring is the use of automation for sampling and extraction post equilibrium dialysis. Acoustic droplet ejection is also a technology beginning to see use as a method to inject nanolitre droplets into the MS source without chromatography (Wang, Dalglish et al. 2020) . Samples are analysed in a few seconds and hence the MS/MS portion of the workflow would be completed in minutes.

-APPENDIX

Appendix 1 Stability of Compounds in Human Serum Albumin and Phosphate Buffered Saline

Stability of Acid Series in Human Serum Albumin

Plate Position_Compound	A1 - CCI6817		B1 - GR62550X		C1 - GR87272X		D1 - GR38714X		E1 - GR70487A	
Sampling Time (Hrs)	T0	T6	T0	T6	T0	T6	T0	T6	T0	T6
Rep 1	8.84	8.43	3.38	3.31	4.9	5.13	2.03	2.33	12.4	12.9
Rep 2	8.49	8.02	3.24	3.26	4.8	5.11	2.29	2.36	13.8	13.3
Rep 3	8.36	8.16	3.38	3.12	5.25	5.20	2.36	2.37	12.6	13.4
Rep 4	8.43	8.44	3.20	3.15	4.87	5.09	2.32	2.37	13.2	13.0
Rep 5	8.36	7.86	3.15	3.09	5.00	4.99	2.64	2.30	12.9	12.6
Rep 6	8.57	7.90	3.15	3.20	4.99	5.16	2.59	2.28	12.4	12.3
Mean Peak Area Ratio	8.51	8.14	3.25	3.19	4.97	5.11	2.37	2.34	12.88	12.92
Std Dev	0.18	0.25	0.11	0.08	0.16	0.07	0.22	0.04	0.55	0.42
CV	2.13	3.13	3.27	2.66	3.16	1.40	9.35	1.64	4.23	3.23
%Diff	-4.39		-1.90		2.92		-1.55		0.26	

Plate Position_Compound	F1 - CCI23760		G1 - CCI120		H1 - GR33000X		A2 - BRL15541Q		B2 - GW289865X		C2 - SB213421-Z	
Sampling Time (Hrs)	T0	T6	T0	T6	T0	T6	T0	T6	T0	T6*	T0	T6
Rep 1	5.64	5.36	21.7	21.2	7.1	7.07	16.7	16.2	34.7	36	4.8	5.03
Rep 2	5.79	5.57	22.8	21	7.07	7.13	16.1	15.7	37.7	36.1	4.08	5.34
Rep 3	5.96	5.71	22.5	20.8	7.06	6.95	16	16.3	37.6	37.2	4.19	5.59
Rep 4	5.59	5.95	23	20.4	7.12	6.9	16.2	16.4	38	35.2	4.3	5.81
Rep 5	5.46	5.49	22	20.5	6.91	7.11	16.1	16.8	37.1	35.7	4.58	6.14
Rep 6	5.74	5.67	21.8	20.5	6.81	6.98	16.4	16.6	36.5	35.6	4.82	6.47
Mean Peak Area Ratio	5.70	5.63	22.30	20.73	7.01	7.02	16.25	16.33	36.93	35.97	4.46	5.73
Std Dev	0.17	0.20	0.54	0.32	0.12	0.09	0.26	0.38	1.21	0.68	0.32	0.53
CV	3.05	3.61	2.44	1.55	1.76	1.33	1.59	2.31	3.29	1.90	7.11	9.18
%Diff	-1.26		-7.03		0.17		0.51		-2.62		28.43	

Plate Position_Compound	D2 - GI235401x		E2 - CCI133*		F2 - GSK275458A		G2 - GR77494A	
Sampling Time (Hrs)	T0	T6	T0	T6	T0	T6	T0	T6
Rep 1	26.3	28.9	3.94	1.25	5.89	5.82	0.0767	0.0907
Rep 2	24.2	30.9	3.79	1.27	5.78	5.69	0.0812	0.11
Rep 3	24.9	30.2	3.91	1.23	5.64	5.56	0.084	0.0815
Rep 4	26.3	30.7	3.73	1.35	5.88	5.58	0.0946	0.0882
Rep 5	27.6	29.8	3.73	1.29	5.52	5.67	0.0879	0.084
Rep 6	29.3	30.1	3.8	1.3	5.69	5.78	0.088	0.0844
Mean Peak Area Ratio	26.43	30.10	3.82	1.28	5.73	5.68	0.09	0.09
Std Dev	1.84	0.71	0.09	0.04	0.14	0.10	0.01	0.01
CV	6.97	2.37	2.34	3.29	2.52	1.83	7.27	11.61
%Diff	13.87		-66.42		-0.87		5.15	

*Compound unstable in HSA and was therefore excluded from the project

HSA		
	C2 - SB213421-Z	
Peak Area	T0	T6
Rep 1	2779220.9	4184764.3
Rep 2	3308716.2	4290160.7
Rep 3	3707519.9	4257443.1
Rep 4	3879558.2	4261823.8
Rep 5	4042983.6	4311990.2
Rep 6	4141167.6	4309688.0
Mean	3643194.40	4269311.68
Std Dev	515002.95	47395.31
CV	14.14	1.11
%Diff	17.2	

Plate Position_Compound	H2 - GR118989X		A3 - AH22182X		B3 - GR87036X		C3 - GW622791X	
Sampling Time (Hrs)	T0	T6	T0	T6	T0	T6	T0	T6
Rep 1	10.0	9.77	12.4	12.8	13.8	14.0	29.7	26.6
Rep 2	9.49	10.2	12.1	13.1	13.3	13.4	29.8	27.8
Rep 3	10.1	10.0	12.9	13.7	13.5	13.0	31.2	27.4
Rep 4	9.63	9.74	12.3	13.9	13.4	14.4	29.2	28.9
Rep 5	9.79	9.83	13.0	13.3	14.3	13.3	30.7	27.8
Rep 6	10.7	9.89	12.6	12.7	13.5	13.4	29.5	27.9
Mean Peak Area Ratio	9.95	9.91	12.55	13.25	13.63	13.58	30.02	27.73
Std Dev	0.43	0.17	0.35	0.48	0.37	0.52	0.77	0.75
CV	4.33	1.73	2.79	3.63	2.69	3.79	2.56	2.70
%Diff	-0.47		5.58		-0.37		-7.61	

Stability of Basic Series in Human Serum Albumin

Plate Position_Compound	A1 - SKF1498A		B1 - SB731710		C1 - CCI3748		D1 - GR30676X		E1 - SKF95914*	
Sampling Time (Hrs)	T0	T6	T0	T6	T0	T6	T0	T6	T0	T6*
Rep 1	11.20	10.3	15.1	15.5	45.5	42.7	8.7	7.99	18.5	5.41
Rep 2	11.00	9.97	15.4	14.8	45.1	42.4	8.68	7.81	18.8	5.34
Rep 3	11.40	9.67	15.3	15.0	46.1	43.3	8.73	7.88	18.3	5.55
Rep 4	10.90	9.93	15.8	15.3	47.2	42.2	8.74	7.80	18.9	7.80
Rep 5	11.20	9.90	14.9	14.8	46.4	43.1	8.94	7.75	15.8	5.08
Rep 6	10.50	9.67	15.9	14.7	45.9	42.6	9.02	7.99	19.3	11.20
Mean Peak Area Ratio	11.03	9.91	15.40	15.02	46.03	42.72	8.80	7.87	18.27	6.73
Std Dev	0.31	0.23	0.39	0.32	0.73	0.42	0.14	0.10	1.26	2.40
CV	2.85	2.35	2.53	2.12	1.59	0.98	1.61	1.29	6.88	35.73
%Diff	-10.21		-2.49		-7.20		-10.59		-63.16	

Variability in sample injections 6hrs. Compound stable in PBS and was included in project

Plate Position_Compound	F1 - GR189721X		H1 - GR43175X		A2 - GF120454X		B2 - GR99941A	
Sampling Time (Hrs)	T0	T6	T0	T6	T0	T6	T0	T6
Rep 1	27.7	24.4	5.65	13.6	8.09	7.83	22.6	22.3
Rep 2	24.1	22.5	5.29	16.5	8.42	7.26	22.7	20.7
Rep 3	24.2	24.0	5.57	6.04	8.42	6.83	22.9	21.4
Rep 4	23.3	24.3	5.18	79.4	8.87	7.73	22.2	20.7
Rep 5	23.0	23.1	5.03	8.60	8.43	7.85	22.3	21.6
Rep 6	23.3	23.5	5.43	6.02	8.45	7.99	23.2	21.8
Mean Peak Area Ratio	24.27	23.63	5.36	21.69	8.45	7.58	22.65	21.42
Std Dev	1.75	0.74	0.24	28.58	0.25	0.45	0.37	0.63
CV	7.21	3.14	4.41	131.75	2.94	5.87	1.65	2.94
%Diff	-2.61		304.85		-10.24		-5.45	

Variability in internal standard at 6hrs. Stability obtained in PBS therefore compound included in project

Plate Position_Compound	C2 - GW300671A		D2 - SB416332AAA		E2 - CC13839		F2 - GR61317X	
Sampling Time (Hrs)	T0	T6	T0	T6	T0	T6	T0	T6
Rep 1	18.4	17.4	9.36	9.62	103	101	3.43	3.25
Rep 2	18.5	17.2	9.14	9.11	100	95.1	3.41	3.22
Rep 3	18.6	17.3	9.40	9.17	104	92.4	3.27	3.17
Rep 4	16.5	18.1	8.79	9.15	98.7	85.9	3.35	3.15
Rep 5	17.5	16.9	9.79	8.8	107	93.9	3.48	2.92
Rep 6	18.7	13.3	9.05	9.68	105	97.4	3.35	3.08
Mean Peak Area Ratio	18.03	16.70	9.26	9.26	102.95	94.28	3.38	3.13
Std Dev	0.87	1.71	0.34	0.33	3.11	5.09	0.07	0.12
CV	4.80	10.25	3.71	3.62	3.02	5.40	2.18	3.81
%Diff	-7.39		0.00		-8.42		-7.4	

Plate Position_Compound	H2 - GW769340X		A3 - CCI120557A		B3 - CCI4001		C3 - GR84804A		D3 - GW787034X	
Sampling Time (Hrs)	T0	T6	T0	T6	T0	T6	T0	T6	T0	T6
Rep 1	15.5	14.8	38.9	36.2	14.9	12.2	23.7	23.4	7.68	7.50
Rep 2	15.4	15.3	40.5	38.6	14.1	13.8	23.6	23.2	6.97	7.49
Rep 3	16.3	15	38.2	38.2	13.3	15.1	22.8	23.0	7.36	7.62
Rep 4	15	27.6	39.8	38.3	14.2	14.7	22.3	23.0	6.92	7.63
Rep 5	15.6	14.9	41.6	37.7	13.8	14.1	23.5	22.9	7.28	7.51
Rep 6	16.4	10.4	38.2	38.8	14.9	14	24.0	23.0	7.21	7.64
Mean Peak Area Ratio	15.70	16.33	39.53	37.97	14.20	13.98	23.32	23.08	7.24	7.57
Std Dev	0.54	5.82	1.36	0.94	0.63	1.00	0.64	0.18	0.28	0.07
CV	3.47	35.64	3.44	2.49	4.41	7.14	2.73	0.79	3.84	0.95
%Diff	4.03		-3.96		-1.53		-1.00		4.54	

Stability of Neutral Series in Human Serum Albumin

Plate Position_Compound	A1 - GR91295X		B1 - CC19371		D1 - CCI22428		E1 - GR104104X	
Sampling Time (Hrs)	T0	T6	T0	T6	T0	T6	T0	T6
Rep 1	18.50	21.50	1.82	1.85	6.14	6.13	14	12.6
Rep 2	18.00	20.90	1.79	1.77	6.3	6.05	13.7	13
Rep 3	19.10	21.20	1.74	1.79	6.29	5.94	14.6	13.3
Rep 4	19.10	22.00	1.83	1.79	6.34	5.97	13.5	13.9
Rep 5	19.00	21.80	1.73	1.94	6.04	5.99	13.8	12.8
Rep 6	20.20	21.50	1.84	1.88	6.09	5.8	14.3	12.7
Mean Peak Area Ratio	18.98	21.48	1.79	1.84	6.20	5.98	13.98	13.05
Std Dev	0.74	0.40	0.05	0.07	0.13	0.11	0.41	0.48
CV	3.88	1.85	2.63	3.57	2.03	1.86	2.91	3.71
%Diff	13.17		2.51		-3.55		-6.67	

Plate Position_Compound	C2 - GF120403X		E2 - GR78367X*		G2 - GI115674X		H2 - AH23463X		A3 - GR35842A	
Sampling Time (Hrs)	T0	T6	T0	T6	T0	T6	T0	T6	T0	T6*
Rep 1	20.60	20.00	0.101	0.0147	14.9	14	18.2	21.4	1.04	0.912
Rep 2	19.90	19.90	0.103	0.0157	14.7	12.6	18.7	20.7	0.941	0.89
Rep 3	21.80	19.50	0.098	0.0127	14.8	13.6	18.1	21	1.07	0.974
Rep 4	20.30	19.40	0.104	0.0155	14.8	14.1	18.5	22.5	1.04	0.887
Rep 5	20.30	19.80	0.101	0.0173	15.5	14.1	19.2	21	1.05	0.946
Rep 6	20.20	18.70	0.102	0.0138	14.8	13.6	18.1	21.8	1.07	0.923
Mean Peak Area Ratio	20.52	19.55	0.10	0.01	14.92	13.67	18.47	21.40	1.04	0.92
Std Dev	0.67	0.48	0.00	0.00	0.29	0.57	0.43	0.66	0.05	0.03
CV	3.25	2.44	2.08	10.72	1.96	4.18	2.34	3.09	4.65	3.64
%Diff	-4.71		-85.27		-8.38		15.88		-10.93	

*split peaks at 0hrs, single peak post incubation and compound therefore not progressed

Plate Position_Compound	F1 - GR33914X		G1 - GR38393X		H1 - GW388185X		A2 - GR119497X	
Sampling Time (Hrs)	T0	T6	T0	T6	T0	T6	T0	T6
Rep 1	4.61	4.92	23.4	23.9	11.5	11.5	12.2	12.6
Rep 2	5.12	5.46	24.1	24.1	11	10.7	12.9	12.2
Rep 3	5.18	5.53	23.5	24.3	10.6	11.7	11.9	12.2
Rep 4	4.72	5.67	24.3	24	11.6	11	12.7	12.8
Rep 5	5.03	5.39	22.2	24.1	10.5	10.4	13.2	11.7
Rep 6	5.04	5.65	24.2	22.8	11.2	10.9	12.3	12.4
Mean Peak Area Ratio	4.95	5.44	23.62	23.87	11.07	11.03	12.53	12.32
Std Dev	0.23	0.28	0.79	0.54	0.45	0.49	0.48	0.38
CV	4.65	5.06	3.34	2.26	4.11	4.43	3.87	3.10
%Diff	9.83		1.06		-0.30		-1.73	

Plate Position_Compound	B2 - GW703803X		D2 - GR64334X		F2 - GI116108X		C1 - GI99296X*	
Sampling Time (Hrs)	T0	T6	T0	T6	T0	T6	T0	T6
Rep 1	121.00	120.00	1.04	1.03	28.6	28.3	15.3	19.4
Rep 2	117.00	115.00	1.09	1.11	27.6	29.1	15.8	21.5
Rep 3	121.00	119.00	1.05	1.09	27.8	27	15.1	19.2
Rep 4	120.00	128.00	0.969	1.09	28.9	27.5	16.3	19.8
Rep 5	118.00	122.00	0.999	1.01	27.3	28.1	15.8	19.4
Rep 6	111.00	122.00	1.12	1.01	28.8	28.1	16	20.6
Mean Peak Area Ratio	118.00	121.00	1.04	1.06	28.17	28.02	15.72	19.98
Std Dev	3.79	4.29	0.06	0.05	0.68	0.72	0.44	0.90
CV	3.22	3.55	5.35	4.26	2.43	2.56	2.83	4.48
%Diff	2.54		1.15		-0.53		27.15	

*Decrease in internal standard peak area at 6hrs causing an increase in peak area ratio. Stability calculated using analyte peak area as shown below. Compound included in project.

	Analyte Peak Area	
Plate Position_Compound	C1 - GI99296X	
Sampling Time (Hrs)	T0	T6
Rep 1	2909665	3002255.4
Rep 2	3021875.3	3066842
Rep 3	3020611.4	3049831.2
Rep 4	3063587.6	3196102.9
Rep 5	3133371.9	3198783.1
Rep 6	3106710.7	3169968.9
Mean Peak Area Ratio	3042636.98	3113963.92
Std Dev	79214.79	84723.00
CV	2.60	2.72
%Diff	4.50	

Stability of Acid Series in Phosphate Buffered Saline

Plate Position_Compound	A1 - CCI6817		B1 - GR62550X		C1 - GR87272X		D1 - GR38714X		E1 - GR70487A	
Sampling Time (Hrs)	T0	T6	T0	T6	T0	T6	T0	T6	T0	T6*
Rep 1	7.74	7.55	7.34	7.63	4.64	4.79	1.59	1.59	10.3	10.3
Rep 2	7.67	7.99	7.37	7.06	4.67	4.93	1.78	1.59	10.4	10.7
Rep 3	7.67	7.97	7.69	7.28	4.71	4.52	1.55	1.61	10.2	10.4
Rep 4	7.60	8.1	7.38	7.5	4.46	4.35	1.48	1.74	9.91	10.3
Rep 5	8.30	8.14	7.44	7.11	4.56	4.51	1.59	1.59	9.96	10.0
Rep 6	7.85	8.29	7.23	7.05	4.45	4.48	1.52	1.52	10.2	10.6
Mean Peak Area Ratio	7.81	8.01	7.41	7.27	4.58	4.60	1.59	1.61	10.16	10.38
Std Dev	0.26	0.25	0.15	0.25	0.11	0.22	0.10	0.07	0.19	0.25
CV	3.29	3.14	2.08	3.37	2.40	4.73	6.59	4.50	1.88	2.39
%Diff	2.58		-1.84		0.33		1.37		2.18	

Plate Position_Compound	F1 - CCI23760		G1 - CCI120		H1 - GR33000X		A2 - BRL15541Q		B2 - GW289865X	
Sampling Time (Hrs)	T0	T6	T0	T6	T0	T6	T0	T6	T0	T6*
Rep 1	5.10	5.17	18.4	20.6	6.80	7.09	17.6	17.3	36.8	39.9
Rep 2	5.26	4.92	20.6	17.7	6.73	6.55	17.6	17.5	37.8	38.3
Rep 3	4.62	5.01	19.0	19.9	6.97	7.13	17.0	17.6	36.6	38.8
Rep 4	4.73	4.80	18.9	19.5	6.52	6.94	17.7	18.2	39.7	37.9
Rep 5	4.58	4.89	18.5	19.2	6.69	7.05	17.5	17.6	38.6	38.6
Rep 6	4.79	5.28	19.5	19.1	6.72	7.26	17.6	17.6	38.7	37.5
Mean Peak Area Ratio	4.85	5.01	19.15	19.33	6.74	7.00	17.50	17.63	38.03	38.50
Std Dev	0.27	0.18	0.81	0.97	0.15	0.25	0.25	0.30	1.20	0.83
CV	5.65	3.63	4.24	5.01	2.18	3.50	1.45	1.71	3.15	2.16
%Diff	3.40		0.96		3.93		0.76		1.23	

	D2 - GI235401x		E2 - CCI133*		F2 - GSK275458A		G2 - GR77494A	
Peak Area Ratio	T0	T6	T0	T6	T0	T6	T0	T6
Rep 1	21.6	26.9	3.67	2.55	5.49	5.47	0.086	0.081
Rep 2	21.2	27.5	3.6	2.42	5.36	5.71	0.0968	0.0716
Rep 3	23.8	26.3	3.74	2.4	5.34	5.56	0.0677	0.069
Rep 4	23.5	26.6	3.64	2.45	5.36	5.35	0.0909	0.0931
Rep 5	23.7	25.6	3.55	2.55	5.40	5.61	0.0956	0.0719
Rep 6	27.6	28.6	3.43	2.66	5.20	5.40	0.0845	0.073
Mean	23.57	26.92	3.61	2.51	5.36	5.52	0.09	0.08
Std Dev	2.27	1.04	0.11	0.10	0.09	0.14	0.01	0.01
CV	9.64	3.86	2.97	3.97	1.76	2.45	12.23	11.81
%Diff	14.21		-30.51		2.95		-11.87	

*Compound unstable in HSA and was therefore excluded from the project

Plate Position_Compound	H2 - GR118989X		A3 - AH22182X		B3 - GR87036X		C3 - GW622791X	
Sampling Time (Hrs)	T0	T6	T0	T6	T0	T6	T0	T6
Rep 1	13.6	12.6	14.3	16.1	15	16.2	25.1	23.2
Rep 2	13.6	13.4	14.0	16.2	15.1	15.4	25.5	23.5
Rep 3	14.6	12.9	14.9	15.8	15	15.9	25.2	24.1
Rep 4	13.4	13.3	15.0	14.2	15.6	15.6	24.5	23.8
Rep 5	13.5	13.5	14.0	15.3	15.9	15.3	24.3	24
Rep 6	13.5	13.2	15.9	15.2	15.3	15.6	24.4	23.5
Mean Peak Area Ratio	13.70	13.15	14.68	15.47	15.32	15.67	24.83	23.68
Std Dev	0.45	0.34	0.74	0.74	0.37	0.33	0.50	0.34
CV	3.26	2.58	5.01	4.80	2.39	2.12	2.00	1.45
%Diff	-4.01		5.33		2.29		-4.63	

Stability of Basic Series in Phosphate Buffered Saline

Plate Position_Compound	A1 - SKF1498A		B1 - SB731710		C1 - CCI3748		D1 - GR30676X	
Sampling Time (Hrs)	T0	T6	T0	T6	T0	T6	T0	T6
Rep 1	1.85	1.43	2.22	2.38	4.21	4.53	1.27	1.37
Rep 2	1.80	1.40	2.20	2.37	4.28	4.62	1.27	1.37
Rep 3	1.83	1.40	2.23	2.38	3.79	4.71	1.25	1.40
Rep 4	1.86	1.39	2.16	2.42	4.30	4.79	1.27	1.42
Rep 5	1.82	1.42	2.26	2.40	4.29	4.75	1.26	1.42
Rep 6	1.82	1.42	2.23	2.42	4.24	4.80	1.22	1.40
Mean Peak Area Ratio	1.83	1.41	2.22	2.40	4.19	4.70	1.26	1.40
Std Dev	0.02	0.02	0.03	0.02	0.20	0.11	0.02	0.02
CV	1.20	1.10	1.53	0.91	4.69	2.25	1.56	1.61
%Diff	-22.95		8.05		12.31		11.14	

	A1 - SKF1498A	
Peak Area	T0	T6
Rep 1	6623195.2	5771357.3
Rep 2	6592574.5	5767774.2
Rep 3	6547908.4	5820017.2
Rep 4	6468763.2	5789195.3
Rep 5	6426885.4	5874880.8
Rep 6	6390033.1	5846073.3
Mean	6508226.63	5811549.68
Std Dev	93862.08	43141.28
CV	1.44	0.74
%Diff	-10.70	

Plate Position_Compound	E1 - SKF95914		F1 - GR189721X		H1 - GR43175X		A2 - GF120454X	
Sampling Time (Hrs)	T0	T6	T0	T6	T0	T6	T0	T6
Rep 1	2.47	2.36	30.4	29.8	4.82	4.32	10.6	10.4
Rep 2	2.50	2.30	30.8	27.2	4.83	3.98	10.5	10.1
Rep 3	2.50	2.28	29.2	29.5	4.7	4.4	9.53	9.85
Rep 4	2.50	2.38	30.6	29.5	4.8	4.37	10.2	9.66
Rep 5	2.42	2.25	29.0	28.3	4.34	4.48	11.4	9.75
Rep 6	2.48	2.36	32.8	28.7	4.55	4.21	11.6	10.7
Mean Peak Area Ratio	2.48	2.32	30.47	28.83	4.67	4.29	10.64	10.08
Std Dev	0.03	0.05	1.37	0.98	0.19	0.18	0.77	0.41
CV	1.26	2.25	4.48	3.40	4.16	4.14	7.22	4.03
%Diff	-6.32		-5.36		-8.13		-5.28	

Plate Position_Compound	B2 - GR99941A		C2 - GW300671A		D2 - SB416332AAA		E2 - CC13839	
Sampling Time (Hrs)	T0	T6	T0	T6	T0	T6	T0	T6
Rep 1	21.3	22.3	15.9	12.9	9.19	8.53	56.7	52.1
Rep 2	21.3	22	14.6	15.6	8.58	8.29	53.1	53.4
Rep 3	20.8	20.7	16.2	15	8.72	8.58	52.8	52.6
Rep 4	22.8	22	15.7	14.6	8.87	8.48	55.4	51.2
Rep 5	21.3	21.2	14.3	14.6	9.13	8.39	60.6	50.4
Rep 6	20.5	20.7	13.2	15.1	8.32	8.2	52.8	48.9
Mean Peak Area Ratio	21.33	21.48	14.98	14.63	8.80	8.41	55.23	51.43
Std Dev	0.79	0.71	1.15	0.93	0.33	0.15	3.08	1.63
CV	3.71	3.30	7.68	6.33	3.77	1.74	5.57	3.16
%Diff	0.70		-2.34		-4.43		-6.88	

Plate Position_Compound	F2 - GR61317X		G2 - GR183544X		H2 - GW769340X		A3 - CCI120557A	
Sampling Time (Hrs)	T0	T6	T0	T6	T0	T6	T0	T6
Rep 1	0.523	0.493	1.24	1.22	1.93	1.83	4.73	4.67
Rep 2	0.515	0.501	1.23	1.27	1.9	1.85	4.69	4.66
Rep 3	0.522	0.491	1.26	1.25	1.91	1.91	4.74	4.48
Rep 4	0.513	0.494	1.24	1.22	1.9	1.88	4.77	4.68
Rep 5	0.509	0.495	1.24	1.24	1.89	1.93	4.85	4.62
Rep 6	0.52	0.485	1.25	1.26	1.93	1.87	4.73	4.59
Mean Peak Area Ratio	0.52	0.49	1.24	1.24	1.91	1.88	4.75	4.62
Std Dev	0.01	0.01	0.01	0.02	0.02	0.04	0.05	0.08
CV	1.07	1.06	0.83	1.66	0.88	1.98	1.15	1.62
%Diff	-4.6		0.00		-1.66		-2.84	

Plate Position_Compound	B3 - CCI4001		C3 - GR84804A		D3 - GW787034X	
Sampling Time (Hrs)	T0	T6	T0	T6	T0	T6
Rep 1	1.99	1.97	3.44	3.41	1.58	1.56
Rep 2	1.98	1.98	3.48	3.33	1.64	1.59
Rep 3	2.02	1.95	3.51	3.39	1.57	1.53
Rep 4	1.97	1.96	3.44	3.39	1.66	1.62
Rep 5	1.98	1.92	3.5	3.37	1.66	1.66
Rep 6	1.98	1.96	3.43	3.46	1.58	1.59
Mean Peak Area Ratio	1.99	1.96	3.47	3.39	1.62	1.59
Std Dev	0.02	0.02	0.03	0.04	0.04	0.05
CV	0.88	1.06	0.99	1.27	2.65	2.85
%Diff	-1.51		-2.16		-1.44	

Stability of Neutral Series in Phosphate Buffered Saline

Plate Position_Compound	A1 - GR91295X		B1 - CC19371		D1 - CCI22428		E1 - GR104104X	
Sampling Time (Hrs)	T0	T6	T0	T6	T0	T6	T0	T6
Rep 1	1.85	1.86	0.470	0.49	0.917	0.881	1.83	1.76
Rep 2	1.83	1.84	0.513	0.489	0.898	0.871	1.77	1.78
Rep 3	1.77	1.85	0.493	0.481	0.868	0.897	1.79	1.79
Rep 4	1.85	1.85	0.505	0.49	0.889	0.882	1.77	1.80
Rep 5	1.84	1.82	0.500	0.497	0.905	0.873	1.72	1.80
Rep 6	1.82	1.82	0.497	0.491	0.885	0.878	1.78	1.79
Mean Peak Area Ratio	1.83	1.84	0.50	0.49	0.89	0.88	1.78	1.79
Std Dev	0.03	0.02	0.01	0.01	0.02	0.01	0.04	0.02
CV	1.65	0.91	2.95	1.05	1.90	1.05	2.00	0.84
%Diff	0.73		-1.34		-1.49		0.56	

Plate Position_Compound	C2 - GF120403X		E2 - GR78367X*		G2 - GI115674X		H2 - AH23463X		A3 - GR35842A	
Sampling Time (Hrs)	T0	T6	T0	T6	T0	T6	T0	T6	T0	T6
Rep 1	2.70	2.70	0.034	0.012	2.66	2.52	1.68	1.67	0.427	0.349
Rep 2	2.73	2.71	0.035	0.013	2.54	2.56	1.67	1.66	0.428	0.351
Rep 3	2.71	2.72	0.038	0.012	2.57	2.56	1.65	1.64	0.434	0.355
Rep 4	2.66	2.65	0.032	0.012	2.59	2.58	1.64	1.67	0.429	0.351
Rep 5	2.65	2.75	0.037	0.013	2.57	2.53	1.67	1.69	0.432	0.356
Rep 6	2.64	2.69	0.033	0.012	2.63	2.54	1.68	1.69	0.437	0.359
Mean Peak Area Ratio	2.68	2.70	0.03	0.01	2.59	2.55	1.67	1.67	0.43	0.35
Std Dev	0.04	0.03	0.00	0.00	0.04	0.02	0.02	0.02	0.00	0.00
CV	1.36	1.23	6.34	2.77	1.70	0.87	0.99	1.14	0.90	1.07
%Diff	0.81		-64.79		-1.74		0.30		-18.01	

*split peaks at 0hrs, single peak post incubation and compound therefore not progressed

Plate Position_Compound	F1 - GR33914X*		G1 - GR38393X		H1 - GW388185X		A2 - GR119497X	
Sampling Time (Hrs)	T0	T6	T0	T6	T0	T6	T0	T6
Rep 1	6.71	5.07	8.39	8.81	5.13	4.78	3.78	4.2
Rep 2	7.82	4.88	9.12	8.31	5.12	5.02	4.08	3.92
Rep 3	7.33	4.84	8.86	8.34	5.04	4.47	3.9	4.09
Rep 4	6.21	4.73	8.79	8.67	5	4.79	3.98	4.05
Rep 5	5.77	4.62	9.33	8.74	5.17	4.91	3.99	4.06
Rep 6	5.74	4.73	9.58	8.64	4.91	4.93	3.93	4.02
Mean Peak Area Ratio	6.60	4.81	9.01	8.59	5.06	4.82	3.94	4.06
Std Dev	0.85	0.16	0.42	0.21	0.10	0.19	0.10	0.09
CV	12.89	3.25	4.69	2.45	1.92	3.99	2.56	2.25
%Diff	-27.06		-4.73		-4.84		2.87	

*Increased peak area of internal standard observed during the analysis attributed to reduced peak area ratio at 6hrs. Compound therefore included in project

Plate Position_Compound	B2 - GW703803X		D2 - GR64334X		F2 - GI116108X		C1 - GI99296X	
Sampling Time (Hrs)	T0	T6	T0	T6	T0	T6	T0	T6
Rep 1	34.8	35.5	1.65	1.26	13.0	12.3	6.54	4.91
Rep 2	34.5	35.7	1.74	1.21	12.7	13.1	6.08	6.39
Rep 3	33.8	35.4	1.65	1.31	12.6	12.4	6.01	5.06
Rep 4	36.3	34.6	1.77	1.40	13.1	12.8	5.77	5.06
Rep 5	37.1	35.3	1.79	1.30	12.8	12.5	5.81	5.15
Rep 6	36.7	35.4	1.88	1.28	12.8	15.3	5.91	5.09
Mean Peak Area Ratio	35.53	35.32	1.75	1.29	12.8	13.1	6.02	5.28
Std Dev	1.34	0.38	0.09	0.06	0.2	1.1	0.28	0.55
CV	3.78	1.07	5.05	4.88	1.5	8.7	4.66	10.44
%Diff	-0.61		-25.95		1.8		-12.35	

Compound is unstable in PBS (outside of $\pm 20\%$) but stable in human serum albumin.

Included as the internal standard performance was inconsistent for the replicate injections at 0 and 6 hr in PBS.

Appendix 2 Mass Spectrometer Acquisition Parameters

Mass Spectrometer Acquisition Parameters of Acid Series

Compound	Plate Position	Precursor	Product	DP	CE	CXP	Ionization Mode
CCI6817	A1	228.9	165.1	-88.9	-31.2	-11.2	Negative
GR62550X	B1	243.3	199.1	-33.9	-9.93	-11.0	
GR87272X	C1	307.2	198.1	-61.8	-38.2	-12	
GR138714X	D1	574.6	462.2	-68.2	-42.5	-15	
GR70487A	E1	423.5	303.3	-75.0	-22.4	-16	
CCI23760	F1	229.1	185.1	-32.8	-9.7	-12	
CCI120	G1	356.1	312.1	-43.2	-12.3	-11.5	
GR33000X	H1	330.4	266.1	-49.6	-18	-14.6	
BRL15541Q	A2	253.2	208.9	-49.3	-11	-11	
GW289865X	B2	286.1	212.1	-68.3	-33.2	-11.5	
SB213421-Z	C2	258.3	118.9	58.5	22.0	10.8	Positive
GI235401X	D2	249.1	156.9	-60.6	-48.1	-10.3	Negative
CCI133	E2	179.1	137.1	-29.6	-9.4	-9.5	
GSK275458A	F2	292.2	220.2	-75.6	-28.5	-11.5	Positive
GR77494A	G2	230.1	171.0	47	25.6	13	
GR118989X	H2	329.2	284.9	-60.8	-20.4	-14.5	Negative
AH22182X	A3	403.2	125.0	-65	-26.9	-9.4	
GR87036X	B3	284.2	240.0	-75.1	-21.7	-14	
GW622791X	C3	427.3	193.1	-85	-35.6	-10.7	

Mass Spectrometer Acquisition Parameters of Basic Series

Compound	Plate Position	Precursor	Product	DP	CE	CXP	Ionization Mode
CCI3993	A1	285.1	198.1	58.5	30	16.5	Positive
SB731710	B1	448.2	285.1	33.9	33.9	15	
CCI3748	C1	376.1	165.1	40	34.9	14.8	
GR30676X	D1	462.4	328.3	29	41	15	
SKF95914	E1	470.4	167.1	22	39	14	
GR189721X	F1	313.3	256.2	51.7	28.6	18	
GR192446A	G1	336.4	261.1	70	26.3	15	
GR43175X	H1	296.3	251.1	22.6	25	21	
GF120454X	A2	314.2	271.0	47.8	34.0	19	
GR99941A	B2	388.9	201.1	50.2	25.7	15.5	
GW300671A	C2	502.3	466.3	88.7	36.6	17	
SB416332AA	D2	278.4	215.1	49.6	22.4	17.5	
CC13839	E2	256.2	167.1	29.5	33	16	
GR61317X	F2	404.4	360.2	30	28.9	12	
GR183544X	G2	288.4	243.2	45.2	24.9	16.5	
GW769340A	H2	256.3	148.3	31	12	12.9	
CCII20557A	A3	455.3	165.1	15	38	15	
CCI4001	B3	260.1	183.1	33.5	25.1	16	
GR84804A	C3	263.9	233.2	53.6	20.9	18	
GW787034X	D3	311.1	259.1	40.3	27.5	15.5	

Mass Spectrometer Acquisition Parameters of Neutral Series

Compound	Plate Position	Precursor	Product	DP	CE	CXP	Ionization Mode
GR91295X	A1	279.3	180.8	41	24.1	13.8	Positive
CC19371	B1	341.4	187.0	70	30.5	13.5	
CC122428	D1	375.4	339.3	27.8	14.3	8.7	
GR104104X	E1	237.2	161.0	36	15.1	13.8	
GF120403X	C2	366.1	259.0	60.4	25.6	14.2	
GR78367X	E2	405.5	199.1	45	17.6	16	
GI115674X	G2	276.1	208.1	71	22	13.5	
AH23463X	H2	249.3	156.0	80	20.6	13.8	
GR35842A	A3	289.2	271.2	49	21.5	16	
GR33914X	F1	417.1	294.3	-27.7	-25.9	-16	Negative
GR38393X	G1	359.1	122.2	-59.4	-25.5	-19.6	
GW388185X	H1	380.1	316.1	-97.4	-30.3	-10	
GR119497X	A2	283.9	242.0	-68.2	-30.9	-12	
GW703803X	B2	429.1	255.1	-48.9	-18.4	-12.40	
GR64334X	D2	382.1	145.0	-52.6	-18	-18.6	
GI116108X	F2	370.1	118.9	-60.7	-21.7	-10	
GI99296X	C1	269.1	159.9	-45.5	-28.4	-12	

Appendix 3 Pilot Study In-Vitro Pharmacokinetic Parameters
Pilot Study *In-Vitro* Pharmacokinetic Parameters of Acid series using CRED Device

Compound Number	CC16817					
	PC 1	PC 2A	PC 3	PC 2B	1% PBS	HSA
Rep 1	1.504	2.344	2.301	2.006	0.929	3.474
Rep 2	1.618	2.073	2.226	2.314	1.006	3.983
Rep 3	1.584	2.214	2.093	2.188	0.950	3.710
Rep 4	1.497	2.265	2.249	2.145	0.964	3.660
Rep 5	1.699	2.144	2.115	1.928	0.948	3.325
Rep 6	1.481	2.302	2.244	2.007	1.117	3.332
Mean	1.564	2.224	2.205	2.098	0.986	3.581
SD	0.09	0.10	0.08	0.14	0.07	0.25
CV	5.5	4.6	3.7	6.8	7.0	7.1
Free Concentration (μm)					0.986	
% HSA Binding						72.5
% PC Binding	36.9	55.7	55.3	53.0		
Free Fraction (fu)	0.631	0.443	0.447	0.470		0.275

Compound Number	CC16817					
	PC 1	PC 2A	PC 3	PC 2B	1% PBS	HSA
Rep 1	2.826	3.970	3.703	3.221	1.286	5.019
Rep 2	3.082	3.705	3.593	3.654	1.617	4.946
Rep 3	3.206	4.017	3.660	3.658	1.849	6.281
Rep 4	2.942	3.957	3.700	3.239	0.846	5.401
Rep 5	3.081	3.818	3.604	3.322	1.069	5.327
Rep 6	2.910	3.824	3.583	3.319	1.069	5.225
Mean	3.008	3.882	3.641	3.402	1.333	5.367
SD	0.14	0.12	0.05	0.20	0.38	0.48
CV	4.6	3.1	1.5	5.9	28.3	9.0
Free Concentration (μm)					1.333	
% HSA Binding						75.2
% PC Binding	55.7	65.7	63.4	60.8		
Free Fraction (fu)	0.443	0.343	0.366	0.392		0.248

Compound Number	CC16817					
	PC 1	PC 2A	PC 3	PC 2B	1% PBS	HSA
Rep 1	0.938	1.114	1.735	1.566	0.816	2.167
Rep 2	0.932	1.143	1.231	1.325	0.805	2.021
Rep 3	1.133	1.341	1.414	1.491	0.733	2.091
Rep 4	0.935	1.210	1.327	1.266	0.795	2.215
Rep 5	1.047	1.235	1.336	1.298	0.829	2.402
Rep 6	1.034	1.263	1.403	1.291	0.703	2.295
Mean	1.003	1.218	1.408	1.373	0.796	2.199
SD	0.08	0.08	0.17	0.12	0.05	0.14
CV	8.2	6.8	12.3	9.1	6.3	6.3
Free Concentration (μM)					0.796	
% HSA Binding						63.8
% PC Binding	20.7	34.7	43.5	42.0		
Free Fraction (fu)	0.793	0.653	0.565	0.580		0.362

Compound Number	GR77494					
	PC 1	PC 2A	PC 3	PC 2B	1% PBS	HSA
Rep 1	0.844	0.936	1.036	1.122	0.886	1.396
Rep 2	0.822	1.025	1.078	1.050	0.984	1.255
Rep 3	0.789	1.015	1.054	1.038	0.860	1.368
Rep 4	0.848	0.972	1.177	1.234	0.918	1.451
Rep 5	0.810	1.061	1.098	1.130	0.826	1.415
Rep 6	0.813	1.020	1.042	1.127	0.883	1.453
Mean	0.821	1.005	1.081	1.117	0.895	1.390
SD	0.02	0.04	0.05	0.07	0.05	0.07
CV	2.7	4.4	4.9	6.3	6.0	5.3
Free Concentration (μM)					0.895	
% HSA Binding						35.6
% PC Binding	[-9.0]	11.0	17.2	19.9		
Free Fraction (fu)	[1.090]	0.890	0.828	0.801		0.644

Compound Number	GR77494					
	PC 1	PC 2A	PC 3	PC 2B	1% PBS	HSA
Rep 1	0.918	1.087	1.531	0.961	1.189	1.533
Rep 2	1.096	1.291	1.037	1.138	1.210	1.437
Rep 3	1.258	1.011	0.945	1.025	0.999	1.340
Rep 4	1.271	1.019	1.303	1.013	1.289	1.683
Rep 5	1.173	1.257	0.964	1.544	1.448	1.619
Rep 6	1.312	1.148	1.206	1.338	1.507	1.762
Mean	1.171	1.136	1.164	1.170	1.274	1.562
SD	0.146	0.119	0.228	0.227	0.185	0.157
CV	12.5	10.5	19.6	19.4	14.6	10.1
Free Concentration (μM)					1.274	
% HSA Binding						18.5
% PC Binding	-8.7	-37.6	-9.4	-8.9		
Free Fraction (fu)	1.087	1.122	1.094	1.089		0.815

Compound Number	GR77494					
	PC 1	PC 2A	PC 3	PC 2B	1% PBS	HSA
Rep 1	1.004	1.259	1.243	*	0.875	1.091
Rep 2	1.002	1.216	*	*	0.738	1.035
Rep 3	1.065	1.330	*	*	0.776	1.125
Rep 4	*	*	*	*	*	1.343
Rep 5	*	*	*	*	*	1.189
Rep 6	*	*	*	*	*	1.268
Mean	1.024	1.268	1.243	N/A	0.796	1.175
SD	0.04	0.06	N/A	N/A	0.07	0.12
CV	3.5	4.5	N/A	N/A	8.9	9.8
Free Concentration (μM)					0.796	
% HSA Binding						32.2
% PC Binding	22.2	37.2	35.9	N/A		
Free Fraction (fu)	0.78	0.63	0.64	N/A		67.8

*Bad injection no data acquired

Compound Number	GI235401					
	PC 1	PC 2A	PC 3	PC 2B	1% PBS	HSA
Rep 1	0.000	0.025	0.074	0.000	0.000	2.611
Rep 2	0.000	0.029	0.100	0.000	0.000	2.594
Rep 3	0.000	0.016	0.091	0.000	0.000	2.427
Rep 4	0.000	0.034	0.095	0.000	0.000	2.514
Rep 5	0.000	0.032	0.092	0.000	0.000	2.505
Rep 6	0.000	0.026	0.093	0.000	0.000	2.723
Mean	0.000	0.027	0.091	0.000	0.000	2.562
SD	0.00	0.01	0.01	0.00	0.00	0.10
CV	N/A	23.7	9.7	N/A	N/A	4.0
Free Concentration (μM)					0.000	
% HSA Binding						99.96
% PC Binding	0.0	96.3	98.9	0		
Free Fraction (fu)	1.00	0.037	0.011	1.00		0.004

Compound Number	GI235401					
	PC 1	PC 2A	PC 3	PC 2B	1% PBS	HSA
Rep 1	0.006	0.031	0.115	0.013	0.000	2.462
Rep 2	0.007	0.025	0.123	0.011	0.000	2.965
Rep 3	0.000	0.018	0.122	0.012	0.000	2.890
Rep 4	0.010	0.030	0.128	0.012	0.004	3.017
Rep 5	0.006	0.025	0.136	0.010	0.002	2.845
Rep 6	0.005	0.025	0.122	0.019	0.000	2.871
Mean	0.006	0.026	0.124	0.013	0.001	2.842
SD	0.00	0.00	0.01	0.00	0.00	0.20
CV	57.6	18.1	5.7	24.8	139.4	6.9
Free Concentration (μM)					0.001	
% HSA Binding						99.96
% PC Binding	78.8	95.3	99.0	90.6		
Free Fraction (fu)	0.212	0.047	0.010	0.094		0.004

Compound Number	GI235401					
	PC 1	PC 2A	PC 3	PC 2B	1% PBS	HSA
Rep 1	0.027	0.036	0.073	0.049	0.025	2.455
Rep 2	0.027	0.035	0.062	0.056	0.011	2.718
Rep 3	0.061	0.036	0.062	0.070	0.009	2.365
Rep 4	0.034	0.059	0.085	0.066	0.023	2.643
Rep 5	0.039	0.038	0.097	0.083	0.018	2.403
Rep 6	0.030	0.046	0.068	0.094	0.019	2.802
Mean	0.036	0.042	0.075	0.070	0.018	2.564
SD	0.013	0.009	0.014	0.017	0.006	0.181
CV	35.6	22.5	18.7	24.0	36.5	7.1
Free Concentration (μM)					0.018	
% HSA Binding						99.32
% PC Binding	51.8	58.0	76.5	74.9		
Free Fraction (fu)	0.482	0.420	0.235	0.251		0.682

Compound Number	GW622791					
	PC 1	PC 2A	PC 3	PC 2B	1% PBS	HSA
Rep 1	0.187	0.267	0.281	0.262	0.146	2.194
Rep 2	0.190	0.317	0.277	0.268	0.151	2.465
Rep 3	0.208	0.281	0.261	0.272	0.172	2.409
Rep 4	0.201	0.277	0.309	0.281	0.156	2.220
Rep 5	0.191	0.260	0.276	0.253	0.147	2.285
Rep 6	0.193	0.272	0.262	0.266	0.153	2.498
Mean	0.195	0.279	0.278	0.267	0.154	2.345
SD	0.01	0.02	0.02	0.01	0.01	0.13
CV	4.1	7.2	6.3	3.5	6.2	5.5
Free Concentration (μM)					0.154	
% HSA Binding						93.4
% PC Binding	21.0	44.8	44.5	42.3		
Free Fraction (fu)	0.790	0.552	0.555	0.577		0.066

Compound Number	GW622791					
	PC 1	PC 2A	PC 3	PC 2B	1% PBS	HSA
Rep 1	0.147	0.240	0.221	0.211	0.103	1.960
Rep 2	0.153	0.239	0.218	0.217	0.107	1.948
Rep 3	0.159	0.236	0.225	0.221	0.109	2.125
Rep 4	0.151	0.237	0.221	0.230	0.109	1.999
Rep 5	0.160	0.226	0.215	0.228	0.110	1.925
Rep 6	0.152	0.223	0.232	0.232	0.101	2.041
Mean	0.154	0.234	0.222	0.223	0.107	2.000
SD	0.005	0.007	0.006	0.008	0.004	0.074
CV	3.2	3.1	2.7	3.7	3.4	3.7
Free Concentration (μM)					0.107	
% HSA Binding						94.6
% PC Binding	30.4	54.2	51.8	52.1		
Free Fraction (fu)	0.696	0.458	0.482	0.479		0.054

Compound Number	GW622791					
	PC 1	PC 2A	PC 3	PC 2B	1% PBS	HSA
Rep 1	0.284	0.258	0.302	0.282	0.160	1.460
Rep 2	0.286	0.384	0.299	0.287	0.167	1.514
Rep 3	0.297	0.254	0.369	0.299	0.193	1.499
Rep 4	0.314	0.306	0.454	0.245	0.142	1.423
Rep 5	0.318	0.217	0.332	0.294	0.152	1.496
Rep 6	0.325	0.249	0.393	0.294	0.220	1.627
Mean	0.304	0.278	0.358	0.284	0.172	1.503
SD	0.017	0.059	0.060	0.020	0.029	0.069
CV	5.7	21.3	16.7	7.0	16.8	4.6
Free Concentration (μM)					0.172	
% HSA Binding						88.6
% PC Binding	43.4	38.1	52.0	39.3		
Free Fraction (fu)	0.566	0.619	0.480	0.607		0.114

Pilot Study *In-Vitro* Pharmacokinetic Parameters of Basic series using CRED Device

Compound Number	CCI3839					
Rep 1	1.275	1.955	2.012	2.064	0.647	0.915
Rep 2	1.269	1.864	2.156	2.009	0.701	1.095
Rep 3	1.329	1.696	2.034	2.032	0.473	1.111
Rep 4	1.322	1.876	1.987	2.092	0.657	1.132
Rep 5	1.320	1.834	2.035	1.888	0.670	1.096
Rep 6	1.311	1.805	2.063	[1.471]*	[No Peak]*	1.129
Mean	1.304	1.838	2.048	2.017	0.630	1.080
SD	0.03	0.09	0.06	0.08	0.09	0.08
CV	2.0	4.7	2.9	3.9	14.3	7.6
Free Concentration (μm)					0.630	
% HSA Binding						41.6
% PC Binding	51.7	65.7	69.2	68.8		
Free Fraction (fu)	0.483	0.343	0.308	0.312		0.584

Compound Number	CCI3839					
Rep 1	1.631	2.455	2.781	2.302	0.769	1.337
Rep 2	1.582	2.520	2.895	2.351	0.817	1.255
Rep 3	1.598	2.467	2.194	2.602	{No Peak}*	1.992
Rep 4	1.458	2.481	2.568	2.535	0.767	1.204
Rep 5	1.525	2.507	2.622	2.636	0.873	1.336
Rep 6	1.450	2.338	[1.539]*	*	0.897	1.319
Mean	1.541	2.461	2.612	2.485	0.807	1.407
SD	0.08	0.07	0.27	0.15	0.06	0.29
CV	4.9	2.6	10.2	6.1	7.3	20.7
Free Concentration (μm)						
% HSA Binding						42.7
% PC Binding	47.6	67.2	69.1	67.5		

Free Fraction (fu)	0.523	0.328	0.309	0.325		0.573
--------------------	-------	-------	-------	-------	--	-------

Compound Number	CCI3839					
Rep 1	1.072	2.350	2.571	2.553	0.827	1.116
Rep 2	1.240	2.348	2.592	2.531	0.825	1.265
Rep 3	1.372	2.212	2.547	2.563	0.778	1.078
Rep 4	1.381	2.423	2.494	2.36	0.778	1.205
Rep 5	1.393	2.473	2.575	2.517	0.814	1.218
Rep 6	1.347	2.291	2.424	2.318	0.812	1.229
Mean	1.301	2.350	2.534	2.474	0.804	1.185
SD	0.13	0.09	0.06	0.11	0.02	0.07
CV	9.6	3.9	2.5	4.3	2.8	6.1
Free Concentration (μm)					0.804	
% HSA Binding						32.2
% PC Binding	38.2	65.8	68.3	67.5		
Free Fraction (fu)	0.618	0.342	0.317	0.325		0.678

Compound Number	GR99941					
	0.818	1.425	1.777	1.493	0.612	1.848
Rep 1	0.804	1.542	1.823	1.614	0.605	1.853
Rep 2	0.879	1.496	1.731	1.603	0.566	1.937
Rep 3	0.927	1.873	1.890	1.729	0.596	1.995
Rep 4	0.961	1.808	1.788	1.684	0.564	2.065
Rep 5	0.967	1.723	[2.566]	1.708	0.750	2.039
Rep 6						
	0.893	1.645	1.802	1.639	0.589	1.956
Mean	0.07	0.18	0.06	0.09	0.07	0.09
SD	7.9	11.1	3.3	5.3	11.7	4.7
CV	0.818	1.425	1.777	1.493	0.612	1.848
Free Concentration (μm)					0.589	
% HSA Binding						69.9
% PC Binding	34.0	64.2	67.3	64.1		
Free Fraction (fu)	0.660	0.358	0.327	0.359		0.301

Compound Number	GR99941					
Rep 1	0.765	1.681	1.624	1.973	0.443	1.714
Rep 2	0.760	1.583	1.701	1.807	0.527	1.837
Rep 3	0.722	1.756	1.641	1.910	0.531	1.876
Rep 4	0.764	1.719	1.680	1.899	0.565	1.937
Rep 5	0.777	1.756	1.709	1.887	0.515	2.018
Rep 6	0.774	1.847	1.732	1.844	0.481	1.988
Mean	0.760	1.724	1.681	1.887	0.516	1.895
SD	0.02	0.09	0.04	0.06	0.04	0.11
CV	2.6	5.1	2.5	3.0	8.3	5.9
Free Concentration (μM)						
% HSA Binding						74.2
% PC Binding	35.8	71.7	71.0	74.1		
Free Fraction (fu)	0.642	0.283	0.290	0.259		0.258

*Bad injection no data acquired

Compound Number	GR99941					
Rep 1	0.462	1.414	1.290	1.282	0.419	2.168
Rep 2	0.551	1.458	1.265	1.376	0.440	2.226
Rep 3	0.549	1.412	1.198	1.354	0.414	2.201
Rep 4	0.641	1.464	1.165	1.342	0.443	2.263
Rep 5	0.676	1.465	1.377	1.347	0.434	2.176
Rep 6	0.679	1.440	1.321	1.300	0.423	2.289
Mean	0.593	1.442	1.269	1.334	0.430	2.221
SD	0.09	0.02	0.08	0.04	0.01	0.05
CV	14.6	1.7	6.2	2.7	2.8	2.2
Free Concentration (μM)					0.430	
% HSA Binding						80.6
% PC Binding	27.5	70.2	66.1	67.8		
Free Fraction (fu)	0.725	0.298	0.339	0.322		0.194

Compound Number	SB416332					
	PC 1	PC 2A	PC 3	PC 2B	1% PBS	HSA
Rep 1	1.648	1.340	1.638	1.515	1.469	1.398
Rep 2	1.489	1.328	1.686	1.719	1.351	1.391
Rep 3	1.487	1.316	1.467	1.893	2.840*	1.347
Rep 4	1.217	1.326	1.732	1.490	1.052	1.711
Rep 5	1.211	1.443	1.553	1.689	1.130	1.594
Rep 6	1.217	1.491	1.497	1.625	4.951*	1.508
Mean	1.378	1.374	1.596	1.655	1.251	1.492
SD	0.19	0.07	0.11	0.15	0.19	0.14
CV	13.6	5.4	6.7	8.9	15.4	9.4
Free Concentration (μM)					1.251	
% HSA Binding						16.1
% PC Binding	9.2	9.0	21.6	24.4		
Free Fraction (fu)	0.907	0.910	0.784	0.756		0.838

*Bad injection no data acquired

Compound Number	SB416332					
	PC 1	PC 2A	PC 3	PC 2B	1% PBS	HSA
Rep 1	1.207	1.452	1.760	1.890	1.306	1.563
Rep 2	1.300	1.743	1.817	1.911	1.196	1.580
Rep 3	1.181	1.910	[8.129]	[No Peak]	[2.486]	1.507
Rep 4	1.355	1.739	1.580	1.545	0.901	1.378
Rep 5	1.305	1.723	1.684	1.954	1.093	1.559
Rep 6	1.245	1.998	1.941	2.142	1.144	1.588
Mean	1.266	1.761	1.756	1.888	1.124	1.529
SD	0.07	0.19	0.14	0.22	0.15	0.08
CV	5.2	10.7	7.8	11.5	13.3	5.2
Free Concentration (μM)					1.124	
% HSA Binding						26.5
% PC Binding	11.2	36.2	36.0	40.5		
Free Fraction (fu)	0.888	0.638	0.640	0.595		0.735

*Bad injection no data acquired

Compound Number	SB416332					
	PC 1	PC 2A	PC 3	PC 2B	1% PBS	HSA
Rep 1	0.897	1.708	1.844	1.819	1.380	1.592
Rep 2	1.072	1.897	1.842	1.870	1.415	1.771
Rep 3	1.300	1.776	1.627	1.740	1.389	1.806
Rep 4	1.265	1.825	1.979	2.090	1.288	1.861
Rep 5	1.219	1.904	1.797	1.727	1.419	1.749
Rep 6	1.167	1.966	1.760	1.857	1.482	1.821
Mean	1.153	1.846	1.808	1.851	1.378	1.767
SD	0.15	0.09	0.12	0.13	0.06	0.09
CV	12.9	5.1	6.4	7.1	4.6	5.3
Free Concentration (μM)					1.378	
% HSA Binding						22.0
% PC Binding	-19.5	25.4	23.8	25.5		
Free Fraction (fu)	1.195	0.747	0.762	0.745		0.780

Compound Number	GR613617					
	PC 1	PC 2A	PC 3	PC 2B	1% PBS	HSA
Rep 1	0.850	1.250	1.310	1.290	0.071	1.719
Rep 2	0.769	1.234	1.340	1.477	0.053	1.836
Rep 3	0.875	1.318	1.210	[3.71]	0.051	1.832
Rep 4	0.740	1.410	1.300	1.202	0.052	1.488
Rep 5	0.771	1.334	1.250	1.241	0.074	1.883
Rep 6	0.930	1.438	1.450	[No Peak]	0.058	1.768
Mean	0.823	1.331	1.310	1.303	0.060	1.754
SD	0.07	0.08	0.08	0.12	0.01	0.14
CV	9.0	6.2	6.3	9.3	16.9	8.1
Free Concentration (μM)					0.060	
% HSA Binding						96.6
% PC Binding	92.7	95.5	95.4	95.4		

Free Fraction (fu)	0.073	0.045	0.046	0.046		0.034
--------------------	-------	-------	-------	-------	--	-------

Compound Number	GR613617					
	PC 1	PC 2A	PC 3	PC 2B	1% PBS	HSA
Rep 1	0.957	1.362	1.426	1.611	0.064	1.581
Rep 2	0.950	1.347	1.624	1.645	0.065	1.665
Rep 3	0.984	1.557	1.280	[3.277]	[No Peak]	[3.477]
Rep 4	0.899	1.470	1.349	1.421	0.066	1.454
Rep 5	0.975	1.549	1.583	1.477	0.057	1.748
Rep 6	1.012	1.483	1.337	[2.308]	0.053	1.643
Mean	0.963	1.461	1.433	1.539	0.063	1.618
SD	0.04	0.09	0.14	0.11	0.01	0.11
CV	4.0	6.1	9.8	6.9	9.0	6.8
Free Concentration (μm)					0.063	
% HSA Binding						96.1
% PC Binding	93.5	95.7	95.6	95.9		
Free Fraction (fu)	0.065	0.043	0.044	0.041		0.039

Compound Number	GR613617					
	PC 1	PC 2A	PC 3	PC 2B	1% PBS	HSA
Rep 1	0.584	0.956	1.062	0.881	0.055	2.067
Rep 2	0.643	1.009	0.973	0.956	0.030	2.031
Rep 3	0.741	0.942	0.944	0.922	0.052	1.923
Rep 4	0.653	0.977	0.803	0.949	0.035	1.921
Rep 5	0.673	1.035	0.852	1.011	0.026	1.890
Rep 6	0.622	0.995	0.841	0.953	0.023	1.863
Mean	0.653	0.986	0.913	0.945	0.040	1.949
SD	0.05	0.03	0.10	0.04	0.01	0.08
CV	8.1	3.5	10.7	4.5	34.2	4.2
Free Concentration (μm)					0.040	
% HSA Binding						97.9

% PC Binding	93.9	95.9	95.6	95.8		
Free Fraction (fu)	0.061	0.041	0.044	0.042		0.021

**Pilot Study *In-Vitro* Pharmacokinetic Parameters of Neutral series
using CRED Device**

Compound Number	GR119497					
	PC 1	PC 2A	PC 3	PC 2B	1% PBS	HSA
Rep 1	1.140	1.318	1.441	1.292	0.786	2.040
Rep 2	1.066	1.405	1.289	1.388	0.774	2.194
Rep 3	1.062	1.431	1.249	1.274	0.824	1.984
Rep 4	1.122	1.305	1.416	1.338	0.888	1.961
Rep 5	0.994	1.271	1.313	1.349	0.842	2.041
Rep 6	0.962	1.291	1.279	1.378	0.839	2.041
Mean	1.058	1.337	1.331	1.337	0.823	2.044
SD	0.07	0.07	0.08	0.05	0.04	0.08
CV	6.6	4.9	5.9	3.4	5.0	4.0
Free Concentration (µm)					0.823	
% HSA Binding						59.7
% PC Binding	22.2	38.4	38.2	38.4		
Free Fraction (fu)	0.778	0.615	0.618	0.616		0.403

Compound Number	GR119497					
	PC 1	PC 2A	PC 3	PC 2B	1% PBS	HSA
Rep 1	1.002	1.173	1.371	1.238	0.765	2.088
Rep 2	1.019	1.180	1.354	1.177	0.675	2.219
Rep 3	1.012	1.211	1.406	1.213	0.784	2.106
Rep 4	1.029	1.052	1.347	1.103	0.775	2.277
Rep 5	1.044	1.141	1.306	1.226	0.753	2.178
Rep 6	0.942	1.194	1.425	1.095	0.777	2.048
Mean	1.008	1.159	1.368	1.175	0.750	2.153
SD	0.04	0.06	0.04	0.06	0.04	0.09
CV	3.5	4.9	3.1	5.3	5.4	4.0

Free Concentration (μm)					0.750	
% HSA Binding						65.2
% PC Binding	25.6	35.3	45.2	36.2		
Free Fraction (fu)	0.744	0.648	0.548	0.638		0.349

Compound Number	GR119497					
	PC 1	PC 2A	PC 3	PC 2B	1% PBS	HSA
Rep 1	0.919	1.190	1.164	0.984	0.897	1.435
Rep 2	0.896	0.985	1.235	0.975	0.932	1.612
Rep 3	0.848	1.031	1.210	1.124	0.867	1.454
Rep 4	0.812	1.238	1.304	1.248	0.901	1.513
Rep 5	0.876	1.144	1.231	1.208	0.817	1.571
Rep 6	0.931	1.121	1.255	1.270	0.893	1.697
Mean	0.880	1.118	1.233	1.135	0.885	1.547
SD	0.04	0.10	0.10	0.13	0.04	0.05
CV	5.1	8.5	8.1	11.5	4.4	3.0
Free Concentration (μm)					0.885	
% HSA Binding						42.8
% PC Binding	-0.5	20.9	28.2	22.0		42.8
Free Fraction (fu)	1.005	0.791	0.717	0.779		0.572

Compound Number	GI116108					
	PC 1	PC 2A	PC 3	PC 2B	1% PBS	HSA
Rep 1	0.489	0.722	0.653	0.720	0.051	1.917
Rep 2	0.556	0.689	0.680	0.720	0.054	2.001
Rep 3	0.546	0.752	0.701	0.726	0.053	1.951
Rep 4	0.583	0.710	0.656	0.749	0.058	1.941
Rep 5	0.587	0.645	0.688	0.697	0.050	2.128
Rep 6	0.592	0.735	0.672	0.720	0.051	2.255
Mean	0.559	0.709	0.675	0.722	0.053	2.032
SD	0.04	0.04	0.02	0.02	0.00	0.13
CV	6.9	5.4	2.8	2.3	5.5	6.5

Free Concentration (μM)					0.053	
% HSA Binding						97.4
% PC Binding	90.5	92.5	92.1	92.6		
Free Fraction (f_u)	0.095	0.075	0.079	0.074		0.026

Compound Number	GI116108					
	PC 1	PC 2A	PC 3	PC 2B	1% PBS	HSA
Rep 1	0.781	1.175	0.815	0.894	0.029	1.948
Rep 2	0.736	1.123	0.903	0.833	0.031	1.915
Rep 3	0.809	1.028	0.839	0.838	0.030	2.308
Rep 4	0.756	0.981	0.866	0.840	0.033	2.059
Rep 5	0.855	1.022	0.878	0.805	0.031	2.207
Rep 6	0.720	1.094	0.819	0.921	0.032	2.118
Mean	0.776	1.071	0.853	0.855		2.093
SD	0.05	0.07	0.03	0.04	0.00	0.15
CV	6.4	6.8	4.1	5.1	4.6	7.2
Free Concentration (μM)					0.031	
% HSA Binding						98.5
% PC Binding	96.0	97.1	96.4	96.4		
Free Fraction (fu)	0.040	0.029	0.036	0.036		0.015

Compound Number	GI116108					
	PC 1	PC 2A	PC 3	PC 2B	1% PBS	HSA
Rep 1	0.941	1.302	1.417	1.137	0.072	1.478
Rep 2	0.885	1.174	1.319	1.316	0.088	1.594
Rep 3	0.945	1.266	1.260	1.204	0.063	1.548
Rep 4	1.022	1.282	1.282	1.111	0.073	1.571
Rep 5	1.071	1.263	1.350	1.097	0.087	1.603
Rep 6	0.901	1.336	1.269	1.012	0.072	1.590
Mean	0.961	1.271	1.316	1.146	0.077	1.564
SD	0.07	0.05	0.06	0.10	0.01	0.05
CV	7.5	4.3	4.5	9.1	12.7	3.0
Free Concentration (μM)					0.077	
% HSA Binding						95.1
% PC Binding	92.0	94.0	94.2	93.3		
Free Fraction (fu)	0.080	0.060	0.058	0.067		0.049

Compound Number	GW703803					
	PC 1	PC 2A	PC 3	PC 2B	1% PBS	HSA
Rep 1	1.124	1.570	1.502	1.572	0.172	2.143
Rep 2	1.032	1.586	1.423	1.512	0.166	2.044
Rep 3	1.105	1.443	1.409	1.526	0.154	2.008
Rep 4	1.096	1.544	1.439	1.497	0.181	2.479
Rep 5	1.092	1.546	1.444	1.563	0.187	2.256
Rep 6	0.975	1.504	1.524	1.575	0.187	2.401
Mean	1.071	1.532	1.457	1.541	0.172	2.222
SD	0.06	0.05	0.05	0.03	0.01	0.19
CV	5.2	3.4	3.1	2.2	7.6	8.6
Free Concentration (μM)					0.172	
% HSA Binding						92.3
% PC Binding	83.9	88.8	88.2	88.8		
Free Fraction (fu)	0.161	0.112	0.118	0.112		0.077

Compound Number	GW703803					
	PC 1	PC 2A	PC 3	PC 2B	1% PBS	HSA
Rep 1	1.098	1.667	1.780	1.893	0.102	2.150
Rep 2	1.320	1.965	2.106	1.923	0.087	1.971
Rep 3	1.187	1.885	1.911	1.885	0.077	1.915
Rep 4	1.274	1.826	1.592	2.118	0.103	2.322
Rep 5	1.194	1.753	1.779	2.064	0.106	2.161
Rep 6	1.433	2.104	1.716	2.024	0.079	2.096
Mean	1.251	1.867	1.814	1.985	0.095	2.103
SD	0.12	0.16	0.18	0.10	0.01	0.15
CV	9.4	8.3	9.7	4.9	13.6	6.9
Free Concentration (μM)					0.095	
% HSA Binding						95.5
% PC Binding	92.4	94.9	94.8	95.2		
Free Fraction (fu)	0.076	0.051	0.052	0.048		0.045

Compound Number	GW703803					
	PC 1	PC 2A	PC 3	PC 2B	1% PBS	HSA
Rep 1	1.654	2.116	2.325	1.884	0.133	1.135
Rep 2	1.734	1.951	2.498	2.100	0.145	1.118
Rep 3	1.808	2.003	2.226	2.097	0.132	1.219
Rep 4	1.553	2.046	2.321	2.049	0.142	1.236
Rep 5	1.661	2.225	2.519	1.963	0.126	1.242
Rep 6	1.693	2.015	2.140	1.905	0.148	1.159
Mean	1.684	2.059	2.338	2.000	0.136	1.185
SD	0.09	0.10	0.15	0.10	0.01	0.05
CV	5.1	4.7	6.4	4.8	6.3	4.6
Free Concentration (μM)					0.136	
% HSA Binding						
% PC Binding	91.9	93.4	94.2	93.2		88.6
Free Fraction (fu)	0.081	0.066	0.058	0.068		0.114

Compound Number	AH23463					
	PC 1	PC 2A	PC 3	PC 2B	1% PBS	HSA
Rep 1	0.533	0.554	0.604	0.618	0.418	0.784
Rep 2	0.472	0.550	0.584	0.675	0.412	0.816
Rep 3	0.456	0.583	0.607	0.679	0.417	0.854
Rep 4	0.405	0.615	0.615	0.746	0.407	1.037
Rep 5	0.445	0.623	0.617	0.697	0.387	0.975
Rep 6	0.447	0.619	0.655	0.743	0.400	1.111
Mean	0.460	0.591	0.614	0.693	0.407	0.930
SD	0.04	0.03	0.02	0.05	0.01	0.13
CV	9.2	5.6	3.8	6.9	2.9	14.1
Free Concentration (μM)					0.407	
% HSA Binding						56.2
% PC Binding	11.5	31.1	33.7	41.3		
Free Fraction (fu)	0.885	0.689	0.663	0.587		0.438

Compound Number	AH23463					
	PC 1	PC 2A	PC 3	PC 2B	1% PBS	HSA
Rep 1	0.906	1.269	1.031	1.005	0.531	1.324
Rep 2	0.938	1.263	1.062	1.122	0.546	1.268
Rep 3	0.897	1.207	1.022	1.086	0.517	1.241
Rep 4	0.956	1.188	1.020	1.054	0.499	1.341
Rep 5	0.881	1.237	1.032	1.065	0.512	1.328
Rep 6	0.878	1.096	0.980	1.072	0.507	1.37
Mean	0.909	1.210	1.025	1.067	0.519	1.312
SD	0.03	0.06	0.03	0.04	0.02	0.05
CV	3.5	5.3	2.6	3.6	3.3	3.7
Free Concentration (μM)					0.519	
% HSA Binding						60.4
% PC Binding	42.9	57.1	49.3	51.4		
Free Fraction (fu)	0.571	0.429	0.507	0.486		0.395

Appendix 4 Main Study In-Vitro Pharmacokinetic Parameters

Main Study In-Vitro Pharmacokinetic Parameters of Acid series using CRED Device

Compound Number	CC16817					
	PC 1	PC 2A	PC 3	PC 2B	1% PBS	HSA
Rep 1	0.499	0.638	0.878	0.650	0.472	2.114
Rep 2	0.595	0.586	0.783	0.670	0.510	1.955
Rep 3	0.565	0.655	0.800	0.682	0.483	2.257
Rep 4	0.632	0.665	0.820	0.679	0.53	1.967
Rep 5	0.567	0.698	0.788	0.691	0.472	1.935
Rep 6	0.575	0.739	0.758	0.758	0.485	2.105
Mean	0.572	0.664	0.805	0.688	0.492	2.056
SD	0.044	0.052	0.041	0.037	0.023	0.126
CV	7.6	7.9	5.1	5.4	4.7	6.1
Free Concentration (μm)					0.492	
% HSA Binding						76.1
% PC Binding	14.0	25.8	38.8	28.5		
Free Fraction (fu)	0.860	0.742	0.612	0.715		0.239
Dilution Factor (D)	10.6	5.3	3.5	5.3		
Free Fraction Undiluted in Tissues (fut)	0.367	0.351	0.308	0.321		
Volume of Distribution (Vdss)	0.651	0.681	0.775	0.745		
Mean Volume of Distribution (Vdss)	0.713					

Compound Number	GR62550					
	PC 1	PC 2A	PC 3	PC 2B	1% PBS	HSA
Rep 1	0.005	0.005	0.007	0.005	0.006	1.950
Rep 2	0.004	0.006	0.006	0.005	0.007	1.808
Rep 3	0.004	0.009	0.006	0.005	0.009	2.312
Rep 4	0.005	0.006	0.005	0.004	0.004	1.902
Rep 5	0.005	0.005	0.004	0.005	0.006	1.975
Rep 6	0.005	0.006	0.007	0.004	0.004	1.826
Mean	0.005	0.006	0.006	0.005	0.006	1.962
SD	0.001	0.001	0.001	0.001	0.002	0.184
CV	11.1	23.9	20.0	11.1	31.6	9.4
Free Concentration (μm)					0.006	
% HSA Binding						99.7
% PC Binding	-28.6	2.7	-2.9	-28.6		
Free Fraction (fu)	1.286	0.973	1.029	1.286		0.003
Dilution Factor (D)	10.6	5.3	3.5	5.3		
Free Fraction Undiluted in Tissues (fut)	1.000	0.8717	1.000	1.000		
Volume of Distribution (Vdss)	0.0030	0.0034	0.0030	0.0030		
Mean Volume of Distribution (Vdss)	0.0031					

Compound Number	GR87272					
	PC 1	PC 2A	PC 3	PC 2B	1% PBS	HSA
Rep 1	0.098	0.144	0.225	0.152	0.050	2.611
Rep 2	0.106	0.155	0.211	0.157	0.063	2.504
Rep 3	0.108	0.150	0.245	0.143	0.056	2.804
Rep 4	0.104	0.152	0.242	0.153	0.060	2.726
Rep 5	0.103	0.152	0.249	0.157	0.060	2.550
Rep 6	0.092	0.144	0.249	0.163	0.048	2.436
Mean	0.102	0.150	0.237	0.154	0.056	2.605
SD	0.006	0.005	0.015	0.007	0.006	0.139
CV	5.8	3.0	6.5	4.3	10.7	5.3
Free Concentration (μm)					0.056	
% HSA Binding						97.8
% PC Binding	44.8	62.4	76.3	63.6		
Free Fraction (fu)	0.552	0.376	0.237	0.364		0.022
Dilution Factor (D)	10.6	5.3	3.5	5.3		
Free Fraction Undiluted in Tissues (fut)	0.104	0.102	0.081	0.098		
Volume of Distribution (Vdss)	0.207	0.212	0.267	0.221		
Mean Volume of Distribution (Vdss)	0.227					

Compound Number	GR138714					
	PC 1	PC 2A	PC 3	PC 2B	1% PBS	HSA
Rep 1	0.009	0.263	0.024	0.016	0.002	1.836
Rep 2	0.013	0.253	0.021	0.011	0.002	1.874
Rep 3	0.010	0.236	0.022	0.011	0.001	1.969
Rep 4	0.010	0.265	0.024	0.012	0.002	1.905
Rep 5	0.010	0.224	0.019	0.013	0.001	2.317
Rep 6	0.010	0.261	0.026	0.013	0.001	1.889
Mean	0.010	0.250	0.023	0.013	0.002	1.965
SD	0.001	0.017	0.003	0.002	0.001	0.178
CV	13.2	6.7	11.0	14.7	34.2	9.1
Free Concentration (μm)					0.002	
% HSA Binding						99.92
% PC Binding	85.5	99.4	93.4	88.2		
Free Fraction (fu)	0.145	0.006	0.066	0.118		0.0008
Dilution Factor (D)	10.6	5.3	3.5	5.3		
Free Fraction Undiluted in Tissues (fut)	0.016	0.001	0.020	0.025		
Volume of Distribution (Vdss)	0.051	[0.705]	0.041	0.032		
Mean Volume of Distribution (Vdss)	0.041					

Compound Number	GR70487					
	PC 1	PC 2A	PC 3	PC 2B	1% PBS	HSA
Rep 1	1.216	1.298	1.005	1.195	1.161	1.97
Rep 2	1.059	1.27	1.244	1.221	1.255	1.862
Rep 3	1.274	1.071	1.248	1.199	1.201	1.713
Rep 4	1.121	1.168	1.226	1.117	1.053	2.004
Rep 5	1.154	1.314	1.212	1.291	1.133	1.796
Rep 6	1.097	1.275	1.434	1.268	1.151	1.755
Mean	1.154	1.233	1.228	1.215	1.159	1.850
SD	0.080	0.094	0.136	0.061	0.068	0.117
CV	6.9	7.6	11.1	5.1	5.8	6.3
Free Concentration (μm)					1.159	
% HSA Binding						37.3
% PC Binding	-0.5	6.0	5.6	4.6		
Free Fraction (fu)	1.005	0.940	0.941	0.954		0.627
Dilution Factor (D)	10.6	5.3	3.5	5.3		
Free Fraction Undiluted in Tissues (fut)	1.000	0.747	0.820	0.796		
Volume of Distribution (Vdss)	0.626	0.838	0.764	0.786		
Mean Volume of Distribution (Vdss)	0.753					

Compound Number	CCI120					
	PC 1	PC 2A	PC 3	PC 2B	1% PBS	HSA
Rep 1	0.025	0.030	0.59	0.531	0.015	2.067
Rep 2	0.032	0.036	0.549	0.579	0.019	1.965
Rep 3	0.024	0.034	0.557	0.554	0.015	2.180
Rep 4	0.027	0.039	0.519	0.54	0.015	2.210
Rep 5	0.026	0.035	0.497	0.58	0.019	2.260
Rep 6	0.027	0.034	0.558	0.551	0.018	2.179
Mean	0.027	0.035	0.545	0.556	0.017	2.144
SD	0.003	0.003	0.033	0.020	0.002	0.108
CV	10.4	8.5	6.0	3.6	12.1	5.0
Free Concentration (μm)					0.017	
% HSA Binding						99.2
% PC Binding	37.3	51.4	96.9	97.0		
Free Fraction (fu)	0.627	0.486	0.031	0.030		0.008
Dilution Factor (D)	10.6	5.3	3.5	5.3		
Free Fraction Undiluted in Tissues (fut)	0.137	0.151	0.009	0.006		
Volume of Distribution (Vdss)	0.058	0.053	0.895	1.367		
Mean Volume of Distribution (Vdss)	0.593					

Compound Number	GR33000					
	PC 1	PC 2A	PC 3	PC 2B	1% PBS	HSA
Rep 1	0.075	0.090	0.099	0.100	0.088	2.188
Rep 2	0.074	0.085	0.087	0.092	0.084	2.032
Rep 3	0.076	0.090	0.088	0.088	0.081	2.151
Rep 4	0.084	0.089	0.093	0.090	0.090	2.249
Rep 5	0.085	0.102	0.101	0.093	0.072	2.218
Rep 6	0.084	0.087	0.087	0.105	0.090	2.350
Mean	0.080	0.091	0.093	0.095	0.084	2.198
SD	0.005	0.006	0.006	0.007	0.007	0.106
CV	6.5	6.6	6.8	6.9	8.2	4.8
Free Concentration (μm)					0.084	
% HSA Binding						96.2
% PC Binding	-5.6	7.0	9.0	11.1		
Free Fraction (fu)	1.056	0.930	0.910	0.889		0.038
Dilution Factor (D)	10.6	5.3	3.5	5.3		
Free Fraction Undiluted in Tissues (fut)	1.000	0.715	0.741	0.602		
Volume of Distribution (Vdss)	0.038	0.053	0.051	0.063		
Mean Volume of Distribution (Vdss)	0.051					

Compound Number	GW289865					
	PC 1	PC 2A	PC 3	PC 2B	1% PBS	HSA
Rep 1	0.070	0.099	0.129	0.103	0.054	2.074
Rep 2	0.065	0.100	0.133	0.091	0.051	1.979
Rep 3	0.065	0.090	0.136	0.099	0.049	2.022
Rep 4	0.070	0.110	0.141	0.104	0.046	1.991
Rep 5	0.075	0.098	0.137	0.109	0.048	1.987
Rep 6	0.070	0.109	0.139	0.095	0.049	2.018
Mean	0.069	0.101	0.136	0.100	0.050	2.012
SD	0.004	0.007	0.004	0.007	0.003	0.035
CV	5.4	7.4	3.2	6.5	5.5	1.7
Free Concentration (μm)					0.050	
% HSA Binding						97.5
% PC Binding	28.4	51.0	63.6	50.6		
Free Fraction (fu)	0.716	0.490	0.364	0.494		0.025
Dilution Factor (D)	10.6	5.3	3.5	5.3		
Free Fraction Undiluted in Tissues (fut)	0.192	0.153	0.140	0.156		
Volume of Distribution (Vdss)	0.130	0.163	0.179	0.161		
Mean Volume of Distribution (Vdss)	0.158					

Compound Number	GSK275458					
	PC 1	PC 2A	PC 3	PC 2B	1% PBS	HSA
Rep 1	0.019	0.016	0.568	0.023	0.002	2.035
Rep 2	0.023	0.016	0.553	0.025	0.004	2.136
Rep 3	0.020	0.018	0.513	0.021	0.010	2.025
Rep 4	0.028	0.025	0.488	0.021	0.000	2.000
Rep 5	0.019	0.013	0.561	0.032	0.002	2.212
Rep 6	0.034	0.015	0.569	0.031	0.001	
Mean	0.024	0.017	0.542	0.026	0.003	2.082
SD	0.006	0.004	0.034	0.005	0.004	0.089
CV	25.4	24.3	6.2	19.2	100.0113.7	4.3
Free Concentration (μm)					0.003	
% HSA Binding						99.8
% PC Binding	86.7	81.6	99.4	87.6		
Free Fraction (fu)	0.133	0.184	0.006	0.124		0.002
Dilution Factor (D)	10.6	5.3	3.5	5.3		
Free Fraction Undiluted in Tissues (fut)	0.014	0.041	0.002	0.026		
Volume of Distribution (Vdss)	0.140	0.049	[1.205]	0.077		
Mean Volume of Distribution (Vdss)	0.089					

Compound Number	GR87036					
	PC 1	PC 2A	PC 3	PC 2B	1% PBS	HSA
Rep 1	0.230	1.119	0.326	0.295	0.255	2.268
Rep 2	0.239	1.014	0.308	0.297	0.252	2.203
Rep 3	0.240	1.182	0.303	0.281	0.245	2.250
Rep 4	0.248	1.023	0.321	0.282	0.264	2.284
Rep 5	0.236	1.121	0.302	0.283	0.260	2.299
Rep 6	0.245	1.069	0.299	0.271	0.245	2.300
Mean	0.240	1.088	0.310	0.285	0.254	2.267
SD	0.006	0.065	0.011	0.010	0.008	0.037
CV	2.7	5.9	3.6	3.4	3.1	1.6
Free Concentration (μm)					0.254	
% HSA Binding						88.8
% PC Binding	-5.8	76.7	18.2	11.0		
Free Fraction (fu)	1.058	0.233	0.818	0.890		0.112
Dilution Factor (D)	10.6	5.3	3.5	5.3		
Free Fraction Undiluted in Tissues (fut)	1.000	0.054	0.560	0.604		
Volume of Distribution (Vdss)	0.112	[2.065]	0.200	0.185		
Mean Volume of Distribution (Vdss)	0.166					

Compound Number	AH22182					
	PC 1	PC 2A	PC 3	PC 2B	1% PBS	HSA
Rep 1	0.041	0.038	0.059	0.038	0.030	1.801
Rep 2	0.041	0.037	0.063	0.035	0.028	1.894
Rep 3	0.037	0.034	0.056	0.036	0.032	1.734
Rep 4	0.034	0.035	0.060	0.044	0.027	1.755
Rep 5	0.038	0.036	0.050	0.045	0.025	1.797
Rep 6	0.038	0.038	0.055	0.042	0.024	1.815
Mean	0.038	0.036	0.057	0.040	0.028	1.799
SD	0.003	0.002	0.005	0.004	0.003	0.056
CV	6.9	4.5	7.9	10.6	10.9	3.1
Free Concentration (μm)					0.028	
% HSA Binding						98.5
% PC Binding	27.5	23.9	51.6	30.8		
Free Fraction (fu)	0.725	0.761	0.484	0.692		0.015
Dilution Factor (D)	10.6	5.3	3.5	5.3		
Free Fraction Undiluted in Tissues (fut)	0.199	0.376	0.210	0.297		
Volume of Distribution (Vdss)	0.075	0.040	0.072	0.050		
Mean Volume of Distribution (Vdss)	0.059					

Compound Number	SB213421					
	PC 1	PC 2A	PC 3	PC 2B	1% PBS	HSA
Rep 1	0.015	0.018	0.027	0.017	0.010	1.394
Rep 2	0.012	0.019	0.024	0.012	0.011	1.648
Rep 3	0.013	0.014	0.031	0.011	0.012	1.986
Rep 4	0.015	0.020	0.025	0.018	0.012	1.895
Rep 5	0.015	0.018	0.021	0.015	0.010	2.008
Rep 6	0.015	0.016	0.019	0.014	0.010	1.787
Mean	0.014	0.018	0.025	0.015	0.011	1.786
SD	0.001	0.002	0.004	0.003	0.001	0.234
CV	9.4	12.4	17.5	18.9	9.1	13.1
Free Concentration (μm)					0.011	
% HSA Binding						99.4
% PC Binding	23.5	38.1	55.8	25.3		
Free Fraction (fu)	0.765	0.619	0.442	0.747		0.006
Dilution Factor (D)	10.6	5.3	3.5	5.3		
Free Fraction Undiluted in Tissues (fut)	0.235	0.2352	0.183	0.358		
Volume of Distribution (Vdss)	0.026	0.026	0.033	0.017		
Mean Volume of Distribution (Vdss)	0.025					

Compound Number	GR118989					
	PC 1	PC 2A	PC 3	PC 2B	1% PBS	HSA
Rep 1	0.067	0.090	0.481	0.083	0.046	1.703
Rep 2	0.065	0.112	0.505	0.073	0.062	1.569
Rep 3	0.059	0.094	0.472	0.073	0.059	1.566
Rep 4	0.068	0.069	0.441	0.079	0.051	1.665
Rep 5	0.070	0.064	0.386	0.084	0.043	1.621
Rep 6	0.071	0.059	0.469	0.084	0.041	1.613
Mean	0.067	0.081	0.459	0.079	0.050	1.623
SD	0.004	0.021	0.041	0.005	0.009	0.054
CV	6.5	25.4	9.0	6.6	17.1	3.3
Free Concentration (μm)					0.052	
% HSA Binding						96.9
% PC Binding	24.5	38.1	89.0	36.6		
Free Fraction (fu)	0.755	0.619	0.110	0.634		0.031
Dilution Factor (D)	10.6	5.3	3.5	5.3		
Free Fraction Undiluted in Tissues (fut)	0.225	0.234	0.034	0.247		
Volume of Distribution (Vdss)	0.138	0.132	[0.920]	0.126		
Mean Volume of Distribution (Vdss)	0.132					

Compound Number	BRL15541					
	PC 1	PC 2A	PC 3	PC 2B	1% PBS	HSA
Rep 1	0.038	0.029	0.030	0.037	0.033	1.489
Rep 2	0.041	0.029	0.031	0.040	0.029	1.593
Rep 3	0.049	0.033	0.032	0.036	0.038	1.733
Rep 4	0.046	0.036	0.041	0.040	0.028	1.793
Rep 5	0.045	0.036	0.036	0.041	0.036	1.797
Rep 6	0.040	0.037	0.043	0.032	0.038	1.625
Mean	0.043	0.033	0.036	0.038	0.034	1.672
SD	0.004	0.004	0.005	0.003	0.004	0.123
CV	9.7	10.8	15.4	9.0	13.1	7.4
Free Concentration (μm)					0.034	
% HSA Binding						98.0
% PC Binding	22.0	-1.0	5.2	10.6		
Free Fraction (fu)	0.780	1.010	0.948	0.894		0.020
Dilution Factor (D)	10.6	5.3	3.5	5.3		
Free Fraction Undiluted in Tissues (fut)	0.251	1.000	0.839	0.613		
Volume of Distribution (Vdss)	[0.080]	0.020	0.024	0.3		
Mean Volume of Distribution (Vdss)	0.025					

Compound Number	GI235401					
	PC 1	PC 2A	PC 3	PC 2B	1% PBS	HSA
Rep 1	0.598	0.099	0.274	0.219	0.029	2.537
Rep 2	0.633	0.085	0.255	0.232	0.032	2.523
Rep 3	0.589	0.068	0.250	0.230	0.012	2.535
Rep 4	0.655	0.152	0.247	0.229	0.022	2.572
Rep 5	0.694	0.135	0.266	0.232	0.024	2.947
Rep 6	0.569	0.140	0.258	0.230	0.011	2.793
Mean	0.623	0.113	0.258	0.229	0.022	2.651
SD	0.047	0.034	0.010	0.005	0.009	0.177
CV	7.5	29.9	3.9	2.1	39.9	6.7
Free Concentration (μm)					0.022	
% HSA Binding						99.1
% PC Binding	96.5	80.9	91.6	90.5		
Free Fraction (fu)	0.035	0.191	0.084	0.095		0.009
Dilution Factor (D)	10.6	5.3	3.5	5.3		
Free Fraction Undiluted in Tissues (fut)	0.003	0.043	0.025	0.019		
Volume of Distribution (Vdss)	[2.359]	0.87	0.317	0.413		
Mean Volume of Distribution (Vdss)	0.306					

Compound Number	GW622791					
	PC 1	PC 2A	PC 3	PC 2B	1% PBS	HSA
Rep 1	0.229	0.321	0.447	0.720	0.159	1.906
Rep 2	0.225	0.299	0.419	0.651	0.141	1.813
Rep 3	0.249	0.309	0.420	0.678	0.177	1.867
Rep 4	0.231	0.295	0.458	0.665	0.149	2.082
Rep 5	0.235	0.324	0.477	0.648	0.156	2.060
Rep 6	0.256	0.295	0.446	0.706	0.166	2.044
Mean	0.238	0.307	0.445	0.678	0.158	1.962
SD	0.012	0.013	0.022	0.029	0.013	0.012
CV	5.2	4.2	5.0	4.3	8.0	5.8
Free Concentration (μm)					0.158	
% HSA Binding						91.9
% PC Binding	34.1	49.1	64.8	76.9		
Free Fraction (fu)	0.659	0.509	0.352	0.231		0.081
Dilution Factor (D)	10.6	5.3	3.5	5.3		
Free Fraction Undiluted in Tissues (fut)	0.158	0.166	0.135	0.054		
Volume of Distribution (Vdss)	0.513	0.487	0.600	[1.495]		
Mean Volume of Distribution (Vdss)	0.533					

***In-Vitro* Pharmacokinetic Parameters of Bases series using CRED Device**

Compound Number	CCII3993					
	PC 1	PC 2A	PC 3	PC 2B	1% PBS	HSA
Rep 1	1.611	2.091	2.344	2.052	0.139	0.554
Rep 2	1.504	2.219	2.461	2.092	0.140	0.519
Rep 3	1.469	2.165	2.269	2.121	0.156	0.559
Rep 4	1.449	2.184	2.588	2.228	0.129	0.564
Rep 5	1.522	2.145	2.663	2.269	0.117	0.482
Rep 6	1.478	2.416	2.308	2.312	0.132	0.535
Mean	1.506	2.203	2.439	2.179	0.136	0.536
SD	0.058	0.113	0.160	0.105	0.013	0.031
CV	3.8	5.1	6.6	4.8	9.6	5.8
Free Concentration (μm)					0.136	
% HSA Binding						74.7
% PC Binding	91.0	93.9	94.4	93.8		
Free Fraction (fu)	0.090	0.061	0.056	0.062		0.253
Dilution Factor (D)	10.6	5.3	3.5	5.3		
Free Fraction Undiluted in Tissues (fut)	0.009	0.012	0.016	0.012		
Volume of Distribution (Vdss)	27.338	20.734	15.452	20.493		
Mean Volume of Distribution (Vdss)	21.004					

Compound Number	SB731710					
	PC 1	PC 2A	PC 3	PC 2B	1% PBS	HSA
Rep 1	0.319	0.341	0.363	0.347	0.219	2.603
Rep 2	0.313	0.328	0.274	0.338	0.227	2.731
Rep 3	0.298	0.295	0.304	0.293	0.212	2.632
Rep 4	0.325	0.312	0.315	0.371	0.201	2.636
Rep 5	0.388	0.309	0.344	0.309	0.170	2.654
Rep 6	0.364	0.325	0.338	0.312	0.226	2.598
Mean	0.335	0.318	0.323	0.328	0.209	2.642
SD	0.034	0.016	0.032	0.029	0.021	0.048
CV	10.2	5.1	9.9	8.8	10.3	1.8
Free Concentration (μm)					0.209	
% HSA Binding						92.1
% PC Binding	37.5	34.3	35.2	36.3		
Free Fraction (fu)	0.625	0.657	0.648	0.637		0.079
Dilution Factor (D)	10.6	5.3	3.5	5.3		
Free Fraction Undiluted in Tissues (fut)	0.138	0.265	0.342	0.249		
Volume of Distribution (Vdss)	0.580	0.298	0.231	0.318		
Mean Volume of Distribution (Vdss)	0.357					

Compound Number	CCI3748					
	PC 1	PC 2A	PC 3	PC 2B	1% PBS	HSA
Rep 1	1.491	2.528	3.459	2.957	0.363	0.857
Rep 2	1.447	2.923	3.319	3.092	0.365	1.023
Rep 3	1.482	2.906	3.197	2.811	0.357	0.831
Rep 4	1.572	2.907	3.602	2.841	0.396	0.937
Rep 5	1.437	2.787	3.251	3.030	0.397	0.854
Rep 6	1.357	2.652	3.340	2.849	0.446	0.906
Mean	1.464	2.784	3.361	2.930	0.387	0.901
SD	0.071	0.163	0.148	0.115	0.034	0.071
CV	4.8	5.8	4.4	3.9	8.7	7.9
Free Concentration (μm)					0.387	
% HSA Binding						57.0
% PC Binding	73.5	86.1	88.5	86.8		
Free Fraction (fu)	0.265	0.139	0.115	0.132		0.430
Dilution Factor (D)	10.6	5.3	3.5	5.3		
Free Fraction Undiluted in Tissues (fut)	0.033	0.030	0.036	0.028		
Volume of Distribution (Vdss)	13.090	14.543	12.098	15.403		
Mean Volume of Distribution (Vdss)	13.783					

Compound Number	GR30676					
	PC 1	PC 2A	PC 3	PC 2B	1% PBS	HSA
Rep 1	0.585	0.620	0.623	0.675	0.028	1.370
Rep 2	0.707	0.678	0.712	0.706	0.04	1.517
Rep 3	0.603	0.634	0.634	0.619	0.01	1.438
Rep 4	0.607	0.731	0.719	0.764	0.069	1.450
Rep 5	0.727	0.696	0.656	0.674	0.065	1.330
Rep 6	0.652	0.652	0.796	0.683	0.04	1.481
Mean	0.647	0.669	0.690	0.687	0.042	1.431
SD	0.059	0.041	0.065	0.047	0.022	0.070
CV	9.1	6.2	9.5	6.9	53.6	4.9
Free Concentration (μm)					0.042	
% HSA Binding						97.1
% PC Binding	93.6	93.8	94.0	93.9		
Free Fraction (fu)	0.064	0.062	0.060	0.061		0.029
Dilution Factor (D)	10.6	5.3	3.5	5.3		
Free Fraction Undiluted in Tissues (fut)	0.006	0.012	0.018	0.012		
Volume of Distribution (Vdss)	4.489	2.343	1.624	2.411		
Mean Volume of Distribution (Vdss)	2.717					

Compound Number	SKF95914					
	PC 1	PC 2A	PC 3	PC 2B	1% PBS	HSA
Rep 1	0.048	0.056	0.054	0.044	0.006	0.889
Rep 2	0.054	0.021	0.033	0.024	0.013	0.818
Rep 3	0.049	0.044	0.043	0.038	0.001	0.844
Rep 4	0.052	0.042	0.050	0.043	0.012	0.848
Rep 5	0.048	0.034	0.042	0.028	0.013	0.844
Rep 6	0.044	0.046	0.022	0.042	0.005	0.878
Mean	0.049	0.041	0.041	0.037	0.008	0.854
SD	0.003	0.012	0.012	0.008	0.005	0.026
CV	7.1	29.4	28.7	23.2	60.6	3.0
Free Concentration (μm)					0.008	
% HSA Binding						99.0
% PC Binding	83.1	79.4	79.5	77.2		
Free Fraction (fu)	0.169	0.206	0.205	0.228		0.010
Dilution Factor (D)	10.6	5.3	3.5	5.3		
Free Fraction Undiluted in Tissues (fut)	0.019	0.047	0.068	0.053		
Volume of Distribution (Vdss)	0.529	0.215	0.147	0.189		
Mean Volume of Distribution (Vdss)	0.270					

Compound Number	GR35842					
	PC 1	PC 2A	PC 3	PC 2B	1% PBS	HSA
Rep 1	1.423	2.909	4.584	2.501	0.458	0.862
Rep 2	1.441	2.764	4.797	2.874	0.424	0.743
Rep 3	1.476	2.923	4.279	2.784	0.434	0.745
Rep 4	1.316	2.853	3.444	2.863	0.436	0.815
Rep 5	1.287	2.798	3.656	2.637	0.656	0.802
Rep 6	1.305	2.547	3.378	2.681	0.425	0.774
Mean	1.375	2.799	4.023	2.723	0.472	0.790
SD	0.081	0.138	0.611	0.145	0.091	0.046
CV	5.9	4.9	15.2	5.3	19.2	5.8
Free Concentration (μm)					0.472	
% HSA Binding						40.2
% PC Binding	65.7	83.1	88.3	82.7		
Free Fraction (fu)	0.343	0.169	0.117	0.173		0.598
Dilution Factor (D)	10.6	5.3	3.5	5.3		
Free Fraction Undiluted in Tissues (fut)	0.047	0.037	0.036	0.038		
Volume of Distribution (Vdss)	12.701	16.230	16.491	15.722		
Mean Volume of Distribution (Vdss)	15.286					

Compound Number	GR43175					
	PC 1	PC 2A	PC 3	PC 2B	1% PBS	HSA
Rep 1	1.240	1.576	1.386	1.510	1.261	1.326
Rep 2	1.243	1.537	1.278	1.439	1.146	1.482
Rep 3	1.416	1.480	1.339	1.384	1.250	1.343
Rep 4	1.245	1.387	1.416	1.567	1.223	1.310
Rep 5	1.218	1.380	1.403	1.524	1.231	1.414
Rep 6	1.232	1.447	1.393	1.520	1.234	1.378
Mean	1.266	1.468	1.369	1.491	1.224	1.376
SD	0.07	0.08	0.05	0.07	0.04	0.06
CV	5.9	5.4	3.8	4.5	3.3	4.7
Free Concentration (μm)					1.224	
% HSA Binding						11.0
% PC Binding	3.3	16.6	10.6	17.9		
Free Fraction (fu)	0.967	0.834	0.894	0.821		0.890
Dilution Factor (D)	10.6	5.3	3.5	5.3		
Free Fraction Undiluted in Tissues (fut)	0.736	0.486	0.705	0.464		
Volume of Distribution (Vdss)	1.209	1.830	1.263	1.918		
Mean Volume of Distribution (Vdss)	1.555					

Compound Number	GF120454					
	PC 1	PC 2A	PC 3	PC 2B	1% PBS	HSA
Rep 1	2.073	2.273	2.177	2.098	0.291	0.947
Rep 2	1.794	1.874	2.447	2.184	0.268	0.939
Rep 3	1.945	1.985	2.142	2.071	0.292	0.990
Rep 4	1.987	2.423	2.351	2.598	0.284	1.143
Rep 5	2.230	2.349	2.136	1.710	0.278	0.887
Rep 6	2.134	2.390	2.270	2.198	0.440	bad injection
Mean	2.027	2.216	2.254	2.143	0.309	0.981
SD	0.153	0.230	0.126	0.285	0.065	0.098
CV	7.6	10.4	5.6	13.3	21.0	9.9
Free Concentration (μm)					0.309	
% HSA Binding						68.5
% PC Binding	84.8	86.1	86.3	85.6		
Free Fraction (fu)	0.152	0.139	0.137	0.144		0.315
Dilution Factor (D)	10.6	5.3	3.5	5.3		
Free Fraction Undiluted in Tissues (fut)	0.017	0.030	0.043	0.031		
Volume of Distribution (Vdss)	18.872	10.632	7.326	10.240		
Mean Volume of Distribution (Vdss)	11.767					

Compound Number	GR99941					
	PC 1	PC 2A	PC 3	PC 2B	1% PBS	HSA
Rep 1	1.095	1.714	2.353	1.635	0.490	1.703
Rep 2	1.002	1.779	2.384	1.505	0.529	1.569
Rep 3	1.077	1.646	2.463	1.585	0.528	1.566
Rep 4	1.058	1.630	2.398	1.548	0.527	1.665
Rep 5	1.035	1.603	2.303	1.498	0.552	1.621
Rep 6	1.016	1.626	2.377	1.611	0.516	1.613
Mean	1.047	1.666	2.380	1.564	0.524	1.623
SD	0.036	0.067	0.053	0.056	0.020	0.054
CV	3.4	4.0	2.2	3.6	3.9	3.3
Free Concentration (μm)					0.524	
% HSA Binding						67.7
% PC Binding	50.0	68.6	78.0	66.5		
Free Fraction (fu)	0.500	0.314	0.220	0.335		0.323
Dilution Factor (D)	10.6	5.3	3.5	5.3		
Free Fraction Undiluted in Tissues (fut)	0.086	0.080	0.074	0.087		
Volume of Distribution (Vdss)	3.742	4.062	4.369	3.726		
Mean Volume of Distribution (Vdss)	3.974					
Compound Number	GW300671					
	PC 1	PC 2A	PC 3	PC 2B	1% PBS	HSA
Rep 1	1.158	1.532	1.896	1.557	0.804	2.007
Rep 2	1.177	1.505	1.991	1.480	0.851	2.086
Rep 3	1.156	1.549	2.028	1.441	0.776	2.113
Rep 4	1.152	1.578	1.856	1.490	0.830	1.923
Rep 5	1.169	1.526	1.784	1.425	0.870	1.996
Rep 6	1.171	1.412	1.760	1.409	0.864	2.072
Mean	1.164	1.517	1.886	1.467	0.833	2.033
SD	0.010	0.057	0.108	0.054	0.037	0.071
CV	0.8	3.8	5.7	3.7	4.4	3.5
Free Concentration (μm)					0.833	
% HSA Binding						59.0
% PC Binding	28.5	45.1	55.9	43.3		
Free Fraction (fu)	0.715	0.549	0.441	0.567		0.410
Dilution Factor (D)	10.6	5.3	3.5	5.3		
Free Fraction Undiluted in Tissues (fut)	0.192	0.187	0.183	0.198		
Volume of Distribution (Vdss)	2.138	2.198	2.243	2.068		
Mean Volume of Distribution (Vdss)	2.162					

Compound Number	SB416332					
	PC 1	PC 2A	PC 3	PC 2B	1% PBS	HSA
Rep 1	1.623	1.957	2.367	2.075	1.324	1.301
Rep 2	1.575	2.065	2.501	1.960	1.359	1.237
Rep 3	1.672	2.100	2.326	2.036	1.317	1.363
Rep 4	1.639	2.022	2.440	2.148	1.355	1.602
Rep 5	1.670	2.001	2.451	2.062	1.281	1.627
Rep 6	1.672	1.936	2.419	2.066	1.282	1.630
Mean	1.642	2.014	2.417	2.058	1.320	1.460
SD	0.039	0.063	0.062	0.061	0.034	0.180
CV	2.3	3.1	2.6	3.0	2.6	12.3
Free Concentration (μm)					1.320	
% HSA Binding						9.6
% PC Binding	19.6	34.5	45.4	35.9		
Free Fraction (fu)	0.804	0.655	0.546	0.641		0.904
Dilution Factor (D)	10.6	5.3	3.5	5.3		
Free Fraction Undiluted in Tissues (fut)	0.279	0.264	0.254	0.252		
Volume of Distribution (Vdss)	3.241	3.425	3.561	3.586		
Mean Volume of Distribution (Vdss)	3.453					

Compound Number	CC13839					
	PC 1	PC 2A	PC 3	PC 2B	1% PBS	HSA
Rep 1	1.982	3.024	3.869	3.087	1.074	1.598
Rep 2	1.928	2.932	4.038	3.179	1.066	1.572
Rep 3	2.084	2.942	3.922	3.135	1.079	1.552
Rep 4	1.970	2.918	3.861	3.034	1.090	1.573
Rep 5	1.983	3.011	3.910	3.053	1.045	1.586
Rep 6	2.139	2.875	3.872	3.132	1.088	1.585
Mean	2.014	2.950	3.912	3.103	1.074	1.578
SD	0.080	0.057	0.066	0.055	0.017	0.016
CV	4.0	1.9	1.7	1.8	1.6	1.0
Free Concentration (μM)					1.074	
% HSA Binding						31.9
% PC Binding	46.7	63.6	72.6	65.4		
Free Fraction (fu)	0.533	0.364	0.274	0.346		0.681
Dilution Factor (D)	10.6	5.3	3.5	5.3		
Free Fraction Undiluted in Tissues (fut)	0.097	0.097	0.097	0.091		
Volume of Distribution (Vdss)	6.998	6.995	7.043	7.510		

Mean Volume of Distribution (Vdss)	7.137
------------------------------------	-------

Compound Number	GR61317					
	PC 1	PC 2A	PC 3	PC 2B	1% PBS	HSA
Rep 1	1.210	1.400	1.925	1.444	0.075	2.507
Rep 2	1.165	1.578	1.840	1.632	0.083	2.362
Rep 3	1.233	1.514	1.748	1.650	0.059	2.167
Rep 4	1.135	1.699	1.918	1.565	0.072	2.431
Rep 5	1.222	1.647	1.924	1.564	0.070	2.534
Rep 6	1.203	1.616	1.833	1.611	0.050	2.415
Mean	1.195	1.576	1.865	1.578	0.068	2.403
SD	0.037	0.106	0.071	0.074	0.012	0.131
CV	3.1	6.8	3.8	4.7	17.3	5.5
Free Concentration (μm)					0.068	
% HSA Binding						97.2
% PC Binding	94.3	95.7	96.3	95.7		
Free Fraction (fu)	0.057	0.043	0.037	0.043		0.028
Dilution Factor (D)	10.6	5.3	3.5	5.3		
Free Fraction Undiluted in Tissues (fut)	0.006	0.008	0.011	0.008		
Volume of Distribution (Vdss)	4.927	3.313	2.636	3.317		
Mean Volume of Distribution (Vdss)	3.548					

Compound Number	GW769340					
	PC 1	PC 2A	PC 3	PC 2B	1% PBS	HSA
Rep 1	1.663	1.524	3.235	2.875	0.314	0.790
Rep 2	1.736	1.509	3.124	2.816	0.290	0.851
Rep 3	1.766	1.641	3.382	2.736	0.285	0.868
Rep 4	1.696	2.748	3.511	2.782	0.286	0.793
Rep 5	1.759	2.748	3.344	2.869	0.300	0.777
Rep 6	1.690	2.744	3.383	2.879	0.272	0.846
Mean	1.718	2.152	3.330	2.826	0.291	0.821
SD	0.041	0.653	0.134	0.059	0.014	0.039
CV	2.4	30.3	4.0	2.1	4.9	4.7
Free Concentration (μm)					0.291	
% HSA Binding						64.5
% PC Binding	83.1	86.5	91.3	89.7		

Free Fraction (fu)	0.169	0.135	0.087	0.103		0.355
Dilution Factor (D)	10.6	5.3	3.5	5.3		
Free Fraction Undiluted in Tissues (fut)	0.019	0.029	0.026	0.021		
Volume of Distribution (Vdss)	8.964	12.392	13.448	16.750		
Mean Volume of Distribution (Vdss)	12.888					

Compound Number	CCII20557					
	PC 1	PC 2A	PC 3	PC 2B	1% PBS	HSA
Rep 1	2.196	3.150	4.336	2.704	0.780	1.267
Rep 2	2.192	3.010	4.222	2.879	0.761	1.138
Rep 3	1.864	3.198	4.176	2.914	0.751	1.234
Rep 4	2.139	2.884	4.147	2.944	0.762	1.178
Rep 5	2.192	3.181	4.062	2.913	0.819	1.328
Rep 6	2.089	3.094	4.167	2.882	0.828	1.194
Mean	2.112	3.086	4.185	2.873	0.784	1.223
SD	0.129	0.120	0.091	0.086	0.032	0.068
CV	6.1	3.9	2.2	3.0	4.1	5.6
Free Concentration (μm)					0.784	
% HSA Binding						35.9
% PC Binding	62.9	74.6	81.3	72.7		
Free Fraction (fu)	0.371	0.254	0.187	0.273		0.641
Dilution Factor (D)	10.6	5.3	3.5	5.3		
Free Fraction Undiluted in Tissues (fut)	0.053	0.060	0.061	0.066		
Volume of Distribution (Vdss)	12.149	10.634	10.476	9.707		
Mean Volume of Distribution (Vdss)	10.742					
Compound Number	CCI4001					
	PC 1	PC 2A	PC 3	PC 2B	1% PBS	HSA
Rep 1	2.409	5.307	5.589	4.910	0.622	1.130
Rep 2	2.745	4.956	5.930	5.357	0.666	1.150
Rep 3	2.554	5.551	5.928	5.035	0.620	1.170
Rep 4	2.402	4.829	5.660	4.495	0.614	1.290
Rep 5	2.548	4.559	5.396	4.992	0.603	1.130
Rep 6	2.325	4.782	5.258	5.791	0.602	1.210
Mean	2.497	4.997	5.627	5.097	0.621	1.180
SD	0.151	0.366	0.274	0.439	0.023	0.062
CV	6.0	7.3	4.9	8.6	3.8	5.2
Free Concentration (μm)					0.621	
% HSA Binding						47.4

% PC Binding	75.1	87.6	89.0	87.8		
Free Fraction (fu)	0.249	0.124	0.110	0.122		0.526
Dilution Factor (D)	10.6	5.3	3.5	5.3		
Free Fraction Undiluted in Tissues (fut)	0.030	0.026	0.034	0.025		
Volume of Distribution (Vdss)	17.346	20.183	15.506	20.629		
Mean Volume of Distribution (Vdss)	18.416					
Compound Number	GR84804					
	PC 1	PC 2A	PC 3	PC 2B	1% PBS	HSA
Rep 1	1.795	2.481	2.711	2.642	0.107	0.419
Rep 2	1.853	2.484	2.609	2.641	0.127	0.405
Rep 3	1.809	2.420	2.694	2.626	0.129	0.428
Rep 4	1.825	2.460	2.837	2.425	0.123	0.444
Rep 5	1.836	2.510	2.792	2.716	0.140	0.450
Rep 6	1.848	2.556	2.808	2.693	0.133	0.427
Mean	1.828	2.485	2.742	2.624	0.127	0.429
SD	0.023	0.046	0.086	0.103	0.011	0.016
CV	1.2	1.8	3.1	3.9	8.8	3.8
Free Concentration (μM)					0.127	
% HSA Binding						70.5
% PC Binding	93.1	94.9	95.4	95.2		
Free Fraction (fu)	0.069	0.051	0.046	0.048		0.295
Dilution Factor (D)	10.6	5.3	3.5	5.3		
Free Fraction Undiluted in Tissues (fut)	0.007	0.010	0.014	0.009		
Volume of Distribution (Vdss)	42.300	29.472	21.849	31.188		
Mean Volume of Distribution (Vdss)	31.202					

***In-Vitro* Pharmacokinetic Parameters of Neutral series using CRED Device**

Compound Number	GR91295					
	PC 1	PC 2A	PC 3	PC 2B	1% PBS	HSA
Rep 1	1.491	0.000	1.241	1.466	1.646	1.769
Rep 2	1.504	0.000	1.366	1.562	1.558	1.791
Rep 3	1.534	0.000	1.391	1.558	1.510	1.808
Rep 4	1.465	0.000	1.533	1.580	1.605	1.849
Rep 5	1.460	0.000	1.594	1.701	1.762	1.888
Rep 6	1.492	0.000	1.589	1.561	1.696	1.932
Mean	1.491	0.000	1.452	1.571	1.630	1.840
SD	0.027	0.000	0.142	0.075	0.092	0.062
CV	1.8	No Data Acquired	9.8	4.8	5.6	3.4
Free Concentration (μm)					1.630	
% HSA Binding						11.4
% PC Binding	-9.3		-12.2	-3.7		
Free Fraction (fu)	1.093		1.122	1.037		0.886
Dilution Factor (D)	10.6		3.5	5.3		
Free Fraction Undiluted in Tissues (fut)	1.000		1.000	1.000		
Volume of Distribution (Vdss)	0.886		0.886	0.886		
Mean Volume of Distribution (Vdss)	0.886					

Compound Number	CC19371					
	PC 1	PC 2A	PC 3	PC 2B	1% PBS	HSA
Rep 1	1.011	0.000	2.011	1.379	0.457	2.200
Rep 2	1.242	0.000	2.024	1.708	0.187	2.381
Rep 3	1.162	0.000	2.077	1.488	0.456	1.816
Rep 4	1.096	0.000	1.726	1.751	0.570	2.364
Rep 5	1.162	0.000	2.034	1.172	0.493	2.432
Rep 6	1.104	0.000	1.967	1.718	0.500	2.259
Mean	1.130	0.000	1.973	1.536	0.444	2.242
SD	0.078		0.126	0.232	0.132	0.225
CV	6.9	No Data Acquired	6.4	15.1	29.9	10.0
Free Concentration (μm)					0.444	
% HSA Binding						80.2
% PC Binding	60.7		77.5	71.1		
Free Fraction (fu)	0.393		0.225	0.289		0.198
Dilution Factor (D)	10.6		3.5	5.3		
Free Fraction Undiluted in Tissues (fut)	0.058		0.052	0.103		
Volume of Distribution (Vdss)	3.436		3.816	1.20		
Mean Volume of Distribution (Vdss)	3.057					

Compound Number	CC122428					
	PC 1	PC 2A	PC 3	PC 2B	1% PBS	HSA
Rep 1	0.942	1.409	1.737	1.459	0.648	1.521
Rep 2	1.221	1.615	1.801	1.407	0.541	1.333
Rep 3	1.110	1.477	1.689	1.358	0.700	1.400
Rep 4	1.102	1.643	1.744	1.544	0.615	1.62
Rep 5	1.121	1.475	1.876	1.656	0.593	1.555
Rep 6	1.009	1.357	1.815	1.479	0.649	1.542
Mean	1.084	1.496	1.777	1.484	0.624	1.495
SD	0.097	0.113	0.067	0.105	0.055	0.107
CV	8.9	7.5	3.8	7.1	8.7	7.2
Free Concentration (μm)					0.624	
% HSA Binding						58.2
% PC Binding	42.4	58.3	64.9	57.9		
Free Fraction (fu)	0.576	0.417	0.351	0.421		0.418
Dilution Factor (D)	10.6	5.3	3.5	5.3		
Free Fraction Undiluted in Tissues (fut)	0.114	0.119	0.133	0.120		
Volume of Distribution (Vdss)	3.678	3.514	3.145	3.470		
Mean Volume of Distribution (Vdss)	3.46352					
Compound Number	GR104104					
	PC 1	PC 2A	PC 3	PC 2B	1% PBS	HSA
Rep 1	0.750	1.209	1.373	1.040	0.249	1.389
Rep 2	0.759	1.242	1.272	1.041	0.261	1.480
Rep 3	0.808	1.172	1.314	1.021	0.263	1.401
Rep 4	0.776	1.179	1.287	1.077	0.241	1.424
Rep 5	0.750	1.146	1.283	1.063	0.248	1.385
Rep 6	0.735	1.184	1.249	1.031	0.248	1.317
Mean	0.763	1.189	1.296	1.046	0.252	1.399
SD	0.026	0.033	0.043	0.021	0.009	0.053
CV	3.4	2.8	3.3	2.0	3.4	3.8
Free Concentration (μm)					0.252	
% HSA Binding						82.02
% PC Binding	66.9	78.8	80.5	75.9		

Free Fraction (fu)	0.331	0.212	0.195	0.241		0.180
Dilution Factor (D)	10.6	5.3	3.5	5.3		
Free Fraction Undiluted in Tissues (fut)	0.044	0.048	0.064	0.056		
Volume of Distribution (Vdss)	4.052	3.735	2.821	3.192		
Mean Volume of Distribution (Vdss)	3.437					
Compound Number	GF120403					
	PC 1	PC 2A	PC 3	PC 2B	1% PBS	HSA
Rep 1	0.224	0.282	0.362	0.290	0.183	1.866
Rep 2	0.228	0.284	0.376	0.285	0.170	1.808
Rep 3	0.225	0.305	0.345	0.297	0.175	1.833
Rep 4	0.306	0.287	0.399	0.364	0.191	2.003
Rep 5	0.269	0.339	0.344	0.327	0.189	1.797
Rep 6	0.281	0.312	0.369	0.303	0.179	1.831
Mean	0.256	0.302	0.366	0.311	0.181	1.856
SD	0.035	0.022	0.021	0.030	0.008	0.076
CV	13.6	7.3	5.7	9.6	4.5	4.1
Free Concentration (μm)					0.181	
% HSA Binding						90.2
% PC Binding	29.1	39.9	50.5	41.7		-
Free Fraction (fu)	0.709	0.601	0.495	0.583		0.098
Dilution Factor (D)	10.6	5.3	3.5	5.3		
Free Fraction Undiluted in Tissues (fut)	0.162	0.222	0.218	0.209		
Volume of Distribution (Vdss)	0.604	0.441	0.449	0.468		
Mean Volume of Distribution (Vdss)	0.491					
Compound Number	GI115674					
	PC 1	PC 2A	PC 3	PC 2B	1% PBS	HSA
Rep 1	0.944	1.229	1.514	1.285	0.799	2.177
Rep 2	0.999	1.309	1.480	1.407	0.71	1.885
Rep 3	0.971	1.277	1.430	1.282	0.768	1.901
Rep 4	0.921	1.361	1.694	1.32	0.784	2.109
Rep 5	0.983	1.202	1.584	1.342	0.752	2.055
Rep 6	0.970	1.410	1.504	1.309	0.693	2.165
Mean	0.965	1.298	1.534	1.324	0.751	2.049
SD	0.028	0.079	0.093	0.046	0.042	0.128
CV	2.9	6.1	6.1	3.5	5.6	6.3
Free Concentration (μm)					0.751	
% HSA Binding						63.4
% PC Binding	22.2	42.2	51.1	43.3		

Free Fraction (fu)	0.778	0.578	0.489	0.567		0.366
Dilution Factor (D)	10.6	5.3	3.5	5.3		
Free Fraction Undiluted in Tissues (fut)	0.249	0.205	0.213	0.198		
Volume of Distribution (Vdss)	1.472	1.782	1.717	1.850		
Mean Volume of Distribution (Vdss)	1.705					

Compound Number	AH24363					
	PC 1	PC 2A	PC 3	PC 2B	1% PBS	HSA
Rep 1	1.181	1.595	1.848	1.446	0.893	1.862
Rep 2	1.074	1.673	1.936	1.627	0.961	1.736
Rep 3	1.162	1.584	1.816	1.570	1.001	1.778
Rep 4	1.283	1.639	2.027	1.565	0.986	1.899
Rep 5	1.228	1.590	1.925	1.769	1.001	1.964
Rep 6	1.250	1.675	1.919	1.583	0.840	1.784
Mean	1.196	1.626	1.912	1.593	0.947	1.837
SD	0.075	0.042	0.074	0.105	0.066	0.086
CV	6.2	2.6	3.9	6.6	7.0	4.7
Free Concentration (μm)					0.947	
% HSA Binding						48.5
% PC Binding	20.8	41.8	50.5	40.6		
Free Fraction (fu)	0.792	0.582	0.495	0.594		0.515
Dilution Factor (D)	10.6	5.3	3.5	5.3		
Free Fraction Undiluted in Tissues (fut)	0.264	0.208	0.217	0.216		
Volume of Distribution (Vdss)	1.951	2.474	2.369	2.379		
Mean Volume of Distribution (Vdss)	2.293					

Compound Number	GW388185					
	PC 1	PC 2A	PC 3	PC 2B	1% PBS	HSA
Rep 1	0.034	0.059	0.047	0.028	0.014	2.527
Rep 2	0.035	0.051	0.042	0.030	0.006	2.298
Rep 3	0.036	0.043	0.048	0.027	0.007	2.392
Rep 4	0.032	0.033	0.040	0.028	0.007	2.312
Rep 5	0.031	0.029	0.033	0.033	0.009	2.331
Rep 6	0.017	0.044	0.032	0.047	0.010	2.265
Mean	0.031	0.043	0.040	0.032	0.009	2.354
SD	0.007	0.011	0.007	0.008	0.003	0.095
CV	22.8	25.7	16.8	23.5	33.1	4.0
Free Concentration (μm)					0.009	
% HSA Binding						99.6
% PC Binding	71.4	79.5	78.1	72.5		
Free Fraction (fu)	0.286	0.205	0.219	0.275		0.004
Dilution Factor (D)	10.6	5.3	3.5	5.3		
Free Fraction Undiluted in Tissues (fut)	0.037	0.046	0.074	0.067		
Volume of Distribution (Vdss)	0.103	0.081	0.051	0.056		
Mean Volume of Distribution (Vdss)	0.073					

Compound Number	GR119497					
	PC 1	PC 2A	PC 3	PC 2B	1% PBS	HSA
Rep 1	0.686	0.868	1.140	0.814	0.472	1.079
Rep 2	0.592	0.783	1.101	0.752	0.491	0.923
Rep 3	0.658	0.897	1.015	0.792	0.467	0.960
Rep 4	0.765	0.809	0.882	0.893	0.481	0.917
Rep 5	0.636	0.881	0.906	0.827	0.452	1.103
Rep 6	0.713	0.795	0.985	0.813	0.535	1.036
Mean	0.675	0.839	1.005	0.815	0.483	1.003
SD	0.061	0.049	0.103	0.046	0.029	0.081
CV	9.0	5.8	10.2	5.7	5.9	8.0
Free Concentration (μm)					0.483	
% HSA Binding						51.8
% PC Binding	28.4	42.4	51.9	40.7		
Free Fraction (fu)	0.716	0.576	0.481	0.593		0.482
Dilution Factor (D)	10.6	5.3	3.5	5.3		
Free Fraction Undiluted in Tissues (fut)	0.192	0.204	0.208	0.215		
Volume of Distribution (Vdss)	2.508	2.363	2.320	2.238		
Mean Volume of Distribution (Vdss)	2.358					

Compound Number	GR33914					
	PC 1	PC 2A	PC 3	PC 2B	1% PBS	HSA
Rep 1	0.757	0.806	0.888	0.769	0.040	2.265
Rep 2	0.675	0.829	0.827	0.728	0.034	2.368
Rep 3	0.674	0.815	0.909	0.789	0.030	2.117
Rep 4	0.731	0.806	0.871	0.817	0.044	2.170
Rep 5	0.843	0.989	0.918	0.866	0.034	2.028
Rep 6	0.845	0.877	0.974	0.848	0.041	2.179
Mean	0.754	0.854	0.898	0.803	0.037	2.188
SD	0.077	0.071	0.049	0.051	0.005	0.118
CV	10.2	8.4	5.5	6.4	14.3	5.4
Free Concentration (μm)					0.036	
% HSA Binding						98.3
% PC Binding	95.1	95.6	95.9	95.4		
Free Fraction (fu)	0.049	0.044	0.041	0.046		0.017
Dilution Factor (D)	10.6	5.3	3.5	5.3		
Free Fraction Undiluted in Tissues (fut)	0.005	0.009	0.012	0.009		
Volume of Distribution (Vdss)	3.487	1.997	1.407	1.873		
Mean Volume of Distribution (Vdss)	2.191					

Compound Number	GR38393					
	PC 1	PC 2A	PC 3	PC 2B	1% PBS	HSA
Rep 1	0.305	0.314	0.390	0.335	0.019	2.490
Rep 2	0.330	0.372	0.350	0.364	0.020	2.294
Rep 3	0.293	0.374	0.356	0.349	0.021	2.300
Rep 4	0.296	0.382	0.342	0.358	0.019	2.113
Rep 5	0.322	0.377	0.363	0.332	0.021	2.171
Rep 6	0.285	0.345	0.442	0.392	0.020	2.019
Mean	0.305	0.361	0.374	0.355	0.020	2.231
SD	0.018	0.026	0.037	0.022	0.001	0.166
CV	5.7	7.3	10.0	6.2	4.5	7.5
Free Concentration (μm)					0.020	
% HSA Binding						99.1
% PC Binding	93.4	94.5	94.7	94.4		
Free Fraction (fu)	0.066	0.055	0.053	0.056		0.009
Dilution Factor (D)	10.6	5.3	3.5	5.3		
Free Fraction Undiluted in Tissues (fut)	0.007	0.011	0.016	0.011		
Volume of Distribution (Vdss)	1.36	0.819	0.569	0.805		
Mean Volume of Distribution (Vdss)	0.889					

Compound Number	GR64334					
	PC 1	PC 2A	PC 3	PC 2B	1% PBS	HSA
Rep 1	0.438	0.488	0.434	0.475	0.512	2.040
Rep 2	0.449	0.455	0.486	0.434	0.510	1.967
Rep 3	0.466	0.447	0.532	0.502	0.504	1.853
Rep 4	0.530	0.518	0.458	0.476	0.505	2.069
Rep 5	0.421	0.500	0.478	0.458	0.486	1.702
Rep 6	0.440	0.513	0.506	0.43	0.461	1.878
Mean	0.457	0.487	0.482	0.463	0.496	1.918
SD	0.039	0.030	0.035	0.028	0.020	0.136
CV	8.4	6.1	7.2	6.0	3.9	7.1
Free Concentration (μm)					0.496	
% HSA Binding						74.1
% PC Binding	-8.5	-2.0	-2.9	-7.3		
Free Fraction (fu)	1.085	1.020	1.029	1.073		0.259
Dilution Factor (D)	10.6	5.3	3.5	5.3		
Free Fraction Undiluted in Tissues (fut)	1.000	1.000	1.000	1.000		
Volume of Distribution (Vdss)	0.259	0.259	0.259	0.259		
Mean Volume of Distribution (Vdss)	0.259					
Compound Number	GW703803					
	PC 1	PC 2A	PC 3	PC 2B	1% PBS	HSA
Rep 1	1.229	1.350	1.328	1.453	0.104	1.740
Rep 2	1.092	1.407	1.316	1.775	0.102	1.917
Rep 3	0.996	1.460	1.308	1.652	0.130	2.026
Rep 4	1.068	1.666	1.303	1.356	0.097	1.916
Rep 5	1.055	1.577	1.509	1.572	0.119	2.070
Rep 6	1.100	1.500	1.199	1.526	0.097	2.406
Mean	1.090	1.493	1.327	1.556	0.108	2.013
SD	0.077	0.115	0.101	0.148	0.013	0.224
CV	7.1	7.7	7.6	9.5	12.4	11.1

Free Concentration (μm)					0.108	
% HSA Binding						94.6
% PC Binding	90.1	92.8	91.8	93.0		
Free Fraction (fu)	0.099	0.072	0.082	0.070		0.054
Dilution Factor (D)	10.6	5.3	3.5	5.3		
Free Fraction Undiluted in Tissues (fut)	0.010	0.015	0.024	0.014		
Volume of Distribution (Vdss)	5.219	3.705	2.1924	3.869		
Mean Volume of Distribution (Vdss)	3.747					
Compound Number	GI116108					
	PC 1	PC 2A	PC 3	PC 2B	1% PBS	HSA
Rep 1	0.525	0.728	0.807	0.756	0.053	1.961
Rep 2	0.543	0.768	0.737	0.654	0.054	1.849
Rep 3	0.561	0.807	0.795	0.720	0.046	2.043
Rep 4	0.570	0.647	0.798	0.805	0.048	2.059
Rep 5	0.594	0.795	0.810	0.807	0.058	2.150
Rep 6	0.596	0.813	0.795	0.718	0.060	1.878
Mean	0.565	0.760	0.790	0.743	0.053	1.990
SD	0.028	0.063	0.027	0.059	0.005	0.115
CV	5.0	8.3	3.4	7.9	10.3	5.8
Free Concentration (μm)					0.053	
% HSA Binding						97.3
% PC Binding	90.6	93.0	93.3	92.8		
Free Fraction (fu)	0.094	0.070	0.067	0.072		0.027
Dilution Factor (D)	10.6	5.3	3.5	5.3		
Free Fraction Undiluted in Tissues (fut)	0.010	0.014	0.020	0.014		
Volume of Distribution (Vdss)	2.749	1.910	1.336	1.866		
Mean Volume of Distribution (Vdss)	1.969					

Compound Number	GI99296					
	PC 1	PC 2A	PC 3	PC 2B	1% PBS	HSA
Rep 1	0.035	0.078	0.141	0.120	0.004	0.448
Rep 2	0.037	0.105	0.145	0.126	0.003	0.506
Rep 3	0.040	0.095	0.154	0.111	0.003	0.424
Rep 4	0.043	0.091	0.154	0.125	0.004	0.514
Rep 5	0.046	0.090	0.134	0.104	0.003	0.535
Rep 6	0.039	0.085	0.143	0.098	0.004	0.526
Mean	0.040	0.091	0.145	0.114	0.004	0.492
SD	0.004	0.009	0.008	0.012	0.001	0.045
CV	10.0	10.1	5.4	10.1	15.6	9.2
Free Concentration (μm)					0.004	
% HSA Binding						99.3
% PC Binding	91.3	96.1	97.6	96.9		
Free Fraction (fu)	0.088	0.039	0.024	0.031		0.007
Dilution Factor (D)	10.6	5.3	3.5	5.3		
Free Fraction Undiluted in Tissues (fut)	0.009	0.008	0.007	0.006		
Volume of Distribution (Vdss)	0.792	0.947	1.024	1.198		
Mean Volume of Distribution (Vdss)	0.990					

Compound Number	GR77494					
	PC 1	PC 2A	PC 3	PC 2B	1% PBS	HSA
Rep 1	0.849	0.678	0.978	0.934	0.530	0.789
Rep 2	0.662	0.665	0.902	0.971	0.575	0.921
Rep 3	0.648	0.661	1.131	0.829	0.456	0.929
Rep 4	0.705	0.646	1.060	0.917	0.466	0.817
Rep 5	0.604	0.685	0.939	0.938	0.535	0.830
Rep 6	0.625	0.679	0.896	1.031	0.500	0.853
Mean	0.682	0.669	0.984	0.937	0.510	0.857
SD	0.089	0.014	0.094	0.066	0.045	0.057
CV	13.0	2.2	9.5	7.1	8.9	6.7
Free Concentration (μm)					0.512	
% HSA Binding						40.4
% PC Binding	25.2	23.7	48.2	45.5		
Free Fraction (fu)	0.748	0.763	0.518	0.545		0.596
Dilution Factor (D)	10.6	5.3	3.5	5.3		
Free Fraction Undiluted in Tissues (fut)	0.219	0.377	0.234	0.184		
Volume of Distribution (Vdss)	2.721	1.579	2.552	3.237		
Mean Volume of Distribution (Vdss)	2.522					

Compound Number	GR189721					
	PC 1	PC 2A	PC 3	PC 2B	1% PBS	HSA
Rep 1	0.111	0.105	0.593	0.137	0.091	0.114
Rep 2	0.117	0.066	0.556	0.116	0.086	0.125
Rep 3	0.105	0.074	0.600	0.147	0.077	0.130
Rep 4	0.091	0.069	0.480	0.121	0.079	0.108
Rep 5	0.131	0.101	0.535	0.177	0.077	0.102
Rep 6	0.129	0.095	0.539	0.139	0.072	0.111
Mean	0.114	0.085	0.551	0.140	0.080	0.115

SD	0.015	0.017	0.044	0.022	0.007	0.011
CV	13.3	20.3	8.0	15.6	8.6	9.2
Free Concentration (μm)					0.080	
% HSA Binding						30.1
% PC Binding	29.5	5.5	85.4	42.4		
Free Fraction (fu)	0.705	0.945	0.146	0.576		0.699
Dilution Factor (D)	10.6	5.3	3.5	5.3		
Free Fraction Undiluted in Tissues (fut)	0.184	0.764	0.046	0.204		
Volume of Distribution (Vdss)	3.801	0.914	15.157	3.430		
Mean Volume of Distribution (Vdss)	5.825					

Appendix 5 Back Calculated Calibration Standard Data and Associated Parameters for Acidic Series

Back Calculated Calibration Standard Data and Associated Parameters for Acidic Series

Calibration Standard Nominal Concentration (µM)												
Analytical Run	0.005	0.010	0.020	0.100	0.500	1.000	4.000	5.000		Slope	Intercept	Corr.Coeff.
CC16817	0.006 0.004	0.011 0.011	0.019 [0.025]	0.097 0.108	0.536 0.583	0.978 0.934	3.960 3.666	4.664 4.298		17.20	0.0279	0.9913
GR622550	0.005 0.005	0.008 0.010	0.017 [0.027]	0.083 [0.133]	0.460 0.628	0.903 1.206	4.132 [5.975]	5.263 [7.238]		4.46	0.0075	0.9862
GR87272	0.005	0.010	0.020	0.101	0.567	1.178	3.443	4.461		1.71	0.0021	0.9940
	0.005	0.010	0.022	0.107	0.486	0.961	3.704	4.338				
GR138714	0.005	0.011	0.024	0.094	0.564	0.968	3.789	5.665		1.21	0.0000	0.9932
	0.004	0.010	0.018	0.096	0.476	0.952	3.547	4.829				
GR70487	0.005	0.009	[0.012]	0.103	0.428	1.037	4.139	4.805		0.301	0.0006	0.9935
	[0.009]	[0.001]	0.018	0.089	0.529	[1.336]	4.498	5.778				
CCI120	0.005	[0.013]	0.019	0.091	0.497	1.092	3.903	5.199		9.30	0.0074	0.9965
	0.005	0.010	0.021	0.082	0.514	1.098	4.199	5.175				
GR33000	0.006	0.009	0.020	0.094	0.522	1.091	3.995	5.398		6.52	0.0024	0.9935
	0.004	0.009	0.017	0.102	0.518	1.056	3.781	4.835				
BRL15541	0.005	0.010	0.018	0.100	0.539	1.062	3.853	4.972		2.30	-0.0031	0.9922
	0.005	0.010	0.017	0.125	0.485	1.144	3.463	4.351				
GW289865X	0.004	0.010	0.022	0.108	0.559	0.985	3.304	4.192		1.39	0.0026	0.9879
	0.005	0.011	0.024	[0.163]	0.519	1.209	3.525	3.936				
SB213421	0.004	0.009	0.018	0.096	0.450	1.031	3.423	4.112		18.50	0.0075	0.9885
	0.005	0.012	0.024	0.117	0.547	1.149	4.030	4.317				
GI235401	0.005	[0.005]	0.016	0.093	0.552	0.991	4.131	5.118		0.10	0.0010	0.9952
	0.005	0.011	0.022	0.091	0.477	1.036	3.961	5.137				
GSK275458	[0.008]	0.008	0.023	0.094	0.483	1.014	3.916	4.782		0.41	0.0024	0.9903
	0.006	[0.015]	0.016	0.125	0.488	1.166	3.688	4.914				
GR77494	0.006	0.010	0.020	0.085	0.448	1.033	4.041	5.542		34.1	0.106	0.9929
	0.004	0.008	[0.013]	0.110	0.477	1.051	4.305	4.950				

GR118989	0.005	0.012	0.020	0.106	0.505	1.050	4.069	5.051		1.19	0.0011	0.9901
	0.005	0.008	[0.013]	0.122	0.406	1.095	3.625	4.118				
AH22182	0.005	0.011	0.023	0.112	0.622	1.130	4.432	5.612		3.39	0.0010	0.9856
	0.005	0.008	0.018	0.079	0.417	0.969	3.421	4.357				
GR87036	0.005	0.010	0.021	0.092	0.520	0.930	3.986	4.751		1.82	0.0033	0.9979
	0.005	0.011	0.020	0.094	0.536	0.994	3.967	5.229				
GW622791	0.005	0.011	0.020	0.091	0.555	1.090	3.365	4.917		1.42	0.0017	0.9945
	0.004	0.011	0.018	0.106	0.528	1.074	3.629	4.821				

Back Calculated Calibration Standard Data and Associated Parameters for Basic Series

Calibration Standard Nominal Concentration (µM)												
Analytical Run	0.005	0.010	0.020	0.100	0.500	1.000	4.000	5.000		Slope	Intercept	Corr.Coeff.
CCI13993	[0.017] [0.011]	0.010 [0.016]	0.021 0.019	0.089 0.113	0.509 0.545	0.920 1.109	3.696 4.230	4.344 4.993		0.786	0.0052	0.9957
SB73110	0.005 0.009	[0.015] [0.014]	0.020 0.022	0.086 0.091	0.546 0.625	0.804 0.934	4.146 4.309	4.810 5.225		3.18	0.0056	0.9916
CCI3748	0.005	0.009	0.019	0.092	0.496	0.978	4.029	4.637		0.738	0.0011	0.9934
	0.007	0.011	0.015	0.093	0.545	1.156	4.579	5.208				
GR30676	0.004	0.010	0.019	0.095	0.534	1.038	3.891	4.808		0.377	0.0001	0.9962
	0.006	0.009	[0.026]	0.100	0.543	0.994	4.051	4.958				
SKF95914	0.005	0.010	0.025	0.087	0.491	0.950	[6.714]	4.839		0.442	0.0003	0.9913
	0.005	0.011	0.019	0.089	0.493	0.992	4.962	4.591				
GR189721	[]	0.011	0.017	0.071	0.392	0.984	4.832	5.734		0.261	0.0022	0.9814
	[]	0.011	0.016	0.078	0.421	1.065	4.843	5.675				
GR43175	0.004	0.010	0.025	0.107	0.523	1.104	3.426	4.278		1.90	0.0019	0.9865
	0.005	0.012	0.022	0.101	0.495	0.988	3.050	[3.528]				
GF120454	0.006	0.009	0.016	[0.062]	0.530	0.782	4.058	5.116		1.04	0.0007	0.9845
	0.012	[0.009]	0.011	[0.071]	[0.585]	0.849	4.686	6.022				
GR99941	0.005	0.010	0.020	0.093	0.552	0.899	3.899	4.491		0.417	0.0005	0.9935
	0.006	[0.015]	0.018	0.095	0.619	1.053	4.237	4.961				
GW300671	0.000	0.011	0.016	0.096	0.604	0.960	4.150	4.857		0.346	0.0015	0.9941
	0.001	0.011	0.019	0.092	0.560	0.985	3.994	4.772				
SB461332	0.004	0.009	[0.014]	0.090	0.533	0.944	4.200	5.359		0.184	0.0002	0.9950
	0.006	0.012	0.019	0.096	0.522	0.979	3.848	5.088				
CC13839	0.006	0.010	0.018	0.090	0.564	0.997	4.105	4.902		0.368	0.0006	0.9942
	0.004	0.010	0.020	0.102	0.541	0.967	4.117	4.914				
GR61317	0.003	0.012	0.021	0.085	0.500	0.804	3.981	4.287		0.621	0.0005	0.9906
	0.004	0.016	0.023	0.104	0.566	0.906	4.365	5.437				
GW769340	0.005	0.009	0.018	0.115	0.550	0.858	3.610	4.592		3.94	0.0022	0.9931
	0.005	0.010	0.022	0.117	0.555	0.881	4.233	4.651				
CCI120557	0.006	0.011	0.021	0.109	0.506	0.857	3.952	4.639		2.43	0.0013	0.9942
	0.004	0.010	0.020	0.099	0.590	0.944	4.047	4.810				
CCI4001	0.005	0.009	0.024	0.093	0.540	0.914	3.929	4.913		2.42	0.0004	0.9950
	0.005	0.009	0.021	0.105	0.544	0.905	4.004	4.851				
GR84804	0.004	0.010	0.019	0.109	0.550	1.005	3.559	4.202		2.11	0.0001	0.9937

	0.005	0.011	0.022	0.108	0.512	1.070	3.733	4.312			
--	-------	-------	-------	-------	-------	-------	-------	-------	--	--	--

Back Calculated Calibration Standard Data and Associated Parameters for Neutral Series

Calibration Standard Nominal Concentration (µM)												
Analytical Run	0.005	0.010	0.020	0.100	0.500	1.000	4.000	5.000		Slope	Intercept	Corr.Coeff.
GR91295	0.005 0.009	0.009 0.014	0.016 0.022	0.094 0.120	0.489 0.582	0.852 1.175	3.393 4.039	4.303 5.556		26.7	0.1020	0.9889
CC19371	0.005 [0.015]	0.011 [0.074]	[0.042] [0.012]	0.091 0.111	0.514 [0.769]	1.298 0.749	5.059 3.318	4.592 4.177				
CC122428	0.001	0.016	0.018	0.088	0.528	0.965	4.192	4.760		2.90	0.0073	0.9945
	0.010	0.011	0.017	0.117	0.507	0.901	4.279	5.310				
GR104104	0.006	0.010	0.024	0.121	0.599	1.164	4.214	5.369		9.50	0.0007	0.9844
	0.004	0.009	0.018	0.089	0.411	0.829	3.730	3.868				
GR33914	0.004	0.010	0.022	0.094	0.503	1.065	3.706	4.681		2.75	0.0001	0.9946
	0.005	0.010	0.024	0.087	0.505	0.921	3.985	5.509				
GR38393	0.005	0.011	0.020	0.106	0.514	0.998	3.412	4.065		11.4	0.0053	0.9943
	0.005	0.009	0.019	0.108	0.569	1.110	4.012	4.601				
GW388185	0.006	[0.007]	0.024	0.102	0.504	0.884	4.504	5.554		2.16	0.0016	0.9909
	0.004	0.010	0.019	0.113	0.482	0.982	3.244	4.446				
GR119497	0.005	0.010	0.017	0.106	0.465	0.942	4.389	4.826		9.67	0.0041	0.9951
	0.005	0.010	0.018	0.087	0.471	1.096	4.434	5.644				
GW703803	0.005	0.010	0.016	0.099	0.541	1.035	3.911	4.462		9.15	0.0065	0.9922
	0.006	0.011	0.020	0.083	0.559	1.046	3.975	5.326				
GF120403	0.004	0.009	0.018	0.090	0.510	0.974	3.874	4.371		7.87	0.0025	0.9945
	0.006	0.010	0.021	0.101	0.567	1.056	4.106	5.400				
GR64334	0.005	0.010	0.021	0.095	0.500	1.067	4.260	4.902		1.29	0.0020	0.9935
	0.006	0.009	0.017	0.090	0.572	0.953	4.147	4.807				
GI116108	0.005	0.009	0.020	0.101	0.583	0.922	4.366	4.339		17.1	0.0042	0.9918
	0.005	0.011	0.019	0.079	0.484	1.119	4.134	4.987				
GI115674	0.004	0.012	0.024	0.109	0.571	0.952	3.377	4.023		2.71	0.0072	0.9834
	0.006	0.009	[0.026]	0.118	0.564	1.006	3.371	4.205				
AH23463	[0.000]	0.012	0.024	0.115	0.521	0.969	3.451	4.014		0.067	0.0003	0.9836
	0.004	0.008	0.025	0.118	0.508	0.889	3.589	4.231				
GR35842	[0.006*]	[0.009*]	0.021	0.093	0.468	1.038	4.248	5.267		0.179	0.0005	0.9981
	[No Peak*]	[0.010*]	0.020	0.090	0.535	0.981	3.975	5.012				

*low signal

Appendix 6

In-Vitro Pharmacokinetic Parameters of Acidic series using CRED Device for Mouse, Rat, Dog and Human Plasma in Parallel with RapidSep and Standard LC for Chromatographic Separation

Compound Number	GW622791 RapidSep					
	Mouse	Rat	Dog	Human	PC	1% PBS
Rep 1	1.770	3.160	1.990	2.010	1.830	0.114
Rep 2	1.830	3.050	2.100	2.050	2.020	0.134
Rep 3	1.890	3.040	2.490	2.090	1.860	0.141
Mean	1.8300	3.083	2.193	2.050	1.9033	0.12967
SD	0.060	0.067	0.263	0.040	0.102	0.014
%CV	3.3	2.2	12.0	2.0	5.4	10.8
Free Drug (peak area ratio)						0.130
% PPPB Binding	92.9	95.8	94.1	93.7	61.7	
Free Fraction (fu)	0.071	0.042	0.059	0.063	0.383	

Compound Number	GW622791 STD LC					
	Mouse	Rat	Dog	Human	PC	E1% PBS
Rep 1	7.180	11.200	8.270	8.630	0.860	0.758
Rep 2	8.200	12.500	8.190	8.600	0.995	0.714
Rep 3	8.080	13.300	10.000	8.550	0.929	0.717
Mean	7.8200	12.333	8.820	8.593	0.9280	0.72967
SD	0.557	1.060	1.023	0.040	0.068	0.025
%CV	7.1	8.6	11.6	0.5	7.3	3.4
Free Drug (peak area ratio)						0.730
% PPPB Binding	90.7	94.1	91.7	91.5	86.0	
Free Fraction (fu)	0.093	0.059	0.083	0.085	0.140	

Compound Number	GR118989 RapidSep					
	Mouse	Rat	Dog	Human	PC	1% PBS
Rep 1	0.624	1.44	0.495	1.48	0.117	0.106
Rep 2	0.703	1.47	0.470	1.51	0.140	0.116
Rep 3	0.686	1.52	0.586	1.55	0.137	0.113
Mean	0.6710	1.477	0.517	1.513	0.1313	0.1117
SD	0.042	0.040	0.061	0.035	0.008	0.007
%CV	6.2	2.7	11.8	2.3	0.01	0.01
Free Drug (peak area ratio)						0.112
% PPPB Binding	83.4	92.4	78.4	92.6	15.0	
Free Fraction (fu)	0.166	0.076	0.216	0.074	0.850	

Compound Number	GR118989 STD LC					
	Mouse	Rat	Do	Human	PC	1% PBS
Rep 1	0.307	0.53	0.194	0.566	0.0755	0.0494
Rep 2	0.321	0.586	0.18	0.569	0.0765	0.0319
Rep 3	0.293	0.603	0.23	0.55	0.0751	0.0329
Mean	0.3070	0.573	0.201	0.562	0.0757	0.0381
SD	0.014	0.038	0.026	0.010	0.008	0.007
%CV	4.6	6.7	12.8	1.8	0.01	0.01
Free Drug (peak area ratio)						0.380
% PPPB Binding	87.6	93.4	81.1	93.2	49.7	
Free Fraction (fu)	0.124	0.066	0.189	0.068	0.503	

Compound Number	AH22182 RapidSep					
	Mouse	Rat	Dog	Human	PC	1% PBS
Rep 1	0.595	0.667	0.305	0.499	0.225	0.024
Rep 2	0.610	0.666	0.323	0.576	0.273	0.028
Rep 3	0.661	0.696	0.338	0.599	0.243	0.026
Mean	0.6220	0.676	0.322	0.558	0.2470	0.0264
SD	0.035	0.017	0.017	0.052	0.008	0.007
%CV	5.6	2.5	5.1	9.4	0.01	0.01
Free Drug (peak area ratio)						0.026
% PPPB Binding	95.8	96.1	91.8	95.3	89.3	
Free Fraction (fu)	0.042	0.039	0.082	0.047	0.107	

Compound Number	AH22182 STD LC					
	Mouse	Rat	Dog	Human	PC	1% PBS
Rep 1	0.708	0.979	0.992	0.901	0.120	0.088
Rep 2	0.649	0.918	0.983	0.968	0.163	0.100
Rep 3	0.757	0.957	0.983	0.962	0.111	0.107
Mean	0.7047	0.951	0.986	0.944	0.1313	0.0984
SD	0.054	0.031	0.005	0.037	0.008	0.007
%CV	7.7	3.2	0.5	3.9	0.01	0.01
Free Drug (peak area ratio)						0.098
% PPPB Binding	86.0	89.7	90.0	89.6	25.1	
Free Fraction (fu)	0.140	0.103	0.100	0.104	0.749	

Compound Number	GR70487 RapidSep					
	Mouse	Rat	Dog	Human	PC	1% PBS
Rep 1	0.16	0.162	0.173	0.208	0.133	0.153
Rep 2	0.169	0.172	0.171	0.225	0.245	0.139
Rep 3	0.175	0.171	0.174	0.211	0.125	0.131
Mean	0.1680	0.168	0.173	0.215	0.168	0.141
SD	0.008	0.006	0.002	0.009	0.008	0.007
%CV	4.5	3.3	0.9	4.2	0.008	0.0
Free Drug (peak area ratio)						0.141
% PPPB Binding	16.1	16.2	18.3	34.3	15.9	
Free Fraction (fu)	0.839	0.838	0.817	0.657	0.841	

Compound Number	GR70487 STD LC					
	Mouse	Rat	Dog	Human	PC	1% PBS
Rep 1	0.0656	0.071	0.0658	0.080	0.128	0.054
Rep 2	0.0587	0.0697	0.0656	0.082	0.212	0.055
Rep 3	0.0711	0.066	0.0604	0.079	0.125	0.055
Mean	0.0651	0.069	0.064	0.080	0.155	0.055
SD	0.006	0.003	0.003	0.002	0.008	0.007
%CV	9.5	3.8	4.8	2.0	0.01	0.01
Free Drug (peak area ratio)						0.055
% PPPB Binding	16.0	20.6	14.4	31.5	64.7	
Free Fraction (fu)	0.840	0.794	0.856	0.685	0.353	

Compound Number	BRL15541 RapidSep					
	Mouse	Rat	Dog	Human	PC	1% PBS
Rep 1	0.273	0.757	0.612	0.939	0.135	0.107
Rep 2	0.446	0.741	0.43	0.942	0.143	0.123
Rep 3	0.353	0.874	0.557	0.925	0.126	0.0867
Mean	0.3573	0.791	0.533	0.935	0.1347	0.1057
SD	0.087	0.073	0.093	0.009	0.008	0.007
%CV	24.2	9.2	17.5	1.0	0.01	0.01
Free Drug (peak area ratio)						0.106
% PPPB Binding	70.5	86.6	80.2	88.7	21.6	
Free Fraction (fu)	0.295	0.134	0.198	0.113	0.784	

Compound Number	BRL15541 STD LC					
	Mouse	Rat	Dog	Human	PC	1% PBS
Rep 1	0.475	0.998	0.678	1.34	0.290	0.29
Rep 2	0.511	1.09	0.676	1.26	0.257	0.257
Rep 3	0.477	1.02	0.815	1.2	0.260	0.26
Mean	0.4877	1.036	0.723	1.267	0.2690	0.2690
SD	0.020	0.048	0.080	0.070	0.007	0.007
%CV	4.1	4.6	11.0	5.5	0.01	0.01
Free Drug (peak area ratio)						0.269
% PPPB Binding	56.7	79.6	70.8	83.3	21.6	
Free Fraction (fu)	0.433	0.204	0.292	0.167	0.784	

Compound Number	GR70487 RapidSep					
	Mouse	Rat	Dog	Human	PC	1% PBS
Rep 1	0.16	0.162	0.173	0.208	0.133	0.153
Rep 2	0.169	0.172	0.171	0.225	0.245	0.139
Rep 3	0.175	0.171	0.174	0.211	0.125	0.131
Mean	0.1680	0.168	0.173	0.215	0.168	0.141
SD	0.008	0.006	0.002	0.009	0.008	0.007
%CV	4.5	3.3	0.9	4.2	0.008	0.0
Free Drug (peak area ratio)						0.141
% PPPB Binding	16.1	16.2	18.3	34.3	15.9	
Free Fraction (fu)	0.839	0.838	0.817	0.657	0.841	

Compound Number	GR70487 STD LC					
	Mouse	Rat	Dog	Human	PC	1% PBS
Rep 1	0.0656	0.071	0.0658	0.080	0.128	0.054
Rep 2	0.0587	0.0697	0.0656	0.082	0.212	0.055
Rep 3	0.0711	0.066	0.0604	0.079	0.125	0.055
Mean	0.0651	0.069	0.064	0.080	0.155	0.055
SD	0.006	0.003	0.003	0.002	0.008	0.007
%CV	9.5	3.8	4.8	2.0	0.01	0.01
Free Drug (peak area ratio)						0.055
% PPPB Binding	16.0	20.6	14.4	31.5	64.7	
Free Fraction (fu)	0.840	0.794	0.856	0.685	0.353	

Compound Number		CCI120 RapidSep				
	Mouse	Rat	Dog	Human	PC	1% PBS
Rep 1	0.1890	0.2200	0.215	0.250	0.096	0.009
Rep 2	0.1720	0.2320	0.189	0.243	0.107	0.010
Rep 3	0.2000	0.2490	0.193	0.212	0.073	0.011
Mean	0.1870	0.234	0.199	0.235	0.092	0.010
SD	0.014	0.015	0.014	0.020	0.017	0.001
%CV	7.5	6.2	7.0	8.6	18.8	9.6
Free Drug (peak area ratio)						0.010
% PPPB Binding	94.6	95.7	94.9	95.7	89.0	
Free Fraction (fu)	0.054	0.043	0.051	0.043	0.110	

Compound Number		CCI120 STD LC				
	Mouse	Rat	Dog	Human	PC	1% PBS
Rep 1	2.0300	2.0100	1.120	1.940	0.142	0.117
Rep 2	2.3000	2.2000	1.010	1.920	0.167	0.098
Rep 3	2.2400	2.4200	1.340	1.850	0.130	0.101
Mean	2.1900	2.210	1.157	1.903	0.146	0.105
SD	0.142	0.205	0.168	0.047	0.019	0.010
%CV	6.5	9.3	14.5	2.5	12.9	9.8
Free Drug (peak area ratio)						05
% PPPB Binding	95.2	95.2	90.9	94.5	28.1	
Free Fraction (fu)	0.048	0.048	0.091	0.055	0.719	

Compound Number	GR87036 RapidSep					
	Mouse	Rat	Dog	Human	PC	1% PBS
Rep 1	0.0514	0.0944	0.046	0.149	0.017	0.014
Rep 2	0.0487	0.1000	0.061	0.179	0.038	0.017
Rep 3	0.0441	0.0937	0.050	0.155	0.022	0.015
Mean	0.0481	0.096	0.052	0.161	0.026	0.015
SD	0.004	0.003	0.008	0.016	0.011	0.002
%CV	7.7	3.6	15.0	9.9	42.2	12.6
Free Drug (peak area ratio)						0.015
% PPPB Binding	94.6	95.7	94.9	95.7	41.2	
Free Fraction (fu)	0.054	0.043	0.051	0.043	0.588	

Compound Number	GR87036 STD LC					
	Mouse	Rat	Dog	Human	PC	1% PBS
Rep 1	0.0824	0.1890	0.095	0.260	0.071	0.049
Rep 2	0.0843	0.1840	0.088	0.292	0.094	0.044
Rep 3	0.0829	0.1760	0.090	0.262	0.070	0.047
Mean	0.0832	0.183	0.091	0.271	0.078	0.046
SD	0.001	0.007	0.003	0.018	0.014	0.002
%CV	1.2	3.6	3.5	6.6	17.471	4.775
Free Drug (peak area ratio)						0.046
% PPPB Binding	44.2	74.6	48.9	82.9	40.5	
Free Fraction (fu)	0.558	0.254	0.511	0.171	0.595	

Compound Number	GI235401 RapidSep					
	Mouse	Rat	Dog	Human	PC	1% PBS
Rep 1	0.482	0.596	0.679	0.715	0.129	0.024
Rep 2	0.503	0.678	0.646	0.779	0.178	0.021
Rep 3	0.588	0.658	0.630	0.742	0.112	0.019
Mean	0.5243	0.644	0.652	0.745	0.140	0.021
SD	0.056	0.043	0.025	0.032	0.034	0.002
%CV	10.7	6.6	3.8	4.3	24.5	11.2
Free Drug (peak area ratio)						0.021
% PPPB Binding	95.9	96.7	96.7	97.1	84.7	
Free Fraction (fu)	0.041	0.033	0.033	0.029	0.153	

Compound Number	GI235401 STD LC					
	Mouse	Rat	Dog	Human	PC	1% PBS
Rep 1	1.390	2.020	1.910	2.000	0.116	0.064
Rep 2	1.330	1.970	1.900	2.230	0.207	0.058
Rep 3	1.360	1.910	1.880	2.130	0.108	0.055
Mean	1.3600	1.967	1.897	2.120	0.144	0.059
SD	0.030	0.055	0.015	0.115	0.055	0.004
%CV	2.2	2.8	0.8	5.4	38.3	7.4
Free Drug (peak area ratio)						0.059
% PPPB Binding	95.7	97.0	96.9	97.2	58.9	
Free Fraction (fu)	0.043	0.030	0.031	0.028	0.411	

In-Vitro Pharmacokinetic Parameters of Basic series using CRED Device for Mouse, Rat, Dog and Human Plasma in Parallel with RapidSep and Standard LC for Chromatographic Separation

Compound Number	SB731710 RapidSep				
	Mouse	Rat	Dog	Human	1% PBS
Rep 1	0.656	0.658	0.636	0.613	0.235
Rep 2	0.668	0.639	0.680	0.658	0.205
Rep 3	0.704	0.697	0.691	0.620	0.253
Mean	0.6760	0.665	0.669	0.630	0.23100
SD	0.025	0.030	0.029	0.024	0.024
%CV	3.7	4.4	4.4	3.8	10.5
Free Drug (peak area ratio)					0.231
% PPPB Binding	65.8	65.2	65.5	63.4	
Free Fraction (fu)	0.342	0.348	0.345	0.366	

Compound Number	SB731710 STD LC				
	Mouse	Rat	Dog	Human	1% PBS
Rep 1	0.342	0.344	0.320	0.316	0.084
Rep 2	0.344	0.348	0.330	0.315	0.087
Rep 3	0.346	0.359	0.339	0.314	0.085
Mean	0.3440	0.350	0.330	0.315	0.08537
SD	0.002	0.008	0.010	0.001	0.002
%CV	0.6	2.2	2.9	0.3	1.9
Free Drug (peak area ratio)					0.085
% PPPB Binding	75.2	75.6	74.1	72.9	
Free Fraction (fu)	0.248	0.244	0.259	0.271	

Compound Number	SB416332 RapidSep				
	Mouse	Rat	Dog	Human	1% PBS
Rep 1	1.6600	1.7400	1.890	1.780	1.18000
Rep 2	1.6900	1.8400	2.010	1.820	1.24000
Rep 3	1.8600	2.0100	1.970	1.670	1.19000
Mean	1.7367	1.863	1.957	1.757	1.20333
SD	0.108	0.137	0.061	0.078	0.032
%CV	6.2	7.3	3.1	4.4	2.7
Free Drug (peak area ratio)					1.203
% PPPB Binding	30.7	35.4	38.5	31.5	
Free Fraction (fu)	0.693	0.646	0.615	0.685	

Compound Number	SB416332 STD LC				
	Mouse	Rat	Dog	Human	1% PBS
Rep 1	0.0394	0.0424	0.0396	0.0453	0.0295
Rep 2	0.0368	0.0419	0.0488	0.0426	0.0282
Rep 3	0.0460	0.0429	0.0412	0.0401	0.0344
Mean	0.0407	0.042	0.043	0.043	0.03070
SD	0.005	0.001	0.005	0.003	0.003
%CV	11.6	1.2	11.4	6.1	10.7
Free Drug (peak area ratio)					0.301
% PPPB Binding	24.6	27.6	28.9	28.0	
Free Fraction (fu)	0.754	0.724	0.711	0.720	

Compound Number	CCI3748 RapidSep				
	Mouse	Rat	Dog	Human	1% PBS
Rep 1	8.180	7.560	8.710	8.190	0.950
Rep 2	8.490	7.790	9.110	8.750	1.000
Rep 3	8.880	8.240	9.190	8.400	0.929
Mean	8.5167	7.863	9.003	8.447	0.95967
SD	0.351	0.346	0.257	0.283	0.036
%CV	4.1	4.4	2.9	3.3	3.8
Free Drug (peak area ratio)					0.96
% PPPB Binding	88.7	87.8	89.3	88.6	
Free Fraction (fu)	0.113	0.122	0.107	0.114	

Compound Number	CCI3748 STD LC				
	Mouse	Rat	Dog	Human	1% PBS
Rep 1	3.76	3.53	3.91	3.56	0.282
Rep 2	3.75	3.52	3.9	3.63	0.28
Rep 3	3.67	3.57	3.94	3.63	0.283
Mean	3.7267	3.540	3.917	3.607	0.28167
SD	0.049	0.026	0.021	0.040	0.002
%CV	1.3	0.7	0.5	1.1	0.5
Free Drug (peak area ratio)					0.282
% PPPB Binding	92.4	92.0	92.8	92.2	
Free Fraction (fu)	0.076	0.080	0.072	0.078	

Compound Number	CCI4001 RapidSep				
	Mouse	Rat	Dog	Human	1% PBS
Rep 1	0.184	0.314	0.228	0.0863	0.040
Rep 2	0.188	0.254	0.215	0.0995	0.028
Rep 3	0.197	0.224	0.258	0.093	0.036
Mean	0.1897	0.264	0.234	0.093	0.03463
SD	0.007	0.046	0.022	0.007	0.006
%CV	3.5	17.4	9.4	7.1	16.6
Free Drug (peak area ratio)					0.035
% PPPB Binding	81.7	86.9	85.2	62.7	
Free Fraction (fu)	0.183	0.131	0.148	0.373	

Compound Number	CCI4001 STD LC				
	Mouse	Rat	Dog	Human	1% PBS
Rep 1	0.281	0.453	0.416	0.2	0.067
Rep 2	0.275	0.468	0.421	0.205	0.0692
Rep 3	0.275	0.474	0.425	0.209	0.07
Mean	0.2770	0.465	0.421	0.205	0.06873
SD	0.003	0.011	0.005	0.005	0.002
%CV	1.3	2.3	1.1	2.2	2.3
Free Drug (peak area ratio)					0.069
% PPPB Binding	75.2	85.2	83.7	66.4	
Free Fraction (fu)	0.248	0.148	0.163	0.336	

Compound Number	CCI3993 RapidSep				
	Mouse	Rat	Dog	Human	1% PBS
Rep 1	0.7320	0.7470	0.669	0.687	0.03540
Rep 2	0.7740	0.7710	0.682	0.691	0.04140
Rep 3	0.6890	0.6560	0.774	0.717	0.04080
Mean	0.7317	0.725	0.708	0.698	0.03920
SD	0.043	0.061	0.057	0.016	0.003
%CV	5.8	8.4	8.1	2.3	8.4
Free Drug (peak area ratio)					0.03920
% PPPB Binding	94.6	94.6	94.5	94.4	
Free Fraction (fu)	0.054	0.054	0.055	0.056	

Compound Number	CCI3993 STD LC				
	Mouse	Rat	Dog	Human	1% PBS
Rep 1	0.3640	0.3520	0.381	0.375	0.01430
Rep 2	0.3730	0.3500	0.394	0.376	0.01420
Rep 3	0.3750	0.3410	0.406	0.363	0.01320
Mean	0.3707	0.348	0.394	0.371	0.01390
SD	0.006	0.006	0.013	0.007	0.001
%CV	1.6	1.7	3.2	1.9	4.4
Free Drug (peak area ratio)					0.014
% PPPB Binding	96.3	96.0	96.5	96.3	
Free Fraction (fu)	0.038	0.040	0.035	0.037	

Compound Number	GR84804 RapidSep				
	Mouse	Rat	Dog	Human	1% PBS
Rep 1	2.1400	2.1400	1.380	0.902	0.10200
Rep 2	2.2800	2.2800	1.390	0.929	0.09610
Rep 3	2.0000	2.0000	1.650	0.939	0.09130
Mean	2.1400	2.140	1.473	0.923	0.09647
SD	0.140	0.140	0.153	0.019	0.005
%CV	6.5	6.5	10.4	2.1	5.6
Free Drug (peak area ratio)					0.096
% PPPB Binding	95.5	95.5	93.5	89.6	
Free Fraction (fu)	0.045	0.045	0.065	0.104	

Compound Number	GR84804 STD LC				
	Mouse	Rat	Dog	Human	1% PBS
Rep 1	1.3900	1.3900	1.160	0.708	0.05400
Rep 2	1.4200	1.4000	1.180	0.749	0.05170
Rep 3	1.4100	1.3600	1.200	0.705	0.05070
Mean	1.4067	1.383	1.180	0.721	0.05213
SD	0.015	0.021	0.020	0.025	0.002
%CV	1.1	1.5	1.7	3.4	3.2
Free Drug (peak area ratio)					0.052
% PPPB Binding	96.3	96.2	95.6	92.8	
Free Fraction (fu)	0.037	0.038	0.044	0.072	

Compound Number	CC13839 RapidSep				
	Mouse	Rat	Dog	Human	1% PBS
Rep 1	7.2400	5.8500	6.090	7.480	1.76000
Rep 2	7.5800	6.4900	6.310	7.680	1.77000
Rep 3	6.2900	5.3000	7.400	8.230	1.82000
Mean	7.0367	5.880	6.600	7.797	1.78333
SD	0.669	0.596	0.701	0.388	0.032
%CV	9.5	10.1	10.6	5.0	1.8
Free Drug (peak area ratio)					1.783
% PPPB Binding	74.7	69.7	73.0	77.1	
Free Fraction (fu)	0.253	0.303	0.270	0.229	

Compound Number	CC13839 STD LCp				
	Mouse	Rat	Dog	Human	1% PBS
Rep 1	3.0400	3.0100	3.100	3.950	0.76700
Rep 2	2.9900	3.0000	3.190	4.050	0.75700
Rep 3	3.0900	2.9000	3.270	3.850	0.72200
Mean	3.0400	2.970	3.187	3.950	0.74867
SD	0.050	0.061	0.085	0.100	0.024
%CV	1.6	2.0	2.7	2.5	3.2
Free Drug (peak area ratio)					0.749
% PPPB Binding	75.4	74.8	76.5	81.0	
Free Fraction (fu)	0.246	0.252	0.235	0.190	

Compound Number	CCI120557A RapidSep				
	Mouse	Rat	Dog	Human	1% PBS
Rep 1	14.4000	18.1000	13.000	14.300	1.67000
Rep 2	14.7000	19.1000	13.700	14.900	1.73000
Rep 3	14.3000	16.9000	15.100	14.900	1.59000
Mean	14.4667	18.033	13.933	14.700	1.66333
SD	0.208	1.102	1.069	0.346	0.070
%CV	1.4	6.1	7.7	2.4	4.2
Free Drug (peak area ratio)					1.663
% PPPB Binding	88.5	90.8	88.1	88.7	
Free Fraction (fu)	0.115	0.092	0.119	0.113	

Compound Number	CCI120557A STD LC				
	Mouse	Rat	Dog	Human	1% PBS
Rep 1	7.3800	10.0000	7.890	8.560	0.96500
Rep 2	7.4800	9.8100	8.210	8.930	0.98200
Rep 3	7.7300	9.8400	8.330	8.480	0.97400
Mean	7.5300	9.883	8.143	8.657	0.97367
SD	0.180	0.102	0.227	0.240	0.009
%CV	2.4	1.0	2.8	2.8	0.9
Free Drug (peak area ratio)					0.974
% PPPB Binding	87.1	90.1	88.0	88.8	
Free Fraction (fu)	0.129	0.099	0.120	0.112	

In-Vitro Pharmacokinetic Parameters of Neutral series using CRED Device for Mouse, Rat, Dog and Human Plasma in Parallel with RapidSep and Standard LC for Chromatographic Separation

Compound Number	GR91295 Rapid Sep				
	Mouse	Rat	Dog	Human	1% PBS
Rep 1	[#DIV/0]	0.758	0.749	[#DIV/0]	0.695
Rep 2	0.868	0.776	0.830	0.796	0.744
Rep 3	0.843	[#DIV/0]	0.822	0.758	[#DIV/0]
Mean	0.8555	0.767	0.800	0.777	0.71950
SD	0.018	0.013	0.045	0.027	0.035
%CV	2.1	1.7	5.6	3.5	4.8
Free Drug (peak area ratio)					0.720
% PPPB Binding	15.9	6.2	10.1	7.4	
Free Fraction (fu)	0.841	0.938	0.899	0.926	

Compound Number	GR91295 STD LC				
	Mouse	Rat	Dog	Human	1% PBS
Rep 1	0.435	0.436	0.452	0.494	[0.558]
Rep 2	0.439	0.429	0.475	0.467	0.432
Rep 3	0.458	0.461	0.487	0.462	0.433
Mean	0.4440	0.442	0.471	0.474	0.43250
SD	0.012	0.017	0.018	0.017	0.001
%CV	2.8	3.8	3.8	3.6	0.2
Free Drug (peak area ratio)					0.433
% PPPB Binding	2.6	2.1	8.2	8.8	
Free Fraction (fu)	0.974	0.979	0.918	0.912	

Compound Number	CCI22428 RapidSep				
	Mouse	Rat	Dog	Human	1% PBS
Rep 1	[#DIV/0!]	0.0473	0.0252	[#DIV/0!]	0.0114
Rep 2	0.0366	0.0337	0.0300	0.045	0.0198
Rep 3	0.0398	[#DIV/0!]	0.0243	0.0374	[#DIV/0!]
Mean	0.0382	0.041	0.027	0.041	0.01560
SD	0.002	0.010	0.003	0.005	0.006
%CV	5.9	23.7	11.6	13.0	38.1
Free Drug (peak area ratio)					0.016
% PPPB Binding	59.2	61.5	41.1	62.1	
Free Fraction (fu)	0.408	0.385	0.589	0.379	

Compound Number	CCI22428 STD LC				
	Mouse	Rat	Dog	Human	1% PBS
Rep 1	0.0818	0.0931	0.0884	0.0968	0.026
Rep 2	0.0825	0.0994	0.0945	0.0957	0.0561
Rep 3	0.086	0.106	0.1010	0.093	0.0477
Mean	0.0834	0.100	0.095	0.095	0.04327
SD	0.002	0.006	0.006	0.002	0.016
%CV	2.7	6.5	6.7	2.1	35.9
Free Drug (peak area ratio)					0.043
% PPPB Binding	48.1	56.5	54.3	54.5	
Free Fraction (fu)	0.519	0.435	0.457	0.455	

Compound Number	GF120403 RapidSep				
	Mouse	Rat	Dog	Human	1% PBS
Rep 1	[#DIV/0!]	0.566	0.363	[#DIV/0!]	0.153
Rep 2	0.712	0.544	0.418	1.03	0.163
Rep 3	0.723	[#DIV/0!]	0.404	0.99	[#DIV/0!]
Mean	0.7175	0.555	0.395	1.010	0.15800
SD	0.008	0.016	0.029	0.028	0.007
%CV	1.1	2.8	7.2	2.8	4.5
Free Drug (peak area ratio)					0.158
% PPPB Binding	78.0	71.5	60.0	84.4	
Free Fraction (fu)	0.220	0.285	0.400	0.156	

Compound Number	GF120403 STD LC				
	Mouse	Rat	Dog	Human	1% PBS
Rep 1	0.748	0.591	0.432	0.44	0.227
Rep 2	0.734	0.592	0.466	0.453	0.175
Rep 3	0.753	0.601	0.471	0.432	0.179
Mean	0.7450	0.595	0.456	0.442	0.19367
SD	0.010	0.006	0.021	0.011	0.029
%CV	1.3	0.9	4.7	2.4	14.9
Free Drug (peak area ratio)					0.194
% PPPB Binding	74.0	67.4	57.6	56.2	
Free Fraction (fu)	0.260	0.326	0.424	0.438	

Compound Number	GR33914 RapidSep				
	Mouse	Rat	Dog	Human	1% PBS
Rep 1	5.01	4.46	5.98	4.5700	0.509
Rep 2	[#DIV/0!]	5.89	7.09	5.0900	0.644
Rep 3	4.74	6.67	6.54	4.7500	[#DIV/0!]
Mean	4.8750	5.673	6.537	4.803	0.57650
SD	0.191	1.121	0.555	0.264	0.095
%CV	3.9	19.8	8.5	5.5	16.6
Free Drug (peak area ratio)					0.577
% PPPB Binding	88.2	89.8	91.2	88.0	
Free Fraction (fu)	0.118	0.102	0.088	0.120	

Compound Number	GR33914 STD LC				
	Mouse	Rat	Dog	Human	1% PBS
Rep 1	2.57	[#DIV/0!]	3.5	2.8500	0.296
Rep 2	2.84	3.35	3.63	2.9800	0.336
Rep 3	3.17	3.04	3.05	3.0100	0.355
Mean	2.8600	3.195	3.393	2.947	0.32900
SD	0.300	0.219	0.304	0.085	0.030
%CV	10.5	6.9	9.0	2.9	9.2
Free Drug (peak area ratio)					0.329
% PPPB Binding	88.5	89.7	90.3	88.8	
Free Fraction (fu)	0.115	0.103	0.097	0.112	

Compound Number	GI116108 RapidSep				
	Mouse	Rat	Dog	Human	1% PBS
Rep 1	3.76	3.76	4.03	4.07	0.357
Rep 2	[#DIV/0!]	4.28	4.96	4.16	0.347
Rep 3	3.45	5.18	4.65	4.61	[#DIV/0!]
Mean	3.6050	4.407	4.547	4.280	0.35200
SD	0.219	0.718	0.474	0.289	0.007
%CV	6.1	16.3	10.4	6.8	2.0
Free Drug (peak area ratio)					0.352
% PPPB Binding	90.2	92.0	92.3	91.8	
Free Fraction (fu)	0.098	0.080	0.077	0.082	

Compound Number	GI116108 STD LC				
	Mouse	Rat	Dog	Human	1% PBS
Rep 1	2.23	[#DIV/0!]	2.42	2.17	0.189
Rep 2	2.21	2.63	2.58	2.28	0.212
Rep 3	2.26	2.55	2.22	2.3	0.221
Mean	2.2333	2.590	2.407	2.250	0.20733
SD	0.025	0.057	0.180	0.070	0.017
%CV	1.1	2.2	7.5	3.1	8.0
Free Drug (peak area ratio)					0.207
% PPPB Binding	90.7	92.0	91.4	90.8	
Free Fraction (fu)	0.093	0.080	0.086	0.092	

Compound Number	GR119497 RapidSep				
	Mouse	Rat	Dog	Human	1% PBS
Rep 1	0.377	0.298	0.394	0.475	0.194
Rep 2	[#DIV/0!]	0.324	0.516	0.405	0.203
Rep 3	0.388	0.406	0.447	0.439	[#DIV/0!]
Mean	0.3825	0.343	0.452	0.440	0.19850
SD	0.008	0.056	0.061	0.035	0.006
%CV	2.0	16.4	13.5	8.0	3.2
Free Drug (peak area ratio)					0.199
% PPPB Binding	48.1	42.1	56.1	54.9	
Free Fraction (fu)	0.519	0.579	0.439	0.451	

Compound Number	GR119497 STD LC				
	Mouse	Rat	Dog	Human	1% PBS
Rep 1	0.816	[#DIV/0!]	0.832	0.884	0.34
Rep 2	0.772	0.839	0.842	0.871	0.392
Rep 3	0.709	0.737	0.832	0.844	0.399
Mean	0.7657	0.788	0.835	0.866	0.37700
SD	0.054	0.072	0.006	0.020	0.032
%CV	7.0	9.2	0.7	2.4	8.6
Free Drug (peak area ratio)					0.377
% PPPB Binding	50.8	52.2	54.9	56.5	
Free Fraction (fu)	0.492	0.478	0.451	0.435	

Compound Number	GR38393 STD LC				
	Mouse	Rat	Dog	Human	1% PBS
Rep 1	19.5	19.5	21.6	21.4	3.45
Rep 2	[#DIV/0!]	22.6	25.3	21.7	3.53
Rep 3	17.6	25.6	25.2	25	[#DIV/0!]
Mean	18.5500	22.567	24.033	22.700	3.49000
SD	1.344	3.050	2.108	1.997	0.057
%CV	7.2	13.5	8.8	8.8	1.6
Free Drug (peak area ratio)					3.49
% PPPB Binding	81.2	84.5	85.5	84.6	
Free Fraction (fu)	0.188	0.155	0.145	0.154	

Compound Number	GR38393 STD LC				
	Mouse	Rat	Dog	Human	1% PBS
Rep 1	9.78	[#DIV/0!]	11.5	10	1.56
Rep 2	10.1	12.4	12.1	10.7	1.72
Rep 3	10.2	11.2	10.4	10.9	1.72
Mean	10.0267	11.800	11.333	10.533	1.66667
SD	0.219	0.849	0.862	0.473	0.092
%CV	2.2	7.2	7.6	4.5	5.5
Free Drug (peak area ratio)					1.667
% PPPB Binding	83.4	85.9	85.3	84.2	
Free Fraction (fu)	0.166	0.141	0.147	0.158	

References

- Acocella, G. J. C. p. (1978). "Clinical pharmacokinetics of rifampicin." **3**(2): 108-127.
- Asano, H., et al. (1993). "Effects of sodium glycocholate and sodium taurocholate on the mixed micelles of bile salts and nonionic surfactant." Journal of the American Oil Chemists' Society **70**(7): 693-697.
- Ascenzi, P., et al. (2015). "Heme-based catalytic properties of human serum albumin." Cell death discovery **1**: 15025.
- Ballard, P., et al. (2012). "The right compound in the right assay at the right time: an integrated discovery DMPK strategy." Drug metabolism reviews **44**(3): 224-252.
- Banker, M. J., et al. (2003). "Development and validation of a 96-well equilibrium dialysis apparatus for measuring plasma protein binding." Journal of Pharmaceutical Sciences **92**(5): 967-974.
- Basavaraj, S. and G. V. J. A. P. S. B. Betageri (2014). "Can formulation and drug delivery reduce attrition during drug discovery and development—review of feasibility, benefits and challenges." **4**(1): 3-17.
- Bito, L., et al. (1966). "The concentrations of free amino acids and other electrolytes in cerebrospinal fluid, in vivo dialysate of brain, and blood plasma of the dog." Journal of neurochemistry **13**(11): 1057-1067.
- Bohnert, T. and L.-S. Gan (2013). "Plasma protein binding: From discovery to development." Journal of Pharmaceutical Sciences **102**(9): 2953-2994.
- Bourne, J. A. (2003). "Intracerebral microdialysis: 30 years as a tool for the neuroscientist." Clinical and Experimental Pharmacology and Physiology **30**(1-2): 16-24.
- Buchanan, N. and C. Eyberg (1974). "Equilibrium dialysis." South African medical journal = Suid-Afrikaanse tydskrif vir geneeskunde **48**(44): 1867-1869.
- Bulbake, U., et al. (2017). "Liposomal formulations in clinical use: an updated review." Pharmaceutics **9**(2): 12.
- Buscher, B., et al. (2014). "Bioanalysis for plasma protein binding studies in drug discovery and drug development: views and recommendations of the European Bioanalysis Forum." Bioanalysis **6**(5): 673-682.

Butler, J. M. and E. J. J. C. p. Begg (2008). "Free drug metabolic clearance in elderly people." **47**(5): 297-321.

Charrois, G. J. and T. M. Allen (2004). "Drug release rate influences the pharmacokinetics, biodistribution, therapeutic activity, and toxicity of pegylated liposomal doxorubicin formulations in murine breast cancer." Biochimica et Biophysica Acta (BBA)-Biomembranes **1663**(1-2): 167-177.

Chefer, V. I., et al. (2001). Overview of Brain Microdialysis. Current Protocols in Neuroscience, John Wiley & Sons, Inc.

Choi, J., et al. (2018). "Comprehensive analysis of phospholipids in the brain, heart, kidney, and liver: brain phospholipids are least enriched with polyunsaturated fatty acids." **442**(1-2): 187-201.

Christie, W. W. (1985). "Rapid separation and quantification of lipid classes by high performance liquid chromatography and mass (light-scattering) detection." Journal of Lipid Research **26**(4): 507-512.

Colclough, N., et al. (2014). "Species differences in drug plasma protein binding." MedChemComm **5**(7): 963-967.

Cook, D., et al. (2014). "Lessons learned from the fate of AstraZeneca's drug pipeline: a five-dimensional framework." Nature reviews Drug discovery **13**(6): 419-431.

Curry, S. (2002). "Beyond Expansion: Structural Studies on the Transport Roles of Human Serum Albumin." Vox Sanguinis **83**: 315-319.

Dickstein, K., et al. (1987). "The pharmacokinetics of enalapril in hospitalized patients with congestive heart failure." **23**(4): 403-410.

Dimitrova, M. N., et al. (2000). "Interaction of albumins from different species with phospholipid liposomes. Multiple binding sites system." **27**(3): 187-194.

Dowhan, W. (1994). Role of Phospholipids in Cell Function. Biological Membranes: Structure, Biogenesis and Dynamics. J. A. F. Op den Kamp. Berlin, Heidelberg, Springer Berlin Heidelberg: 1-21.

Du Souich, P., et al. (1993). "Plasma protein binding and pharmacological response." **24**(6): 435-440.

Dua, J., et al. (2012). "Liposome: methods of preparation and applications." Int J Pharm Stud Res **3**(2): 14-20.

Fan, Y. and Q. Zhang (2013). "Development of liposomal formulations: From concept to clinical investigations." Asian Journal of Pharmaceutical Sciences **8**(2): 81-87.

Fasano, M., et al. (2005). "The extraordinary ligand binding properties of human serum albumin." IUBMB Life **57**(12): 787-796.

Ghuman, J., et al. (2005). "Structural Basis of the Drug-binding Specificity of Human Serum Albumin." Journal of Molecular Biology **353**(1): 38-52.

Ghuman, J., et al. (2005). "Structural basis of the drug-binding specificity of human serum albumin." **353**(1): 38-52.

Giacomini, K. M., et al. (2010). "Membrane transporters in drug development." **9**(3): 215.

Gleeson, M. P. J. J. o. m. c. (2008). "Generation of a set of simple, interpretable ADMET rules of thumb." **51**(4): 817-834.

Gross, A. S., et al. (1988). "Stereoselective protein binding of verapamil enantiomers." Biochemical pharmacology **37**(24): 4623-4627.

Hashimoto, S. and A. J. C. p. Kobayashi (2003). "Clinical pharmacokinetics and pharmacodynamics of glyceryl trinitrate and its metabolites." **42**(3): 205-221.

Hausken, T., et al. (1998). "Estimation of the human liver volume and configuration using three-dimensional ultrasonography: effect of a high-caloric liquid meal." Ultrasound in Medicine & Biology **24**(9): 1357-1367.

Hood, B., et al. (1961). "Cholesterol and Phospholipid Levels in Human Liver and Muscle in Relation to the Serum Cholesterol Level." Acta Medica Scandinavica **169**(6): 707-712.

Jeffrey, P. and S. Summerfield (2007). "Challenges for blood–brain barrier (BBB) screening." Xenobiotica **37**(10-11): 1135-1151.

Jeffrey, P. and S. Summerfield (2010). "Assessment of the blood-brain barrier in CNS drug discovery." Neurobiology of disease **37**(1): 33-37.

Jessome, L. L. and D. A. Volmer (2006). "Ion suppression: a major concern in mass spectrometry." Lc Gc North America **24**(5): 498.

Joukhadar, C. and M. Müller (2005). "Microdialysis." Clinical Pharmacokinetics **44**(9): 895-913.

Kalvass, J. C., et al. (2007). "Use of Plasma and Brain Unbound Fractions to Assess the Extent of Brain Distribution of 34 Drugs: Comparison of Unbound Concentration Ratios to in Vivo P-Glycoprotein Efflux Ratios." Drug Metabolism and Disposition **35**(4): 660-666.

Klotz, U. J. C. p. (1976). "Pathophysiological and disease-induced changes in drug distribution volume: pharmacokinetic implications." **1**(3): 204-218.

Kola, I. (2008). "The state of innovation in drug development." Clinical Pharmacology & Therapeutics **83**(2): 227-230.

Kratochwil, N. A., et al. (2002). "Predicting plasma protein binding of drugs: a new approach." **64**(9): 1355-1374.

Kraus, V. B. (2018). "Biomarkers as drug development tools: discovery, validation, qualification and use." Nature Reviews Rheumatology **14**(6): 354-362.

Krishna, S. and N. J. White (1996). "Pharmacokinetics of Quinine, Chloroquine and Amodiaquine." Clinical Pharmacokinetics **30**(4): 263-299.

Malaria is associated with a reduction in the systemic clearance and apparent volume of distribution of the cinchona alkaloids; this reduction is proportional to the disease severity. There is increased plasma protein binding, predominantly to α 1-acid glycoprotein, and elimination half-lives (in healthy adults quinine $t_{1/2}$ = 11 hours, quinidine $t_{1/2}$ =8 hours) are prolonged by 50%. Systemic clearance is predominantly by hepatic biotransformation to more polar metabolites (quinine 80%, quinidine 65%) and the remaining drug is eliminated unchanged by the kidney. Quinine is well absorbed by mouth or following intramuscular injection even in severe cases of malaria (estimated bioavailability more than 85%). Quinine and chloroquine may cause potentially lethal hypotension if given by intravenous injection.

Lee, K.-J., et al. (2003). "Modulation of Nonspecific Binding in Ultrafiltration Protein Binding Studies." Pharmaceutical Research **20**(7): 1015-1021.

Purpose. The aim of this study was to reduce or prevent nonspecific binding (NSB) of compounds to ultrafiltration (UF) protein binding (PB) testing units.

Li, J., et al. (2015). "A review on phospholipids and their main applications in drug delivery systems." Asian Journal of Pharmaceutical Sciences **10**(2): 81-98.

Li, J., et al. (2015). "A review on phospholipids and their main applications in drug delivery systems." **10**(2): 81-98.

Lobell, M. and V. J. M. d. Sivarajah (2003). "In silico prediction of aqueous solubility, human plasma protein binding and volume of distribution of compounds from calculated pK_a and AlogP98 values." **7**(1): 69-87.

Lu, X., et al. (2014). "Limitations of Microdialysis in Measuring Unbound Drug Concentrations in the Brain." LATIN AMERICAN JOURNAL OF PHARMACY **33**(10): 1609-1617.

Manallack, D. T., et al. (2013). "The significance of acid/base properties in drug discovery." **42**(2): 485-496.

Martínez-Gómez, M. A., et al. (2007). "Evaluation of enantioselective binding of antihistamines to human serum albumin by ACE." Electrophoresis **28**(15): 2635-2643.

McGinnity, D. F., et al. (2007). "Evaluation of Human Pharmacokinetics, Therapeutic Dose and Exposure Predictions Using Marketed Oral Drugs." Current Drug Metabolism **8**(5): 463-479.

Mehn, D., et al. (2020). "Analytical ultracentrifugation for measuring drug distribution of doxorubicin loaded liposomes in human serum." Journal of Nanoparticle Research **22**(6): 1-7.

Molina, D. K. and V. J. M. DiMaio (2012). "Normal Organ Weights in Men: Part II—The Brain, Lungs, Liver, Spleen, and Kidneys." The American Journal of Forensic Medicine and Pathology **33**(4): 368-372.

Monteiro, N., et al. (2014). "Liposomes in tissue engineering and regenerative medicine." J R Soc Interface **11**(101): 20140459.

Morgan, P., et al. "Can the flow of medicines be improved." Fundamental pharmacokinetic and.

Morris, B. and F. C. Courtice (1955). "THE PROTEIN AND LIPID COMPOSITION OF THE PLASMA OF DIFFERENT ANIMAL SPECIES DETERMINED BY ZONE ELECTROPHORESIS AND CHEMICAL ANALYSIS." Quarterly Journal of Experimental Physiology and Cognate Medical Sciences **40**(2): 127-137.

1. The electrophoretic patterns and chemical composition of the plasma proteins and lipids of different animal species have been examined by zone electrophoresis on filter paper and by chemical analysis. 2. Significant differences have been found in the absolute amount and relative distribution of both the protein and lipid constituents of different animal plasmas. 3. Dog and cat plasma showed high levels of an alpha-type lipoprotein which contained most of the plasma cholesterol, whereas in human plasma cholesterol was mainly present in the large betalipoprotein fraction. 4. The herbivora in general had low levels of plasma lipoprotein and the concentration of alpha-type lipoprotein was relatively high. The horse had the highest concentrations of plasma lipids and lipoproteins of these animals. 5. The mouse constantly, and the rat and guinea-pig in some samples, showed the presence of a rapidly migrating fraction termed a pre-albumin lipoprotein. In the mouse this lipoprotein had a high proportion of lipid to protein and contained a large percentage of the plasma lipids.

Mross, K., et al. (1990). "Pharmacokinetics and metabolism of iodo-doxorubicin and doxorubicin in humans." European journal of clinical pharmacology **39**(5): 507-513.

Mukker, J. K., et al. (2016). Methodologies for Protein Binding Determination in Anti-infective Agents. Antibiotic Pharmacodynamics. J. C. Rotschafer, D. R. Andes and K. A. Rodvold. New York, NY, Springer New York: 109-125.

Murakami, T., et al. (2011). "Role of phosphatidylserine binding in tissue distribution of amine-containing basic compounds." **7**(3): 353-364.

Nilsson, L. (2013). "The bioanalytical challenge of determining unbound concentration and protein binding for drugs." Bioanalysis **5**(24): 3033.

O'Leary, E. I., et al. (2018). "Effects of phosphatidylcholine membrane fluidity on the conformation and aggregation of N-terminally acetylated α -synuclein." Journal of Biological Chemistry **293**(28): 11195-11205.

Obach, R. S., et al. (2008). "Trend analysis of a database of intravenous pharmacokinetic parameters in humans for 670 drug compounds." Drug Metabolism and Disposition **36**(7): 1385-1405.

Obach, R. S., et al. (2008). "Trend analysis of a database of intravenous pharmacokinetic parameters in humans for 670 drug compounds." **36**(7): 1385-1405.

Pacifici, G. M. and A. Viani (1992). "Methods of Determining Plasma and Tissue Binding of Drugs." Clinical Pharmacokinetics **23**(6): 449-468.

Påhlman, I. and P. Gozzi (1999). "Serum protein binding of tolterodine and its major metabolites in humans and several animal species." Biopharmaceutics & Drug Disposition **20**(2): 91-99.

Pajouhesh, H. and G. R. J. N. Lenz (2005). "Medicinal chemical properties of successful central nervous system drugs." **2**(4): 541-553.

Pammolli, F., et al. (2011). "The productivity crisis in pharmaceutical R&D." **10**(6): 428-438.

Plock, N. and C. Kloft (2005). "Microdialysis—theoretical background and recent implementation in applied life-sciences." European Journal of Pharmaceutical Sciences **25**(1): 1-24.

Prentis, R., et al. (1988). "Pharmaceutical innovation by the seven UK-owned pharmaceutical companies (1964-1985)." British Journal of Clinical Pharmacology **25**(3): 387-396.

Rahman, A. M., et al. (2007). "Anthracycline-induced cardiotoxicity and the cardiac-sparing effect of liposomal formulation." International journal of nanomedicine **2**(4): 567.

Reichel, A. (2009). "Addressing Central Nervous System (CNS) Penetration in Drug Discovery: Basics and Implications of the Evolving New Concept." Chemistry & Biodiversity **6**(11): 2030-2049.

Abstract Despite enormous efforts, achieving a safe and efficacious concentration profile in the brain remains one of the big challenges in central nervous system (CNS) drug discovery and development. Although there are multiple reasons, many failures are due to

underestimating the complexity of the brain, also in terms of pharmacokinetics (PK). To this day, PK support of CNS drug discovery heavily relies on improving the blood–brain barrier (BBB) permeability in vitro and/or the brain/plasma ratio (K_p) in vivo, even though neither parameter can be reliably linked to pharmacodynamic (PD) and efficacy readouts. While increasing BBB permeability may shorten the onset of drug action, an increase in the total amount in brain may not necessarily increase the relevant drug concentration at the pharmacological target. Since the traditional K_p ratio is based on a crude homogenization of brain tissue, it ignores the compartmentalization of the brain and an increase favors non-specific binding to brain lipids rather than free drug levels. To better link exposure/PK to efficacy/PD and to delineate key parameters, an integrated approach to CNS drug discovery is emerging which distinguishes total from unbound brain concentrations. As the complex nature of the brain requires different compartments to be considered when trying to understand and improve new compounds, several complementary parameters need to be measured in vitro and in vivo, and integrated into a coherent model of brain penetration and distribution. The new paradigm thus concentrates on finding drug candidates with the right balance between free fraction in plasma and brain, and between rate and extent of CNS penetration. Integrating this data into a coherent model of CNS distribution which can be linked to efficacy will allow it to design compounds with an optimal mix in physicochemical, pharmacologic, and pharmacokinetic properties, ultimately mitigating the risk for failures in the clinic.

Roberts, J. A., et al. (2013). "The Clinical Relevance of Plasma Protein Binding Changes." Clinical Pharmacokinetics **52**(1): 1-8.

Controversy reigns as to how protein binding changes alter the time course of unbound drug concentrations in patients. Given that the unbound concentration is responsible for drug efficacy and potential drug toxicity, this area is of significant interest to clinicians and academics worldwide. The present uncertainty means that many questions relating to this area exist, including "How important is protein binding?", "Is protein binding always constant?", "Do pH and temperature changes alter binding?" and "How do protein binding changes affect dosing requirements?". In this paper, we seek to address these questions and consider the data associated with altered pharmacokinetics in the presence of changes in protein binding and the clinical consequences that these may have on therapy, using examples from the critical care area. The published literature consistently indicates that a change in the protein binding and unbound concentrations of some drugs are common in certain specific patient groups such as the critically ill. Changes in pharmacokinetic parameters, including clearance and apparent volume of distribution (V_d), may be dramatic. Drugs with high protein binding, high intrinsic clearance (e.g. clearance by glomerular filtration) and where dosing is not titrated to effect are most likely to be affected in a clinical context. Drugs such as highly protein bound antibacterials with multiple half-lives within a dosing interval and that have some level of renal clearance, such as ertapenem, teicoplanin, ceftriaxone and flucloxacillin, are commonly affected. In response to these challenges, clinicians need to adapt dosing regimens rationally based on the pharmacokinetic/pharmacodynamic characteristics of the drug. We propose that further pharmacokinetic modelling-based research is required to enable the design of robust dosing regimens for drugs affected by altered protein binding.

Rodgers, T., et al. (2005). "Tissue distribution of basic drugs: Accounting for enantiomeric, compound and regional differences amongst β -blocking drugs in rat." Journal of Pharmaceutical Sciences **94**(6): 1237-1248.

Sandy, P. K., et al. (2019). "Commentary: Hepatic Clearance Concepts and Misconceptions: Why the Well-Stirred Model Is Still Used Even Though It Is Not Physiologic Reality?".

Seddon, A. M., et al. (2009). "Drug interactions with lipid membranes." Chemical Society Reviews **38**(9): 2509-2519.

Shepherd, A. M., et al. (1977). "Age as a determinant of sensitivity to warfarin." British Journal of Clinical Pharmacology **4**(3): 315-320.

Small, H., et al. (2011). "Measurement of Binding of Basic Drugs to Acidic Phospholipids Using Surface Plasmon Resonance and Incorporation of the Data into Mechanistic Tissue Composition Equations to Predict Steady-State Volume of Distribution." Drug Metabolism and Disposition **39**(10): 1789-1793.

Acidic phospholipid binding plays an important role in determining the tissue distribution of basic drugs. This article describes the use of surface plasmon resonance to measure binding affinity (KD) of three basic drugs to phosphatidylserine, a major tissue acidic phospholipid. The data are incorporated into mechanistic tissue composition equations to allow prediction of the steady-state volume of distribution (Vss). The prediction accuracy of Vss using this approach is compared with the original methodology described by Rodgers et al. (J Pharm Sci 94:1259–1276), in which the binding to acidic phospholipids is calculated from the blood/plasma concentration ratio (BPR). The compounds used in this study [amlodipine, propranolol, and 3-dimethylaminomethyl-4-(4-methylsulfanyl-phenoxy)-benzenesulfonamide (UK-390957)] showed higher affinity binding to phosphatidylserine than to phosphatidylcholine. When the binding affinity to phosphatidylserine was incorporated into mechanistic tissue composition equations, the Vss was more accurately predicted for all three compounds by using the surface plasmon resonance measurement than by using the BPR to estimate acidic phospholipid binding affinity. The difference was particularly marked for UK-390957, a sulfonamide that has a high BPR due to binding to carbonic anhydrase. The novel approach described in this article allows the binding affinity of drugs to an acidic phospholipid (phosphatidylserine) to be measured directly and demonstrates the utility of the binding data in the prediction of Vss.%U
<http://dmd.aspetjournals.org/content/dmd/39/10/1789.full.pdf>

Spector, A. A. J. J. o. l. r. (1975). "Fatty acid binding to plasma albumin." **16**(3): 165-179.

Summerfield, S. and P. Jeffrey (2009). "Discovery DMPK: changing paradigms in the eighties, nineties and noughties." Expert Opinion on Drug Discovery **4**(3): 207-218.

Svensson, C. K., et al. (1986). "Free Drug Concentration Monitoring in Clinical Practice." Clinical Pharmacokinetics **11**(6): 450-469.

Recent advances in techniques to determine free drug concentrations have lead to a substantial increase in the monitoring of this parameter in clinical practice. The majority of drug binding to macromolecules in serum can be accounted for by association with albumin and α 1-acid glycoprotein. Albumin is the primary binding protein for acidic drugs, while binding to α 1-acid glycoprotein is more commonly observed with basic lipophilic agents.

Alterations in the concentrations of either of these macromolecules can result in significant changes in free fraction. Diseases such as cirrhosis, nephrotic syndrome and malnourishment can result in hypoalbuminaemia. Burn injury, cancer, chronic pain syndrome, myocardial infarction, inflammatory diseases and trauma are all associated with elevations in the concentration of α 1-acid glycoprotein. Treatment with a number of drugs has also been shown to increase α 1-acid glycoprotein serum concentrations.

Switzar, L., et al. (2013). "Protein digestion: an overview of the available techniques and recent developments." J Proteome Res **12**(3): 1067-1077.

Several proteomics approaches are available that are defined by the level (protein or peptide) at which analysis takes place. The most widely applied method still is bottom-up proteomics where the protein is digested into peptides that can be efficiently analyzed with a wide range of LC-MS or MALDI-TOF-MS instruments. Sample preparation for bottom-up proteomics experiments requires several treatment steps in order to get from the protein to the peptide level and can be very laborious. The most crucial step in such approaches is the protein digestion, which is often the bottleneck in terms of time consumption. Therefore, a significant gain in throughput may be obtained by speeding up the digestion process. Current techniques allow for reduction of the digestion time from overnight (~15 h) to minutes or even seconds. This advancement also makes integration into online systems feasible, thereby reducing the number of tedious sample handling steps and the risk of sample loss. In this review, an overview is given of the currently available digestion strategies and recent developments in the acceleration of the digestion process. Additionally, tailored approaches for classes of proteins that pose specific challenges are discussed.

Talbert, R. L. J. T. J. o. C. P. (1994). "Drug dosing in renal insufficiency." **34**(2): 99-110.

Taylor, S. and A. Harker (2006). "Modification of the ultrafiltration technique to overcome solubility and non-specific binding challenges associated with the measurement of plasma protein binding of corticosteroids." Journal of Pharmaceutical and Biomedical Analysis **41**(1): 299-303.

Thies, R. L., et al. (1990). "Method for rapid separation of liposome-associated doxorubicin from free doxorubicin in plasma." Analytical biochemistry **188**(1): 65-71.

Toutain, P. L. and A. Bousquet-MÉLou (2004). "Volumes of distribution." Journal of Veterinary Pharmacology and Therapeutics **27**(6): 441-453.

Tucker, G. J. B. j. o. c. p. (1981). "Measurement of the renal clearance of drugs." **12**(6): 761.

Valkó, K. L., et al. (2011). "Estimating unbound volume of distribution and tissue binding by in vitro HPLC-based human serum albumin and immobilised artificial membrane-binding measurements." Journal of pharmaceutical sciences **100**(3): 849-862.

Wang, J. and L. J. D. D. W. Urban (2004). "The impact of early ADME profiling on drug discovery and development strategy." **5**(4): 73-86.

Wang, L., et al. (2020). "Integration of Acoustic Liquid Handling into Quantitative Analysis of Biological Matrix Samples." SLAS TECHNOLOGY: Translating Life Sciences Innovation **25**(5): 463-473.

Waters, N. J., et al. (2008). "Validation of a rapid equilibrium dialysis approach for the measurement of plasma protein binding." Journal of Pharmaceutical Sciences **97**(10): 4586-4595.

Wilkinson, G. R. and D. G. Shand (1975). "A physiological approach to hepatic drug clearance." Clinical Pharmacology & Therapeutics **18**(4): 377-390.

A physiological approach has been developed recognizing that hepatic blood flow, the activity of the overall elimination process (intrinsic clearance), drug binding in the blood, and the anatomical arrangement of the hepatic circulation are the major biological determinants of hepatic drug clearance. This approach permits quantitative prediction of both the unbound and total drug concentration/time relationships in the blood after intravenous and oral administration, and any changes that may occur as a result of alterations in the above biological parameters. These considerations have led to a classification of drug metabolism based on the hepatic extraction ratio. The proposed classification allows prediction and interpretation of the effects of individual variations in drug-metabolizing activity, route of administration, pharmacokinetic interactions, and disease states on hepatic drug elimination.

Xu, X., et al. (2014). "Quantitative determination of free/bound atazanavir via high-throughput equilibrium dialysis and LC-MS/MS, and the application in ex vivo samples." Bioanalysis **6**(23): 3169-3182.

Yap, C. and Y. J. J. o. p. s. Chen (2005). "Quantitative Structure-Pharmacokinetic Relationships for drug distribution properties by using general regression neural network." **94**(1): 153-168.

Yata, N., et al. (1990). "Phosphatidylserine as a Determinant for the Tissue Distribution of Weakly Basic Drugs in Rats." Pharmaceutical Research **7**(10): 1019-1025.

Interorgan variation in tissue distribution of weakly basic drugs such as quinidine, propranolol, and imipramine was investigated as a function of binding to phosphatidylserine (PhS) in tissues. Tissue distributions of these drugs were determined using 10 different tissues at a steady-state plasma concentration and were expressed as tissue-to-plasma partition coefficients (K_p values). The concentration of PhS in the tissue was determined by two-dimensional thin-layer chromatography. Plotting of K_p values, except for brain, against the tissue PhS concentrations showed a linear relationship, indicating that PhS is a determinant in the interorgan variation of these tissue distributions. Further, differences in tissue distribution among the drugs was considered to be due to the difference in binding potency to PhS. Drug binding parameters to individual standard phospholipid were determined using a hexane-pH 4.0 buffer partition system. Binding was highest to PhS, and a linear relationship was found between the log nK [product of the number of binding sites (n) and the association constant (K) for PhS binding] obtained in vitro and K_p values of drugs in tissues in vivo. The empirically derived equation, $K_p = 14.3 \times (\log nK) \times (\text{PhS conc.}) - 8.09$, was found to predict K_p values in vivo of weakly basic drugs. Thus, a determinant of

interorgan variation in the tissue distribution of the weakly basic drugs studied was the tissue concentration of PhS and the drug binding affinity to PhS.

Zhang, F., et al. (2012). "Compilation of 222 drugs' plasma protein binding data and guidance for study designs." Drug Discovery Today **17**(9–10): 475-485.

Bulbake, U., et al. (2017). "Liposomal formulations in clinical use: an updated review." Pharmaceutics **9**(2): 12.

Charrois, G. J. and T. M. Allen (2004). "Drug release rate influences the pharmacokinetics, biodistribution, therapeutic activity, and toxicity of pegylated liposomal doxorubicin formulations in murine breast cancer." Biochimica et Biophysica Acta (BBA)-Biomembranes **1663**(1-2): 167-177.

Fan, Y. and Q. Zhang (2013). "Development of liposomal formulations: From concept to clinical investigations." Asian Journal of Pharmaceutical Sciences **8**(2): 81-87.

Li, J., et al. (2015). "A review on phospholipids and their main applications in drug delivery systems." Asian Journal of Pharmaceutical Sciences **10**(2): 81-98.

Mehn, D., et al. (2020). "Analytical ultracentrifugation for measuring drug distribution of doxorubicin loaded liposomes in human serum." Journal of Nanoparticle Research **22**(6): 1-7.

Monteiro, N., et al. (2014). "Liposomes in tissue engineering and regenerative medicine." J R Soc Interface **11**(101): 20140459.

Mross, K., et al. (1990). "Pharmacokinetics and metabolism of iodo-doxorubicin and doxorubicin in humans." European journal of clinical pharmacology **39**(5): 507-513.

O'Leary, E. I., et al. (2018). "Effects of phosphatidylcholine membrane fluidity on the conformation and aggregation of N-terminally acetylated α -synuclein." Journal of Biological Chemistry **293**(28): 11195-11205.

Rahman, A. M., et al. (2007). "Anthracycline-induced cardiotoxicity and the cardiac-sparing effect of liposomal formulation." International journal of nanomedicine **2**(4): 567.

Thies, R. L., et al. (1990). "Method for rapid separation of liposome-associated doxorubicin from free doxorubicin in plasma." Analytical biochemistry **188**(1): 65-71.